A PRAYER FOR GRAD STUDENTS

Dankwoord

Niet te geloven, hij is gewoon afgeraakt. Hij ligt nu in jouw handen, mijn thesis. Het een meesterwerk noemen is misschien een tikje hoogmoedig, maar je houdt nu toch één van de meest indrukwekkende dingen vast die ik –naar eigen mening- al geproduceerd heb. De kers op de taart van mijn voorlopig academische carrière. Een samenvatting van iets meer dan 4 jaar prullen aan pyrolysereactors, bedenken van experimenten, potjes vullen, filteren, meten en kritisch analyseren. Het merendeel van het experimentele werk dat ik gedaan heb zijn adsorptieproeven, en ik heb het voor jullie even nageteld: ik heb doorheen die 5 jaar ongeveer 2000 keer de volgende handeling uitgevoerd: potje gevuld met actieve kool, vloeistof toegevoegd, laten schudden, vloeistof afgefiltreerd, staalname en meting gedaan (oké, laten doen soms!) en daarna dat potje terug uitgewassen. Ik denk dus dat ik na deze 5 jaar vooral een expertise heb opgedaan in wegen, filteren en afwassen.

Om te zorgen dat ik doorheen deze 5 jaar niet zot geworden ben -of zotter, dit laat ik in het midden- heb ik volcontinu de steun gehad van een hele hoop familie, vrienden en collega's die zowel op praktisch als op minder praktische vlakken inspiratie en hulp boden. Het schrijven van een bedanklijst is een zware taak voor iemand als ik met de hersencapaciteit van een pinda als het gaat om het onthouden van mensen, namen en bezigheden. Ik wil maar gewoon even stellen: het kan zijn dat ik mensen vergeet neer te pennen, maar dat wil niet zeggen dat ik hun hulp minder apprecieer! ☺

Allereerst wil ik graag het TANCpersoneel bedanken. Hun expertise is me vaak goed van pas gekomen en ze hebben me de kans gegeven veel te leren. Jullie stonden altijd paraat om metingen te doen en me te helpen bij het analyseren van de resultaten. Maar vooral ook jullie aanwezigheid op de belangrijkste momenten van de dag (KOFFIE! LUNCH!) in de koffiekamer staan me bij. Gezellige momenten, al dan niet vergezeld van taart of mozzarella en een hoop lachende collega's. De teambuildingactiviteiten en feestjes die we samen hebben kunnen doen zijn alvasy in mijn geheugen gebrand.

Ik weet dat ik de chemische expertise van Linda, Jenny en Jan weinig heb kunnen leren kennen, maar net door die koffiekamermomenten heb ik jullie toch persoonlijk mogen leren kennen! Guy, je stond altijd klaar voor de TGA's, ook al moesten we daar zelf braaf af blijven: nu heeft dat toestel alsnog de geest gegeven, dankzij uw goede zorgen... Laten we hopen dat de toekomst even goede TGA's brengt. Martine, je was altijd een en al luisterend oor als ik weer eens kwam mopperen en ook al heb je voor mij persoonlijk niet veel metingen moeten doen, toch was het telkens fijn om met je samen te werken. Als ik weer iets zocht kon ik altijd terecht bij Yvo, of ik nu labomateriaal zocht (van sommige dingen weet ik nog steeds niet uit welke magische kast ze komen,) of advies over een proef of opstelling. Ik hoop dat je van je aankomende pensioen kan genieten!

En dan de twee dames die het hardste hebben 'afgezien' van al mijn experimenten: Greet en Elsy. Zonder jullie was mijn thesis niet eens de helft zo dik! Dus, een speciaal paragraafje voor de ICP-meisjes. Greet, jij die net als Yvo van die magische kast weet en altijd kan aanduiden waar alles ligt, jij die alles netjes houdt (oef!) en die eerlijk durft te zeggen waarop het staat als we het weer te bont maakten: merci! Ook voor de honderden ICP metingen, waarvoor je telkens zonder klagen stalen ingaf, ijkreeksen maakte en de resultaten analyseerde: nen héle dikke merci. Elsy, ook aan jou een dikke dankuwel voor de vele babbels, metingen –niet allemaal even eenvoudig-, en hilarische verhalen aan de koffietafel. Je kon me op moeilijke dagen altijd opfleuren met een babbel of weer een wild verhaal!

De collega-doctorandi bij TANC is natuurlijk ook een grote groep die ik niet mag vergeten. Koen, Jens, Marco en Inge ben ik heel dankbaar voor het doorgeven van hun kennis en specialiteiten, ook al heb ik niet met iedereen van jullie even veel tijd doorgebracht. De aanstormende nieuwe garde (Tom V, Bram) heb ik ook maar kortelings leren kennen, maar wil ik vooral veel succes toewensen en de moed om vol te houden – al heb ik een vermoeden dat dat helemaal goed komt.

To all foreign PhD-students: thank you. Thank you for granting me the opportunity to work with people from different cultures and different backgrounds. Teaching me new things in the lab and about the world! Ying, Lenia, Shahin: always there to help and explain things about their work and techniques. It was always a joy

to have you around. The Cuban Crew: Thayset, Monica, Jeamichel, Roberto, Harold thank you for bringing some tropical sun into the lab and also for the kind reception in Cuba! Your creativity is your strength and I hope your research will open many people's eyes.

Dan nog die andere 3 mede-doctorandi, die over die 4 jaar soms een beetje meer geworden zijn dan collega's. Ik weet dat jullie liefst allemaal een halve pagina lof over jezelf zien verschijnen, maar mannekes: kalm aan he! Allereerst de persoon waaraan ik al mijn labo-skills en kennis te danken heb, dankzij hem ben ik eigenlijk in dit doctoraat gerold: Kenny. Altijd de eerste om een practical joke uit te halen en de eerste om iemand tegen zijn voeten te geven, maar ook plichtsbewust en correct. Ik ben je dankbaar voor al uw hulp, kennis en ideeën de afgelopen paar jaar, en ik hoop dat je met je bedrijf een rooskleurige toekomst tegemoet gaat. Tom, ik leerde je eerst kennen als een student in Valencia en moet zeggen dat ik u als mens en collega hartelijk apprecieer! Helpen in het labo, labotaken overnemen, niks is je teveel: merci. En ten slotte: de Maggen. Al vond ik u eerst maar een rare snuiter en een chemie-nerd, toch is dat blijkbaar wel goed gekomen over de jaren. Er waren weinig doodse momenten op onze gedeelde bureau en door samen de lessen biomedische te leiden/lijden hebben we ook steen en been tegen elkaar kunnen klagen. Handig, zo hetzelfde traject doorlopen. Ik hoop dat je snel je thesis afkrijgt (2020?) en dat je jezelf ook doctor kan kronen!

En dan: mijn promotoren. Die volgens mij in het begin harder in mij geloofden dan ik zelf deed, maar door hun aanhoudende advies, steun en wijsheid me toch tot aan de eindstreep gepusht hebben. Robert, Jan, Sonja, jullie zijn een knap team. In tegenstelling tot andere doctorandi (...van horen zeggen...) heb ik promotoren die makkelijk bereikbaar en aanspreekbaar zijn, waardevolle suggesties doen én een gevoel voor menselijkheid en humor hebben. Sonja, je onstopbare stroom vragen deden me kritisch nadenken over elke stap en hebben deze thesis zeker mee gevormd. Robert, dankjewel voor alle wetenschap, feiten en wijsheden te delen, die allemaal recht uit het geheugen komen. Ook een extra dikke merci aan Jan, mijn hoofdpromotor, voor zijn kritische bedenkingen, praktische benaderingen en ook voor de kans om mee te gaan naar Cuba!

En dan gaan we over naar de lange lijst van mensen die niet in het academische wereldje verblijven. Ik kan jammer genoeg niet al mijn vrienden en kennissen oplijsten, dus ik wilde even speciaal de volgende mensen bedanken.

Toen ik afstudeerde als ingenieur vond ik dat het eindelijk tijd was om te beginnen specialiseren in een hobby waarvoor ik nooit eerder de tijd had: zingen. Op dat moment is dan ook Cathubodua ontstaan uit de gedachten van Katrien. Een plek waarin in creativiteit, opgekropte frustraties en energie kan uiten, en waar nog mensen naar komen kijken ook! Dankuwel aan iedereen in (Kenny, William, Kyron, Peter) en rond deze band (fotograven, liefdes, andere bands, ...), die samen met m'n doctoraat gegroeid is. Hopelijk kan er hier ook een groots werk rond groeien in de nabije toekomst.

Verder wil ik graag Leen bedanken, steunpilaar, klaagmuur van dienst en mede-liefhebber van alles wat mooi is en glittert. En katten! Samen met jou op café zitten, zagen over koetjes, kalfjes en serieuze dingen zoals thesissen is altijd een pak van mij hart. Aan Hans wil ik een speciaal bedankje doen voor de vele culinaire ontdekkingen de afgelopen paar jaar en de goede vriendschap. Ik weet dat ook 27 april een avond wordt om niet te vergeten. Jordi en Margo, jullie zijn zeker mijn 'oudste' vrienden, en ik weet dat ik altijd op jullie kan rekenen!

De domme-vrienden-groep [You know who you are], jullie zijn geweldig. Of het nu gaat om schrale roadtrips, ijskoude kerstmarkten of marginale weekends in de ardennen, er valt altijd wel iets te beleven (al dan niet veroorzaakt door copieuze hoeveelheden alcohol.) Als dit hele doctoreer-avontuur over is kan ik me eindelijk samen met Dr. Q kronen tot de intelligente keizer en keizerin van deze groep. Zodat we intense debat-avonden en kwissen kunnen organiseren. Ofzoiets.

Verder is er niets zo gezellig als het delen van lief en leed met mijn familie. Geen verjaardag gaat voorbij zonder bergen eten, dessert en wijn en een hele hoop gezelligheid! Papa, Linda, Heidi, Nico, Rita, Stan, Elly, Solange en Freddy: merci om er altijd voor me te zijn en in me te geloven!

En dan uiteindelijk nog de mens waar ik ook een hele thesis over zou willen (kunnen?!) schrijven, maar waarvoor woorden soms gewoon te kort schieten. Dankuwel aan Tom: al ietsje meer dan 9 jaar aan mijn zijde, waarvan 4.5 jaar

doctoraat. Binnenkort is voor het eerst uw vriendin officieel student-af en gaat het "echte" leven beginnen zeker? Altijd klaar voor steun en liefde, maar ook om de afwas te doen, stof te zuigen en alles achter mijn gat op te ruimen (sorry!) als ik wéér eens geen tijd heb. Ge zijt geweldig, en ge weet het. Daarom gaat de grootste merci alvast naar u, want zonder u had ik hier alvast niet gestaan. <3

Table of contents

IX

List of tables

List of figures

Outline

With global population rising and general wealth increasing, the demand for resources is reaching an all-time high. Natural resources are rapidly depleting, waste materials are accumulating in soils and water and the use of fossil fuels is contributing dramatically to the greenhouse effect. All of these consequences of an industrialized lifestyle substantially damage the earth's environment. Modern industry and R&D are challenged to minimize these effects to the environment to provide a better future earth for generations to come.

One of the major solutions is the development of a circular economy. Following this ideology, materials will be re-used, upcycled and recycled to create a closed material loop: there will be no waste material left, only valuable resources. Energy conservation and the use of renewable energy are also important factors to reduce global warming.

Production of new materials from waste is a valuable contribution to the development of this circular economy. Pyrolysis and activation are able to produce activated carbons from waste material, that can be used for remediation of water supplies. Furthermore, excess energy is produced during this process, providing possibilities for green energy production.

Brewer's spent grain, which is a biomass now only used as animal feed for ruminants, can also be used for the production of activated carbons (AC), a material with higher added value. The economic value of this concept has already been proven by previous research. The present study describes the application of these AC as improved adsorbents with better selectivity characteristics for the adsorption of ionic species.

Chapter 1 presents a general introduction and describes the origin of biomass, its components, uses, legislation and main physical and chemical properties. More details are provided about brewer's spent grain. The pyrolysis and activation processes are described, as well as physical and chemical properties of activated

carbon and adsorption processes. The most important models for adsorption isotherms and adsorption kinetics are summarized.

Chapter 2 and **chapter 3** describe the effect of different modifications on the adsorption properties of activated carbons. They are conceived as a summary of scientific manuscripts that are preceded by a general introduction toward the specific topic, as that differs in each chapter.

Chapter 2 handles the adsorption of chromium (Cr) and the modification of AC for its adsorption. The atypical adsorption behavior of Cr is explained in a first manuscript, together with a description of the adsorption kinetics. The second published paper explores two modification possibilities to improve the efficiency of the activated carbon for adsorption and kinetics.

Chapter 3 focuses on the measurement method for cesium and the enhanced removal by creation of a hybrid material. Description of the set-up for measurement of Cs-134 and the removal of cesium by AC is the focus of the first published paper, whereas the second paper focuses on enhanced removal of Cs by a hybrid material from different aqueous media.

In **chapter 4**, the removal of several heavy metal (HM) ions from waste water is investigated. Effects of metal concentrations, water medium and mixtures are investigated by a newly developed two-point method to estimate the effect of low and high dosage of activated carbon.

The outline is summarized in the following scheme.

Chapter 1: Introduction
Chapter 2: Chromium removal by activated carbons
Introduction
Chromium(VI) removal using activated carbon prepared from brewers' spent grain
Activated carbons from brewers' spent grain and their modifications: enhanced removal of chromium(VI)
Chapter 3: Cesium removal by activated carbons
Introduction
Adsorption of cesium on different types of activated carbon
Enhanced cesium removal from real matrices by modified activated carbons
Chapter 4: The use of activated carbons as adsorbent for problematic metals in Flemish surface water.
Summary and conclusion

Schematic representation of the outline of this work

1 Introduction

1.1 Biomass in a circular economy[1]

Estimates show that 10-15% of the world's energy today is supplied by biomass. Increased use of this resource is one of the key points in the Europe 2020 goals to halt climate change. This chapter will shortly discuss what biomass is, how it can be used and points out the current issues regarding agriculture and environment.

1.1.1 Types of biomass

Plant materials are created when sunlight energy is converted to chemical bonds by photosynthesis. The CO_2 in the atmosphere is used following the general unbalanced equation:

$$CO_2 + 2\,H_2A + \text{light energy} \rightarrow (CH_2O) + H_2O + A_2 \qquad \text{Equation 1-1}$$
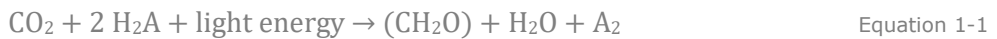
Where H_2A is an oxidisable compound. In algae and green plants H_2A represents water, creating oxygen gas after the conversion. There are however some photosynthetic bacteria that use hydrogen sulfide and form sulphur gas. "A" can also represent an organic radical or in extreme cases 'nothing'. The organic compounds that are generated are carbohydrates which are incorporated in the growing plant matter. Photosynthesis occurs during two stages: light-dependent reactions and dark (light-independent) reactions. The first reactions can be sped up by increasing light intensity and are independent of temperature. The dark reaction rate can be enhanced by increasing the temperature (within certain limits), but is independent of light intensity. Converting this light energy into chemical energy has a low average yield, but occurs on a worldwide scale. Energy is stored in plants to use as food, as a direct fuel or it is transformed into fossil fuels. All organic matter is considered as biomass, including manure and aquatic plants [1, 2].

Depending on the source, biomass is classified into several categories. The National Energy Education Development defines 4 categories: wood and agricultural wastes, other solid wastes, biogas and biofuels [3]. Most other

---

[1] References for this introduction can be found on page 51 in section 1.8

classifications do not categorize ethanol or biodiesel as biomass, but as products of biomass conversion. Here, biomass is classified according to their biological origin or their industrial source. This classification divides biomass into the following categories [1, 4, 5]:

- Wood / woody biomass
- Herbaceous and agricultural biomass
- Aquatic biomass
- Animal and human biomass wastes
- Contaminated biomass and industrial biomass wastes (semi-biomass)

Lignocellulosic biomass consists mostly of cellulose, hemicellulose and lignin. Some smaller molecules, like water, inorganic ions or small organic molecules are incorporated within these structures. Their relative ratios are determined by plant species and growth circumstances. Cellulose is a bio-polymer built up from glucose, composed of linear chains of D-glucose linked by β-1,4-glycosidic bonds (see Figure 1-1). Thousands to ten thousand of (1,4)-D-glucopyranose units are linked and create macromolecules with a molecular weight (MW) of about 100 000. The hydroxyl groups on these linear chains have a strong tendency to form intra- and intermolecular hydrogen bonds, enabling a crystalline structure [1, 6, 7].
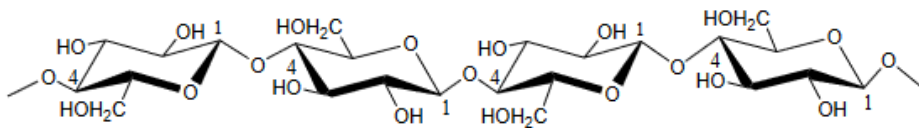
Figure 1-1 Structure of cellulose

Hemicellulose is best described as a mixture of linked polysaccharides. The compound is generally smaller than cellulose (MW of about 30 000), and has a more branched structure. This polysaccharide is also able to form hydrogen bonds, making it possible to bind closely to cellulose. The biggest difference between cellulose and hemicellulose are the monosaccharides that constitute the hemicellulose. Where cellulose is a chain of hexagonal carbon rings, hemicellulose is mostly made up of 5-carbon and 6-carbon monosaccharides. These include glucose, manose, xylose, arabinose and several acid groups, as can be seen in Figure 1-2 [1, 7].
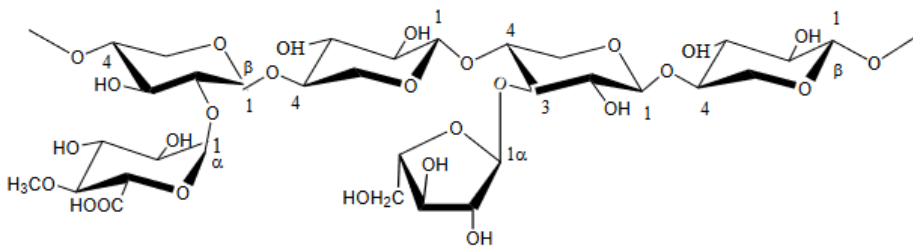
Figure 1-2 A possible structure of hemicellulose

The last structural biomass component is lignin. It is a group of chemically related compounds that are three-dimensional amorphous polymers with a high MW. Lignin is built from chains of three carbons connected to phenyl rings – phenylpropanes. On the ring, up to 2 methoxyl groups can be attached. The degree of methoxylation gives rise to three phenylpropane units: p-hydroxyphenyl, guaicyl and syringyl. These units are randomly linked through different ether and carbon bridges, as proposed in Figure 1-3 [1, 7].

The use of biomass for energy and industrial purposes is dependent on some intrinsic biomass properties, which shall be shortly discussed (according to [1, 5]). The composition and applicability of biomass are mainly dependent on four parameters: moisture, ash content, volatile matter (VM) and fixed carbon (FC) content.
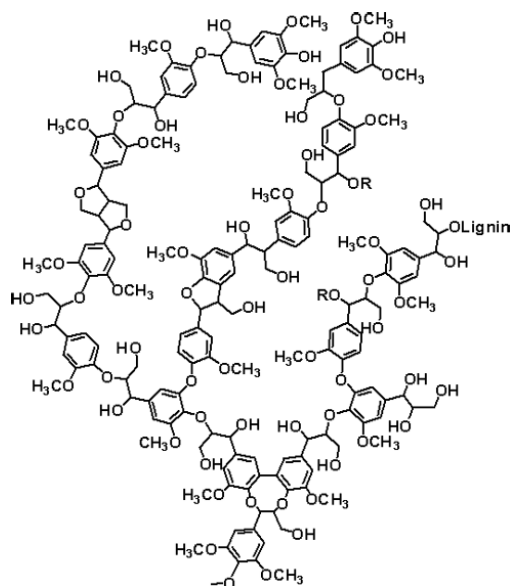
Figure 1-3 The randomised structure of lignin

Moisture is present in biomass in two forms: intrinsic and extrinsic. Intrinsic moisture is the moisture within in the biomass itself, whereas extrinsic moisture is added due to circumstances like the weather. Intrinsic moisture content is much higher in living biomass, especially in herbaceous biomass. The moisture in the biomass is a highly mineralized aqueous solution, resulting in a precipitate when evaporated. The moisture content is an important parameter for the choice of the correct processing method. Woody and other low-moisture biomass are generally more suited for thermal conversion since less heating is required. High-moisture biomass is better suited for biochemical conversion methods such as digestion or fermentation.

The *ash* content of biomass is dependent on biomass type, environmental conditions, harvesting method and processing. Ashes and inorganic ions in biomass can work catalytically for conversion, breaking down phenolic components into CO and char, but they can also react to form slags. Ash content is a highly studied parameter, but its influence is still poorly understood. Metal-oxygen groups are Lewis bases that can donate electrons and initiate a variety of reactions, which include hydrogenation, dehydrogenation, hydrogen transfer, polymerization, …

10

Volatile matter (VM) and *fixed carbon* (FC) provide an estimate for ignition and gasification efficiencies. VM is defined as the gas driven off from the materials after heating up (to 950 °C in 7 minutes in an inert atmosphere). These gasses include light hydrocarbons, CO, CO_2, H_2 and tars. The remaining organic matter (without ash and moisture) is considered as the FC content. In contrast to peat and coal, biomass typically has more volatile matter and less fixed carbon. The thermal degradability of the biomass constituents greatly influences the VM and FC content. Determination of VM and FC in cellulose showed that only 2-14% of the material remains as FC because of its linear structure. For hemicellulose, about 27-32% of the materials remains as FC, whereas the FC of the more aromatic lignin is about 40-47% [8].

Table 1-1 shows the influence of biomass group on a few parameters. It also expands to different inorganic molecules. The results are displayed as enriched/depleted compared to the chemical properties (mean values) among the biomass groups.

Another important parameter for thermo-chemical conversion is the biomass *bulk density*. This parameter mainly has an effect on the transport cost of the biomass to the conversion plant, but is also related to the energy density. This density, together with the *calorific value* of the biomass, determines the ability to power the conversion set-up by pyrolysis oil and gas.

Table 1-1 Characteristic enrichment and depletion of chemicals in biomass groups. A = ash content; VM= volatile matter; M = moisture; taken from [5]

Biomass group and sub-group	Enriched in	Depleted in
1. Wood and woody biomass (WWB)	CaO, M, MgO, Mn, VM	A, Cl, N, P_2O_5, S, SiO_2, SO_3
2. Herbaceous and agricultural biomass (HAB)	FC, K_2O, O, VM	C, H, CaO
2.1. Grasses (HAG)	K_2O, O, SiO_2, VM	Al_2O_3, C, CaO, H, Na_2O
2.2. Straws (HAS)	Cl, K_2O, O, SiO_2	C, H, Na_2O
2.3. Other residues (HAR)	FC, K_2O, MgO, P_2O_5	Cl
3. Animal biomass (AB)	A, C, CaO, Cl, H, N, Na_2O, P_2O_5, S, SO_3	Al_2O_3, Fe_2O_3, M, MgO, Mn, O, SiO_2, TiO_2, VM
4. Contaminated biomass (CB)	A, Al_2O_3, C, Cl, Fe_2O_3, H, N, S, TiO_2	FC, K_2O, P_2O_5

1.1.2 Biomass for sustainable energy and value added chemicals

According to [9] and [10]

In order to maintain economic growth that is sustainable, the European Union has developed a new Circular Economy Package. Instead of following the linear economy model (take-make-dispose), resources are used optimally, so that their finite sources do not deplete and run out. The biggest challenge in this circular economy model is to find environmentally and economically sustainable processes to maintain product value for as long as possible, including the minimisation of the amount of waste products. Products can be used longer, smarter and in different life cycles. Consumers can be provided with innovative durable products, save money and improve their quality of life.

In order to reach this circular economy, the basic concept of 'closing the loop' is used to create action plans for the market and legislature. The impact of a product on environment and waste production is studied during all phases in the lifecycle of a product: from production to consumption to waste, including the possibilities to use a product as a secondary raw resource. This will result in better product design and make products easier to repair and more durable, resulting in the prevention of waste.

But even when making the most out of current-day technology, waste is still generated at the end of a lifecycle. The EU waste hierarchy (as defined in DIRECTIVE 2008/98/EC [11] and displayed in Figure 1-4) creates a list of priorities for the application of waste. If the product cannot be re-used as such, they should be recycled. If that is not possible, a recovery of materials or energy is preferred over disposal in landfills.

Figure 1-4 The EU waste hierarchy [11]

As stated before, biomass can be categorised as a raw resource (e.g. wood) or as biomass waste (e.g. wood waste, pulp). Both resources can be used for production, to recover materials or directly as an energy source. The EU encourages the production of new biomass-based products [9]. These materials provide an alternative for fossil-based products. The cascading use of renewable sources can lead to innovative new materials and chemicals and create an entire bio-industry, focussing also on renewable, biodegradable and compostable materials in production processes. The strategic goals for the use of biomass in Flanders have five main focus points [12]. The first focus lies on the creation of a coherent policy and legislation. Secondly, multidisciplinary research should be supported, as well scientifically as practically, with demonstration plants and business model innovations. Thirdly, the goal is to optimally use and produce biomass in the entire value chain. A cascade system is used to valorise biomass in each step with an optimal socio-economic value creation. A fourth focus is to strengthen the market for the use of bio-based materials: create support for businesses willing to change to greener opportunities, but also creating awareness with the general population. The last focus is to strengthen international relationships and to become a developer of sustainability criteria up to the European level.

The European Union has set the target for renewable energy to 20% by 2020. The current use of wood and wood waste for production of heat and electricity creates the biggest source of renewable energy in the EU today[2]. A reporting and monitoring system for sustainability was suggested to the member states of the EU in 2010. These non-binding recommendations judge the greenhouse gas performance criteria in comparison to fossil fuels for several types of biomass and their energy conversion efficiency [9]. Large scale use of biomass was however considered to lead to a negative impact on the environment and the EU changed their view on this matter: the new aim is to focus on efficient use of biomass and the balance between sustainability policies, energy security and competitiveness [10].

The consumption of biomass for heating and electricity in the EU is expected to rise from 86.5 million of tonnes of oil equivalent (Mtoe) in 2012 up to 110.5 Mtoe in 2020. Of this, about 90 Mtoe of biomass will be used for heating and 20 Mtoe for electricity. Import from third world countries is expected to rise if the EU cannot meet the goals with domestic supplies. Technical, institutional and financial support is needed to provide agricultural and forest biomass, as well as waste materials in the coming years [10].

At this moment, forest areas in the EU are still growing because of the anti-deforestation policies. Abandoned farmlands and natural vegetation growth have increased the forest area with 2% over the last decade. Agricultural residues are more likely to come from dedicated crops or waste materials [10].

---

[2] Wood and wood waste constitute 49% of the share of energy from renewable sources in the EU. See: Eurostat (2012), Statistics in focus, renewable energy.

1.1.3 Advantages and disadvantages of using biomass

The EU states several energetic, economic, employment and environmental benefits if biomass will be used more often in the future [13, 14]. Biomass can be dried and stored easily. When there is a high seasonal demand, biomass can then be used to balance the variability in the availability of wind and solar energy. This also ensures the energy supply in the EU if the biomass is produced domestically and sources are diversified. Furthermore, biomass is a diverse source and benefits both farmers and forest owners, possibly aiding in rural development. The raised awareness might motivate small forest owners to invest in sustainable and active forest management. From an environmental point of view, both landfill space and greenhouse emissions can be reduced [15].

Vassilev et al. [5] summarized the more technical advantages and disadvantages. These are displayed in Table 1-2.

Table 1-2 Major advantages and disadvantages of biomass or biomass fuels [5].

Advantages	Disadvantages
Renewable energy source for natural biomass	Incomplete renewable energy resource for biomass fuel with respect to the complete life cycle assessment
CO_2 neutral conversion and climate change benefits	Miss of accepted terminology, classification systems and standards worldwide
Commonly low contents of ash, C, S, N, and trace elements	Insufficient knowledge and variability of composition, properties and quality
Normally high concentrations of volatile matter, Ca, H, Mg, O, and P	Commonly high contents of moisture, Cl, K, Na, Mn, and some trace elements
Great reactivity during conversion	Low energy density
Mitigation of hazardous emissions (CH_4, CO_2, NO_X, SO_X, trace elements) and wastes separated	Potential competition with food and feed production
Capture of some hazardous components by ash during combustion	Possible soil damage and loss of biodiversity
Huge availability and relatively cheap resource	Odour, potential emission and leaching of hazardous components during disposal
Diversification of fuel supply and energy security	Possible hazardous emissions during heat treatment
Rural revitalization with creation of new jobs	Potential technological problems during heat treatment
Potential use of oceans and low-quality soils, and restoration of degraded lands	Regional availability
Reduction of biomass-containing wastes	Great collection, transportation, storage and pre-treatment costs
Cheap resource for production of sorbents, fertilizers, liming and neutralizing agents, building materials, and for some synthesis or recovery of certain elements and compounds	Unclear utilization of waste products

1.2 Brewery waste: origin and properties

1.2.1 Brewing process

Beer is an age-old example of biotechnology. Thousands of years ago, beers were already produced without any knowledge of fermentation, yeast or enzymes. Even though tradition and beer style have strongly influenced the process, a general idea of a brewing scheme is displayed in Figure 1-5. There are roughly four steps in the brewing of beer. During the first stage, the malting, barley is set to steep in water until germination. A variety of enzymes will become active during this stage, but there is a small risk of infection with fungi species. To prevent this, a lactic acid starter culture may be added to control excessive growth of harmful micro-organisms. During the second step, wort is produced during hydrolysis and extraction of the malt. The wort is filled with enzymes, sugars and starches. Hops can be added during this stage to provide bitterness and conservational properties. After this step, the mixture is filtrated to remove the husk of the barley: brewer's spent grain. A third phase is the actual fermentation of the wort into beer, using yeast. During this phase, sugars are converted into ethanol. The last phase consists of all down-stream processing (filtration, stabilization, bottling) [16].

It is mostly the fermentation process that determines the flavour of the beer. There is also a small influence from the grain and hops. The malted grain can be roasted, providing less simple sugars. This results in more toasted and caramel flavours in the final beer. Hops contribute to the bitterness of the beer, but are also a surfactant, stabilising bubbles by increasing surface tension. Yeast is the product that provides the most flavours. Yeasts are categorised into 3 types: ale, lager and wild yeasts. Ale yeasts ferment at the top of the wort and are able to ferment at higher temperatures, producing more esters. Lager yeasts ferment at the bottom, at lower temperatures and produce a simpler, crisp taste. Wild yeasts produce more unusual compounds and an acquired, acidic taste. The taste of beer is mostly determined by: the carbon chain length of the alcohol, the amount of alcohol, amount and type of esters and residual sulphur compounds [17].
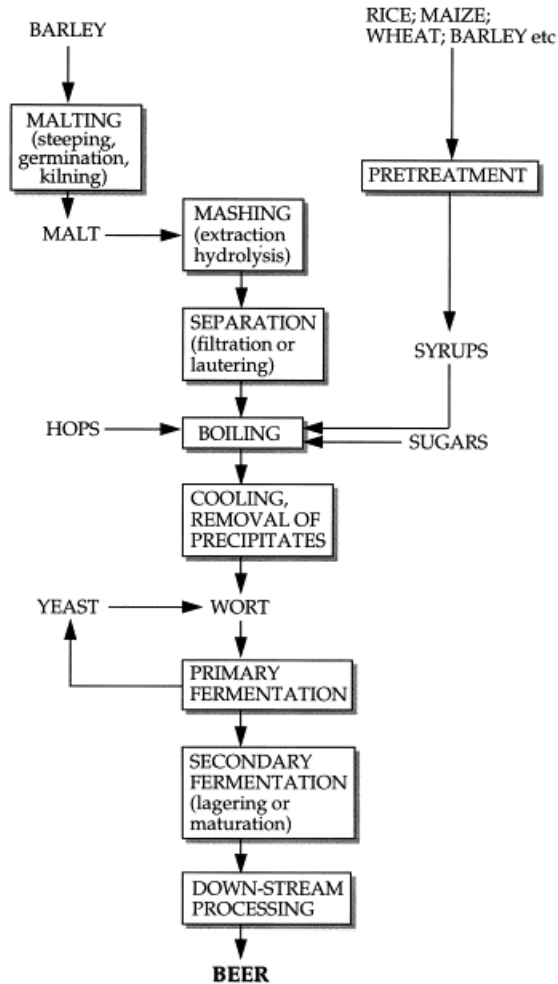
Figure 1-5 The general brewing process. From [12].

1.2.2 Brewer's spent grain

When the malted barley is converted to wort, starches are converted to fermentable and non-fermentable sugars. A part of the protein will also convert to amino acids and peptides. The external husk and the pericarp and seed coat (see Figure 1-6) do not convert and remain in the filter when the sweet wort is extracted. This mixture is brewer's spent grain (BSG) and contains the fibrous remains of the barley. Depending on the brewing conditions and type of beer, some sugars or other grains (maize, rice, wheat) may be present in this BSG. The starch content is assumed to be negligible [18].

18
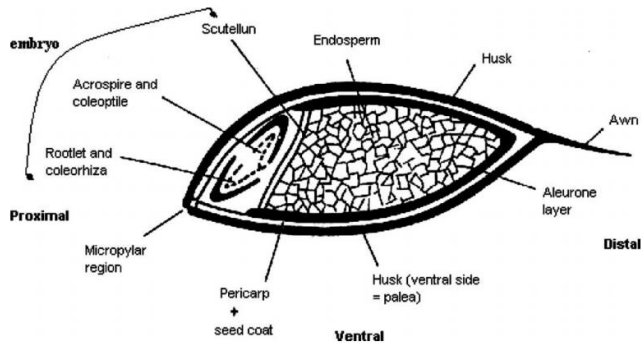
Figure 1-6 A longitudinal representation of a barney kernel. From [14]

The exact chemical composition of the BSG depends on many factors: barley variety, harvest time, malting and mashing conditions, and the type and quality of added products during the brewing process. At the source, BSG has a typical moisture content (MC) of about 70-85%. In general, BSG is a lignocellulosic biomass with roughly 20% of protein and 70-80% of fibre in its composition (on a dry basis). This fibre consists of approximately 48% of hemicellulose, 11% lignin and 20% of cellulose. Furthermore, there are also some lipids and ash present in the BSG. The fibrous material consists mainly of arabinoxylan, lignin and cellulose [18-20]. Micro-constituents are several vitamins and mineral elements such as calcium, cobalt, copper, iron, magnesium, manganese, phosphorus, potassium, sodium and sulphur, all in concentrations lower than 0.5% [21].

The high moisture content and carbon-rich composition make BSG very prone to microbiological degradation, certainly in warmer climates. To avoid growth of mould and general spoilage, a drying process can be used, or the BSG should be used in the proximity of the producing plant [20, 22]. BSG is most often sold to farmers as animal feed for ruminants that can cope with the high fibre content. The latter is hard to digest and promotes methane production, strongly contributing to the greenhouse effect. From the economic point of view, the readily available, locally sourced BSG can compete in the market with the imported soy. Research is currently focussing on fractionating the BSG to wider application in animal nutrition [20, 23]. Apart from use as animal feed, BSG can also be used for other food and biotechnological applications. The simplest solution is to use BSG as an energy source by combustion or bioethanol production. It is also

possible to produce biogas using anaerobic digestion. For combustion, BSG has a rather high moisture content and biomass boilers are needed to efficiently regain a fraction of the energy. Bioethanol production is based on the fermentation of the remaining cellulose and hemicellulose in the BSG and it is theoretically possible to produce 150 L of fuel ethanol from 1000 kg BSG. Anaerobic digestion uses microorganisms to generate biogas and is mostly applied to a mixture of BSG with spent yeasts, hops and water [20, 24]. Further novel applications include the use as a food ingredient [25-27], as a growth medium for mushrooms or specialty chemicals [19, 28], as a sawdust substitute in brick-making, as a soil conditioner and as adsorbent for heavy metals [29]. It can also be converted into activated carbon (AC) after pyrolysis and activation [30, 31]. A techno-economic evaluation has shown that this process is economically viable [32].

When comparing these technologies to the waste hierarchy as proposed by the EU, care should be taken to also include the visions of the food waste prevention programme [33]. For some categories of food waste, priority should be given to use foodstuffs as animal feed over composting, creation of energy and landfill. However, this priority is strongly dependent on the characteristics of the foodstuffs and should consider as well economic circumstances as health and quality standards. For BSG, the high moisture content can lead to microbial activity that is not in line with the feed safety and animal health standards and other options can result in economically and environmentally better applications.

The amount of BSG produced during the brewing accounts for 85% of the by-products of the process. For every 100 L of beer, approximately 14-20 kg of (wet) BSG is produced [18, 34]. Brewers of Europe [35] estimate the beer production in 2014 in Europe (total EU 28) to be approximately 38 454x10^6 L, of which Belgium produced roughly 1 820 10^6 L. Eurostat [31] reports 37 463x10^6 L for the EU 27 and 2 000.2x10^6 L for Belgium in 2015. The Food and Agriculture Organization of the United Nation (FAO) [37] estimated the production in 2014 at 180 332.5x10^6 kg beer, and at 1 800x10^6 kg for Belgium. An approximate calculation (15 kg of BSG per 100 L of beer) provides a rough estimate of the BSG production of 270 000 tons of BSG for Belgium, 5,6 Mtons for Europe and 27 Mtons worldwide.

1.3 Thermo-chemical conversion - pyrolysis

Conversion of biomass into value added chemicals or fuel can be divided into two categories: bio-chemical conversion and thermo-chemical conversion. Bio-chemical conversion includes fermentation, anaerobic digestion, mechanical extraction among other methods. These will not be discussed here. Thermo-chemical conversion uses heat to convert the biomass into energy or new materials and include pyrolysis, combustion, gasification and torrefaction. Only pyrolysis will be discussed in depth here [38].

1.3.1 Major principles of pyrolysis

Pyrolysis is a thermal conversion method that cracks organic molecules at high temperatures in an oxygen-deficient atmosphere. The organic constituents of the biomass break down into smaller parts and form three fractions: condensable gases (bio-oil), non-condensable gases (pyrolytic gas) and a solid fraction ((bio-)char). This is displayed schematically in Figure 1-7. Pyrolysis happens in a series of degradation reactions such as depolymerisation, hydrolysis, oxidation, dehydration and decarboxylation. The used material, particle size, heating rate, pyrolysis temperature and reaction atmosphere mostly determine the amount and characteristics of the products [38-40].
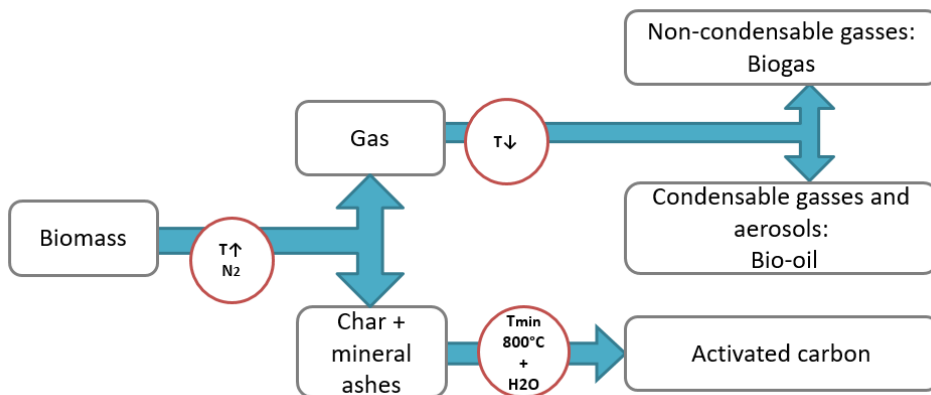
Figure 1-7 A schematic representation of the pyrolysis process

The ideal precursor for pyrolysis has a high organic carbon and low inorganic content. Most lignocellulosic material (biomass) is subsequently fit for pyrolysis after drying. [41] Cellulose and hemicellulose are relatively easy broken down into volatile matter, contributing mostly to the bio-oil and gas yield. Cellulose decomposes in a narrow temperature range (300-430°C) and results in a low char yield. Hemicellulose is thermally the most unstable and already decomposes at lower temperatures (from 250 °C), but has a somewhat higher (approx. 30%) char yield. Lignin is harder to fragment, resulting in a wider decomposition temperature range (400-700 °C). The char yield is the highest from lignin, about 40-50% [12, 42-44].

The effect of pyrolysis temperature seems to be clear from the last paragraph. At low temperatures (<300 C - torrefaction), mostly hemicellulose decomposes, resulting in a tarry bio-oil. At higher temperatures (<500 °C), the cellulose also decomposes into bio-oil and gas. At temperatures higher than 500 °C, the biomass is massively fragmented and this results in possible secondary decomposition of the pyrolysis gases. The most important product will be the bio-char.

However, it is not only the pyrolysis temperature that determines the characteristics and amount of product. A most important parameter is the heating rate. In fast pyrolysis, heating rates are higher, causing quick fragmentation of the biomass constituents and enhancing the yield of volatiles, resulting in high yields of gas and bio-oil. The bio-oil is also quite tarry: there is only a short time available for secondary reactions that could crack and repolymerise the tar. There is a maximum heating rate for each biomass, mostly determined by the mass and heat transfer limitations. This can be influenced by adjusting particle size and reactor set-up [42, 43, 45].

1.3.2 Pyrolysis products and applications

1.3.2.1 Pyrolytic gas

Pyrolytic gas consists of the smallest molecules released during pyrolysis. It consists mainly of carbon dioxide and carbon monoxide (CO_2 and CO), hydrogen gas (H_2) and low-carbon number hydrocarbons such as methane, ethane and ethylene (CH_4, C_2H_6, C_2H_4). Furthermore, small traces of other gases might be

present: propane (C_3H_8), ammonia (NH_3), nitrogen oxides (NO_x), sulphur oxides (SO_x) and some low-carbon alcohols. Carbon oxides originate from the decomposition of carbonyl (C=O) and carboxyl (COOH) groups. The light hydrocarbons (methane) are produced during the decomposition of weakly bonded methoxyl (-O-CH_3) and methylene (-CH_2-) groups and during the secondary decomposition of oxygenated compounds. Hydrogen gas originates from decomposing and reforming at high temperatures. Up to 40% higher hydrogen gas yields can be obtained when using wet instead of dry biomass. The lower heating value (LHV) of pyrolytic gas is in the range of 5.5 – 7.0 MJ/m³, compared to approximately 37 MJ/m³ for natural gas [43, 46, 47].

Pyrolytic gas and uncondensed bio-oil are mostly used to power the pyrolysis reactor on site. Both fuels would need to be upgraded by separation techniques, improving their poor thermal stability and tackling their corrosivity.

1.3.2.2 Bio-oil

Bio-oil is a complex mixture of several organic and inorganic species. Organic molecules present can be acids, esters, alcohols, ketones, aldehydes, phenols, alkenes, nitrogen compounds, furans, sugars and other miscellaneous oxygenates. Inorganic species are either associated with counter ions, connected to organic acids or related to enzymatic compounds [43]. A comparison between bio-oil and fossil fuel diesel is made according to [39, 46, 48].

The *water content* in bio-oil originates from the biomass feed and from chemical reactions in the oil itself. Depending on the biomass feedstock, this water content can be as high as 30%, reducing the heating value drastically. The benefits of a higher water content are a decrease in viscosity and increase in fluidity, a lower flame temperature and consequently, lower NO_x emissions. The high water content makes bio-oil unfavourable for use in engines because it lowers local temperature, vaporisation rates and negatively influences ignition. Water in bio-oil is typically homogeneously dissolved and drying is not sufficient.

As mentioned, *viscosity* of bio-oil is quite high compared to fossil fuel (kinematic viscosity up to 400 mm²/s, compared to diesel: up to 5 mm²/s according to EN590). The design of the injection system and fuel supply to an engine gravely depends on the expected viscosity of the fuel, so fuels are not easily

interchangeable. The viscosity can be reduced by addition of alcohols or pre-heating. Aging of the bio-oil can cause polymerisation and condensation reactions, leading to a higher viscosity. The *density* of bio-oil is typically higher than that of water and fossil diesel fuel, in the range of 1.15-1.25 kg/m³.

The *acidity* of bio-oil is also problematic for engine use. As mentioned before, bio-oil contains many carboxylic acids, such as formic and acetic acid. The pH of bio-oil is typically in the range of 2-4. The acidity causes corrosion and materials need to be selected for acid resistance. Furthermore, the *solid content* of bio-oil causes erosion and coking in engine injectors. Small char particles and *ashes* also cause higher particulate matter (PM) emissions. Finally, ash can cause further corrosion and kicking problems in the engine.

The *calorific value* of bio-oil depends strongly on its chemical composition and density. The presence of oxygen and other compounds in bio-oil decreases the LHV of bio-oil to about 40-50% of that of diesel. The *carbon content* of bio-oil is around 40-60% compared to fossil diesel fuel, and the *oxygen content* can be as high as 35-50%.

1.3.2.3 Char

Char, biochar or charcoal, is the solid product of pyrolysis. It contains unconverted organic solids, carbonaceous residues from the biomass thermal decomposition and a mineral fraction. The physical, chemical and mechanical properties are highly dependent on pyrolysis parameters and biomass feedstock. As discussed before, slow pyrolysis results in a higher amount of char compared to fast pyrolysis [43].

There are many applications for which char can be used. It can be used as a substitute for fossil coal if the char has a sufficiently high LHV. This is strongly dependent on the used biomass and used pyrolysis parameters. Biochar can also be applied as a soil amendment to enhance water/nutrient retention and improve soil structure. It can contain a broad range of macronutrients (N, P, K, Ca, Mg, S) and micronutrients (Na, Mn, Cu, Fe, Zn), leading to a valuable fertilizer. Adding char to soil also contributes to carbon sequestration. There are however no conclusive long-term results known for the application of biochar in soils. Most literature reports agronomic benefits [50], but there are also contradictory results

showing negative results or no result at all. Furthermore, the economics of biochar production and trade are often marginally viable and strongly bound to the expected duration of agronomic benefits [43, 49, 50].

Another possibility is activation of the char into activated carbon (AC). Biomass typically has a higher amount of volatile matter compared to coal, creating a more porous char. The fixed carbon has a graphitic-like structure but is not graphitisable, which is ideal for AC production, since the structure is more randomized. Activation will enhance the porosity until a sufficient surface area is achieved, simultaneously creating specific organic surface functional groups [41].

1.4 Production of activated carbons using thermal activation

(after [51] and [52])

Char can be converted into AC via activation. This activation will develop the available pore structure and surface functionalities chemically or thermally. Chemical activation can be performed during co-pyrolysis with an impregnated precursor or in a stepwise manner. Only thermal activation will be discussed in more detail here.

Although a char exhibits some porosity, further "extraction" of carbon molecules is needed to enhance its surface area. Two gasifying agents are suitable for this application: water vapour (steam) and carbon dioxide, removing carbon from the char following reactions 1-2 and 1-3 at high temperatures:

$$C + CO_2 \rightarrow 2CO \qquad\qquad \Delta H = +159 \; kJ \; mol^{-1} \qquad\qquad \text{Equation 1-2}$$

$$C + H_2O \rightarrow CO + H_2 \qquad\qquad \Delta H = +117 \; kJ \; mol^{-1} \qquad\qquad \text{Equation 1-3}$$
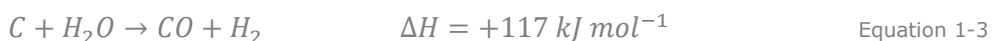
Both reactions are endothermic and play a role in steam activation. For carbon dioxide activation, only reaction 1-2 is important. Even though only water is present during steam activation, CO_2 is also produced during a water gas shift reaction (see Eq. 1-4). This reaction is catalysed by the char surface and uses the CO produced in reaction 1-3. This reaction is also exothermic but has low kinetics and occurs significantly less often than reaction 1-3 itself. The produced H_2 gas is also able to react with the carbon surface to produce methane gas according to reaction 1-5.

$$CO + H_2O \leftrightarrow CO_2 + H_2 \qquad\qquad \Delta H = -41 \; kJ \; mol^{-1} \qquad\qquad \text{Equation 1-4}$$

$$C + 2H_2 \leftrightarrow CH_4 \qquad\qquad \Delta H = -88 \; kJ \; mol^{-1} \qquad\qquad \text{Equation 1-5}$$

The results of the activation with steam or carbon dioxide are not the same. During the activation process surface complexes are formed with oxygen and, in case of steam, hydrogen.

$$C + CO_2 \rightarrow CO + C(O)$$

$$2C + H_2 \rightarrow 2C(H)$$
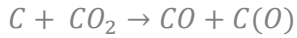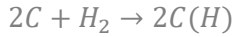
Where C(O) is a surface oxygen complex, C(H) is chemisorbed hydrogen on the surface and reaction (1-7) takes place after reaction (1-3).

The surface oxygen complexes exhibit a broad range of chemical stabilities and their exact chemistry is a function of temperature and thermal treatment. Both C(O) and C(H) complexes inhibit further reaction at that site. C(H) complexes are more stable than C(O) complexes, resulting in a stronger inhibition when steam is used. The inhibition effect is useful for reaction control in industrial environment, preventing the burning of the carbon by oxygen present. Activation with steam is thus more easily controlled, even up to temperatures of 1000 °C.

1.5 Properties of activated carbons

The most characteristic property of an AC is its porous structure. This gives rise to a high surface area. Furthermore, this surface has functional groups and heteroatoms that make it possible to bind chemicals. The characteristics that make AC such a good adsorbent will be discussed here, as well as the adsorption mechanisms that take place.

1.5.1 Porous structure

The main physical property of an AC is its porous structure. It drastically increases the surface area on which adsorption can take place. The pores can be categorized according to IUPAC recommendations: micropores (< 2 nm), mesopores (2-50 nm) and macropores (> 50 nm), as seen in Figure 1-8. The pore size distribution is an important factor to determine which applications the AC is best suited for [41, 52, 53].
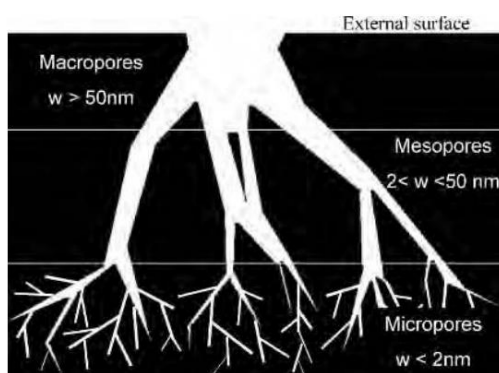
Figure 1-8 Schematic representation of AC pore network

The structure of an AC can be imagined as stacks of randomly distributed and crosslinked poorly developed aromatic sheets (graphene sheets). These sheets are separated by disorganised organic and inorganic matter from the raw material. This alignment is associated with voids between the sheets. The channels through graphitic regions and interstices between the crystallites make up the porous structures with a large surface area [41, 52, 54].

ACs have relatively high surface areas, mainly due to the contribution of the microporous network. Up to 95% of the surface area of an AC can correspond to micropores. However, meso- and macropores should not be disregarded in any adsorption process. Although the associated surface area might be quite low, most ACs have a well-developed mesoporosity. These mesopores serve as channels through which the adsorbate reaches the micropores. In the mesopores, capillary condensation might take place with the formation of a meniscus in the adsorbate. Depending on the size of the adsorbate molecules, molecular sieve effects may occur. This is mostly the case for some large size organic molecules when the pore width is narrower than the molecules of the adsorbate. This prevents the adsorbate of reaching the micropores which therefore become inaccessible. The specific surface area of an AC is not necessarily proportional to the adsorption capacity of the AC: the pore size distribution should also be taken in account. In general, adsorption of gases and vapours are performed on highly porous ACs, while an AC with well-developed meso- and macroporosity is better suited for adsorption of solutes from solutions [52].

1.5.2 Surface functionalities

Carbon atoms located at the edges of the graphene sheets are unsaturated carbon atoms with unpaired electrons. This gives rise to surface groups through bonds with heteroatoms. The surfaces with functional groups only represent a small fraction of the total surface area and even small variations in the surface chemistry can produce dramatic changes in the adsorption properties of an AC. Their presence can influence adsorption properties in two significant ways: modification of the hydrophobic/hydrophilic nature of the AC and the acidic/basic character. Oxygen- and nitrogen-containing functionalities are shortly discussed in this chapter. Furthermore, there are also hydrogen-carbon complexes and other heteroatoms that can be present in the AC, such as sulphur or phosphorous.
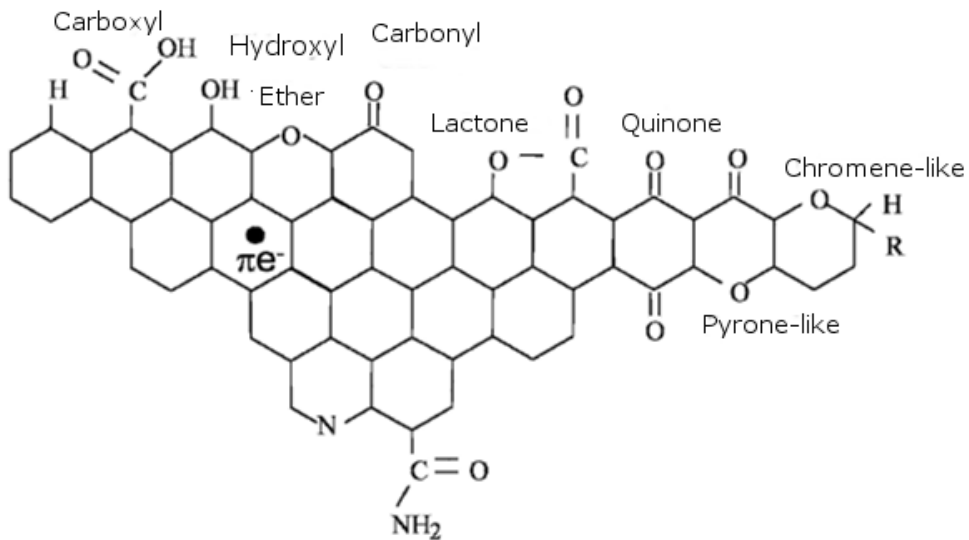
Figure 1-9 A summary of the most important surface functionalities on an AC surface [52]

The overall acidic/basic character of an AC is determined by the concentration and the acidic strength of the surface groups. This influences the point of zero charge (pH_{PZC}) of the AC. The point of zero charge is the pH of the medium where the total charge on the AC equals zero. If the pH > pH_{PZC}, more acidic surface groups will dissociate and leave a negatively charged AC surface. If the pH < pH_{PZC}, basic surface groups will combine with protons in the medium and create a positively charged surface area. The surface groups also influence the AC's isoelectric point (IEP), which is a representative of the charges of the external surface of AC in solution instead of the total surface charge. Typically, the pH_{IEP} of an activated carbon is smaller than the pH_{PZC}, suggesting that the external surface is more negatively charged than the internal surface [55]. The charge of the AC can be important for adsorption of ionic species by electrostatic forces [52, 56].

1.5.2.1 Oxygen-containing surface groups

The relatively large 'edge' areas of the graphene sheets have a strong tendency for oxygen chemisorption, making oxygen-containing surface groups the most common on AC. Oxidation of the AC by molecular oxygen already occurs at room temperature, but is enhanced with increasing temperature. Oxidised surface groups can also be formed by reaction with other oxidising gases (ozone, carbon

dioxide, nitrous oxide…) or solutions (hydrogen peroxide, nitric acid,…). The surface functionalities of an AC can be tailored by controlled oxidation with several chemicals to create oxygen functionalities. It has been proven that nitric acid only alters the surface chemistry of an AC and does not change its porosity. To deplete an AC of its oxygen functionalities, heat treatment can be applied. The most important types of oxygen groups on AC are displayed in Figure 1-9 [52, 54, 57].

Normally, an AC is hydrophobic, but the presence of polar oxygen-containing surface groups increases the hydrophilicity of the AC. These surface groups can form hydrogen bonds between water molecules and the surface. This property increases the wetting of the surface when the AC is used for treatment of liquids, but can be detrimental for gas adsorption: moisture adsorption may cause blockages to a part of the micropores [52].

Carboxyl, hydroxyl and lactone groups behave as acidic groups on the amphoteric surface of an AC when the pH of the medium is higher than the individual pK_a of the surface group. Pyrone-like and chromene-like surface groups are basic functionalities. The influence of surface functionalities is dependent on two factors and difficult to predict. The first factor is the relative concentration of the surface groups; the second factor is their relative acidic strength on the carbon surface (pK_a). [53]

1.5.2.2 Nitrogen-containing surface groups

In contrast to oxygen groups, the amount of nitrogen in an AC is limited: there is little to no spontaneous reaction with nitrogen when an AC has air contact. To create an AC with high concentration of nitrogen, this nitrogen should already be present in the precursor. A lot of research has also been performed recently using nitrogen-containing reagents such as ammonia or melamine [54].

The chemistry of the AC surface is also determined by the nitrogen-containing functionalities, as discussed for the oxygen functionalities. Their amount and acidic or basic strength are important to estimate its effect. The overall amount of nitrogen is mostly much lower than the oxygen content and its impact is less pronounced compared to oxygen functionalities. Treatment with nitrogen-containing reagents at low temperature gives rise to slightly acidic functionalities: lactams, imides and amines. Using nitrogen-containing reagents at high

temperature increases the amount of quaternary N (incorporated in the graphitic rings), pyridine and pyrrole-type structures. Both pyridine and pyrroles exhibit basic properties, and all these structures increase the surface polarity of an AC [54].

Literature studies suggest that nitrogen-containing surface groups have a major influence on adsorption. Treatment with nitrogen-containing chemicals (urea, ammonia, …) has proven to increase the adsorption capacity for phenol, in a similar way as using nitrogen-rich precursors. [32, 56, 58, 59]

1.5.3 Granulometry

(according to [60])

AC can be produced in many forms and shapes. Each form has their own merits and disadvantages. AC can be milled and sieved to different sizes, giving rise to Granular AC (GAC) and Powdered AC (PAC). When extruded with or without binder, the extruded AC can be produced in very specific shapes.

1.5.3.1 Granular Activated Carbon (GAC)

GAC has particles with irregular shapes, ranging in size from 0.2 to 5 mm. Figure 1-10 displays some irregularly shaped GAC. During production, blocks of (coagulated) carbon are activated in a kiln and milled and sieved to the requisite particle size afterwards. There are a lot of handling benefits to GAC: they are harder and longer lasting than PAC, clean to handle, can be regenerated many times and have a reasonable adsorption capacity. They can be used for both liquid and gas phase applications, in both fixed and rotating systems.

For application in liquid phases, GAC is mostly packed in columns or towers through which the solution flows. They are used in a continuous flow when there is a single product to be produced or refined in large quantities. Batch adsorption is also possible, where the GAC is sieved off of the purified solution after the adsorption reaches equilibrium. For gas phase applications, GAC has the benefit of a lower pressure drop in a filter due to a sufficient flow between the particles.

1.5.3.2 Powdered Activated Carbon (PAC)

Different particle size distributions (PSD) are commercially available for PAC, but most PAC have a PSD ranging from 5 to 150µm. Their powdery structure can be seen in Figure 1-11. They are generally cheaper to process and have great flexibility in operation. The dosage of PAC can be altered easily according to changing process parameters. They are mostly used for liquid-phase applications in a batch process, where they are mixed with the solution that is to be treated. Afterwards, the PAC is removed by sedimentation or filtration. Recycling the powder is associated with technical problems and spent PAC is often not regenerated but incinerated or placed in landfills.

1.5.3.3 Extruded carbon

Extruded carbons can take various shapes, depending on the shape of the extrusion mold. Binders can be used prior to or after activation of the carbon. Most extruded carbons are cylindrical pellets with ranging diameters, assuring a low pressure drop. This makes the extruded AC perfect for gas-phase applications like solvent recovery, gas purification or emission control, as the gas can move easily between the particles. The specific shape of the AC can also make them physically strong for heavy duty operations. Different shapes are also possible: there are even spherical AC beads that are perfect for flowing applications, as can be seen in Figure 1-12.

Figure 1-10 Irregularly shaped GAC

Figure 1-11 A powdered AC

Figure 1-12 Extruded and spherical AC

1.5.4 Activated carbon market

AC is a product that is used for many applications, mainly in AC filters which are present in a multitude of companies in different sectors. It is used to purify drinking water, waste water, chemicals, pharmaceuticals, flue gasses…). As legislation becomes stricter to protect the environment, more AC is used and a global market growth rate (Compound Average Growth Rate, CAGR) of 8-10% is expected: from 1.45 Mton in 2013 to 2.88 Mton in 2023 worldwide [61]. The European CAGR is estimated at 6-7% for that same period, with a demand that increases from 351 700 tons in 2013 to 660 000 ton in 2023. Furthermore, prices of AC are expected to increase worldwide by 2.5% annually: from approximately €2000 per ton in 2013 to €2570 per ton in 2023 [61]. Of the global consumption of AC 35% is used for water treatment, 45% for air and gas purification, 8% for chemical and pharmaceutical processing and the rest for a variety of applications [62].

From the AC that is currently available on the market, approximately 52% is produced using bituminous coal, 23% is based on wood, 18% on coconut shell, 5% on lignite coal and other sources like pits and nutshells constitute approximately 2.5% of production [61]. Biomass-based ACs are considered as a threat to the wood-based AC since the cost for the raw materials is relatively low and stable and the ACs are qualitatively comparable [63]. The wood-based AC market has an estimated CAGR of 8.2% in volume and 9.4% in revenue between 2015 and 2024 [63]. Average global prices of wood based AC are estimated at US $1700/ton (2017) and are expected to rise up to US $1800/ton in 2024. Wood-based AC is mostly used in gas adsorption (21.3%), recycling of organic solvents (22.7%) and removal of dyes (25.7%) [63].

1.6 Adsorption

Adsorption is defined as a phenomenon of mass transfer and interactions between a molecule present in a liquid or gaseous phase and a solid surface. These molecules or atoms (adsorbates) are fixed (adsorbed) on the AC surface (adsorbent), often by physical interactions (electrostatic and dispersive forces, physisorption) and/or chemical bonds (chemisorption). A relatively large specific surface area is one of the most important properties, as discussed before [52, 64]

The general mass balance approach assumes neither biological nor chemical reaction between a molecule in a solution and an AC surface. There is only a mass transfer from the liquid to the solid phase, the mass balance can be written:

$$m(q_t - q_0) = V(C_0 - C_t)$$

Equation 1-8

With:

m = the mass of adsorbent (g)

q_t = the concentration of the solute on the surface at a time t (mg g^{-1})

q_0 = the initial concentration of the solute on the surface, for a virgin AC q_0 = 0 (mg g^{-1})

V = the volume of the solution (L)

C_0 = initial concentration of the adsorbate in the solution (mg L^{-1})

C_t = concentration of the adsorbate in the solution at time t (mg L^{-1})

The reactions of an adsorbate molecule with the surface of an adsorbent can mostly be attributed to two interactions: physisorption and chemisorption.

Physisorption includes all non-specific interactions, such as dispersion forces (Van der Waals) and short range (Pauli) repulsion. The combination of these two forces may produce a minimum in the potential energy. This can be visualised by the Lennard-Jones potential as in Figure 1-13. The interaction energy (E) is displayed on the y axis, the x axis shows the distance between the particles in Å. R_m is the distance at which the potential reaches its lowest value, corresponding to a depth of the potential well of ε. The finite distance at which the potential is equal to zero is displayed as σ. Apart from this interaction, there are some specific physical interactions that involve electrostatic forces between ions, dipoles and

quadrupoles. Electrostatic interactions are strongly dependent on the radii of the atoms involved and the magnitude of charge [65].
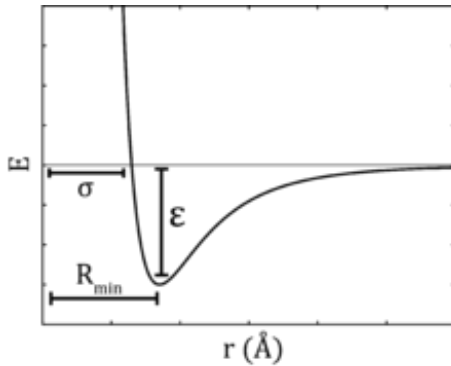
Figure 1-13 Lennard-Jones potential [66]

Chemisorption includes all adsorption processes that form a chemical bond between the adsorbate and the adsorbent. The elementary step in chemisorption involves an activation energy and certain molecules will only occupy specific adsorption sites, forming only a monolayer. Chemisorption can be followed by physisorption [65].

Adsorption systems are described using two important parameters. The first one describes the amount of adsorbate adsorbed at equilibrium as a function of end concentration or pressure at a fixed temperature and is called the adsorption isotherm. The second parameter are associated with the adsorption kinetics that describe the rate at which adsorption takes place.

1.6.1 Adsorption isotherms

(according to [67])

Adsorption isotherms describe the behaviour of adsorption of an adsorbate (gaseous or liquid) on the surface of an adsorbent. It expresses the change of adsorbed amount (adsorption capacity at equilibrium q_m in mg/g) as a function of the change in pressure or concentration of the adsorbate at a constant temperature. IUPAC defined 6 'main types' of adsorption isotherms for the physisorption of gases, these are displayed in Figure 1-14. Three adsorption isotherm equations are discussed.
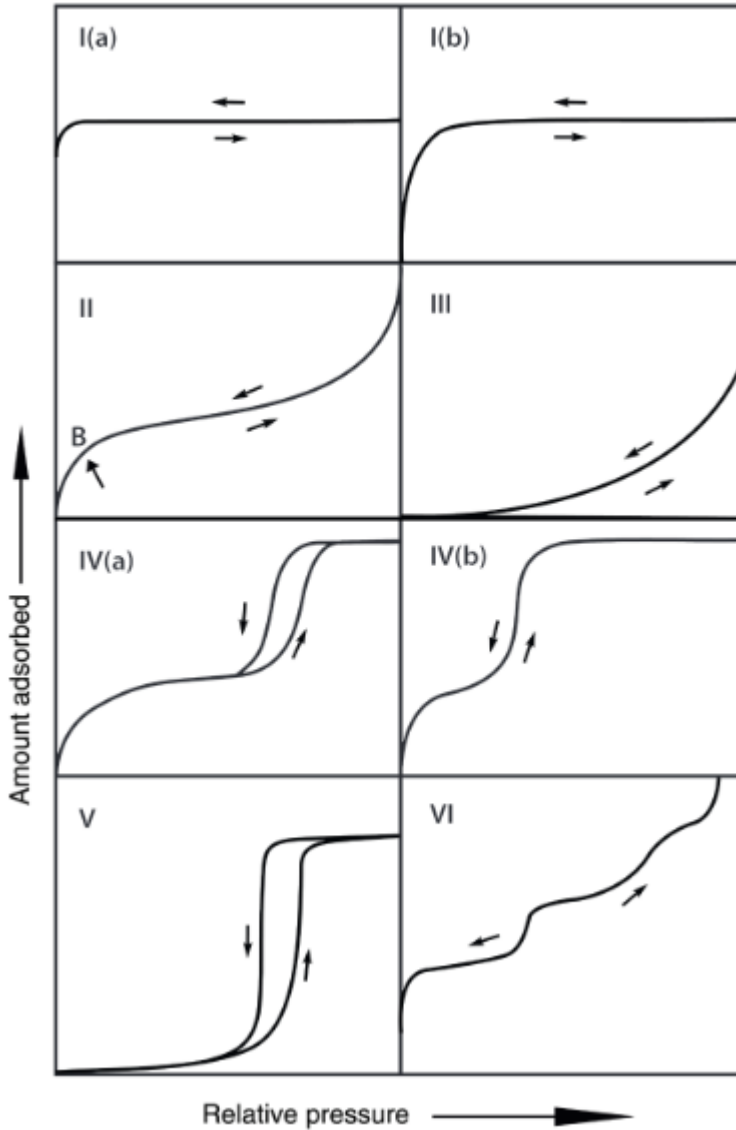
Figure 1-14 The six isotherm types, as defined by IUPAC [66]

The type I adsorption isotherm describes monolayer adsorption and can easily be explained by the Langmuir equation. At a certain pressure, the monolayer is saturated and the adsorbed amount stabilises. This is the typical isotherm found for microporous adsorbents. Types II and III describe adsorption on macroporous adsorbents with either strong or weak adsorbate-adsorbent interactions. The type

II isotherm is much like the type I isotherm, but adsorption is not limited to a monolayer and at a certain pressure molecules start a condensation-like stacking in the micro- and mesopores upon the monolayer. The type III isotherm indicates no monolayer formation and deviates largely from the Langmuir model. Adsorption happens instantly in a multilayer system, indicating there is no real adsorption at the surface of the adsorbent, but adsorbates are adsorbing to already adsorbed adsorbates.

Type IV and V describe adsorption isotherms with hysteresis, typical for mesoporous adsorbents. The adsorption and desorption isotherm exhibit different shapes. This effect is attributed to different effects in a randomly organised adsorbent, such as slit-shaped or inkbottle pores. Isotherm IV displays distinct monolayer formation, isotherm type V doesn't. Type VI isotherms exhibit a step-wise adsorption profile.

The **Langmuir equation** describes an adsorbate/adsorbens system where adsorption is limited to a monolayer on the surface of the adsorbens. It best describes a system of chemisorption but is often successfully applied to other systems as well. It can be adjusted to describe different adsorption mechanisms.

The Langmuir isotherm is based on a dynamic equilibrium between the adsorbed and unadsorbed phase of a molecule in gaseous phase. The rate at which the adsorbate molecules come into contact with the surface is considered proportional to the partial pressure p of the gas and the fraction of the surface that is not covered by the adsorbate $(1-\theta)$. This surface is still available for adsorption. At the same time, desorption also happens. Langmuir poses that the rate of desorption is proportional to the amount of surface that was already covered: θ. At equilibrium, the rate of adsorption is considered equal to the desorption rate:

$$k_a p \left(1 - \theta\right) = k_d \theta \hspace{4cm} \text{Equation 1-9}$$

In equation 1.9 k_a represents the kinetic adsorption constant and k_d represent the kinetic desorption constant. A more practical representation of the equation can be seen in Eq 1.10.

$$\theta = \frac{q}{q_m} = \frac{bp}{(1+bp)}$$

Where k_a/k_d equals b and q_m equals the amount of adsorbate in a monolayer. q/q_m can be expressed in several ways. The easiest expression is the ratio of the amount of moles of adsorbate adsorbed to the number of moles of that adsorbate that could be adsorbed in one layer. Other possibilities use a volume of gas adsorbed or on a weight basis. To obtain the Langmuir isotherm, a few assumptions have to be made:

- Adsorption heat Q is constant and independent of the coverage fraction θ
- Every adsorbate molecule occupies one specific site on the surface
- Adsorption is localized: the adsorbed molecules stay on the same site until desorption

In practice, the adsorption heat does not remain constant during adsorption, but it decreases. The **Freundlich equation** (Eq 1.11) assumes a logarithmic decrease in Q. This implies that the adsorption sites exhibit an exponential adsorption energy distribution, different for each functional group.

$$\theta = kp^{1/n}$$

Where θ is the coverage fraction, p is the equilibrium pressure of the adsorbate and both k and n (n>1) are constants for a specific adsorbate/adsorbent system at a particular temperature. This isotherm shows a similar behavior as the Langmuir equation for average coverage ($0 < \theta < 1$), but there is no limit to a monolayer adsorption ($\theta = 1$). The Freundlich equation has been proven most useful for description of adsorption of organic molecules on AC.

A third equation is the **Brunauer–Emmett–Teller (BET) equation**. It is mostly used to determine specific surface area by calculation of the adsorption of N_2 at 77 K. BET theory assumes a monolayer is adsorbed on surface sites of uniform adsorption energy and multilayers build up via a process analogous to the condensation of the liquid adsorbate (N_2). It assumes that there are no specific interactions between individual molecules. Generally expressed as [69]:

$$\frac{\frac{p}{p_0}}{n(1-\frac{p}{p_0})} = \frac{1}{n_m C} + \frac{C-1}{n_m C}\frac{p}{p_0}$$

Where p and p_0 are the equilibrium and saturation pressure of adsorbates at the adsorption temperature, n is the adsorbed amount of adsorbate, n_m is the monolayer adsorbed gas quantity, and C is the BET constant, defined as:

$$C = \exp(\frac{Q_1 - Q_L}{RT})$$

Where Q_1 is the adsorption heat for the first adsorbed layer and Q_L is the liquefaction heat, corresponding to the next layers. The BET equation requires a linear relationship between $(p/p_0)/(n(1-p/p_0))$ and p/p_0. From this relationship the monolayer capacity n_m (mmol/g) can be calculated. In AC the linearity is mostly restricted to p/p_0 range of 0.05-0.2.

The BET equation has some severe limitations when applied to microporous AC. Constrictions in the microporous network may cause molecular sieve effects and selectivity for the molecular shape. When N_2 at 77 K is used as adsorbate, there are diffusion effects possible: at this low temperature the kinetic energy may be insufficient to penetrate the available micropores. Therefore, adsorption of CO_2 at higher temperatures (273 K) is also used. As a result, CO_2 and N_2 isotherms are complementary. CO_2 is used for micropores up to 1 nm, N_2 for larger pores. The use of argon adsorption at 87K is considered to be more reliable and has been recommended by IUPAC since 2015 [66]. This method is particularly interesting for micropore size analysis. Despite limitations BET surface is the most commonly used parameter to characterize specific surface area of an AC.

The BET equation can be used for the description of most isotherms by making the right choices for C and q_m. However, a monolayer is required, so types III and V cannot be described using the BET equation. The type I Langmuir isotherm can also be described by the BET equation if p/p_0 is small.

All three of these models have initially been developed for the description of adsorption from the gaseous phase. Both Langmuir and Freundlich equations can also be used to describe adsorption from aqueous solutions.

1.6.2 Adsorption kinetics

Adsorption kinetics describe the rates at which an adsorbate is adsorbed to an AC surface. It is generally acknowledged that this rate is not primarily determined by the actual physical (or chemical) attachment of the adsorbate to the AC surface. On the contrary: the intraparticle transport within the porous structure to the available surface seems to be the limiting step. Sometimes the interparticle transport from the bulk fluid to the external surface of the AC might also limit adsorption rates. The overall rate of adsorption is mostly determined by the following transport resistances (according to [68]).

Interparticle transport describes the mass and heat transfer of the adsorbate to and from the exterior surface of the adsorbent. It is assumed that mass and heat flux are driven by a difference in concentration (mass transport) or temperature (heat transport) between the flowing solution and the AC surface. It is displayed in Figure 1-15 as a film surrounding a particle of AC. Intraparticle diffusion is the diffusion of the molecules in the porous network of a particle and is a parallel of three diffusion types. A first type is intracrystalline diffusion, describing the movement of individual particles in channels and cage-like structures such as zeolites. This type of diffusion is less important for the randomly organised AC. A second type is diffusion inside the porous structure. Diffusion in macropores is described by Maxwellian or bulk diffusion, based on the molecular collisions within the pore. If the free path of the molecules is much greater than the pore diameter, molecules start colliding with the pore walls. This process is described by Knudsen diffusion. The third type is surface diffusion for physisorbed molecules. Adsorbed molecules might not be permanently fixed on the surface but possess some ability to move over the surface to other vacant adsorption sites. This diffusion only happens when the adsorbate is already adsorbed and the attractive forces are not too strong to prevent this. Adsorbents with a high surface area and many narrow pores are more prone to have a strong surface diffusion. Lastly, the adsorption rate is also determined by the heat transfer during the exothermic adsorption process.
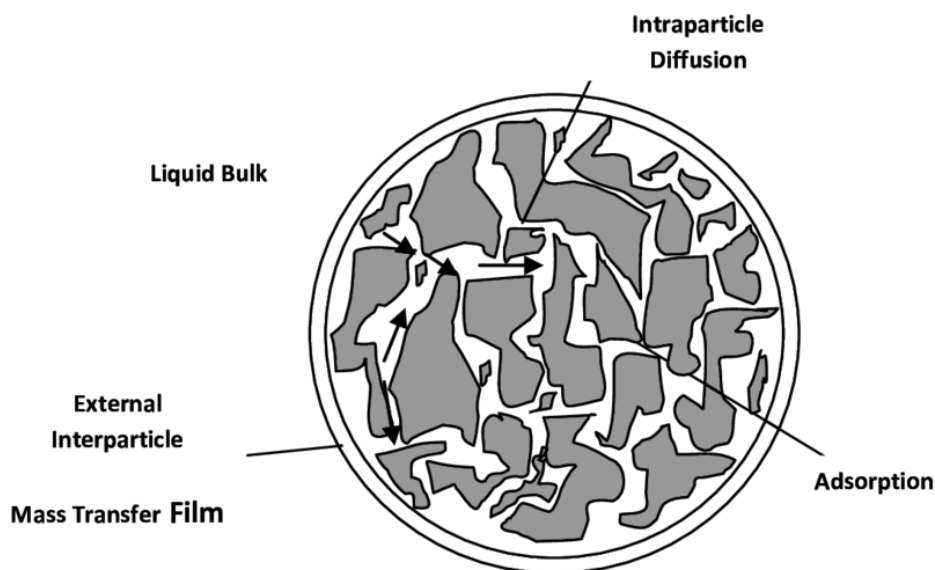
The kinetic results of experiments can be analysed by the intraparticle diffusion model as proposed by Weber and Morris [71] to determine the rate controlling step. This model is expressed as:

$$q_t = k_{id}\sqrt{t} + C_i$$

Equation 1-14

Were k_{id} (mg/g h$^{1/2}$) expresses the rate constant of intraparticle transport and C_i (mg/g) the intercept of a stage i, associated with the thickness of the boundary layer [55, 69]. When the plotted values form linear regions that pass through zero, intraparticle diffusion is the rate limiting step.

Evaluation of the adsorption kinetics are typically performed using both Lagergrens pseudo first order (PFO) model [72, 73] and the pseudo second order (PSO) model as proposed by Ho and McKay [74]. The PFO model generally suits adsorption systems that show physisorption, while the PSO model suits chemisorption processes, especially in the initial stages of adsorption.

The PFO model can be expressed as:

$$q_t = q_e(1 - e^{-k_1 t})$$ Equation 1-15

where q_t and q_e are the adsorption capacities (in mg / g AC) at time t and at time of equilibrium and k_1 (1/ min) is the PFO rate constant.

The PSO model can be expressed as:

$$q_t = \frac{k_2 q_e^2 t}{1 + k_2 q_e t}$$ Equation 1-16

Where q_t and q_e are the adsorption capacities (in mg/ g AC) at time t and at time of equilibrium and k_2 (1/min) the PSO rate constant. It is important to use a non-linear regression for the calculations of the kinetic parameters [73].

1.7 Research questions

A previous study described the chemical properties of AC produced from BSG, its adsorption properties and a techno-economic evaluation. The ACBSG production is shortly re-discussed in the relevant scientific manuscripts, focusing on the activation parameters used. The production process has also been described in detail in [31,32] by Dr. Ing. Kenny Vanreppelen. An important factor in that research was the applicability of the AC in industry.

The main focus in this dissertation is to improve the knowledge regarding this nitrogenised ACBSG. To prove and promote the technical applications of this research, the performance of lab-scale ACBSG is always compared to industrial ACs and the adsorption experiments are performed using 'realistic' concentrations and AC dosages simulating industrial waste water and treatment.

The main research objective is **to explore the potential of activated carbon from brewer's spent grain for the adsorption of ionic species, from a scientific and an industrial point of view.**

AC is mostly known for its ability to adsorb organic molecules. However, the AC from BSG has more nitrogen functionalities and more specific sites compared to AC in general. The potential to chemisorb other adsorbates, such as ionic species is intrinsically present because of these functionalities. In this dissertation, the following ionic species are selected: Cs, Cr(VI)/Cr(III) and a mixed solution of Cd, Co, U, V and Zn (heavy metal ions, HM).

This first chapter, the introduction, provided an in-depth description of biomass, conversion techniques, activated carbon and adsorption behavior. This introduction is considered as general knowledge for the remainder of the thesis: each of the specialized chapters (2, 3 and 4) have a topic-specific introduction. The AC produced from BSG is the core element in all three specialized chapters.

In order to tackle the main research objective, the work is divided into 3 sub-objectives. A conceptual summary of the research sub-objectives is displayed in Figure 1-16. The colours of the blocks correspond to the chapters in which this information can be found. Orange refers to chapter 2, green to chapter 3 and grey to chapter 4.
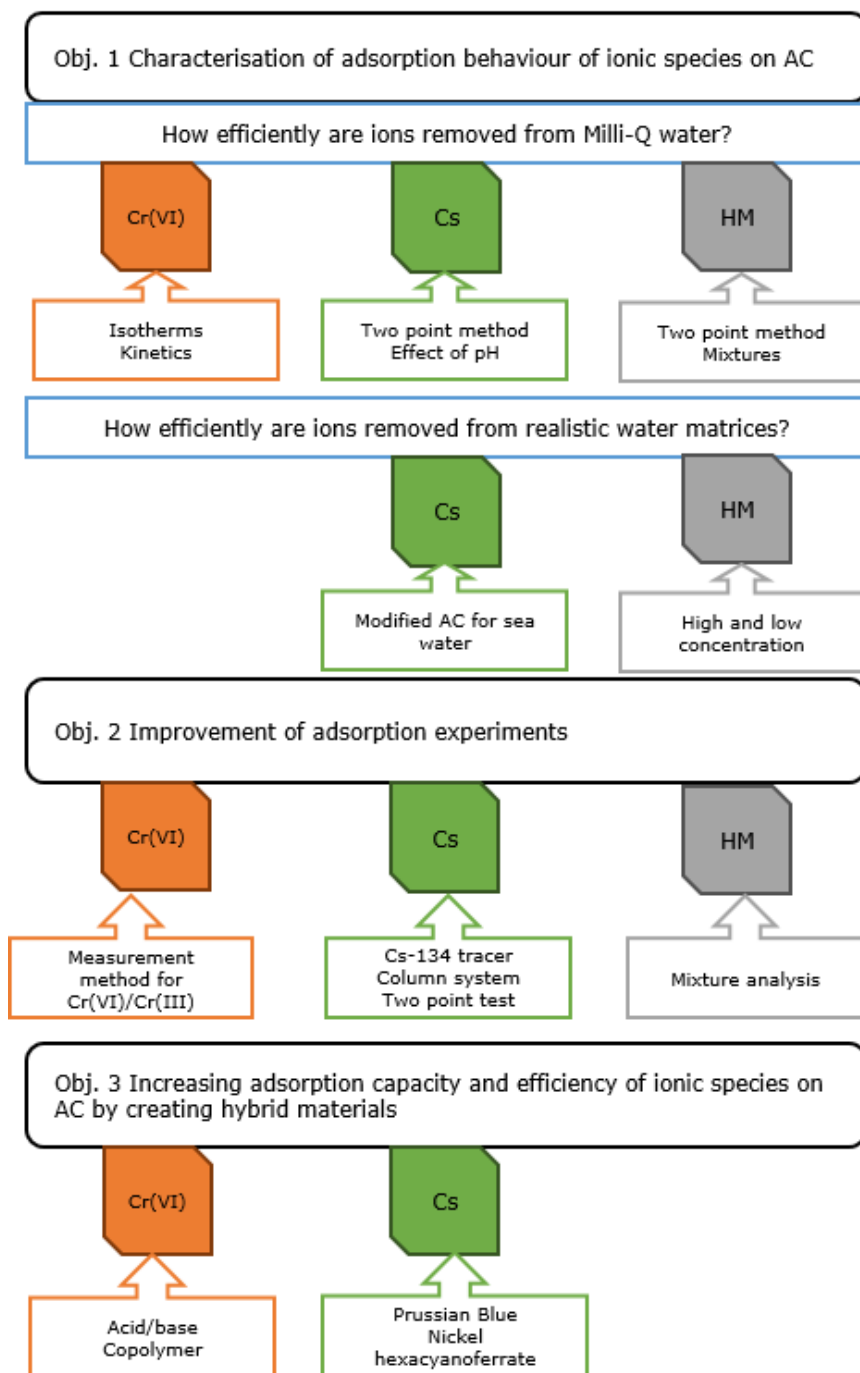
Figure 1-16 Schematic representation of the research sub-objectives

1. Characterisation of adsorption behaviour of ionic species on AC

The first research sub-objective is to determine the adsorption characteristics for each of the goal pollutants. Adsorption efficiency is either evaluated by the determination of adsorption isotherms [**Chapter 2: Cr(VI)**] or the use of a two-point method [**Chapter 3: Cs**, **Chapter 4: mixture of HM**]. The adsorption kinetics of Cr on different types of AC are also discussed. *Realistic* water matrices are also used in the two last chapters [**Chapter 3: Cs**, **Chapter 4: mixture of HM**].

The specific research questions for this sub-objective are:

Can Cr(VI) be removed by activated carbons? What are the characteristics for adsorption isotherms and kinetics? [**Chapter 2**]

How efficient are ACs at removing Cs at different pH? [**Chapter 3**]

Can modified adsorbents remove Cs from reconstituted 'realistic' water matrices? [**Chapter 3**]

Can AC remove individual heavy metals from Milli-Q and reconstituted water at high concentration? [**Chapter 4**]

Can AC efficiently remove mixtures of heavy metals at a very low concentration? [**Chapter 4**]

> 2. Improvement of adsorption experiments

The second sub-objective is to improve the current methods used for adsorption experiments. Improvements can be made to measurement techniques or to the method itself. Development of a quick determination method for the efficiency of ACs will lead to a more efficient AC selection in future research. The specific research questions for this objective are:

How can the oxidation/reduction reaction between Cr(VI) and AC be accounted for in adsorption data? [**Chapter 2**]

Can Cs-134 be used as a tracer in Cs adsorption experiments? [**Chapter 3**]

Is it possible to create a column system to adsorb Cs? [**Chapter 3**]

Does a two-point adsorption test provide reliable results? [**Chapter 3**]

Can the adsorption of a mixture of heavy metals give an estimate for the adsorption of each of the individual metals? [**Chapter 4**]

How do metals influence each other's adsorption at very low concentrations? [**Chapter 4**]

3. Increasing adsorption capacity and efficiency of ionic species on AC by creating hybrid materials

The last research objective is to increase the adsorption capacity and efficiency of AC by creating hybrid materials. A selection of modification methods is used to improve the AC performance and to create hybrid materials for adsorption of Cr(VI) and Cs.

Can an AC be modified to become more efficient and selective for Cr(VI) removal by either acid/basic washing or incorporation of a copolymer? [Chapter 2]

Can incorporation of Prussian Blue on AC be a possible modification method? [Chapter 3]

Is it possible to create a hybrid material that has selective Cs adsorption properties, even in sea water? [Chapter 3]

1.8 References

[1] P. McKendry, Energy production from biomass (part 1): overview of biomass, Bioresource Technology, **2002**, 83, 37-46.

[2] E. Rabinowitch, Govindjec, Photosynthesis, John Wiley and Sons, Inc., **1969**.

[3] Biomass at a glance, National Energy Education Development, online: http://www.need.org/Files/curriculum/Energy%20At%20A%20Glance/BiomassAtAGlance_11x17.pdf, accessed 15 june **2017.**

[4] J.S. Tumuluru, S. Sokhansanj, C.T. Wright, R.D. Boardman, N.A. Yancey, A Review on Biomass Classification and Composition, Co-Firing Issues and Pretreatment Methods, **2011**.

[5] S. Vassilev, D. Baxter, L. Andersen, C. Vassileva, An overview of the chemical composition of biomass, Fuel, **2010**, 89, 913-933.

[6] D. Klemn, B. Heublein, H.-P. Fink, A. Bohn, Cellulose: Fascinating biopolymer and sustainable raw material, Angewandte Chemie International Edition, **2005**, 44, 3358-3393.

[7] F.-X. Collard, J. Blin, A review on pyrolysis of biomass constituents: Mechanisms and composition of the products obtained from the conversion of cellulose, hemicelluloses and lignin, Renewable and Sustainable Energy Reviews, **2014**, 38,594-608.

[8] K.G. Raveendran, A.; Khilar, K.C., Pyrolysis characteristics of biomass and biomass components, Fuel, **1996**, 75, 987-998.

[9] European Commision, Fact sheet, Circular Economy Package, Brussels, **2015**.

[10] European Commision, Communication, Towards a circular economy: A zero waste programme for Europe**,** Brussels, **2014**.

[11] European Commision, Directive 2008/98/EC of the European Parliament and of the Council of 19 November 2008 on waste and repealing certain Directives, Brussels, **2008**.

[12] Vlaamse Overheid, Departement Leefmilieu, Natuur en Energie, Bio-Economie in Vlaanderen, Brussels, **2013**.

[13] European Commision, REPORT FROM THE COMMISSION TO THE COUNCIL AND THE EUROPEAN PARLIAMENT on sustainability requirements for the use of solid and gaseous biomass sources in electricity, heating and cooling in, European Commission, **2010**, 66.

[14] European Commision, COMMISSION STAFF WORKING DOCUMENT,State of play on the sustainability of solid and gaseous biomass used for electricity, heating and cooling in the EU, in, European Commision, Brussels, **2014**.

[15] K. Blennow, E. Persson, M. Lindner, S.P. Faias, M. Hanewinkel, Forest owner motivations and attitudes towards supplying biomass for energy in Europe, Biomass and Bioenergy,**2014**, 67, 223-230.

[16] M. Linko, A. Haikara, A. Ritala, M. Penttilä, Recent advances in the malting and brewing industry1, Journal of Biotechnology, **1998**, 65, 85-98.

[17] S. Oppelt, The Science of Brewing Beer, online: https://biology.mit.edu/sites/default/files/Sarah%20Oppelt%20Science%20of%20Brewing%20Beer%20PPT.pdf, accessed 3 september **2017**.

[18] S.I. Mussatto, G. Dragone, I.C. Roberto, Brewer's spent grain: generation, characteristics and potential applications, Journal of Cereal Science, **2006**, 1-14.

[19] C. Xiros, P. Christakopoulos, Biotechnological potential of brewers spent grain and its recent applications, Waste and Biomass Valorization, **2012**, 2, 213-232.

[20] D. Cook, Brewers' grains: opportunities about, in: Brewers' guardian, **2011**.

[21] Y. Pomeranz, E. Dikeman, From barley to beer--a mineral study. , Brewers digest, **1976**, 51, 30-32.

[22] J.A. Robertson, K.J.A. I'Anson, J. Treimo, C.B. Faulds, T.F. Brocklehurst, V.G.H. Eijsink, K.W. Waldron, Profiling brewers' spent grain for composition and microbial ecology at the site of production, LWT - Food Science and Technology, **2010**, 43 , 890-896.

[23] L. Fillaudeau, P. Blanpain-Avet, G. Daufin, Water, wastewater and waste management in brewing industries, Journal of Cleaner Production, **2006**, 463-471.

[24] Veolia, Distilling Bio-energy, online: https://www.veolia.co.uk/distilling-bio-energy, accessed 29 february **2016**.

[25] A. Ktenioudaki, N. O'Shea, E. Gallagher, Rheological properties of wheat dough supplemented with functional by-products of food processing: Brewer's spent grain and apple pomace, Journal of Food Engineering, **2013**, 116, 362-368.

[26] E. Vieira, M.A.M. Rocha, E. Coelho, O. Pinho, J.A. Saraiva, I.M.P.L.V.O. Ferreira, M.A. Coimbra, Valuation of brewer's spent grain using a fully recyclable integrated process for extraction of proteins and arabinoxylans, Industrial Crops and Products, **2014**, 52, 136-143.

[27] S.R. Reis, N. Abu-GHannam, Antioxidant capacity, arabinoxylans content and in vitro glycaemic index of cereal-based snacks incorporated with brewer's spent grain, LWT - Food Science and Technology, **2014**, 55, 269-277.

[28] S.I. Mussatto, J. Moncada, I.C. Roberto, C.A. Cardona, Techno-economic analysis for brewer's spent grains use on a biorefinery concept: The Brazilian case, Bioresource Technology, **2013**, 148, 302-310.

[29] C. Chen, J. Wang, Removal of Pb2+, Ag+, Cs+ and Sr2+ from aqueous solution by brewery's waste biomass Journal of Hazardous Materials, **2008**, 151, 65-70.

[30] A.S.N. Mahmood, J.G. Brammer, A. Hornung, A. Steele, S. Poulston, The intermediate pyrolysis and catalytic steam reforming of Brewers spent grain, Journal of Analytical and Applied Pyrolysis, **2013**, 103, 328-342.

[31] K. Vanreppelen, S. Vanderheyden, T. Kuppens, S. Schreurs, J. Yperman, R. Carleer, Activated carbon from pyrolysis of brewer's spent grain: Production and adsorption properties, Waste Management & Research, **2014**, 32(7), 634-45

[32] K. Vanreppelen, Towards a circular economy – Development, characterisation, techno-economic analysis and applications of activated carbons from industrial rest streams, UHasselt, **2016**.

[33] European commission, REGULATION (EC) No 767/2009 OF THE EUROPEAN PARLIAMENT AND OF THE COUNCIL of 13 July 2009 on the placing on the market and use of feed, Brussels,**2009**

[34] D. Deconinck, L. Capon, B. Clerinx, J. Couder, Indicatoren voor duurzame ontwikkeling in de Belgische industrie, DWTC Federale Diensten voor Wetenschappelijke, Technische en Culturele Aangelegenheden, **2001**.

[35] Beer statistics, Brewers of Europe, **2015.**

[36] Sold production, exports and imports by PRODCOM list (NACE Rev. 2) - annual data, Eurostat , **2015.**

[37] Crops processed, Food and Agriculture Organisation of the United Nations, **2014.**

[38] P. McKendry, Energy production from biomass (part 2): conversion technologies, Bioresource Technology, **2002**, 83, 47-54.

[39] M.M. Küçük, A. Demirbaş, Biomass conversion processes, Energy Conversion and Management, **1997**, 38, 151-165.

[40] J.E. White, W.J. Catallo, B.L. Legendre, Biomass pyrolysis kinetics: A comparative critical review with relevant agricultural residue case studies, Journal of Analytical and Applied Pyrolysis, **2011**, 1-33.

[41] M.A. Yahya, Z. Al-Qodah, C.W.Z. Ngah, Agricultural bio-waste materials as potential sustainable precursors used for activated carbon production: A review, Renewable and Sustainable Energy Reviews, **2015**, 46, 218-235.

[42] J. Akhtar, N. Saidina Amin, A review on operating parameters for optimum liquid oil yield in biomass pyrolysis, Renewable and Sustainable Energy Reviews, **2012**, 16, 5101-5109.

[43] T. Kan, V. Strezov, T.J. Evans, Lignocellulosic biomass pyrolysis: A review of product properties and effects of pyrolysis parameters, Renewable and Sustainable Energy Reviews, **2016**, 57, 1126-1140.

[44] A. Gani, I. Naruse, Effect of cellulose and lignin content on pyrolysis and combustion characteristics for several types of biomass, Renewable Energy, **2007**, 649-661.

[45] M. Tripathi, J.N. Sahu, P. Ganesan, Effect of process parameters on production of biochar from biomass waste through pyrolysis: A review, Renewable and Sustainable Energy Reviews, **2016**, 55, 467-481.

[46] A.K. Hossain, P.A. Davies, Pyrolysis liquids and gases as alternative fuels in internal combustion engines – A review, Renewable and Sustainable Energy Reviews, **2013**, 21, 165-189.

[47] H.B. Goyal, D. Seal, R.C. Saxena, Bio-fuels from thermochemical conversion of renewable resources: A review, Renewable and Sustainable Energy Reviews, **2008**, 12, 504-517.

[48] S.I. Yang, T.C. Hsu, C.Y. Wu, K.H. Chen, Y.L. Hsu, Y.H. Li, Application of biomass fast pyrolysis part II: The effects that bio-pyrolysis oil has on the performance of diesel engines, Energy, **2014**, 66, 172-180.

[49] J. Li, J. Dai, G. Liu, H. Zhang, Z. Gao, J. Fu, Y. He, Y. Huang, Biochar from microwave pyrolysis of biomass: A review, Biomass and Bioenergy, **2016**, 94 , 228-244.

[50] K.A. Spokas, K.B. Cantrell, J.M. Novak, D.W. Archer, J.A. Ippolito, H.P. Collins, A.A. Boateng, I.M. Lima, M.C. Lamb, A.J. McAloon, R.D. Lentz, K.A. Nichols, Biochar: A synthesis of its agronomic impact beyond carbon sequestration, Journal of Environmental Quality, **2012**, 41, 973-989.

[51] H. Marsh, F. Rodríguez-Reinoso, Activated carbon, Elsevier Science & Technology books, **2006**.

[52] J.A. Menéndez-Díaz, I. Martin-Gullón, Types of carbon adsorbents and their production, in: B. T.J. (Ed.) Activated Carbon Surfaces in Environmental Protection, Elsevier Ltd., **2005**.

[53] M. Inagaki, J.M.D. Tascón, Pore formation and control in carbon materials, in: T.J. Bandosz (Ed.) Activated Carbon Surfaces in Environmental Remediation, Elsevier Ltd., 2006.

[54] T.J. Bandosz, C.O. Ania, Surface chemistry of activated carbons and its characterization, T.J. Bandosz (Ed.) Activated Carbon Surfaces in Environmental Remediation, Elsevier, **2006**, 159-229.

[55] J.A. Menéndez, M.J. Illán-Gómez, C.a. León y León, L.R. Radovic, On the difference between the isoelectric point and the point of zero charge of carbons, Carbon, 33, 1655-1659, **1995**.

[56] E.G. Lorenc-Grabowska, G.; Diez, M.A., Kinetics and equilibrium study of phenol adsorption on nitrogen-enriched activated carbons, Fuel, **2012**.

[57] J.M.V. Nabais, J.A. Gomes, Suhas, P.J.M. Carrot, C. Laginhas, S. Roman, Phenol removal onto novel activated carbons made from lignocellulosic precursors: Influence of surface properties, Journal of Hazardous Materials, **2009**, 904-910.

[58] G.G. Stavropoulos, P. Samaras, G.P. Sakellaropoulos, Effect of activated carbons modifications on porosity, surface structure and phenol adsorption, Journal of Hazardous Materials, **2008**, 414-421.

[59] G. Yang, H. Chen, H. Qin, Y. Feng, Amination of activated carbon for enhancing phenol adsorption: Effect of nitrogen-containing functional groups, Applied Surface Science, **2014**, 293, 299-305.

[60] Haycarb, Activated Carbon | What is activated carbon?, **2017**.

[61] Freedonia Group, World Activated Carbon, **2014**.

[62] Marketing Research Report Activated Carbon, Chemical economics handbook, **2010**.

[63] Woord activated carbon market, Transparancy Market Research, **2016**.

[64] P. Le Cloirec, C. Faur, Adsorption of organic compounds onto activated carbon - applications in water and air treatments, in: T.J. Bandosz (Ed.) Activated Carbon Surfaces in Environmental Remediation, Elsevier, **2006**.

[65] IUPAC, Chemisorption and physisorption, **2001**.

[66] M. Thommes, K. Kaneko, A.V. Neimark, J. P. Olivier, F.Rodriguez-Reinoso, J. Rouguerol, K.S.W. Sing, Physisorption of gases, with special reference to the evaluation of surface area and porze size distribution (IUPAC Technical Report), **2015**.

[67] Wikibooks, The Lennard-Jones Potential, **2017**.

[68] W.J. Thomas, B. Crittenden, Adsorption Technology & Design, Elsevier Science & Technology Books, **1998**.

[69] A. Bagreev, J.A. Menendez, I. Dukhno, Y. Tarasenko, T.J. Bandosz, Bituminous coal-based activated carbons modified with nitrogen as adsorbents of hydrogen sulfide, Carbon, **2004**, 42, 469-476.

[70] M.H. El-Naas, M.A. Alhaija, Modeling of Adsorption Processes, Mathematical Modelling, in: C.R. Brennan, Mathematical Modelling, Nova Publishers, **2011**.

[71] H. Qiu, B.-C. Pan, Q.-j. Zhang, W.-m. Zhang, Q.-x. Zhang, Critical review in adsorption kinetic models, Journal of Zhejiang university science A, **2009**, 10.

[72] S.Y. Lagergren, Zur theorie der sogenannten adsorption gelöster stoffe, Kungliga Svenska Vetenskapsakademiens, Handlingar, **1898**, 24, 1-39.

[73] R.-L. Tseng, F.-C. Wu, R.-S. Juang, Characteristics and applications of the Lagergren's first-order equation for adsorption kinetics, Journal of the Taiwan Institute of Chemical Engineers, **2010**, 41, 661-669.

[74] Y.S. Ho, G. McKay, Kinetic Models for the Sorption of Dye from Aqueous Solution by Wood, Process Safety and Environmental Protection, **1998**, 76, 183-191.

2 Chromium removal by activated carbons

2.1 Introduction[3]

Chromium is introduced into the environment by natural and human activities. Chromite is a mineral present in soils, rocks, volcanic ashes and dust, water and living creatures and is the only chromium containing ore [1, 2]. However, the biggest source of chromium in the environment is the improper disposal from industrial applications. Extracting chromium compounds from chromite is still inefficient and chromium-containing wastes are not always treated properly [3]. Effluents and waste water from several industries are heavily polluted with chromium. Metallurgical applications of chromium include steel production, chrome-plated objects or materials with special properties such as resistance to corrosion and temperature [1, 4]. The chemical industry also uses chromium in electroplating, as pigments or in tanneries for leather production. Chromium compounds are found in wastes and waste waters and can pose a great environmental and biological risk [4]. A summary of chromium prevalence in the biosphere is displayed in Figure 2-1.

Chromium can display oxidation states between 0 and +6. Figure 2-2 displays the Pourbaix diagram for chromium, showing the oxidation states present in water depending on different circumstances. Chromium is typically only found in the environment in three speciation states (according to [1, 4, 6-8]):

- Chromium(0) or metallic chromium is found as a solid particle in alloys such as stainless steel or chrome-plated pieces of metal.

- Chromium(III) or trivalent chromium. It is mostly present in water in hydrolyzed form or bound to humic acid or colloidal particles. It is an essential micronutrient for humans and animals, playing an important role in lipid and sugar metabolism. Plants are able to accumulate chromium(III), but do not need it for their metabolism.

---

[3] References for this introduction can be found on page 67 in section 2.3

- Chromium(VI) or hexavalent chromium can be present as CrO_4^{2-}, $HCrO_4^-$ or $Cr_2O_7^{2-}$, depending on pH (see Figure 2-3). Its mutagenic and carcinogenic properties make this the most troubling chromium ion in the environment. The WHO guidelines for drinking water are set at 0.05 mg/L of total chromium because of chromium(VI) toxicity. Chromium(VI) is able to replace SO_4^{2-} in biochemical pathways (as CrO_4^{2-} and $HCrO_4^-$) making it toxic to many species. It is also much more mobile in slightly acidic media compared to chromium(III).
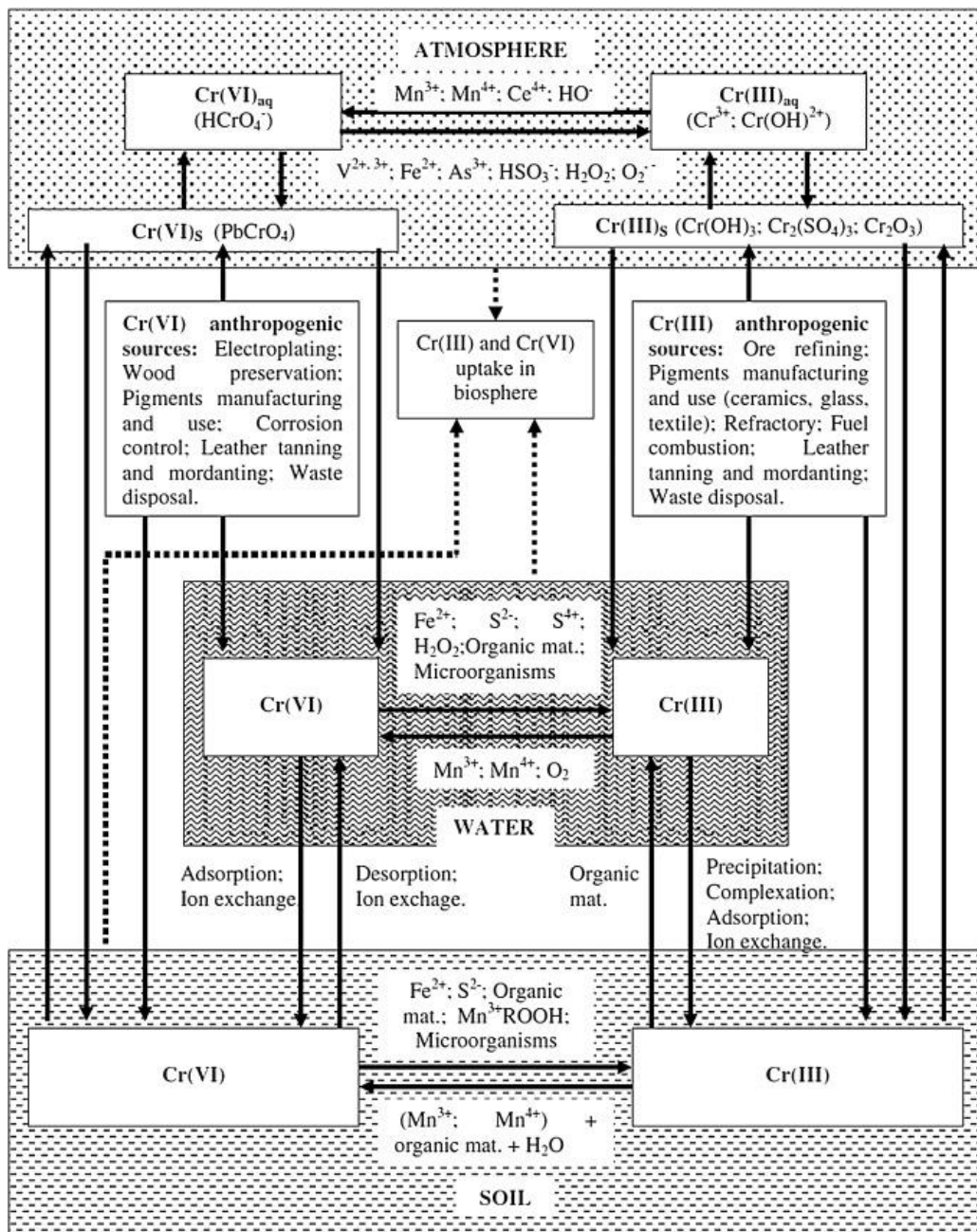
Figure 2-1 Chromium prevalence in the biosphere.

Taken from [5]
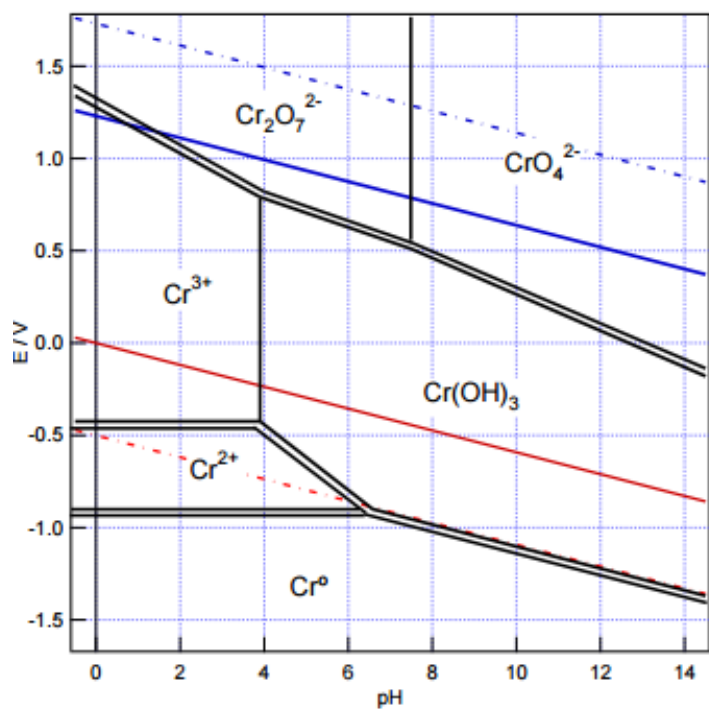
Figure 2-2 Pourbaix diagram for chromium [9]
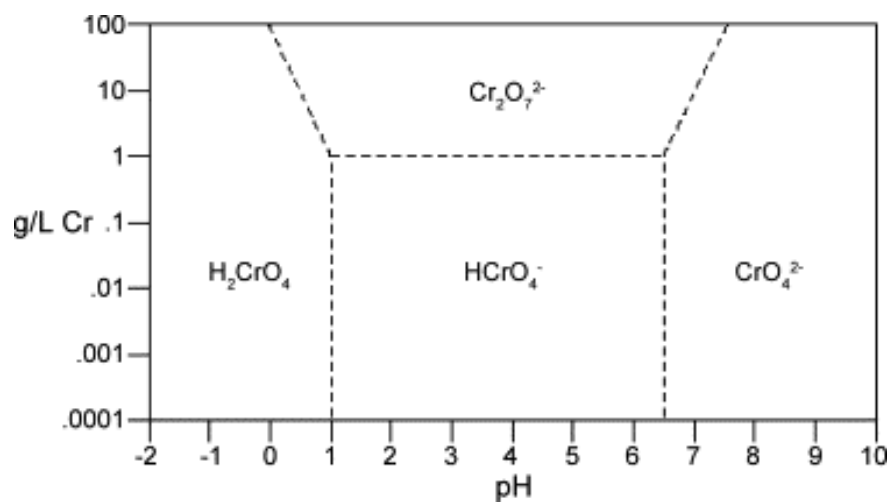
Figure 2-3 Speciation diagram of Cr(VI) [10]

Several methods are available to remove chromium from waste water. A short description is given here, based on [11, 12].

Liquid-liquid extraction (LLE) (or: solvent extraction) was the standard method for chromium removal. LLE is based on the distribution of chromium (or any other chemical compound) between two immiscible phases. The efficiency is highly dependent on the distribution ratio, that expresses the ratio of the concentration of all different species between the two phases. Many factors contribute to a high distribution ratio and general efficiency, such as pH, complexation, formation of a third phase and solvent toxicity. In order to have an economically viable process, also the regeneration and reusability of the extractant solution should be taken into account. For chromium removal, chelating and ion association systems are used, where the chromium anions are able to interact electrostatically with the extractants. These extractants are mostly amine-based, such as quaternary or tertiary amine based compounds (trioctylmethylammonium hydroxide, benzyldodecyldimethylammonium bromide, …). Another possibility is the use of ionic liquids. Ionic liquids are long chain quaternary ammonium salts with a low melting point.

Electrochemical removal methods have also been proposed for the removal of chromium, using chemical reduction. Reducing agents change the oxidation state of hexavalent chromium into trivalent chromium, which can then be precipitated as a hydroxide using alkali or lime or create a sulphate precipitate by adding sulphite. Recovery of the chromium can be performed using sulfuric acid. The biggest disadvantage of this technique is the production of a solid sludge, which increases the process costs. It is also possible to use specific biomass materials as bioreducers. Plant species, fungi, algae have shown bioreduction capacity. Chromium-reducing bacteria have also shown very effective bioreduction in a variety of solution conditions (pH, temperature, contact time, …)

Solid phase extraction (SPE) has emerged in the last few years as a viable alternative removal method. A solid material is added to polluted chromium solutions and the chromium adsorbs to the extracting materials. Electrostatic forces, complexation, ion exchange and hydrophobic interactions are the most common mechanisms in SPE, dependent on the type of solid phase. The most

important process parameters for SPE are the selectivity, adsorption kinetics, isotherms and thermodynamics. Adsorbents can be broadly classified into two categories: inorganic (clays, alumina, silica, …) and organic (divinylbenzene resins, graphene oxides, chitosan,…). However, modern adsorbents are often comprised of both organic and inorganic parts, as the production of functionalized products increases.

Removal of chromium(VI) by activated carbons (ACs) is a well-researched topic. It is generally assumed that the adsorption mechanism consists of two uptake modes[10]:

1. Adsorption of chromium(VI) onto the surface of the AC
2. Reduction of chromium(VI) to chromium(III), which then adsorbs

Because of a great variety in parameters used for adsorption experiments, different adsorbents cannot easily be compared. Different starting concentrations, AC dosage, pH, shaking parameters and reaction set-up (continuous/batch) can make all the difference in the adsorption capacities that are found. In contrast with adsorption of organic species, the adsorption of metal ions cannot be correlated to the AC surface [10]. Adsorption efficiency is much more dependent on ion exchange and precipitation of the metals. A lot of researchers have investigated the introduction of functional groups into the AC by modification [13]. Impregnation of AC with cationic surfactants, other metals or ion exchanging materials has been performed, but also impregnation of the input biomass with nitrogen-containing chemicals. The enhanced nitrogen functionalities in the resulting AC will lead to an improved adsorption specificity and efficiency.

2.2 Research questions

In order to create a valuable addition to current state-of-the-art literature, the research is conducted in two parts.

A first part handles the applicability of biomass-based AC from brewer's spent grain (ACBSG) for removal of chromium(VI) from industrial waste waters. Six ACs are produced using the BSG and involved in the adsorption experiments. A comparison is made to the performance of industrial AC by using two commercially available ACs in the same experiments: Norit GAC1240 and Filtrasorb F400. The most important focus points are:

- Characterization of the ACBSGs and comparison to the commercial ACs
- Removal of chromium (VI) by all the ACs, measuring both chromium(VI) and total chromium
- Modelling of adsorption isotherms and kinetics
- Correlation of AC properties to the adsorption isotherms and kinetics

This study will prove whether the use of ACBSG for chromium(VI) removal can be technically viable and provide insights on the experimental settings for chromium adsorption. This part is described in section 2.4: *"Chromium(VI) removal using activated carbon prepared from brewers' spent grain"*

The second part handles the improvement of the adsorption capacity and kinetics for a selection of ACs from the first part. Two modification methods are selected, after which the new adsorbents are characterized and used for adsorption experiments (isotherms and kinetics). Focus points are :

- Using two completely different modification techniques, 4 ACs (2 ACBSGs, Norit GAC1240 and Filtrasorb F400) are used to prepare new adsorbents.

- Characterisation of the new adsorbents

- Adsorption experiments are carried out for each of these modifications

- Comparison of advantages and disadvantages of the modified adsorbents

All used techniques and results are discussed in 2.5: *"Activated carbons from brewers' spent grain and their modifications: enhanced removal of chromium(VI)".*

2.3 References

[1] V. Gómez, M.P. Callao, Chromium determination and speciation since 2000, TrAC Trends in Analytical Chemistry, **2006**, 25, 1006-1015.

[2] G. Chen, X. Wang, J. Wang, H. Du, Y. Zhang, S.-L. Zheng, Y. Zhang, A new metallurgical process for the clean utilization of chromite ore, International Journal of Mineral Processing, **2014**, 131, 58-68.

[3] J.P. Beukes, S.P. du Preez, P.G. van Zyl, D. Paktunc, T. Fabritius, M. Päätalo, M. Cramer, Review of Cr(VI) environmental practices in the chromite mining and smelting industry – Relevance to development of the Ring of Fire, Canada, Journal of Cleaner Production, **2017**, 165, 874-889.

[4] J. Kotaś, Z. Stasicka, Chromium occurrence in the environment and methods of its speciation, Environmental Pollution, **2000**, 107, 263-283.

[5] M. Gheju, Water, air and soil pollution, **2011**, 222, 103

[6] M. Shahid, S. Shamshad, M. Rafiq, S. Khalid, I. Bibi, N.K. Niazi, C. Dumat, M.I. Rashid, Chromium speciation, bioavailability, uptake, toxicity and detoxification in soil-plant system: A review, Chemosphere, **2017**, 178, 513-533.

[7] N.A. Qambrani, J.-H. Hwang, S.-E. Oh, Comparison of chromium III and VI toxicities in water using sulfur-oxidizing bacterial bioassays, Chemosphere, **2016**, 160, 342-348.

[8] World Health Organization, Chromium in drinking water - Background document for developtment of WHO guidelines for drinking-water quality, **1996**.

[9] Geological Survey of Japan, Open File Report No419, Atles of eE-pH diagrams, intercomparison of thermodynamic databases, **2005**.

[10] D.P. Mohan, C.U. Jr., Activated carbons and low cost adsorbents for remediation of tri- and hexavalent chromium from water, Journal of Hazardous Materials, **2006**, 762-811.

[11] S. Kalidhasan, A. Santhana Krishna Kumar, V. Rajesh, N. Rajesh, The journey traversed in the remediation of hexavalent chromium and the road ahead toward greener alternatives—A perspective, Coordination Chemistry Reviews, **2016**, 317, 157-166.

[12] D. Pradhan, L.B. Sukla, M. Sawyer, P.K.S.M. Rahman, Recent bioreduction of hexavalent chromium in wastewater treatment: A review, Journal of Industrial and Engineering Chemistry, **2017**, 55, 1-20.

[13] X. Xu, B. Gao, B. Jin, Q. Yue, Removal of anionic pollutants from liquids by biomass materials: A review, Journal of Molecular Liquids, **2016**, 215, 565-595.

2.4 Chromium(VI) removal using in-situ nitrogenized activated carbon prepared from brewers' spent grain[4]

S. R. H. Vanderheyden[a*], K. Vanreppelen[a b], J. Yperman[a], R. Carleer[a], S. Schreurs[b],

[a] Hasselt University, Centre for Environmental Sciences, Research Group of Analytical and Applied Chemistry, Agoralaan – Building D, 3590 Diepenbeek, Belgium; e-mail: kenny.vanreppelen@uhasselt.be; jan.yperman@uhasselt.be; robert.carleer@uhasselt.be

[b] Hasselt University, Centre for Environmental Sciences, Research Group of Nuclear Technology, Agoralaan – Building H, 3590 Diepenbeek, Belgium; e-mail: sonja.schreurs@uhasselt.be

* Corresponding author: Sara R.H. Vanderheyden, sara.vanderheyden@uhasselt.be +3211 268211

ABSTRACT

In-situ nitrogenised activated carbons (ACs) are prepared from brewers' spent grain (BSG) using different activation procedures. Cr(VI) adsorption (10 mg/L, pH 2) on these ACs is compared to adsorption on commercial Norit GAC 1240 and Filtrasorb F400. The adsorption isotherms for both Cr(VI) and Cr total (Cr_{tot}) are determined for each AC, of which the best performing ones are chosen for kinetic experiments. The adsorption mechanism towards Cr(VI) is accompanied by its reduction to Cr(III), removing almost all Cr(VI) even at low dosages for all tested ACs. An optimal dosage (0.75 g/L) is found for each AC. For the best performing AC this dosage results in removal rates of over 99% of Cr(VI) and 88% of Cr_{tot}.

---

[4] [4] References for this article can be found on page 90 in section 2.4.7

The amount of reduced Cr(VI) increases with AC dosage, resulting in a higher Cr(III) equilibrium concentration above this optimal dosage. The redox reaction is more dominant in the commercial ACs. However, a faster removal rate for the ACBSGs for both Cr(VI) and Cr_{tot} is demonstrated.

2.4.1 Introduction

Brewers' spent grain (BSG) accounts for 85% of brewery waste [1,2], with an average production of 14-20 kg per 100 L of beer [3]. The total production of beer in Europe (EU-27, for 2011) amounts up to 38400 ML/year, producing up to 5.38 – 7.68 Mt of wet BSG to be disposed of every year [4]. Worldwide production of BSG is estimated at 30 Mt per year [5]. This vast amount of wet biomass is most often used as animal feed, but is difficult to store owing to its microbial activity. Furthermore, BSG is hard to digest and its use as an animal feed for ruminants causes an increased methane production [5]. It is rich in fibers (70-80% of the dry mass) and proteins (20% of the dry mass) and is attractive for the production of value-added chemicals [2].

Using pyrolysis followed by steam activation, BSG can be converted into activated carbon (AC) for the purification of liquid or gaseous waste streams [6]. AC has different surface functionalities, high mechanical strength [7,8], and stability towards chemicals, heat and radiation [8]. Above all, it is an excellent adsorbent for both organic and inorganic pollutants [9-13]. As BSG contains relatively high levels of nitrogen of about 4% [14,15], it can be used for in-situ generation of nitrogen functionalities in AC. Nitrogenised AC has already shown excellent adsorption properties for different pollutants [15-20]. This enhanced adsorption is a result of the overall change in acidic/basic functionalities of the AC [21] and a possible combination of physisorption and chemisorption [17].

Chromium appears in two oxidation states in the environment: Cr(VI) and Cr(III), which differ strongly in chemical and toxicological properties [22,23]. Cr(VI) is toxic, mutagenic and carcinogenic. It is currently mostly produced by industrial processes such as welding and is often applied as pigment in paints and plastics

[24]. The high mobility and solubility of Cr(VI) create a substantial environmental risk. Cr(III), an essential trace element in mammalian metabolism, exhibits lower toxicity and mobility [23].

The goal of this work is to adsorb Cr from a 10 mg/L Cr(VI) solution using in-situ nitrogenised ACs made from BSG. These ACBSG have a nitrogen content of 2% and higher. It has been proven that a low pH promotes adsorption of Cr(VI), present in the solution as $HCrO_4^-$, on the positively charged surface of the adsorbent [25-28]. Adsorbents with a higher nitrogen content (approximately 1%) show a higher Cr(VI) adsorption and reduction compared to non-nitrogenised adsorbents and a more efficient removal [29]. At higher amounts of nitrogen, the risk exists that the benefit for the adsorption is outweighed by the reduction to Cr(III) and results in a less efficient total removal [29].

Adsorption performance of the nitrogenised AC is compared with values found in literature and for commercial samples. A comparison between the adsorption isotherms and kinetics for both Cr(VI) and Cr_{tot} is made. To the best of our knowledge, nitrogenised ACBSG have not been researched in Cr removal studies.

2.4.2 Materials and methods

For every experiment, Milli-Q water (18.2 MΩ cm^{-1} conductivity) and analytical grade reagents are used. For comparison between ACs, two commercially available ACs are used: Norit GAC 1240 and Filtrasorb 400, supplied by Cabot Carbon and Calgon Carbon respectively.

2.4.2.1 Pyrolysis and activation

Preparation of the AC is conducted in a horizontal semi-continuous reactor as described in [15] and displayed in Figure 2-4 : a continuously stirred horizontal tube reactor with steam/nitrogen gas inlet (Schott TR100 pump for water). BSG is dried, sieved and pyrolysis and activation are performed in a two-step process. First, the reactor is heated up (10 °C/min) up to the activation temperature, while 80 mL/min of nitrogen gas is flowing. This will pyrolyse the BSG particles. Then, steam is added and the char particles are activated. The reactor is able to convert 40 g of biomass. Different ACBSGs are prepared according to the varying pyrolysis and steam activation parameters, as shown in Figure 2-5.
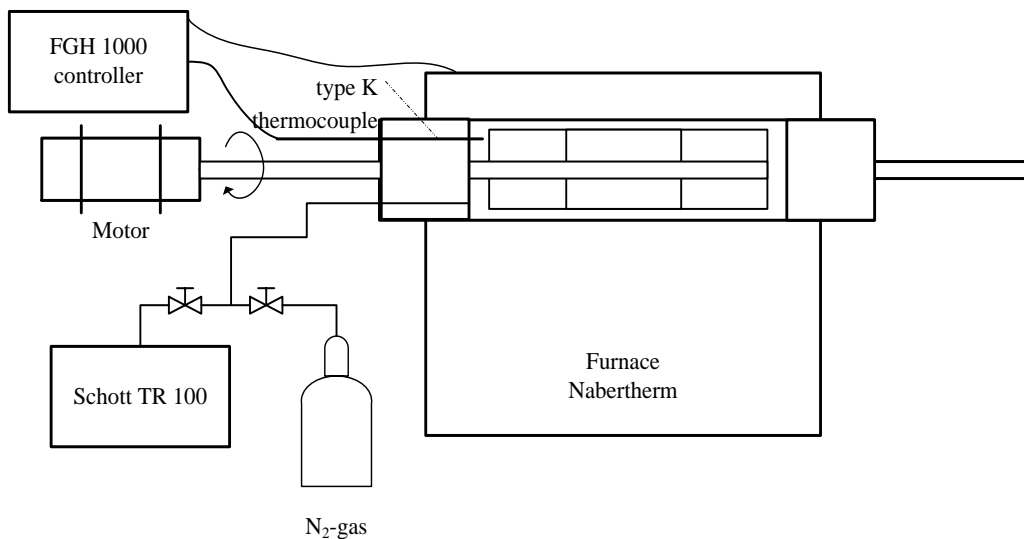
Figure 2-4 Horizontal semi-continuous reactor set-up
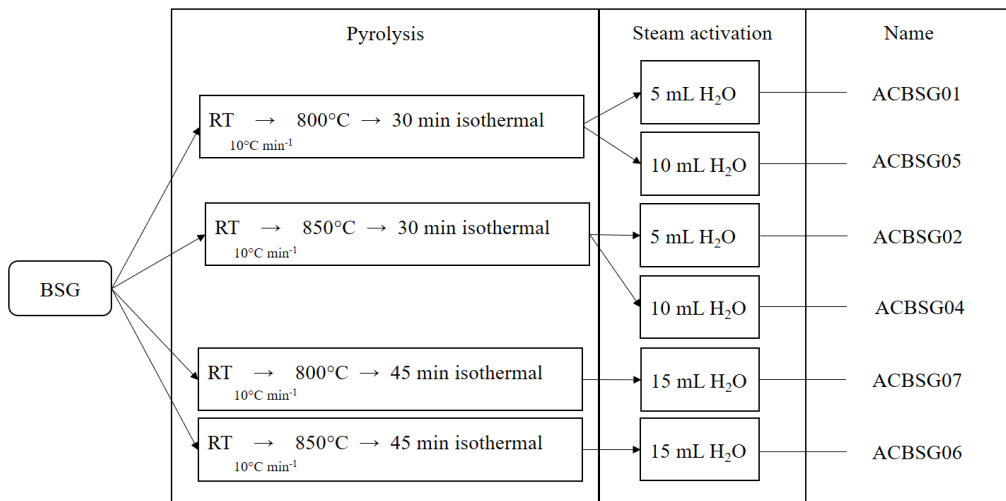
Figure 2-5 Schematic representation of the produced ACBSGs

2.4.2.2 AC characterisation

The point of zero charge of the activated carbons was determined in [15] and is displayed in Table 2-1.

Table 2-1 Point of zero charge of selected ACs [15]

	pH_{PZC}
Norit GAC1240	11,76
Filtrasorb F400	11,54
ACBSG05	10,59
ACBSG07	10,7

Both ACBSGs and commercial ACs are sieved to a particle size between 63 μm and 1 mm for the adsorption study. Bulk density is determined in triplicate according to ASTM D 2854 – 96 based on a vibrating feed system. Particle size distribution (PSD) is determined using laser diffraction in a Malvern Mastersizer S after dispersion in Milli-Q water. PSD is determined again after 20 minutes of stirring to study rigidity of the particles.

The ash content is determined according to ASTM 2866-11. A Thermo Finnigan Element Analysis Flash EA 1112 is used for CHNS analysis after standardisation with BBOT (2,5-bis (5-tert-butyl-benzoxazol-2-yl) thiophene)). O content is calculated by difference. Samples are measured in quadruplicate.

2.4.2.3 Adsorption isotherms and adsorption kinetics

For the determination of adsorption isotherms and kinetics a solution of 10 mg/L Cr(VI) at pH 2 is prepared using potassium dichromate and hydrochloric acid. Between 5 and 100 mg of AC is placed into closed vials together with 25 mL of the 10 mg/L Cr(VI) solution. A vial without AC is treated accordingly to determine initial Cr concentrations. The vials are shaken for 24 h at 25 °C to ensure adsorption equilibrium. A solution of 1 M of hydrochloric acid is used to re-adjust the pH 2 after 4 and 20 h. After shaking for 24 h, the solution is filtered using ashless Whatman 40 filters and both Cr(VI) and Cr_{tot} concentrations are determined. The concentration of Cr(VI) is measured using the diphenylcarbazide method (DPC), measuring absorbance at 540 nm for the samples and calibration

standard solutions [31]. The total Cr concentration is determined via ICP-AES (PE Optima 8300).

A kinetic study is performed by bringing 20 mg of AC into contact with 25 mL of 10 mg/L Cr(VI) solution (corresponding to an AC dosage of 0.8 g/L) in different vials. The Cr(VI) and Cr_{tot} concentrations are measured at eleven time intervals after filtration with ashless Rotilabo 14A filters.

2.4.3 Literature survey

Table 2-2 summarizes values for adsorption capacities q_e from literature for adsorption of Cr(VI) on different types of adsorbents with details of the experimental parameters. The most important parameters that influence the found q_e are adsorbent dosage and Cr(VI) concentration. The pollutant/adsorbent ratio increases when using low doses of AC or high Cr(VI) concentrations, resulting in an increased q_e value. Only those papers were selected where the experimental parameters were comparable to the one applied in this manuscript. However, in most research, only Cr(VI) concentrations are measured by the DPC method and Cr_{tot} is not measured at all. This implies that q_e values measured by DPC or FAAS in Table 2 can only be considered as *apparent* adsorption capacity values and are an overestimation of the Cr(VI) removal, as this is the result of the total decrease which is a sum of adsorption and reduction to Cr(III). Measuring Cr_{tot} concentrations as well is thus crucial to demonstrate the effects of adsorption and reduction. This effect is seldom accounted for in literature concerning AC.

Table 2-2 Adsorption capacities for Cr(VI) found in literature.

Category	Adsorbent	Temperature (°C)	Measurement method	Adsorption capacity q_e (mg Cr(VI)/g AC)	Optimum pH	Dosage (g AC/L)	Concentration of Cr(VI) (mg/L)	References
Low-cost adsorbent	Rice Husk Ash	30	DPC	25.64	2	2.5-30	3-50	[32]
	Clarified sludge	30	DPC	26.31	2	2.5-30	3-50	[32]
	Activated alumina	30	DPC	25.57	2	2.5-30	3-50	[32]
	Fuller's earth	30	DPC	23.58	2	2.5-30	3-50	[32]
	Fly Ash	30	DPC	23.86	2	2.5-30	3-50	[32]
	Sawdust	30	DPC	20.7	2	2.5-30	3-50	[32]
	Neem bark	30	DPC	19.6	2	2.5-30	3-50	[32]

Table 2-2 continued

Category	Adsorbent	Temperature (°C)	Measurement method	Adsorption capacity q_e (mg Cr(VI)/g AC)	Optimum pH	Dosage (g AC/L)	Concentration of Cr(VI) (mg/L)	References
AC	AC from acrylonitrile-divinylbenzene	22	DPC	55.85	2	0.04-1.2	30	[25]
	AC from acrylonitrile-divinylbenzene	45	DPC	73.65	2	0.04-1.2	30	[25]
	Microporous AC from *Aegle Marmelos* fruit shell	20-50	DPC	43.54	2	1.0-3.0	2-10	[33]
	Used tyres AC	38	DPC	58.47	2	8	60	[34]
	Sawdust AC	38	DPC	2.28	2	8	60	[34]
	F400	38	DPC	53.19	2	8	60	[34]
	Hevea Brasilinesis sawdust activated carbon	50	DPC	64.44	2	1	50-200	[35]

Table 2-2 continued

Category	Adsorbent	Temperature (°C)	Measurement method	Adsorption capacity q_e (mg Cr(VI)/g AC)	Optimum pH	Dosage (g AC/L)	Concentration of Cr(VI) (mg/L)	References
AC	Bamboo bark-based activated carbon	30	DPC/ICP-MS	9.99	4	0.25	1-8	[36]
	AC from red algae	25	DCP	66.67	1-7	3-10	5-100	[37]
	PICACHEM-200.P	N.S.	FAAS	131.6	2-10	0.6, 2	30-100	[38]
	AC from peanut shells	N.S.	FAAS	140.8	2-10	0.6, 2	30-100	[38]
	AC from Jatropha	N.S.	FAAS	106.4	2-10	0.6, 2	30-100	[38]

*N.S. = Not Specified

2.4.4 Results and discussion

2.4.4.1 Study of Cr adsorption on ACBSGs

Figure 2-6 and Figure 2-7 display the adsorption isotherms (q_{app} in mg Cr(VI) or q_e in mg Cr$_{tot}$ adsorbed per gram of AC at equilibrium in function of the equilibrium concentration c_e in mg Cr(VI) or Cr$_{tot}$ /L after 24 h of shaking) and removal percentages (percentage of Cr(VI) or Cr$_{tot}$ removed in function of AC dosage) for all studied ACs. ACBSG01 is not displayed in the graphs because it had significantly lower adsorption capacity compared to all other ACSBGs. These substandard adsorption properties have also been found for phenol adsorption in [15]. The lower amount of steam used during activation results in a less developed pore structure, lowering the adsorption capacity. Therefore, it is not investigated further. Through the data points of the best performing AC (ACBSG07) a trend line is drawn to highlight the special adsorption behaviour within this system.

For Cr(VI), all ACs remove almost all Cr(VI) at dosages of approximately 1 g/L and higher (removal percentage higher than 98%) as can be seen in the bottom of Figure 2-6. This results in an adsorption isotherm that is almost tangential to the y-axis (Figure 2-6 top), as c_e equals approximately zero at most carbon dosages. At the lowest AC dosage (20 mg/L), corresponding to the upper right set of data points (7 in total) in the adsorption isotherm an apparent adsorption capacity q_{app} of approximately 35 to 45 mg Cr(VI)/g AC is reached for all ACs. The amount of Cr(VI) actually adsorbed is lower because of a partial reduction to Cr(III), as will be discussed later. The low dosage of approximately 0.2g AC/L corresponds to a Cr(VI) removal percentage between 68 (ACBSG05) and 87% (ACBSG06). ACBSG06 was produced using the most extreme activation conditions, resulting in the most developed pore structure. At higher dosages, the effect of activation conditions is no longer relevant for Cr(VI) adsorption.
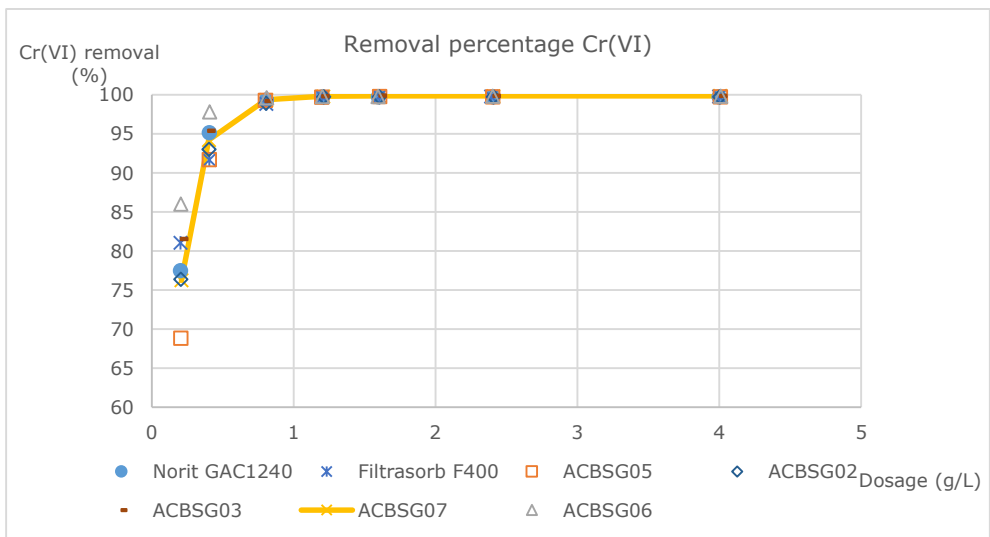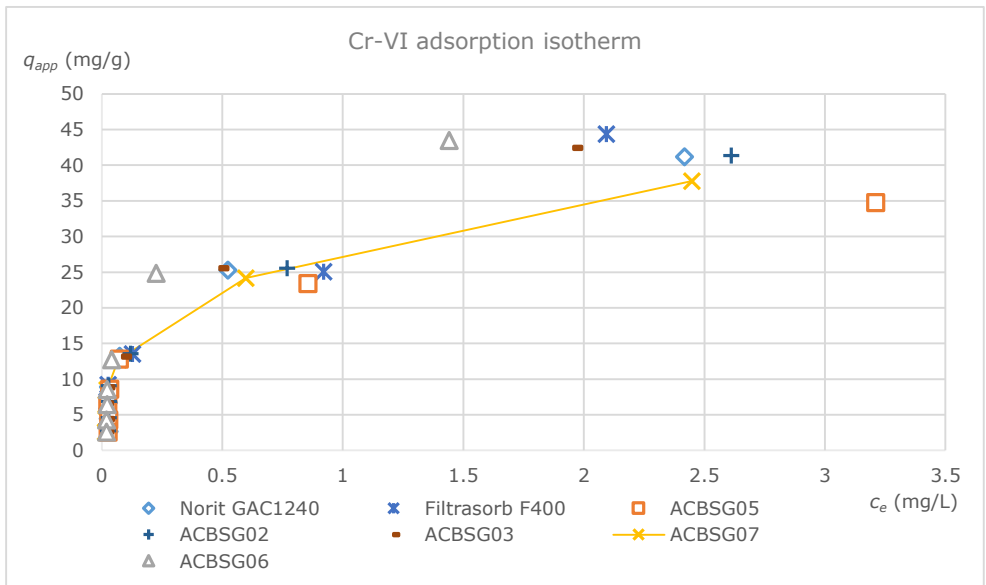
Figure 2-6 (top) Adsorption isotherm for Cr(VI) on different ACs. (bottom) Removal percentage of Cr(VI) as a function of AC dosage Experiment was performed by adding 5-100 mg of AC to 25 mL of 10 mg/L Cr(VI) solution at pH 2
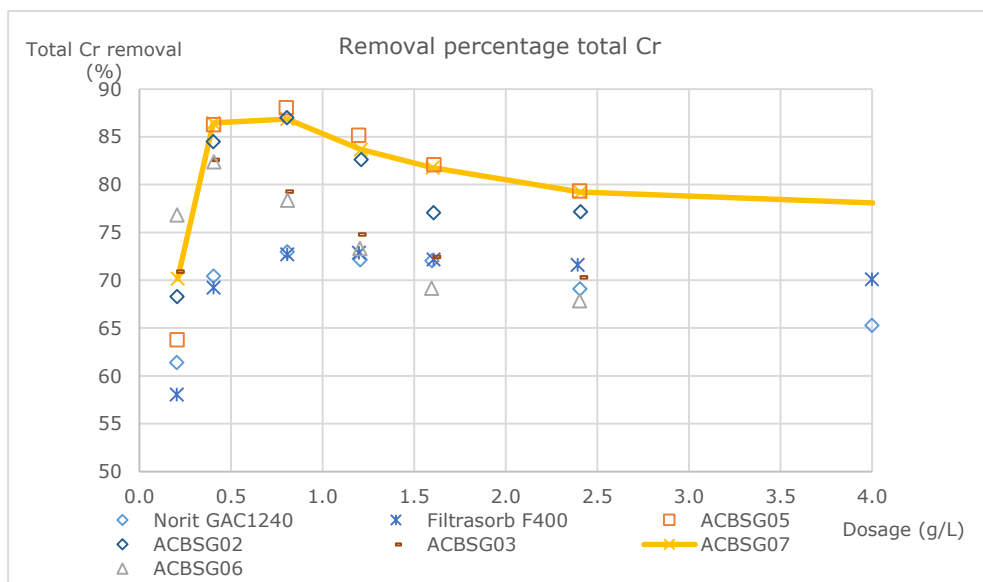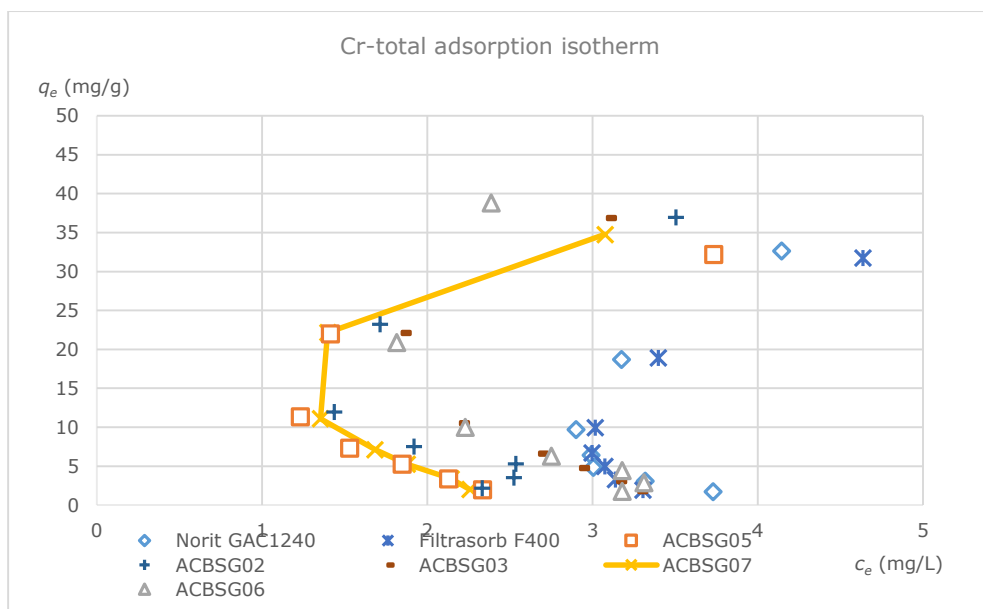
Figure 2-7 (top) Adsorption isotherm for Cr$_{tot}$ on different ACs. (bottom) Removal percentage of Crtot as a function of AC dosage. Experiment was performed by adding 5-100 mg of AC to 25 mL of 10 mg/L Cr(VI) solution at pH 2 (optimal dosage at about 0.75 g AC/L)

Cr_{tot} adsorption measurements reveal the influence of both adsorption and reduction of Cr(VI) to Cr(III). As the AC dosage increases from 0 to 0.5 g/L, the removal percentage of total Cr increases to a maximum of 88% for ACBSG05 at a dosage of approximately 0.75 g/L (bottom of Figure 2-7). Above this critical point, the removal percentage decreases, caused by oxidation of the AC surface and a reduction of Cr(VI) to the less toxic Cr(III). The Cr(III)-cation is adsorbed less efficiently than Cr(VI) at pH 2, since the AC is positively charged [39]. This effect can also be seen at the top graph of Figure 2-7. The upper right hand corner set of data points (7 in total) are the result of a low dosage test. Increasing the dosage reduces c_e (data points in the middle of the plot) but only to a certain point. At higher dosages, the c_e for Cr_{tot} increases again, as Cr(III) is released into the solution. These correspond to the data points in the lower part of the top half of Figure 2-7. This combination of adsorption and reduction results in an optimal dosage for the removal of both Cr species of approximately 0.75 g/L. Cr(VI) is removed effectively at all dosages equal to or above this optimal dosage (bottom of Figure 2-6). Due to the combination of adsorption and reduction mechanisms, both Langmuir and Freundlich isotherm calculations have an extremely low R² value and are considered irrelevant for this complex adsorption system. The isotherms for Cr_{tot} cannot be fitted by the classical models as the found end concentration c_e increases again with increasing dosage, which is counterintuitive. The classical models are based on a straightforward adsorption, which is not the case. The isotherms for Cr(VI) would only yield parameters for an apparent capacity. The effect of combined adsorption and reduction properties has been described for biosorption in several research articles. The typical isotherm behaviour as seen in Figure 2-7 can be explained by various theories that are also presented for biosorption. [40-42]

The difference in adsorption properties between the commercial ACs (Norit GAC1240 and Filtrasorb F400) is strongly pronounced in the adsorption of Cr_{tot}. Both commercial ACs reach equilibrium solution concentrations of approximately 3 mg/L of Cr_{tot} (Figure 2-7, top), compared to approximately 1.3 mg/L for the best ACBSGs. As Cr(VI) is still removed efficiently, this results in a higher equilibrium concentration of Cr(III) for the commercial ACs compared to the ACBSGs and thus a lower Cr_{tot} removal percentage (Figure 2-7, bottom). It can

be concluded that, based on these results, both commercial ACs exhibit stronger reductive properties than the ACBSGs and ACBSG can be used in the same or lower dosages as the two commercial ACs. The best results are achieved for ACBSG05 and ACBSG07, both reaching a removal percentage of approximately 87% of Cr_{tot} after 24h with a dosage of 0.75 g/L. These ACs were chosen for further characterisation (see also [15]) and kinetic experiments. These ACBSG perform similarly compared to other ACs from biomass as listed in Table 2-2, keeping in account the different experimental parameters.

2.4.4.2 Characterisation of the ACs

Results from the ash determination and elemental analysis for BSG, selected ACBSGs and commercial ACs are displayed in Table 2-3. Pyrolysis of the BSG causes a part of the nitrogen functionalities to volatilise, resulting in a decrease from 4.4 to about 2.6%. The ACBSG still shows higher amounts of nitrogen compared to the commercially available ACs by a factor of three. At pH 2, -NH functionalities on the AC surface are protonated to $-NH_2^+$ groups, efficiently attracting the negatively charged Cr(VI) species. The benefit of the nitrogen functionalities towards adsorption outweighs the increased reduction effects that are associated with the functionalities, as suggested by [29]. Furthermore, more reduction of Cr(VI) at the surface of the commercial ACs can be attributed to their lower O content, where ACBSG has roughly double the amount of O in its chemical structure. The higher amount of O in the AC can be beneficial in 2 ways for the adsorption of chromium: less reduction of Cr(VI) to Cr(III), and more possibilities to make oxygen-Cr(III) complexes, resulting in a lower concentration of total chromium in the final solution [43,44].

Results for the bulk density determination are displayed in Table 2-6 on page 95. Both Norit GAC1240 and Filtrasorb F400 have significantly higher bulk densities compared to ACBSG. The ACBSGs are prepared from biomass, typically having a lower bulk density than bituminous coal.

The results of the PSD are displayed in Table 2-7 on page 96 as the percentage of particles that fall into a specific size category and in Figure 2-11 on page 97 as the cumulative amount of particles that have a size lower than an indicated value. Even though the samples were sieved to particle sizes bigger than 63 μm prior to

use, a small percentage of each sample is still present in the category <65.5 µm. Both Norit GAC1240 and Filtrasorb F400 have a narrow PSD, with the most particles having a size between 409 and 878 µm. ACBSG05 and ACBSG07 have a smaller size distribution with most particles between 191 and 351 µm. Intensive stirring for 10 or 20 minutes breaks down bigger particles and moves the distribution towards lower sizes. This effect is more notable for the commercial ACs, whereas the ACBSGs are more rigid.

Table 2-3 Ash content and elemental analysis of BSG with standard deviations of selected ACBSGs and commercial ACs, in wt%

	BSG	ACBSG05 [21]	ACBSG07 [21]	Norit GAC1240	Filtrasorb F400
Ash (%)	3.2 ± 0.1	14.4 ± 0.5	14.6 ± 0.3	7.9± 0.1	7.0 ± 0.1
C (%)	59.5 ± 0.2	71.0 ± 1.4	70.5 ± 0.9	85.3 ± 2.1	83.7± 1.4
H (%)	6.9 ± 0.2	1.6 ± 0.1	1.5 ± 0.1	0.6 ± 0.1	0.7± 0.1
N (%)	4.4 ± 0.2	2.7 ± 0.1	2.5 ± 0.1	0.8 ± 0.1	0.9±0.1
S (%)	<DL	<DL	<DL	<DL	<DL
O (%) (from difference)	36.1 ± 1.4	10.4 ± 1.5	10.9 ± 0.9	5.4 ± 1.5	7.7 ± 0.4
N/C atomic ratio	0.09	0.04	0.04	0.01	0.01
O/C atomic ratio	0.73	0.15	0.15	0.01	0.09

(*) <DL : below detection limit limit (for S, approximately 0.2%)   (**) O calculated as 100% - Ash – C – H – N – S

2.4.4.3 Adsorption kinetics

Evaluation of the Cr(VI) and Cr$_{tot}$ adsorption kinetics is performed using both Lagergrens pseudo first order (PFO) model [45-47] and the pseudo second order (PSO) model as proposed by Ho and McKay [48,49]. The goodness of fit is evaluated using the correlation coefficient value (R^2). Both models are fitted using non-linear regression. The PFO model can be expressed as:

$$q_t = q_e(1 - e^{-k_1 t})$$
<div align="right">Equation 2-1</div>

where q_t and q_e are the Cr adsorption capacities (in mg Cr/ g AC) at time t and at time of equilibrium and k_1 (min^{-1}) is the PFO rate constant.

The PSO model can be expressed as:

$$q_t = \frac{k_2 q_e^2 t}{1 + k_2 q_e t}$$
<div align="right">Equation 2-2</div>

Where k_2 (min^{-1}) is the PSO rate constant.

Diffusion into the pores of the AC plays an important role in the rate of adsorption. The kinetic results are also analysed by the intraparticle diffusion model as proposed by Webber and Morris [50] to determine the rate controlling step. This model is expressed as:

$$q_t = k_{id}\sqrt{t} + C$$
<div align="right">Equation 2-3</div>

Were k_{id} (mg/g h$^{1/2}$) expresses the rate constant of intraparticle transport and C_i (mg/g) the intercept of a stage i, associated with the thickness of the boundary layer [19,51].

The results of the kinetic experiments up to 24 h for ACBSG05, ACBSG07, Norit GAC1240 and Filtrasorb F400 are displayed in Figure 2-8 and Figure 2-9. After 16 h, equilibrium is reached for all ACs. 90% of the adsorbed equilibrium concentration is already reached after 6 h for all ACs. The ACBSGs show a slightly faster adsorption response to Cr(VI) compared to both Norit GAC 1240 and Filtrasorb 400.
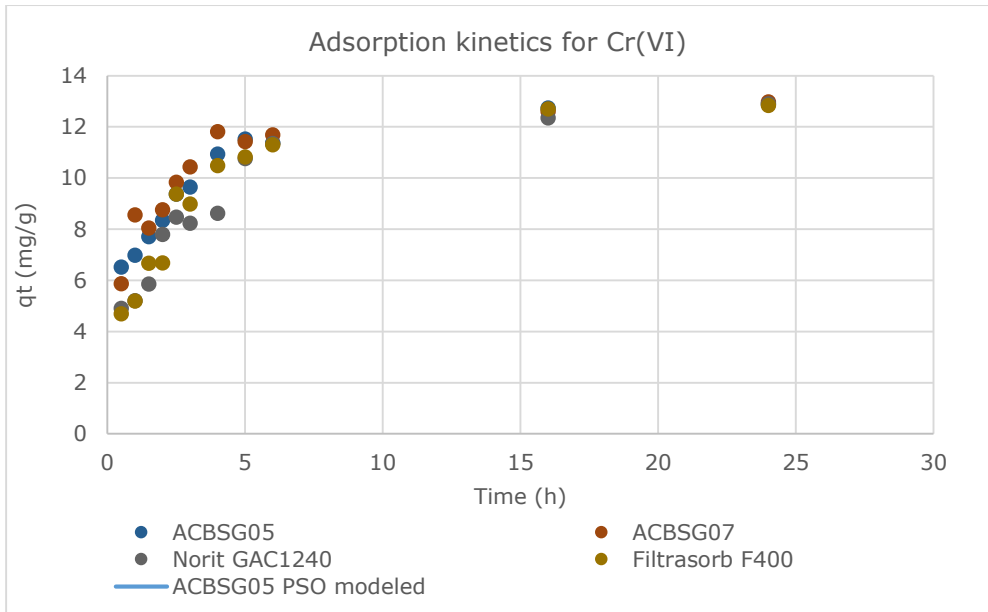
Figure 2-8 Adsorption kinetics for Cr(VI) on unmodified ACs (20 mg AC + 25 mL 10 mg/L Cr(VI) solution at pH 2)
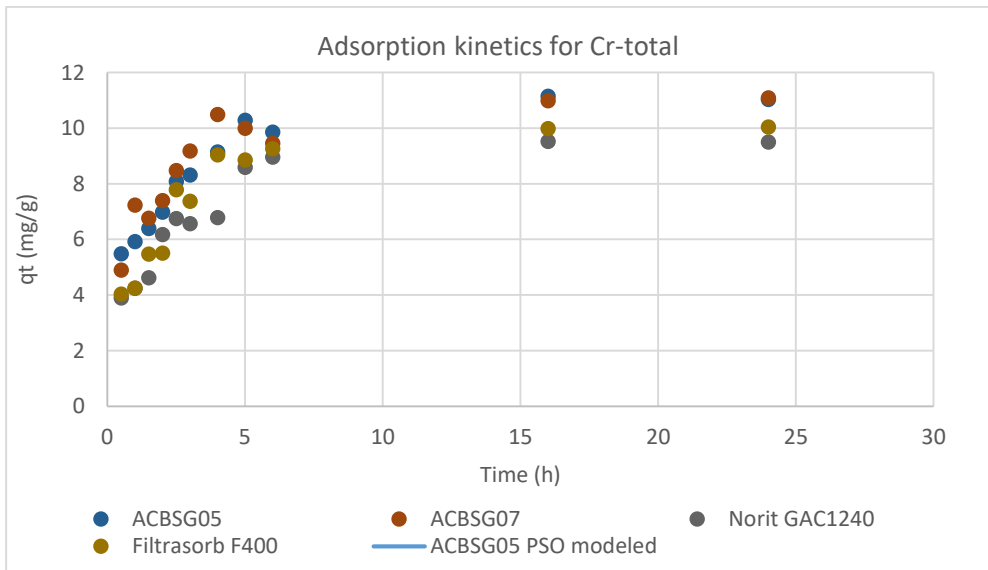
Figure 2-9 Adsorption kinetics for Crtot on unmodified ACs (20 mg AC + 25 mL 10 mg/L Cr(VI) solution at pH 2)

PFO and PSO reaction rates are determined for ACBSGs as well as for the commercially available ACs, both for Cr(VI) and total Cr. The reaction kinetics are slightly better fitted by the PSO model, Table 2-8 on page 98 displays the results for all kinetic experiments. This suggests that chemisorption is the main uptake mechanism. The kinetic constant for the PSO model shows that ACBSG adsorbs Cr(VI) faster than commercial AC (kinetic constant k_2= 0.091 min^{-1} and k_2= 0.107 min^{-1} for ACBSG05 and ACBSG07 respectively). This higher kinetic rate might be due to the combination of adsorption and reduction of the Cr(VI). For Cr$_{tot}$, the kinetic constant is the highest for the ACBSG07 (k_2 = 0.118 min^{-1}). For both ACBSG samples the kinetics constants for total chromium are similar to the Cr(VI) kinetic constants. This implies that the rate at which Cr(VI) is removed is approximately equal to the rate of the removal of Cr$_{tot}$ and that little Cr(III) is formed. For the commercially available ACs the Cr(VI) kinetic constant is significantly lower than the one for Cr$_{tot}$. This implies that Cr(VI) is removed slower than all the Cr species available and that Cr(III) is removed simultaneously. The in-situ formed Cr(III) must be formed almost immediately after the introduction of the AC. The oxidation/reduction mechanism taking place at the surface with less oxygen slows down the adsorption of Cr(VI) significantly on the commercial ACs.
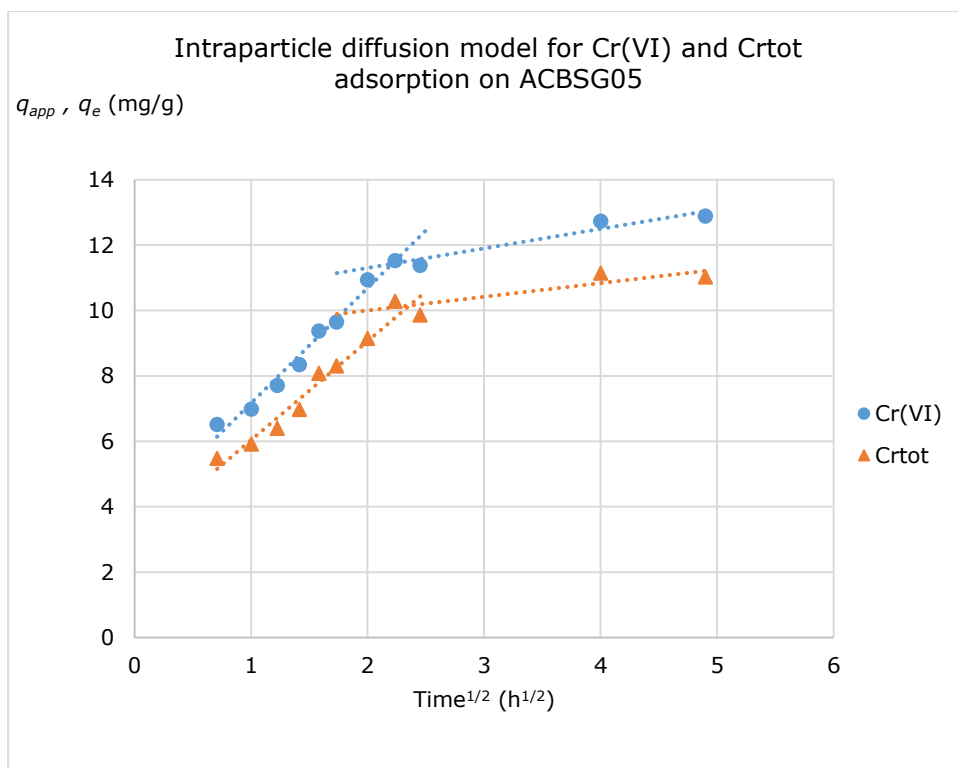
Figure 2-10 Intraparticle diffusion model for Cr(VI) and Cr$_{tot}$ adsorption on ACBSG05 with q_{app} for Cr(VI) and q_e for Cr$_{tot}$

The application of the intraparticle diffusion model shows two distinct linear regions in each of the plots for each of the ACs. As example, Figure 2-10 displays one of these plots for Cr(VI) (q_{app}) and Cr$_{tot}$ (q_e) for ACBSG05. Since none of the lines pass through zero, intraparticle diffusion is not the rate limiting step in the observed time period, but boundary layer determines the adsorption rate. After the chromium ions passes through the mesopores, the diffusion into the micropores becomes slower. The lower slope of the second part of the plot indicates this micropore diffusion as the rate limiting step. Results for the first rate constant of all ACs were summarised in Table 2-4 and Table 2-5. The initial boundary layer (C) is the thinnest for Filtrasorb F400 and during the diffusion in the micropores the boundary effect is the same for the commercial samples. The ACBSG also exhibit similar boundary layers in the second phase. The ACBSGs have plenty of heteroatoms and display a higher boundary effect compared to the

commercial samples. The initial diffusion rates are the highest for Filtrasorb F400 and ACBSG07. The stronger reduction mechanism in Norit GAC1240 and Filtrasorb F400 slows down the adsorption process itself and not the intraparticle diffusion. During the micropore diffusion, the diffusion rates are almost equal for each AC for chromium total, but a higher rate is found for the commercial ACs for Cr(VI). This effect can also be attributed to the reduction that is taking place.

Table 2-4 Calculated kinetic constants for the intraparticle diffusion model for the first linear part of the model

	Chromium-VI			Chromium-total		
Sample	K_{1d} (mg/g h$^{1/2}$)	C (mg/g)	R^2	K_{1d} (mg/g h$^{1/2}$)	C (mg/g)	R^2
Norit GAC 1240	3.45	2.26	0.874	2.68	1.88	0.869
Filtrasorb F400	4.80	0.83	0.924	4.08	0.58	0.909
ACBSG05	3.52	3.65	0.972	3.02	3.02	0.761
ACBSG07	4.48	2.63	0.994	4.14	1.84	0.985

Table 2-5 Calculated kinetic constants for the intraparticle diffusion model for the second linear part of the model

	Chromium-VI			Chromium-total		
Sample	K_{2d} (mg/g h$^{1/2}$)	C (mg/g)	R^2	K_{2d} (mg/g h$^{1/2}$)	C (mg/g)	R^2
Norit GAC 1240	0.75	9.31	0.96	0.32	8.05	0.84
Filtrasorb F400	0.76	9.32	0.93	0.43	8.08	0.90
ACBSG05	0.60	10.1	0.93	0.42	9.16	0.76
ACBSG07	0.50	10.6	0.92	0.43	9.10	0.94

2.4.5 Conclusion

AC from BSG is a viable adsorbent for removal of chromium from waste water streams at the tested concentration of 10 mg/L Cr at pH 2, using realistic industrial AC dosages. It is able to remove all the toxic Cr(VI) from the solutions combining adsorption and reduction. To remove most of total chromium, an optimum dosage of approximately 0.75 g AC/L was found, resulting in an increased reduction to the less efficiently adsorbed Cr(III). The reduction is enhanced in the commercial ACs, Filtrasorb F400 and Norit GAC 1240, due to their lower oxygen and nitrogen content. This resulted in higher residual concentrations of total chromium. The benefit of enhanced adsorption due to the nitrogen content outweighs the possible increase in reduction sites on the ACBSG. Redox reactions during adsorption experiments are hardly accounted for in current literature and not investigated. Kinetic experiments also reveal that the ACBSGs have a faster removal rate than the two commercially available ACs. The adsorption on these ACs is slowed down by the less pronounced reduction reaction, producing Cr(III) which adsorbs less favourably, since the AC surface at pH 2 is positively charged.

2.4.6 Funding

2.4.7 References

[1] C. Xiros, P. Christakopoulos, Biotechnological potential of brewers spent grain and its recent applications, Waste and Biomass Valorization, **2012**, 2, 213-232.

[2] S.I. Mussatto, G. Dragone, I.C. Roberto, Brewer's spent grain: Generation, characteristics and potential applications, Journal of Cereal Science, **2006**, 1-14.

[3] D. Deconinck, L. Capon, B. Clerinx, J. Couder, Indicatoren voor duurzame ontwikkeling in de belgische industrie, **2001**.

[4] Eurostat. Prodcom -statistics by product, **2011**.

[5] D. Cook, Brewers' grains: Opportunities about, Brewers' guardian, Advantage Publishing Ltd: 2011; Vol. November/December **2011**.

[6] S.I. Mussatto, M. Fernandes, G.J.M. Rocha, J.J.M.T. Orfao, I.C. Roberto, Production, characterization and application of activated carbon from brewer's spent grain lignin, Bioresource Technology, **2010**, 2450-2457.

[7] H. Marsh, F. Rodríguez-Reinoso, Activated carbon, Elsevier Science & Technology books: **2006**.

[8] S. Biniak, G. Szymanski, J. Siedlewski, A. Swiatkowski, The characterization of activated carbons with oxygen and nitrogen surface groups, Carbon, **1997**, 35, 1799-1810.

[9] A. Nieto-Márquez, A. Pinedo-Flores, G. Picasso, E. Atanes, R. Sun Kou, Selective adsorption of Pb^{2+}, Cr^{3+} and Cd^{2+} mixtures on activated carbons prepared from waste tires, Journal of Environmental Chemical Engineering, **2017**, 5, 1060-1067.

[10] B.H. Hameed, A.A. Rahman, Removal of phenol from aqueous solutions by adsorption onto activated carbon prepared from biomass material, Journal of Hazardous Materials, **2008**, 576-581.

[11] G. Yang, H. Chen, H. Qin, Y. Feng, Amination of activated carbon for enhancing phenol adsorption: Effect of nitrogen-containing functional groups. Applied Surface Science, **2014**, 293, 299-305.

[12] U. Beker, B. Ganbold, H. Dertli, D.D. Gülbayir, Adsorption of phenol by activated carbons: Influence of activation methods and solution ph. Energy Conversion and Management, **2010**, 235-240.

[13] B. Wanassi, I. Ben Hariz, C.M. Ghimbeu, C. Vaulot, M. Ben Hassen, M. Jeguirim, Carbonaceous adsorbents derived from textile cotton waste for the removal of alizarin s dye from aqueous effluent: Kinetic and equilibrium studies, Environmental Science and Pollution Research, **2017**, 24, 10041-10055.

[14] A.S.N. Mahmood, J.G. Brammer, A. Hornung, A. Steele, S. Poulston, The intermediate pyrolysis and catalytic steam reforming of brewers spent grain, Journal of Analytical and Applied Pyrolysis, **2013**, 103, 328-342.

[15] K. Vanreppelen, S. Vanderheyden, T. Kuppens, S. Schreurs, J. Yperman, R. Carleer, Activated carbon from pyrolysis of brewer's spent grain: Production and adsorption properties, Waste Management & Research, **2014**, 32(7), 634-45

[16] A. Bagreev, S. Bashkova, T.J. Bandosz, Adsorption of SO_2 on activated carbons: The effect of nitrogen functionality and pore size, Langmuir, **2002**, 18, 1257-1264.

[17] A. Bagreev, J.A. Menendez, I. Dukhno, Y. Tarasenko, T.J. Bandosz, Bituminous coal-based activated carbons modified with nitrogen as adsorbents of hydrogen sulfide, Carbon, **2004**, 42, 469-476.

[18] R.A. Hayden, Method for reactivating nitrogen-treated carbon catalysts, Google Patents: **1995**.

[19] E.G. Lorenc-Grabowska, M.A. Diez, Kinetics and equilibrium study of phenol adsorption on nitrogen-enriched activated carbons, Fuel, **2013**, 114, 235-243.

[20] S. Matzner, H.P. Boehm, Influence of nitrogen doping on the adsorption and reduction of nitric oxide by activated carbon, Carbon, **1998**, 36, 1697-1709.

[21] T.J. Bandosz, C.O. Ania, Surface chemistry of activated carbons and its characterization. In Activated carbon surfaces in environmental remediation, Bandosz, Elsevier: **2006**; 159-229.

[22] VMM, Zware metalen in het grondwater in Vlaanderen, Vlaamse Milieumaatschappij, **2013**.

[23] D.P. Mohan, C.U. Pittman Jr., Activated carbons and low cost adsorbents for remediation of tri- and hexavalent chromium from water, Journal of Hazardous Materials, **2006**, 762-811.

[24] U.S. Department of Labor - Occupational Safety and Health Administration, Hexavalent chromium, **2009**.

[25] D.T. Duranoglu, A.W. Trochimczuk, U. Beker, Kinetics and thermodynamics of hexavalent chromium adsorption onto activated carbon derived from acrylonitrile-divinylbenzene copolymer, Chemical Engineering Journal, **2012**, 193-202.

[26] F. Di Natale, A. Lancia, A. Molino, D. Musmarra, Removal of chromium ions form aqueous solutions by adsorption on activated carbon and char, Journal of Hazardous Materials, **2007**, 381-390.

[27] A. Kumar, H.M. Jena, Adsorption of cr(vi) from aqueous phase by high surface area activated carbon prepared by chemical activation with $ZnCl_2$, Process Safety and Environmental Protection, **2017**, 109, 63-71.

[28] M.K. Rai, G. Shahi, V. Meena, R. Meena, S. Chakraborty, R.S. Singh, B.N. Rai, Removal of hexavalent chromium Cr(VI) using activated carbon prepared from mango kernel activated with H_3PO_4, Resource-Efficient Technologies, **2016**, 2, Supplement 1, S63-S70.

[29] M. Valix, W.H. Cheung, K. Zhang, Role of heteroatoms in activated carbon for removal of hexavalent chromium from wastewaters, Journal of Hazardous Materials, **2006**, 135, 395-405.

[30] S.R.H. Vanderheyden, R. Van Ammel, K. Sobiech-Matura, K. Vanreppelen, S. Schreurs, W. Schroeyers, J. Yperman, R. Carleer, Adsorption of cesium on different types of activated carbon, Journal of Radioanalytical and Nuclear Chemistry, **2016**, 1-10.

[31] ASTM. Standard test method for the determination of hexavalent chromium in workplace air by ion chromatography and spectrophotometric measurement using 1,5-diphenylcarbazide; **2002.**

[32] A.K. Bhattacharya, T.K. Naiya, S.N. Mandal, S.K. Das, Adsorption, kinetics and equilibrium studies on removal of cr(vi) from aqueous solutions using different low-cost adsorbents, Chemical Engineering Journal, **2008**, 137, 529-541.

[33] R. Gottipati, S. Mishra, Preparation of microporous activated carbon from aegle marmelos fruit shell and its application in removal of chromium(vi) from aqueous phase, Journal of Industrial and Engineering Chemistry, **2016**, 36, 355-363.

[34] N.K. Hamadi, X.D. Chen, M.M. Farid, M.G.Q. Lu, Adsorption kinetics for the removal of chromium(vi) from aqueous solution by adsorbents derived from used tyres and sawdust. Chemical Engineering Journal, **2001**, 84, 95-105.

[35] T. Karthikeyan, S. Rajgopal, L.R. Miranda, Chromium(vi) adsorption from aqueous solution by hevea brasilinesis sawdust activated carbon, Journal of Hazardous Materials, **2005**, 124, 192-199.

[36] Y.-J. Zhang, J.-L. Ou, Z.-K. Duan, Z.-J. Xing, Y. Wang, Adsorption of Cr(VI) on bamboo bark-based activated carbon in the absence and presence of humic acid, Colloids and Surfaces A: Physicochemical and Engineering Aspects, **2015**, 481, 108-116.

[37] A. El Nemr, A. El-Sikaily, A. Khaled, O. Abdelwahab, Removal of toxic chromium from aqueous solution, wastewater and saline water by marine red alga pterocladia capillacea and its activated carbon, Arabian Journal of Chemistry, **2015**, 8, 105-117.

[38] M. Gueye, Y. Richardson, F.T. Kafack, J. Blin, High efficiency activated carbons from african biomass residues for the removal of chromium(VI) from wastewater, Journal of Environmental Chemical Engineering, **2014**, 2, 273-281.

[39] J. Rivera-Utrilla, M. Sánchez-Polo, Adsorption of Cr(III) on ozonised activated carbon, Importance of cπ—cation interactions, Water Research, **2003**, 37, 3335-3340.

[40] P. Miretzky, A.F. Cirelli, Cr(VI) and Cr(III) removal from aqueous solution by raw and modified lignocellulosic materials: A review, Journal of Hazardous, Materials **2010**, 180, 1-19.

[41] D. Park, Y.-S. Yun, J.M. Park, XAS and XPS studies on chromium-binding groups of biomaterial during Cr(VI) biosorption, Journal of Colloid and Interface Science, **2008**, 317, 54-61.

[42] Z.-G. Ng, J.-W. Lim, H. Daud, S.-L. Ng, M.J.K. Reassessment of adsorption–reduction mechanism of hexavalent chromium in attaining practicable mechanistic kinetic model, Process Safety and Environmental Protection, **2016**, 102, 98-105.

[43] Z. Reddad, C. Gerente, Y. Andres, P.L Cloirec, Mechanisms of Cr(III) and Cr(VI) removal from aqueous solutions by sugar beet pulp, Environmental Technology, **2003**, 24, 257-264.

[44] J. Chang, S. Chen, H. Zhang, X. Wang, Removal behaviors and mechanisms of hexavalent chromium from aqueous solution by cephalosporin residue and derived chars, Bioresource Technology, **2017**, 238, 484-491.

[45] S.Y. Lagergren, Zur theorie der sogenannten adsorption gelöster stoffe, kungliga svenska vetenskapsakademiens, Handlingar, **1898**, 24, 1-39.

[46] R.-L. Tseng, F.-C. Wu, R.-S. Juang, Characteristics and applications of the lagergren's first-order equation for adsorption kinetics, Journal of the Taiwan Institute of Chemical Engineers, **2010**, 41, 661-669.

[47] N. Pradhan, E.R. Rene, P.N.L. Lens, L. Dipasquale, G. D'Ippolito, A. Fontana, A.E. Panico, G. Esposito Adsorption behaviour of lactic acid on granular activated carbon and anionic resins: Thermodynamics, isotherms and kinetic studies, Energies, **2017**, 10, 665.

[48] Y.S. Ho, G. McKay, Kinetic models for the sorption of dye from aqueous solution by wood, Process Safety and Environmental Protection, **1998**, 76, 183-191.

[49] L. Limousy, I. Ghouma, A. Ouederni, M. Jeguirim, Amoxicillin removal from aqueous solution using activated carbon prepared by chemical activation of olive stone, Environmental Science and Pollution Research, **2017**, 24, 9993-10004.

[50] W.J. Weber, J.C. Morris, Kinetics of adsorption on carbon from solution, Journal of the Sanitary Engineering Division, **1963**, 89, 31-59.

[51] H. Qiu, B.-C. Pan, Q.-J. Zhang, W.-M. Zhang, Q.-X. Zhang, Critical review in adsorption kinetic models, Journal of Zhejiang university science A, **2009**, 10, 716-724.

2.4.8 Supplementary materials

Table 2-6 Bulk density (in g/cm³) for each of the ACs according to ASTM D 2854 – 96

Sample	Bulk density (g/cm³)		
Norit GAC1240	0.453	±	0.012
Filtrasorb F400	0.428	±	0.008
ACBSG02	0.356	±	0.01
ACBSG05	0.361	±	0.008

Table 2-7 Particle size distribution (in %) of the used ACs before and after stirring

Particle size (µm)	Norit GAC 1240		Filtrasorb F400		ACBSG02		ACBSG05	
	T=0 min	T=10 min	T= 0 min	T = 20 min	T= 0 min	T = 20 min	T= 0 min	T = 20 min
< 65.5	1.42	7.86	2.23	16.62	2.69	3.83	1.22	1.97
65.5 - 140.6	0.45	2.14	1.21	4.74	13.74	14.26	10.48	10.75
140.6 - 163.8	0.04	0.21	0.17	0.73	5.11	5.28	5.7	5.81
163.8 - 190.8	0.07	0.27	0.33	0.93	5.98	6.18	7.28	7.41
190.8 - 222.3	0.17	0.52	0.66	1.36	6.84	7.05	8.63	8.77
222.3 - 259.0	0.37	0.9	1.15	1.95	7.62	7.82	9.56	9.68
259.0 - 301.7	0.69	1.33	1.87	2.67	8.26	8.39	9.99	10.07
301.7 - 351.5	1.2	1.85	3.01	3.71	8.78	8.79	10.15	10.17
351.5 - 409.5	2.12	2.67	4.93	5.46	9.28	9.12	9.53	9.4
409.5 - 477.0	3.91	4.23	7.83	8.36	9.04	8.65	8.57	8.3
477.0 - 555.7	7.8	7.61	11.87	11.87	8.2	7.67	7.25	6.84
555.7 - 647.4	14.35	13.45	16.46	15.33	6.83	6.23	5.68	5.25
647.4 - 754.2	26.32	24.18	23.9	16.44	4.99	4.42	3.98	3.66
754.2 - 878.7	41.15	32.78	24.38	9.85	2.63	2.29	2.02	1.91

Percentages calculated as the percentage of the particles in a certain particle size range
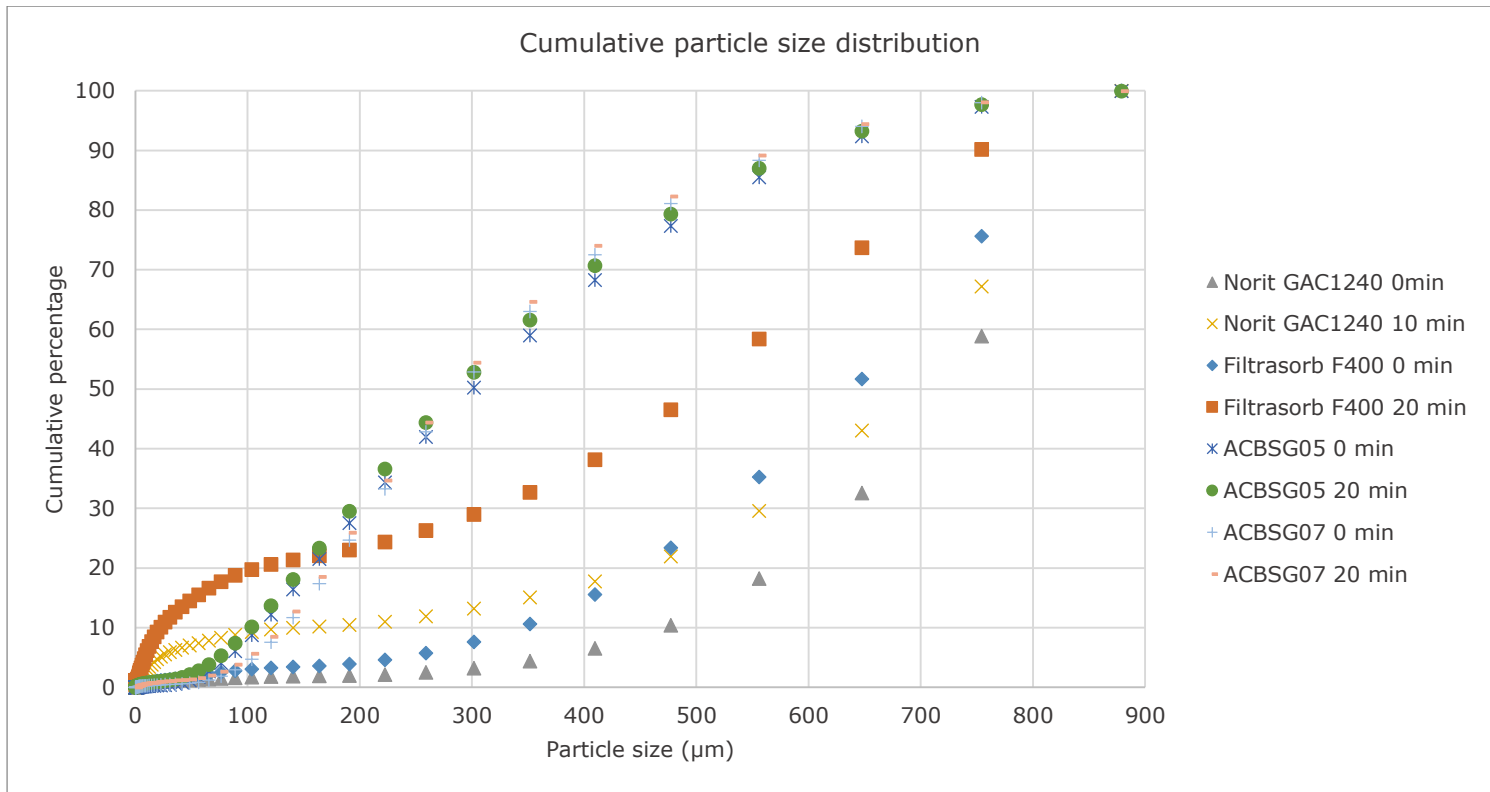
Figure 2-11 Cumulative particle size distribution of selected ACs

Table 2-8 Calculated kinetic constants for pseudo first order (PFO) and pseudo second order (PSO) kinetic models

Sample name	Chromium-VI						Chromium-total					
	PFO			PSO			PFO			PSO		
	k_1 (min^{-1})	q_{max} (mg/g)	R^2	k_2 (min^{-1})	q_{max} (mg/g)	R^2	k_1 (min^{-1})	q_{max} (mg/g)	R^2	k_2 (min^{-1})	q_{max} (mg/g)	R^2
Norit GAC 1240	0.47	12.08	0.904	0.047	13.55	0.934	0.52	9.16	0.899	0.072	10.21	0.92
Filtrasorb F400	0.5	12.31	0.94	0.049	13.84	0.953	0.55	9.78	0.926	0.071	10.92	0.924
ACBSG02	0.77	11.82	0.823	0.091	13.04	0.915	0.7	10.36	0.842	0.094	11.41	0.909
ACBSG05	0.92	11.87	0.838	0.107	13.1	0.838	0.88	10.26	0.836	0.118	11.33	0.911

2.5 Activated carbon modification resulting in an enhanced Cr(VI) removal[5]

Sara Rita H. Vanderheyden[a], Jan Yperman[a], Robert Carleer[a], Sonja Schreurs[b],

[a] Hasselt University, Centre for Environmental Sciences, Research Group of Analytical and Applied Chemistry, Agoralaan – Building D, 3590 Diepenbeek, Belgium; e-mail: jan.yperman@uhasselt.be; robert.carleer@uhasselt.be

[b] Hasselt University, Centre for Environmental Sciences, Research Group of Nuclear Technology, Agoralaan – Building H, 3590 Diepenbeek, Belgium; e-mail: sonja.schreurs@uhasselt.be

* Corresponding author: Sara R.H. Vanderheyden, sara.vanderheyden@uhasselt.be +3211 268211

ABSTRACT

Two modification methods are used to enhance the adsorption properties of Cr(VI) of several activated carbons (AC). AC performance from brewer's spent grain (BSG) is compared to two commercials ACs: Norit GAC 1240 and Filtrasorb F400. The first modification consists of an oxidation of the surface using acidic and basic reagents. Elemental analysis reveals the oxidation of AC, but a removal of surface groups deteriorates adsorption properties. The second modification incorporates a copolymer with a quaternary ammonium end group on the surface of the AC. After copolymer modification a significant increase of nitrogen functionalities (+10%) is realized. An outspoken improvement (a factor 5) in adsorption capacity and kinetics are proven to be solely caused by the copolymer. No synergic effect is found. Unmodified ACBSG is proven to exhibit the fastest adsorption kinetics for Cr(VI), but Cr_{tot} is removed fasted by copolymerised AC.

---

[5] References for this article can be found on page 122 in section 2.5.6

2.5.1 Introduction

Hexavalent chromium, Cr(VI), is present in all surface waters due to industrial and geological deposits [1, 2]. In contrast to the essential Cr(III), Cr(VI) is carcinogenic and a toxic pollutant for both plants and living organisms [3-6]. The removal of Cr(VI) from aqueous solutions has been investigated using different adsorbents and composite materials [7-9]. The combination of adsorptive and reductive properties on both biomass, bio-char, activated carbon (AC) or composite materials can remove Cr(VI) while also reducing it to Cr(III) [10-13]

To improve specific adsorption of Cr(VI), different modification techniques are investigated [14-17]. This work focuses on two types of modification in particular. The first modification is oxidation/acidification of the AC surface using nitric acid. Rivera-Utrilla et al. [14] concluded that treatment of AC with HNO_3 chemically enhanced the amount of surface oxygen functionalities such as carboxylic, phenolic and lactonic groups. This enhancement can lead to a better adsorption of metal ions, as a result of possible formation of complexes on the AC [18]. Especially for removal of chromium, Liu et al. [15] suggest a dual pathway process, where Cr(VI) is both adsorbed and reduced to Cr(III) by oxidation of the AC surface. The second modification technique involves the treatment of the AC with amine-crosslinked copolymers for improved chelation properties towards metal ions, Cr(VI) in particular [16]. In this approach a nitrogen-rich copolymer is grafted on the available hydroxyl surface groups of the AC [17].

The goal of this work is to modify two commercial AC and AC derived from brewers' spent grain (BSG) for enhanced Cr(VI) adsorption and to test each of these for Cr(VI) adsorption. Worldwide BSG production is estimated at 30 Mt per year [19] and this waste is currently mostly fed to ruminants [20]. Possibilities for its use in different applications have been researched [19-29]. Production of in-situ nitrogenized AC is proven to be an economically feasible process [30]. Two modifications are performed, acid treatment and grafting by a copolymer, to

improve adsorption properties towards Cr(VI) and total Cr. Secondly, these ACs are characterized using complementary analytical techniques to monitor both modifications. Finally, a comparison between the adsorption isotherms and kinetics for Cr(VI) and total Cr is made.

2.5.2 Materials and methods

Milli-Q Millipore water (18.2 MΩ cm^{-1} conductivity) and analytical grade reagents are used in each experiment. Triethylamine, diethylenetriamine and epichlorohydrin are all 'for synthesis' grade. Norit GAC 1240 (Cabot Carbon) and Filtrasorb 400 (Calgon Carbon) are used to compare results of lab-scale AC with industrially available ACs.

2.5.2.1 Pyrolysis and activation

A two-step pyrolysis/activation reactor is used to prepare the AC from BSG, this set-up is described in [30]. Oven-dried BSG is inserted in the reactor and pyrolysed from room temperature to 800°C with a continuous heating rate of 10 °C/min in a nitrogen flow of 80 mL/min. An isothermal period at 800 °C with water injection is used for activation. ACBSG05 is activated at 800 °C for 30 min with 10 mL of water. ACBSG07 is also activated at 800 °C but for a period of 45 min with 15 mL of water. These ACs were also produced for previous work in [13, 21, 30].

2.5.2.2 AC modification

Two modifications are applied to ACBSG and to both commercially available ACs. The first modification is based on Liu et al. [15] and uses an acid/base (A/B) modification with HNO$_3$. Approximately 8 g of AC with 40 mL of 7 M HNO$_3$ solution is refluxed at 90 °C for 15 h and subsequently dried at 105 ± 5 °C for 24 h. The dried AC is then added to 160 mL of a 1 M NaOH solution and shaken for 72 h at room temperature. The sample is washed until the effluent has a pH of approximately 7. Then it is dried again at 105 ± 5 °C for 24 h. The acid/base modified ACs are denoted with their name followed by the A/B notation.

The second modification consists of grafting an amino-crosslinked copolymer (CP) on AC [16, 17]. In a typical preparation, 2 g of AC is introduced into a three-neck round bottom flask, then stirred and heated to 80 °C. 5 mL of N,N-

dimethylformamide (DMF) and 5 mL of epichlorohydrin are added. After one hour, 3 mL of diethylenetriamine is added dropwise. Additionally, 10 mL of DMF is added to assure homogeneity of the mixture. After another one hour, 5 mL of triethylamine is added. Finally, the sample is filtered after one hour, washed with Milli-Q and dried in an oven at 70 ± 5 °C for 72 h. The percentage of CP was calculated gravimetrically, and checked by elemental analysis These ACs are denoted with their name followed by the CP notation. Apart from this standard preparation, different dilutions of reagent concentration (a half, a fifth and a tenth of the reagents) are applied to the best performing AC (ACBSG07) to achieve lower modification grades of the AC, and their percentage was calculated based on the reagent amounts. The adsorption capacity of these ACs with different grades of CP-modification is compared to determine a possible synergic effect.

2.5.2.3 AC characterisation

Characterisation of non-modified ACBSGs has already been performed [13, 30]. All modified ACs are analysed in a similar way as described in [18]. The AC and their modifications are sieved to particle size between 63 μm and 1 mm for characterisation and adsorption experiments.

Samples are mixed with liquid nitrogen and ground with mortar and pestle for Elemental Analysis (Thermo Finnigan Element Analysis Flash EA 1112). Calibration of the equipment is performed with BBOT (2,5-bis (5-tert-butyl-benzoxazol-2-yl) thiophene)). Samples are measured in quadruplicate. The ash content is calculated according ASTM 2866-11, based on dry oxidation at 650 ± 25 °C for 3-6 h. Oxygen is calculated by difference.

To determine surface groups, a modified Boehm titration is performed as proposed by Velghe et al. [31]. 200 mg of AC is put into contact with 25 mL of either a 0.100 M HCl or NaOH solution and shaken for 24 h in a thermostatic shaker. Titration is done by a Metrohm 794 Basic Titrino with 0.100 M NaOH or HCl respectively, in a nitrogen atmosphere.

SEM imaging is performed using a Hitachi TM3000 microscope for ACBSG02 and Norit GAC1240 and their modifications. The effect of AC type and modification is expected to be the same for ACBSG05 and Filtrasorb F400.

2.5.2.4 Adsorption isotherms and adsorption kinetics

Adsorption isotherm and kinetic experiments are performed using a solution of 10 mg/L Cr(VI) at pH 2. This solution is prepared using potassium dichromate and hydrochloric acid. The pH is chosen to promote Cr(VI) adsorption [32, 33] and is monitored during the adsorption process by measuring after 4 and 20 h. Drifting pH was adjusted using a 1 M HCl solution.

5 to 100 mg of unmodified AC or modified AC is placed into closed vials and 25 mL of a 10 mg/L Cr(VI) solution is added and shaken for 24 h at room temperature. Based on the obtained adsorption isotherms of unmodified ACs, three additional experiments are performed by adding 10 mg of AC to 100, 200 and 500 mL of the same Cr(VI) solution. After shaking, the solution is filtered using ashless filters (A14, Carl Roth, Karlsruhe). The residual concentration of Cr(VI) is measured using the diphenylcarbazide method (DPC), measuring absorbance at 540 nm for both filtered and standard solutions [34]. Cr_{tot} is determined via inductively coupled plasma atomic emission spectroscopy (ICP-AES, PE Optima 8300). This experiment is performed in duplo.

The adsorption capacity at equilibrium (q_e, in mg Cr/g AC) is calculated as follows:

$$q_e = \frac{(c_{initial} - c_{equilibrium}) * V}{m_{AC}}$$
<div align="right">Equation 2-4</div>

Where $c_{initial}$ (mg/L) is the concentration of the Cr solution added to the vial, $c_{equilibrium}$ (mg/L) the concentration of Cr after filtration, V the added volume (L) and m_{AC} (g) is the amount of AC added to the vial. These adsorption capacities are calculated for both Cr(VI) and Cr_{tot}. For Cr(VI) adsorption capacities, an apparent adsorption capacity is calculated in the same way to provide a q_{app}. This capacity is partially determined by adsorption and partially by reduction of the Cr(VI) to Cr(III). Removal percentage is calculated as follows:

$$Removal\ percentage = \frac{c_{initial} - c_{equilibrium}}{c_{initial}} * 100\%$$
<div align="right">Equation 2-5</div>

To determine whether the adsorbed amount (q_{app} in mg Cr(VI)/g AC or q_e in mg Cr_{tot}/g AC) is the result of a synergic effect between the copolymer and the AC, adsorption of Cr(VI) and total Cr are compared to unmodified AC adsorption

results. ACs with different amounts of copolymer are added in two dosages: 25 mg of AC is added to 25 mL of a 10 mg/L Cr(VI) solution for an intermediate dosage setting (1 g AC/L), while 10 mg of AC is added to 200 mL of 10 mg/L Cr(VI) solution for a low dosage setting (50 mg AC/L).

Kinetic studies are performed for both the unmodified [13] and modified ACs. 25 mL of a 10 mg/L Cr(VI) solution is added to 20 mg of AC in different vials and shaken during different time intervals. Samples are filtrated using ashless filters (Roth A14) and measured as described above. This test is performed in duplo.

Lagergrens pseudo first order (PFO) model [35, 36] and the pseudo second order (PSO) model [37] are used to evaluate the results. The goodness of fit is evaluated using the correlation coefficient value (R^2). Both models are fitted using non-linear regression. The PFO model can be expressed as:

$$q_t = q_e(1 - e^{-k_1 t})$$

<div align="right">Equation 2-6</div>

q_t and q_e are the Cr adsorption capacities (in mg Cr/ g AC) at time t and at time of equilibrium and k_1 (min^{-1}) is the PFO kinetic rate constant.

The PSO model can be expressed as:

$$q_t = \frac{k_2 q_e^2 t}{1 + k_2 q_e t}$$

<div align="right">Equation 2-7</div>

k_2 (min^{-1}) is the PSO kinetic rate constant.

2.5.3 Results and discussion

2.5.3.1 Characterisation of the ACs

Results from ash determination and elemental analysis are displayed in Table 2-9. A/B modification results in a lower carbon content due to oxidation of the surface. This is reflected in an increase in O/C atomic ratio. For Norit GAC 1240 and Filtrasorb 400, the O/C atomic ratio increases with a factor 8 and 4 respectively. The ACs from BSG are less oxidised by the treatment, as they have higher initial oxygen content of approximately 10%. Their O/C ratio still increases with a factor of almost 2. The presence of oxygen-containing surface groups can promote the adsorption of Cr(VI) in two ways: preventing the reduction to Cr(III) and making more sites available for complexation [13, 38]**.**

The amino-crosslinked copolymer modifications (CP) drastically increase N and H concentrations? C content decreases, as there is less carbon present in the copolymer. The high nitrogen content in the copolymer itself leads to an increased N/C atomic ratio for all modified samples. There is also a sulphur impurity in one of the reagents, leading to approximately 0.5% sulphur present in all CP modified samples. There is a slight increase in the O content of Norit GAC1240, a stable amount for Filtrasorb F400 and a decrease for the ACBSG. Since the reaction mechanism is not known in literature, this could be caused by the removal of O (as O_2, CO,…) as a result of a side reaction with the AC. However, this remains unclear.

Table 2-10 shows the amount of acidic and basic surface groups in mmol/g on all ACs and their modifications. A/B modification drastically reduces all surface functionalities, acidic as well as basic. E.g. for Norit GAC 1240, this leads to a reduction of acidic surface groups **of 89%** and a reduction of basic groups **of 83%.**

The incorporation of the copolymer changes the surface functionalities towards the properties of the copolymer itself. The properties of Filtrasorb 400 are less influenced by the copolymer, resulting in a slightly higher acidic group number and a lower amount of basic groups than the other copolymerised ACs. This is also confirmed by the lower N/C ratio for Filtrasorb 400.

The CP/AC ratio is determined gravimetrically and checked by calculation from the elemental analysis data. The AC-CP adsorbent contains approximately 66% CP for each of the ACs.

SEM images of ACBSG05 and Norit GAC1240 and their modifications are shown in Table 2-11. Comparing the two raw ACs the difference between the coal-based Norit GAC1240 and the biomass-based ACBSG05 becomes clear. The structure of ACBSG02 is more unorganized and is similar to the structure of the biomass, whereas Norit GAC1240 has a smoother, organized surface. A/B modification does not alter the surface significantly. The PM modification leads to the formation of copolymer on the surface, completely blocking the original AC surface for both ACs.

Table 2-9 Ash content and elemental analysis (in wt%) of non-modified and modified ACs based on dry weight

Name	Ash (%)	C (%)	H (%)	N (%)	S (%)	O (%)** (by difference)	N/C atomic ratio	O/C atomic ratio
Norit GAC 1240 [13]	7.9 ± 0.1	85.3 ± 2.1	0.6 ± 0.1	0.8 ± 0.1	<DL*	5.4 ± 1.5	0.01	0.06
Norit GAC 1240 A/B	11.9 ± 0.3	58.1 ± 0.3	1.0 ± 0.1	0.7 ± 0.1	<DL	28.3 ± 0.4	0.01	0.49
Norit GAC 1240 CP	2.6 ± 0.1	68.4 ± 4.3	8.0 ± 1.2	12.1 ± 1.7	0.5 ± 0.1	8.4 ± 2.5	0.18	0.12
Filtrasorb 400 [13]	7.0 ± 0.1	83.7 ± 1.4	0.7 ± 0.1	0.9 ± 0.1	<DL	7.7 ± 0.4	0.01	0.09
Filtrasorb 400 A/B	9.4 ± 0.1	65.3 ± 0.5	1.6 ± 0.2	0.9 ± 0.1	<DL	22.7 ± 0.7	0.01	0.35
Filtrasorb 400 CP	2.2 ± 0.1	74.3 ± 2.3	6.0 ± 0.6	9.7 ± 0.6	0.5 ± 0.1	7.3 ± 3.0	0.13	0.10

(*) <DL : below detection limit (for S, approximately 0.2%)   (**) O calculated as 100% - Ash – C – H – N – S

Table 2-8 continued

Name	Ash (%)	C (%)	H (%)	N (%)	S (%)	O (%)** (by difference)	N/C atomic ratio	O/C atomic ratio
ACBSG05 [30]	14.4 ± 0.5	71.0 ± 1.4	1.6 ± 0.1	2.7 ± 0.1	<DL	10.4 ± 1.5	0.04	0.15
ACBSG05 A/B	16.5 ±0.1	60.8 ± 0.7	1.9 ± 0.1	3.2 ± 0.1	<DL	17.7 ± 0.8	0.05	0.29
ACBSG05 CP	4.5 ± 0.1	66.4 ± 0.3	8.1 ± 0.2	12.7 ± 0.6	0.5 ± 0.1	7.7 ± 0.9	0.19	0.12
ACBSG07 [30]	14.6 ± 0.3	70.5 ± 0.9	1.5 ± 0.1	2.5 ± 0.1	<DL	10.9 ± 0.9	0.04	0.15
ACBSG07 A/B	14.3 ± 0.1	62.5 ± 0.8	1.9 ± 0.1	3.3 ± 0.1	<DL	17.9 ± 1.0	0.05	0.29
ACBSG07 CP	4.8 ± 0.2	66.3 ± 0.8	7.7 ± 0.3	12.3 ± 0.4	0.5 ± 0.1	8.3 ± 0.3	0.19	0.13
Pure CP	<DL	50.7 ± 0.9	9.3 ± 0.2	15.3 ± 0.5	0.8 ± 0.2	23.9 ± 0.9	0.30	0.47

(*) <DL : below detection limit   (**) O calculated as 100% - Ash – C – H – N – S

Table 2-10 Acidic and basic surface functionalities of non-modified and modified ACs with standard deviations

Name	Acidic surface groups (mmol/g)	Basic surface groups (mmol/g)
Norit GAC 1240 [13]	0.96 ± 0.01	0.48 ± 0.01
Norit GAC 1240 A/B	0.10 ± 0.01	0.08±0.01
Norit GAC 1240 CP	0.11 ±0.01	0.21 ± 0.02
Filtrasorb 400 [13]	0.58 ± 0.01	0.47± 0.01
Filtrasorb 400 A/B	0.12 ± 0.01	0.06 ±0.01
Filtrasorb 400 CP	0.14 ± 0.01	0.20 ±0.01
ACBSG05 [13]	0.70 ± 0.01	0.65 ± 0.01
ACBSG05 A/B	0.07 ± 0.01	0.18 ± 0.01
ACBSG05 CP	0.12 ±0.01	0.25 ± 0.01
ACBSG07 [13]	0.78 ± 0.01	0.80 ± 0.01
ACBSG07 A/B	0.13 ±0.01	0.15 ±0.01
ACBSG07 CP	0.12 ±0.02	0.26 ± 0.01
Pure CP	0.18 ± 0.01	0.25 ±0.01

Table 2-11 SEM images of ACBSG05 and Norit GAC1240 and their modifications
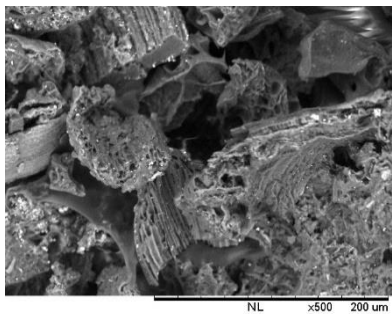
ACBSG05
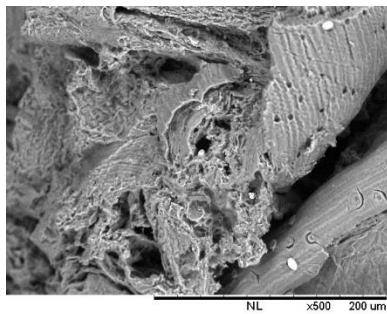
ACBSG05 A/B
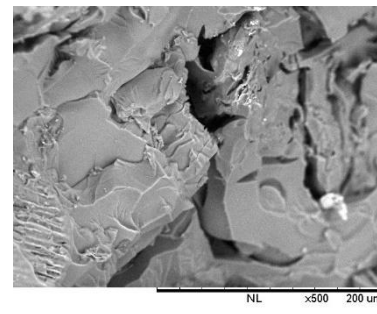
ACBSG05 PM
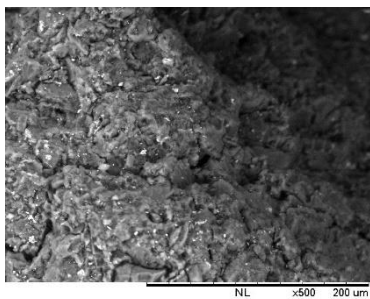
Norit GAC1240
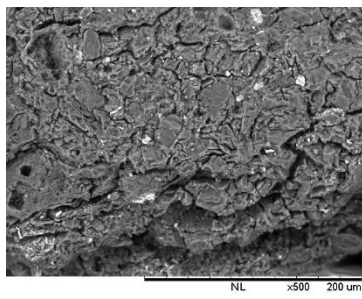
Norit GAC1240 A/B
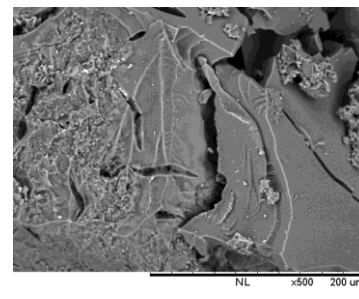
Norit GAC1240 PM

2.5.3.2 Adsorption isotherms of Cr(VI) on modified ACs

For clarity, only graphs of the ACBSG05 data are displayed. The data for ACBSG05, Norit GAC 1240 and Filtrasorb F400 all show the same trends.

Figure 2-12 and Figure 2-13 display the adsorption isotherms for Cr(VI) and Cr_{tot} respectively using ACBSG05 and its two modifications. Due to the reduction of Cr(VI) to Cr(III), the adsorption capacity for Cr(VI) is only an apparent adsorption capacity [13]. Not all the Cr(VI) is adsorbed on the surface, a part of the Cr ions is still present in the solution as Cr(III). The AC treated with the CP modification reaches significantly higher q_{app} values for Cr(VI) as well as higher q_e values for Cr_{tot} removal. Both A/B and CP modified ACs do not show an optimum AC dosage to combine adsorption and reduction as the unmodified AC does [13]. The Cr_{tot} adsorption isotherm of the copolymer modified AC shows an S-type isotherm, suggesting clustering of the Cr ions on the surface of the adsorbent. For adsorption on the A/B modified AC, both isotherms seem to be of the L-type, but very low values of q_e are reached, making this the least effective adsorbent, especially at low dosage. Even though a higher concentration of oxygen in the AC is expected to improve Cr(VI) adsorption, the removal of acidic surface functionalities seems to limit adsorption severely. For ACBSG07, Norit GAC1240 and Filtrasorb and their modifications the same conclusion can be formulated.

Table 2-12 summarizes values for adsorption capacities q_e from the adsorption studies performed in this chapter (based on the maximal found value for a low dosage of 0.2 g AC/L) and for comparison with literature values for adsorption of Cr(VI). Different types of adsorbents and details of experimental parameters are displayed, such as measurement method and concentration ranges. The most important parameters that influence the found q_{app} and q_e are adsorbent dosage and Cr(VI) concentration. The pollutant/adsorbent ratio increases when using low doses of AC or high Cr(VI) concentrations, resulting in an increased q_{app}/q_e value. In most research, only Cr(VI) concentrations are measured by the DPC method. Some authors mention the monitoring of both Cr(VI) and Cr_{tot}, but do not report separate q_e values. Reduction of Cr(VI) also plays a role in adsorption performance on AC and therefore measurement of both Cr(VI) and Cr_{tot} is necessary. Comparing solely the q_e values, ACBSG performs averagely compared to other

ACs from biomass as listed in Table 2-12 (keeping in account their higher starting concentrations).
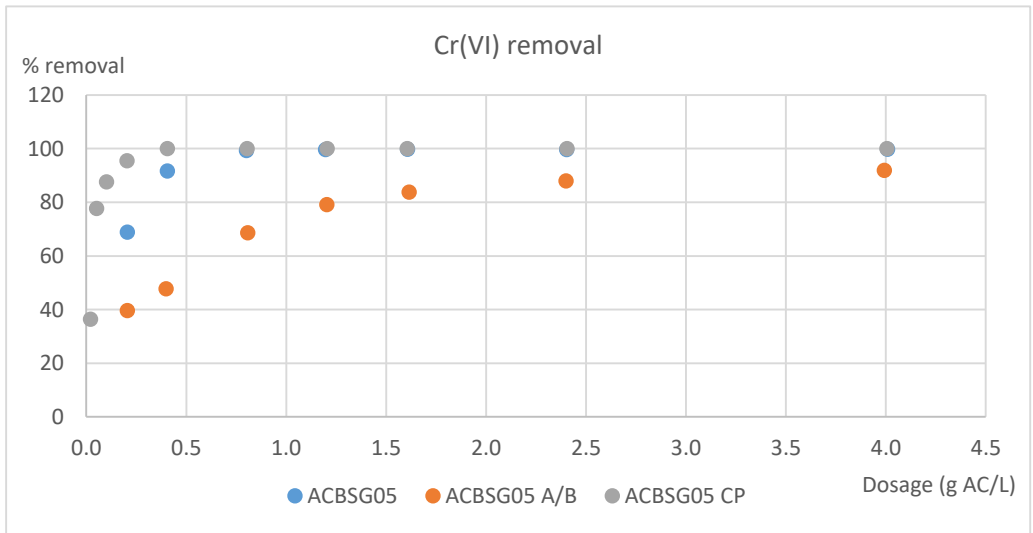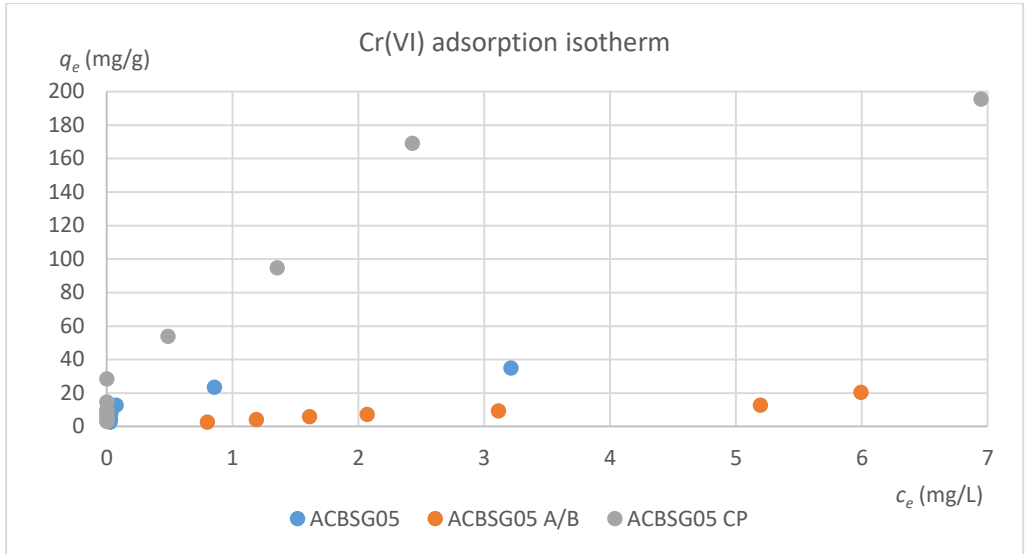
Figure 2-12 Adsorption isotherm and removal percentage for Cr(VI) on unmodified and modified ACBSG05.
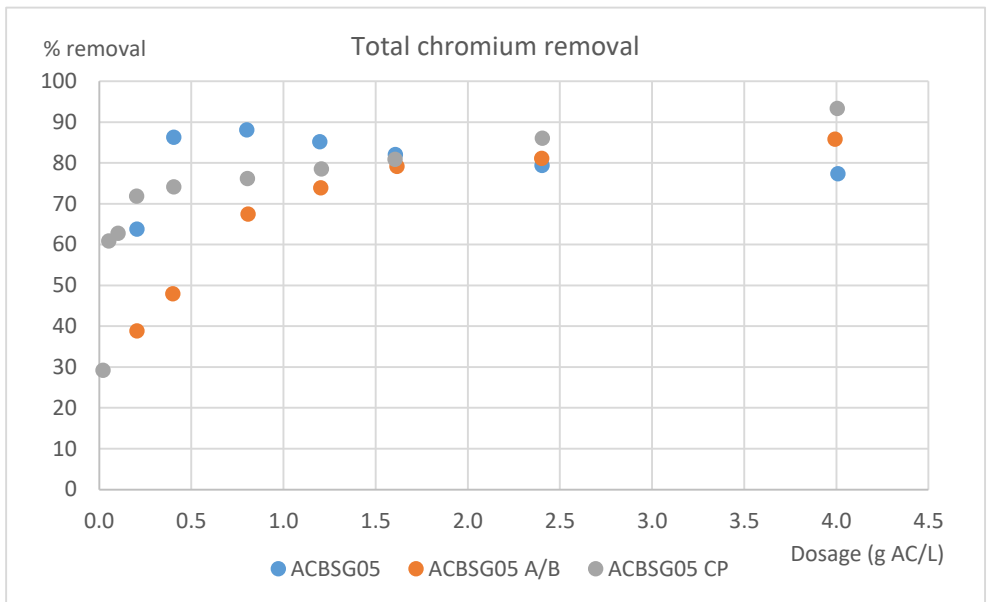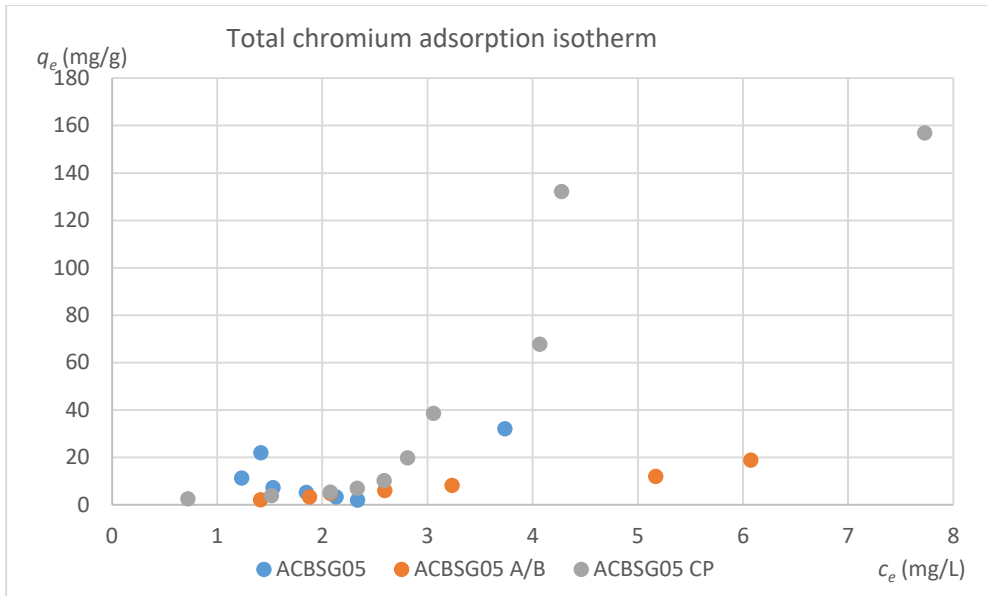
Figure 2-13 Adsorption isotherm and removal percentage for Cr_{tot} on unmodified and modified ACBSG05

Table 2-12 Adsorption capacities for Cr(VI) found in literature and in the present study. *N.S. = Not Specified ** q_e for Cr(VI)/total chromium

Adsorbent	Temperature (°C)	Measurement method	Adsorption capacity q_e (mg/g)	Optimal pH	Dosage (g AC/L)	Concentration of Cr(VI) (mg/L)	References
Arundo donax Linn AC	N.S.*	DPC/AAS	90.99	5	1	10-100	[16]
Arundo donax Linn AC - EDT	N.S.	DPC/AAS	102.88	5	1	10-100	[16]
Groundnut husk AC	30	AAS	7.01	3	0.625-7.5	10	[11]
Groundnut husk AC silver impregnated	30	AAS	11.4	3	0.625-7.5	10	[11]
CoFe$_2$O$_4$/activated carbon composite	N.S.	DPC	32.4	2	4	50-150	[9]
Carya peels based activated carbon (Changnan Activated Carbon Co)	N.S.	DPC	33.8	2	4	50-150	[9]

Table 2-11 continued

Adsorbent	Temperature (°C)	Measurement method	Adsorption capacity q_e (mg/g)	Optimal pH	Dosage (g AC/L)	Concentration of Cr(VI) (mg/L)	References
Norit GAC1240	25	DPC/ICP OES	84/60**	2	0.2-4	10	Present study
Norit GAC1240 A/B	25	DPC/ICP OES	33/31**	2	0.2-4	10	
Norit GAC1240 CP	25	DPC/ICP OES	181/156**	2	0.2-4	10	
Filtrasorb F400	25	DPC/ICP OES	76/58**	2	0.2-4	10	
Filtrasorb F400 A/B	25	DPC/ICP OES	30/30**	2	0.2-4	10	
Filtrasorb F400 CP	25	DPC/ICP OES	178/135**	2	0.2-4	10	
ACBSG05	25	DPC/ICP OES	20/13**	2	0.2-4	10	
ACBSG05 A/B	25	DPC/ICP OES	16/14**	2	0.2-4	10	
ACBSG05 CP	25	DPC/ICP OES	195/157**	2	0.2-4	10	
ACBSG07	25	DPC/ICP OES	35/30**	2	0.2-4	10	
ACBSG07 A/B	25	DPC/ICP OES	19/16**	2	0.2-4	10	
ACBSG07 CP	25	DPC/ICP OES	207/169**	2	0.2-4	10	

2.5.3.3 Influence of AC/CP ratio on adsorption capacity

In Figure 2-14 and Figure 2-15 the q_e values for Cr(VI) and total Cr adsorption are displayed for different ratios of copolymer to AC. On the left hand the results indicate q_e values for pure AC (0% copolymer), the result to the right is compared to pure copolymer (100%). At both low (0.05 g/L) and intermediate (0.8 g/L) dosage of AC there is a decrease in efficiency of the adsorbent grafted with 6 to 11% of copolymer. This result suggests that the copolymer does not increase the efficiency of the AC, but the copolymer itself is important for the improved adsorption at higher levels. Furthermore, the copolymer blocks the porous structure of the AC. There is not enough copolymer to increase the adsorption efficiency in order to compensate for this effect. At copolymer concentrations above 30%, the AC only works as a carrier material and does not significantly contribute to the adsorption and only reflects the adsorption potential of the copolymer. In contrast, only at higher levels of copolymer (>30%) and at intermediate AC dosages, q_e values are comparable with pure activated carbon reflecting no real added adsorption value of the copolymer.
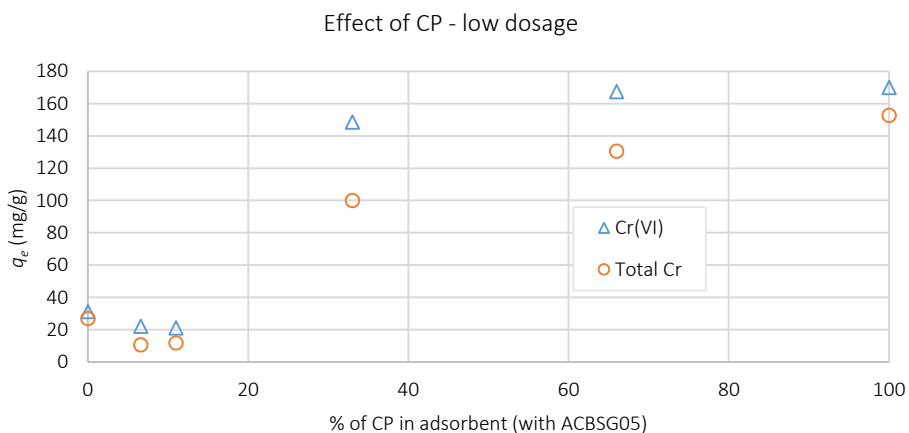
Figure 2-14 Adsorption capacity of ACBSG05 CP with different levels of copolymer at low dosage (0.05 g AC/L, 10 mg AC + 200 mL of 10 mg/L Cr(VI) solution at pH 2)
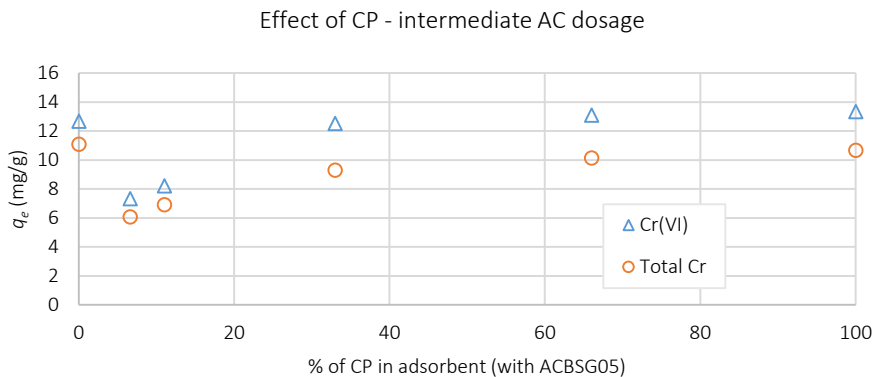
Figure 2-15 Adsorption capacity of ACBSG05 CP with different levels of copolymer at intermediate dosage (1 g AC/L, 25 mg AC + 25 mL of 10 mg/L Cr(VI) solution at pH 2)

2.5.3.4 Adsorption kinetics

Figure 2-16 and Figure 2-17 show the kinetic adsorption data of ACBSG05 and its A/B and CP modifications for Cr(VI) and Cr_{tot}. Plotted lines represent the PSO model.

The other ACs (ACBSG07, Norit GAC 1240 and Filtrasorb 400, and their A/B and CP modifications) showed the same graphical trends. All ACs reach equilibrium after 16 h. PFO and PSO reaction rates are determined for ACBSGs as well as for the commercially available ACs, both for Cr(VI) and Cr_{tot}. The reaction kinetics are slightly better fitted by the PSO model, displaying the results in Table 4 for all kinetic experiments. The kinetic constant for the PSO model shows that unmodified ACBSG adsorbs Cr(VI) faster than any other AC (kinetic constant k_2= 0.091 min^{-1} and k_2=0.107 min^{-1} for ACBSG02 and ACBSG05 respectively). This higher kinetic rate might be due to the combination of adsorption and reduction of Cr(VI).

For total Cr, the kinetic constant is the highest for the copolymerized ACs, suggesting a rapid uptake of all Cr ions. The copolymerized ACBSGs have a somewhat smaller particle size distribution, resulting in a higher k_2 value. The oxidized ACs are slower than the unmodified ACs because of reduced interaction sites as a result of lower amounts of surface groups.
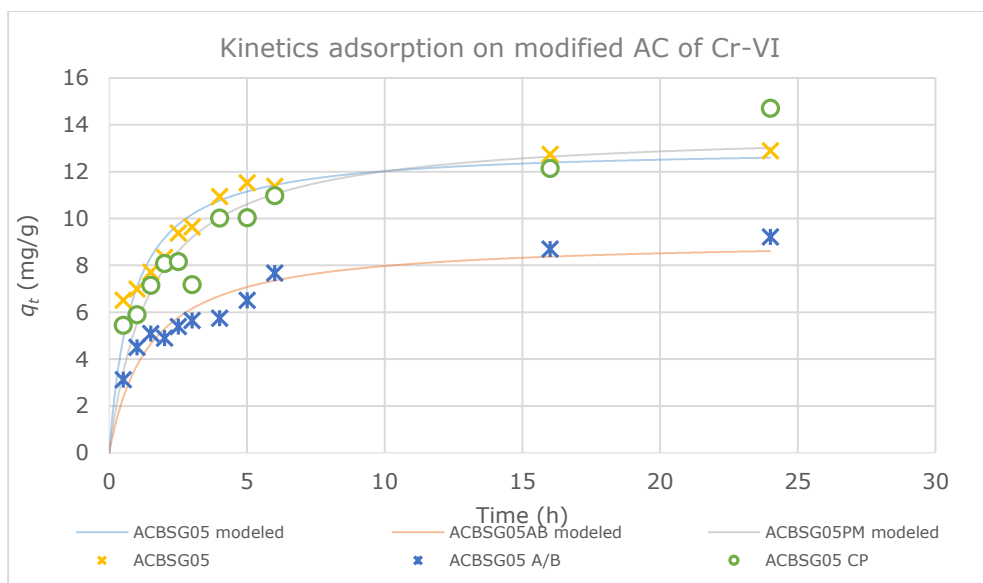
Figure 2-16 Kinetics of the adsorption of Cr(VI) on unmodified and modified ACBSG05 (20 mg AC + 25 mL 10 mg/L Cr(VI) solution at pH 2)
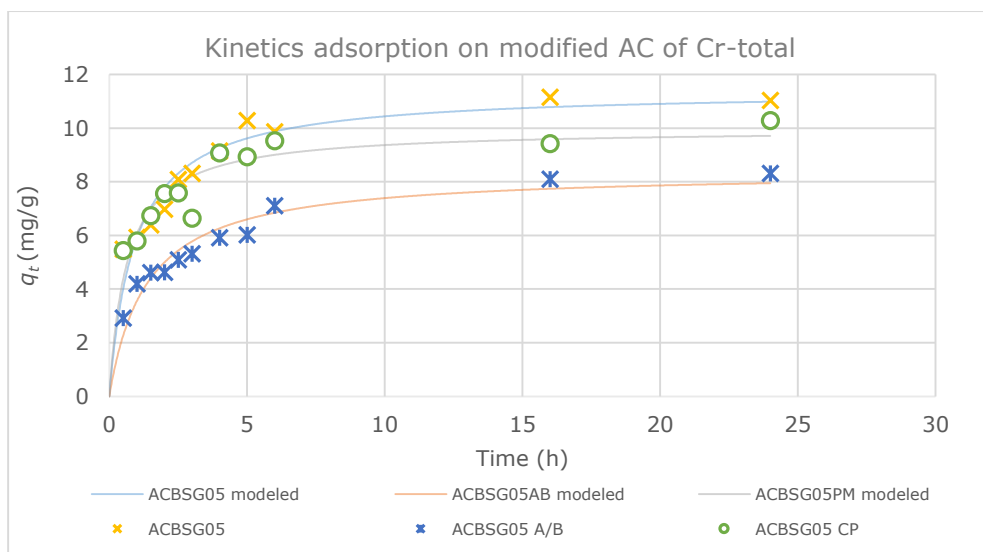
Figure 2-17 Kinetics of the adsorption of Cr_{tot} on unmodified and modified ACBSG05 (20 mg AC + 25 mL 10 mg/L Cr(VI) solution at pH 2).

Table 2-13 Calculated kinetic constants according to PSO and PFO models for each AC and their modifications, for both Cr(VI) and Cr_{tot}

Sample name	Cr(VI)						Cr_{tot}					
	PFO			PSO			PFO			PSO		
	k_1 (min⁻¹)	q_{max} (mg/g)	R^2	k_2 (min⁻¹)	q_{max} (mg/g)	R^2	k_1 (min⁻¹)	q_{max} (mg/g)	R^2	k_2 (min⁻¹)	q_{max} (mg/g)	R^2
Norit GAC1240	0.47	12.08	0.904	0.047	13.55	0.934	0.52	9.16	0.899	0.072	10.21	0.920
Norit GAC1240 A/B	0.29	11.70	0.955	0.026	13.52	0.977	0.30	10.41	0.958	0.030	11.99	0.977
Norit GAC1240 CP	0.52	11.70	0.934	0.054	13.12	0.980	0.82	9.18	0.950	0.124	9.18	0.970
Filtrasorb F400	0.50	12.31	0.940	0.049	13.84	0.953	0.55	9.78	0.926	0.071	10.92	0.924
Filtrasorb F400 A/B	0.24	11.46	0.979	0.019	13.63	0.980	0.27	10.41	0.956	0.026	12.09	0.960
Filtrasorb F400 CP	0.53	11.73	0.854	0.056	13.16	0.938	0.78	9.14	0.863	0.114	10.13	0.952

Table 2-12 continued

Sample name	Cr(VI)						Cr$_{tot}$					
	PFO			PSO			PFO			PSO		
	k_1 (min^{-1})	q_{max} (mg/g)	R^2	k_2 (min^{-1})	q_{max} (mg/g)	R^2	k_1 (min^{-1})	q_{max} (mg/g)	R^2	k_2 (min^{-1})	q_{max} (mg/g)	R^2
ACBSG05	0.77	11.82	0.823	0.091	13.04	0.915	0.7	10.36	0.842	0.094	11.41	0.909
ABSG05 A/B	0.49	8.21	0.811	0.075	9.14	0.898	0.52	7.5	0.847	0.087	8.4	0.93
ACBSG05 CP	0.47	12.35	0.787	0.047	13.84	0.863	0.99	9.06	0.691	0.155	9.97	0.828
ACBSG07	0.92	11.87	0.838	0.107	13.1	0.838	0.88	10.26	0.836	0.118	11.33	0.911
ACBSG07 A/B	0.44	9.51	0.91	0.054	10.75	0.963	0.49	8.66	0.9	0.067	9.76	0.962
ACBSG07 CP	0.56	11.7	0.869	0.06	13.07	0.937	1.05	9.17	0.759	0.168	10.03	0.896

2.5.4 Conclusion

A first modification of AC by acidic/basic treatment does not improve the surface characteristics of any of the produced ACs from brewer's spent grain. Even though the oxygen content increases, the amount of acidic surface groups is reduced. This amount is more critical for the adsorption of Cr(VI). The adsorption capacity q_e decreases by this modification method. Incorporation of a copolymer with quaternary ammonium end groups on the surface of the AC greatly enhances the adsorption, especially at low dosage, but the effect is solely caused by the copolymer. There is no synergy between the copolymers and the surface of the AC. The AC only served as a bulk carrier for the copolymer and its chemical and physical properties were of minor importance. In an industrial setting, other carrier materials are probably better economically suited for this purpose. Kinetic experiments also show that ACBSGs have a faster removal rate for Cr(VI) than the two commercially available ACs and their modified versions. The removal of Cr_{tot} was fastest on all copolymerized ACs, where smaller particle size promotes adsorption kinetics.

2.5.5 Funding

2.5.6 References

[1] Vlaamse Milieumaatschappij, Zware metalen in het grondwater in Vlaanderen, Afdeling Operationeel waterbeheer VMM, Dienst Grondwaterbeheer, Aalst, **2015**.

[2] N. Kazakis, N. Kantiranis, K. Kalaitzidou, E. Kaprara, M. Mitrakas, R. Frei, G. Vargemezis, P. Tsourlos, A. Zouboulis, A. Filippidis, Origin of hexavalent chromium in groundwater: The example of Sarigkiol Basin, Northern Greece, Science of The Total Environment, **2017**, 593–594, 552-566.

[3] J.-H. Kim, J.-C. Kang, Effects of dietary chromium exposure to rockfish, Sebastes schlegelii are ameliorated by ascorbic acid, Ecotoxicology and Environmental Safety, **2017**, 139, 109-115.

[4] K.L. Nguyen, H.A. Nguyen, O. Richter, M.T. Pham, V.P. Nguyen, Ecophysiological responses of young mangrove species Rhizophora apiculata (Blume) to different chromium contaminated environments, Science of The Total Environment, **2017**, 574, 369-380.

[5] U.S. Department of Labor - Occupational Safety and Health Administration, Hexavalent chromium, **2009**.

[6] M. Sittig, Handbook of toxic and hazardous chemicals and carcinogens, Noyes Publications, **1985**.

[7] R. Kumar, S.-J. Kim, K.-H. Kim, S.-h. Lee, H.-S. Park, B.-H. Jeon, Removal of hazardous hexavalent chromium from aqueous phase using zirconium oxide-immobilized alginate beads, Applied Geochemistry, **2017**.

[8] C. Hua, R. Zhang, F. Bai, P. Lu, X. Liang, Removal of chromium (VI) from aqueous solutions using quaternized chitosan microspheres, Chinese Journal of Chemical Engineering, **2017**, 25, 153-158.

[9] W. Qiu, D. Yang, J. Xu, B. Hong, H. Jin, D. Jin, X. Peng, J. Li, H. Ge, X. Wang, Efficient removal of Cr(VI) by magnetically separable $CoFe_2O_4$/activated carbon composite, Journal of Alloys and Compounds, **2016**, 678, 179-184.

[10] J. Zhang, C. Zhang, G. Wei, Y. Li, X. Liang, W. Chu, H. He, D. Huang, J. Zhu, R. Zhu, Reduction removal of hexavalent chromium by zinc-substituted magnetite coupled with aqueous Fe(II) at neutral pH value, Journal of Colloid and Interface Science, **2017**, 500, 20-29.

[11] S.P. Dubey, K. Gopal, Adsorption of chromium(VI) on low cost adsorbents derived from agricultural waste material: A comparative study, Journal of Hazardous Materials, **2007**, 145, 465-470.

[12] A.K. Bhattacharya, T.K. Naiya, S.N. Mandal, S.K. Das, Adsorption, kinetics and equilibrium studies on removal of Cr(VI) from aqueous solutions using

different low-cost adsorbents, Chemical Engineering Journal, **2008**, 137, 529-541.

[13] S. Vanderheyden, K. Vanreppelen, J. Yperman, R. Carleer, S. Schreurs, Chromium(VI) removal using activated carbon prepared from brewers' spent grain, Adsorption, **2017**, 24, 147-156.

[14] J. Rivera-Utrilla, M. Sánchez-Polo, V. Gómez-Serrano, P.M. Álvarez, M.C.M. Alvím-Ferraz, J.M. Dias, Activated carbon modifications to enhance its water treatment applications. An overview, Journal of Hazardous Materials, **2011**, 1-23.

[15] S.X. Liu, X. Chen, X.Y. Chen, Z.F. Liu, H.L. Wang, Activated carbon with excellent chromium(VI) adsorption performance prepared by acid-base surface modification, Journal of Hazardous Materials, **2007**, 315-319.

[16] Y. Sun, Q. Yue, B. Gao, Y. Gao, Q. Li, Y. Wang, Adsorption of hexavalent chromium on Arundo donax Linn activated carbon amine-crosslinked copolymer, Chemical Engineering Journal, **2013**, 217, 240-247.

[17] X. Xu, Y. Gao, B. Gao, X. Tan, Y.-Q. Zhao, Q. Yue, Y. Wang, Characteristics of diethylenetriamine-crosslinked cotton stalk/wheat stalk and their biosorption capacities for phosphate, Journal of Hazardous Materials, **2011**, 192, 1690-1696.

[18] A. Bhatnagar, W. Hogland, M. Marques, M. Sillanpää, An overview of the modification methods of activated carbon for its water treatment applications, Chemical Engineering Journal, **2013**, 499-511.

[19] S.I. Mussatto, G. Dragone, I.C. Roberto, Brewer's spent grain: generation, characteristics and potential applications, Journal of Cereal Science, **2006**, 1-14.

[20] D. Cook, Brewers' grains: opportunities about, Brewers' guardian, Advantage Publishing Ltd, **2011**.

[21] S.R.H. Vanderheyden, R. Van Ammel, K. Sobiech-Matura, K. Vanreppelen, S. Schreurs, W. Schroeyers, J. Yperman, R. Carleer, Adsorption of cesium on different types of activated carbon, Journal of Radioanalytical and Nuclear Chemistry, **2016**, 310, 301-310.

[22] C. Xiros, P. Christakopoulos, Biotechnological potential of brewers spent grain and its recent applications, Waste and Biomass Valorization, **2012**, 2, 213-232.

[23] A.S.N. Mahmood, J.G. Brammer, A. Hornung, A. Steele, S. Poulston, The intermediate pyrolysis and catalytic steam reforming of Brewers spent grain, Journal of Analytical and Applied Pyrolysis, **2013**, 103, 328-342.

[24] S.I. Mussatto, M. Fernandes, G.J.M. Rocha, J.J.M.T. Orfao, J.A., I.C. Roberto, Production, characterization and application of activated carbon from brewer's spent grain lignin, Bioresource Technology, **2010**, 2450-2457.

[25] M. Linko, A. Haikara, A. Ritala, M. Penttilä, Recent advances in the malting and brewing industry1, Journal of Biotechnology, **1998**, 65, 85-98.

[26] C. Chen, J. Wang, Removal of Pb^{2+}, Ag^+, Cs^+ and Sr^{2+} from aqueous solution by brewery's waste biomass Journal of Hazardous Materials, **2008**, 151, 65-70.

[27] A. Ktenioudaki, N. O'Shea, E. Gallagher, Rheological properties of wheat dough supplemented with functional by-products of food processing: Brewer's spent grain and apple pomace, Journal of Food Engineering, 116 (2013) 362-368.

[28] S.I. Mussatto, J. Moncada, I.C. Roberto, C.A. Cardona, Techno-economic analysis for brewer's spent grains use on a biorefinery concept: The Brazilian case, Bioresource Technology, **2013**, 148, 302-310.

[29] E. Vieira, M.A.M. Rocha, E. Coelho, O. Pinho, J.A. Saraiva, I.M.P.L.V.O. Ferreira, M.A. Coimbra, Valuation of brewer's spent grain using a fully recyclable integrated process for extraction of proteins and arabinoxylans, Industrial Crops and Products, **2014**, 52, 136-143.

[30] K. Vanreppelen, S. Vanderheyden, T. Kuppens, S. Schreurs, J. Yperman, R. Carleer, Activated carbon from pyrolysis of brewer's spent grain: Production and adsorption properties, Waste Management & Research, **2014**, 32, 634-645.

[31] I. Velghe, R. Carleer, J. Yperman, S. Schreurs, J. D'Haen, Characterisation of adsorbents prepared by pyrolysis of sludge and sludge/disposal filter cake mix, Water Research, **2012**, 46, 2783-2794.

[32] D.T. Duranoglu, A.W.; Beker, U., Kinetics and thermodynamics of hexavalent chromium adsorption onto activated carbon derived from acrylonitrile-divinylbenzene copolymer, Chemical Engineering Journal, **2012**, 193-202.

[33] F. Di Natale, A. Lancia, A. Molino, D. Musmarra, Removal of chromium ions form aqueous solutions by adsorption on activated carbon and char, Journal of Hazardous Materials, **2007**, 381-390.

[34] ASTM, Standard test method for the determination of hexavalent chromium in workplace air by ion chromatography and spectrophotometric measurement using 1,5-diphenylcarbazide, **2002**.

[35] S.Y. Lagergren, Zur theorie der sogenannten adsorption gelöster stoffe, Kungliga Svenska Vetenskapsakademiens, Handlingar, **1898**, 24, 1-39.

[36] R.-L. Tseng, F.-C. Wu, R.-S. Juang, Characteristics and applications of the Lagergren's first-order equation for adsorption kinetics, Journal of the Taiwan Institute of Chemical Engineers, **2010**, 41, 661-669.

[37] Y.S. Ho, G. McKay, Kinetic Models for the Sorption of Dye from Aqueous Solution by Wood, Process Safety and Environmental Protection, **1998**, 76, 183-191.

[38] Z. Reddad, C. Gerente, Y. Andres, P.L. Cloirec, Mechanisms of Cr(III) and Cr(VI) removal from aqueous solutions by sugar beet pulp, Environmental Technology, **2003**, 24, 257-264.

2.6 Chapter conclusions

The first paper proved that AC from BSG can be used as an adsorbent for chromium(VI). A combined mechanism of reduction and adsorption was found. This mechanism was more pronounced for the ACBSG compared to both industrially available ACs. The nitrogen surface functionalities of the ACBSG are better adsorption sites for chromium(VI), producing less chromium(III) compared to commercially available ACs. In literature studies this effect is hardly accounted for. This might cause misinterpretation of adsorption results, where the apparent adsorption capacity might be misinterpreted as the actual adsorption capacity. In kinetic experiments, the reduction to chromium(III) and the consequent adsorption result in slower adsorption. Nevertheless, the ACBSGs adsorb chromium(VI) significantly faster.

The second paper focused on the improvement of ACs by using acid/base washing and the grafting of a copolymer on the AC. The first modification method used washing with acid and basic solutions and is supposed to improve the amount of oxygenized surface functionalities. This method does not improve the adsorption capacity, nor does it improve the adsorption kinetics. The second method grafted a copolymer onto the surface of the AC and drastically improves the adsorption capacity. The copolymer blocks the porous structure of the AC and the increase in adsorption capacity is only due to the copolymer itself. The copolymer removes the total chromium concentrations faster than any other AC, but for chromium(VI) the ACBSGs still show the highest kinetic parameters.

The following results can be listed:

- Measurement of both chromium(VI) and total chromium should be accounted for, since there are reduction effects alongside adsorption.

- An optimum dosage of activated carbon is found for removal of chromium(VI). Above this optimum dosage, the reduction is enhanced and chromium(III) is produced in-situ.

- Modification of AC by acid/base washing does not improve adsorption properties for Cr(VI)

- Copolymerized AC is able to remove chromium very efficiently, but the economic costs should be taken into account.

- Grafting a copolymer to an AC physically blocks the surface of the AC. More economic bulk materials such as biomass itself are probably better suited for this purpose.

3 Cesium removal by activated carbons

3.1 Introduction[6]

According to [1].

On Friday 11 March 2011, The Great East Japan Earthquake shook up the east coast of Japan. With a magnitude of 9.0 it created a tsunami that hit land 130 km away in the Miyagi prefecture. This resulted in the physical geographic movement of Japan, vast damage to ports and coastal towns and a death toll of approximately 19 000 people. Eleven reactors in four nuclear power plants (NPP) that were operating at the moment the earthquake hit, were all shut down automatically to prevent seismic damage. However, the effect of the tsunami that hit 40 minutes later was grossly underestimated. Most sites achieved shutdown by removing residual heat using grid power or backup generators, but the Fukushima Daiichi site was hit severely.

3.1.1 Fukushima Daiichi Nuclear Power Plant disaster

According to [1].

A 15 m high tsunami hit the Fukushima Daiichi site. Tsunami countermeasures were designed in the 1960s according to scientific knowledge at that time. When newer research showed a realistic risk of higher tsunamis in 1993, the plant operator (Tepco) did not take any actions. The tsunami flooded the halls and disabled 12 of the 13 available backup generators. Three of the reactors were slowly overheating and reactor waste and heat had to be released into the sea. Reactor cooling and water circulation systems were lost. Injection of sea water was initiated, but the temperature of the exposed fuel still rose to 2800 °C and central parts started to melt. The combined heat and absence of decent venting systems caused steam, noble gasses, hydrogen and aerosols to collect at the top floors of the reactor building of unit 1. The mixture combined with air exploded, blowing off the roof of the building. The fuel in units 2 and 3 melted more slowly, but the gases of unit 3 back flowed into the unit 4 building, also causing a hydrogen explosion there.

---

[6] References for the introduction can be found at page 145 in section 3.3

The volatile fission products were released early on, during the explosions. All remaining fuel was contained in the buildings, being cooled by closed recycled water systems. Some water leaking has occurred, but the situation was considered as stable. In mid-December 2011, Tepco declared "cold shutdown condition" as the releases had reduced to minimal levels.

3.1.2 Release of radionuclides

Radionuclides were mostly released into the air, after which rain deposited them in soils and surface water. Volatile iodine-131, xenon-133 and cesium-134 and 137 were the main radionuclides released to air and water [1]. Noble gases like xenon do not react with species and are not deposited on the soil, so they are not considered a long-term danger [2]. With a half-life of 8 days and tendency to accumulate in the thyroid, effects of I-131 are important in the critical phase of the disaster. Cesium-137 is the other main radionuclide that was released in the plume. As a strong gamma emitter with a half-life of approximately 30 years, it causes a major contamination problem [3]. Table 3-1 summarizes nuclear fission products according to their volatility [4]. Iodine and cesium are present in the most volatile group, explaining their presence in the plume.

The total release of Cs-137 into the atmosphere by explosions and steam venting is estimated between 1.0 and 5.0×10^{16} Bq, not considering release of the contaminated waste water into the ocean [3]. At ambient temperatures, Cs is not volatile and it distributes onto aerosol particles [5]. Rain is then able to wash out the aerosols, depositing the Cs on soil and in water [6]. The soil activity concentration due to Cs-137 within a 80 km radius of the Fukushima NPP is displayed in Figure 3-1.

Table 3-1 Classification of fission products (FP) according to volatility [4]

Group	Major elements	Characteristics for leakage and transport	Leakage rate (>2350 °C)
Volatile FP (including noble gases)	Xe, Kr, I, Cs, Sb, Te, Cd, Rb, Ag	- High volatility - Very easily leaked from fuel pellet - Move very long distance in the environment	100%
Semi-volatile FP	Mo, Ba, Rh, Pd, Tc	- Medium volatility - Easily leaked from fuel pellet - Move long distance in the environment	50–100%
Low-volatile FP	Ru, Ce, Sr, Y, Eu, Nb, La	- Low volatility - Difficult to be leaked from fuel pellet - Move short distance in the environment	3–10% (for some nuclides: 20–40%)
Non-volatile FP	Zr, Nd, Pr	- No volatility - Very difficult to be leaked from fuel pellet	Not measured
Actinides	U, Pu	- Different leakage features depending on nuclides - Move short distance in the environment	U: at most 10% Pu: less than 1%
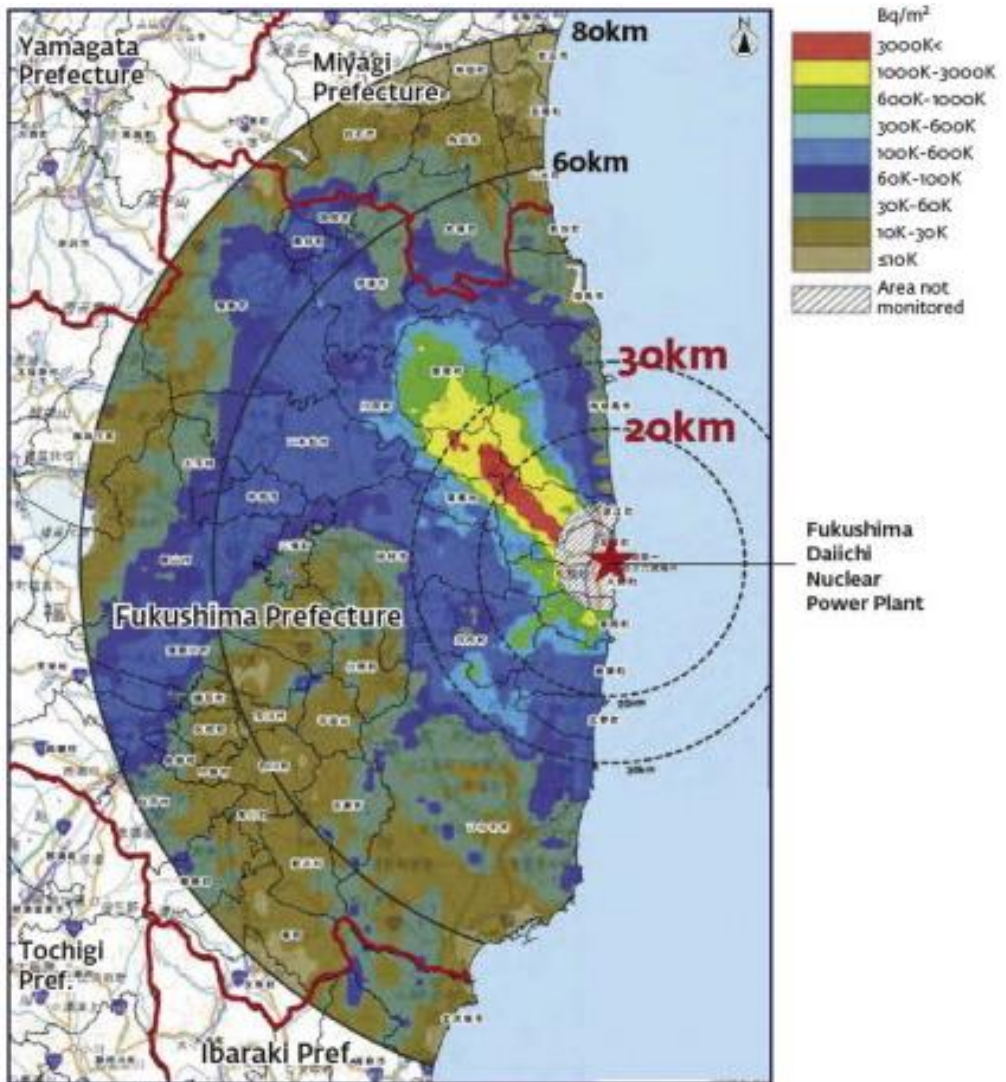
Figure 3-1 Soil activity concentration for Cs-137 corrected to July 2, 2011 in a 80 km radius of the Fukushima NPP [7]

Cs concentrations in soils were always maximal at the top layer and decreased exponentially along the depth of the site. Even though there are strong differences in soil characteristics, more than 70% of radioactive Cs is present in the top 2 cm of the soil and 90% of it is present in the top 5 cm [8, 9]. Seawater within a 30 km radius of the plant site exceeded 10 Bq/L of Cs and concentrations up to 68 000 Bq/L were measured in the immediate vicinity of the plant [10].

3.1.3 Cesium characteristics

As seen from a toxicological point of view, stable cesium is neither genotoxic nor carcinogenic. Stable cesium overdosing might cause hyperirritability and muscle spasms as it displaces potassium in the body [11]. The LD50 of stable Cs varies between 800 and 2000 mg/kg depending on its chemical form [12]. It only poses a health hazard when ingested in large quantities [13]. Stable Cs is only found in two minerals, pollucite and rhodozite, all other isotopes are only produced by industrial activities [14].

Cs-137 ($T_{1/2}$ 30.2 y) is the main Cs isotope produced in nuclear reactors and accelerators, along with Cs-134 ($T_{1/2}$ 2.2 y). The decay schemes of Cs-137 and Cs-134 are displayed in Figure 3-2 and Figure 3-3.

Apart from the releases from its use in medicine and industrial applications, the greatest release into the environment comes from the Tchernobyl and Fukushima nuclear disasters. When it is rained out of the radioactive plume, it deposits on land and concentrates at the top of the soil. It enters the food chain by consumption of contaminated water, plants, mushrooms, meat, fish and milk. The LD50/30 [the dose that kills 50% of the population in 30 days] in rats was found to be 1 GBq of Cs-137/kg [15]. Cs-137 contamination strongly influences the reproduction system but it is also able to result in tumors, mostly in the liver and nose [14].
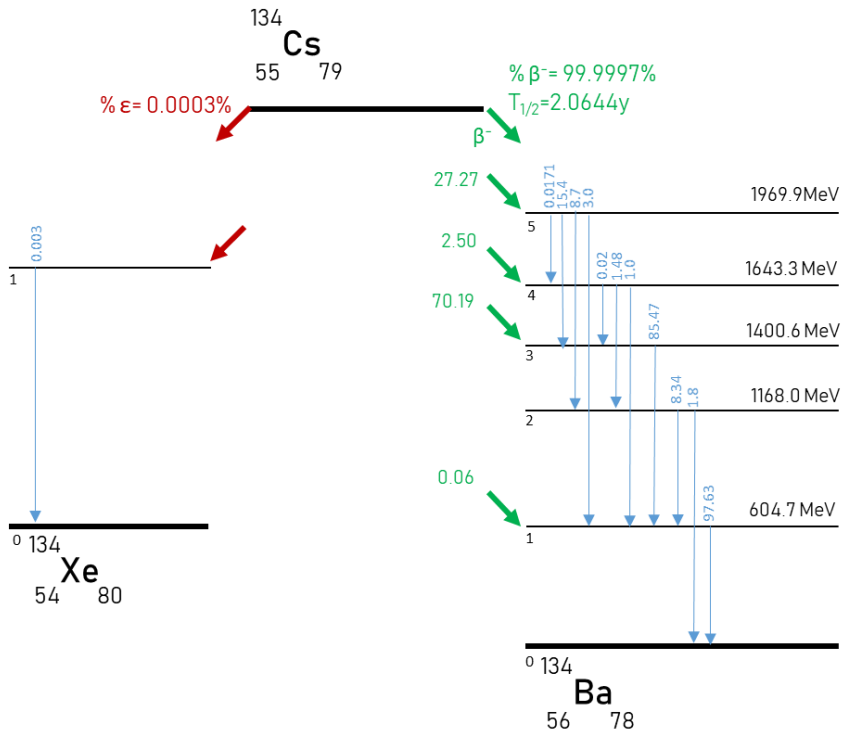
Figure 3-2 Decay scheme for Cs-134 [16,17]
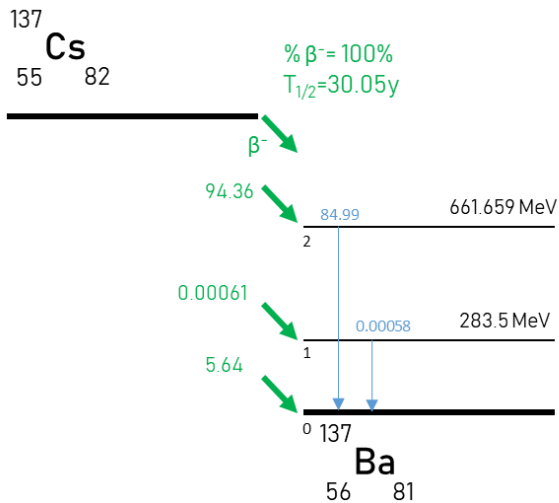
Figure 3-3 Decay scheme for Cs-137 [16,17]

136

3.1.4 Cesium removal

Removal of radioactive Cs isotopes from the gastrointestinal tract of humans and livestock is performed by Prussian Blue (PB), also named iron(II,III) hexacyanoferrate (II,III). Its formula is $Fe_4[Fe(CN)_6]_3$. It is a dispersible blue powder and can be administered pure or mixed with several binders (e.g. saltlicks for ruminants) [18-20]. There are some drawbacks to the use of PB, such as its powder structure and dissociation at pH lower than 5 or larger than 8 [21, 22].

The capacity to bind with Cs is not limited to PB alone, but a variety of hexacyanoferrate (HCF) compounds also exhibit this behaviour because of their typical crystal lattice. This lattice is able to let the small hydrated Cs ions pass through, while the larger hydrated Na and K ions are unable to penetrate the structure [23-25]. A schematic representation can be found in Figure 3-4. Some other HCFs such as ferrocyn (5% $KFe[Fe(CN)_6]$ and 95% $Fe_4[Fe(CN)_6]$) [17], Cu-, Ni-, Co-, Zn- and mixed HCFs have been tried and tested in literature, of which some have shown promising adsorption results.
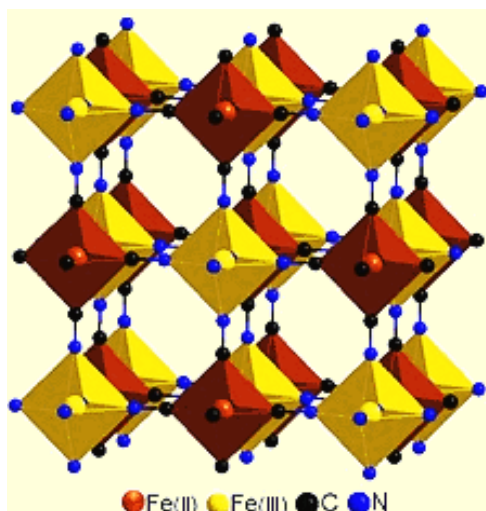
Figure 3-4 Schematic representation of hexacyanoferrate lattice without counterions

To tackle the problems usually present with fine powdery materials, several HCFs have been combined with other materials to create hybrid materials with alluring

properties. It is possible to incorporate the HCF in normal filter materials, such as fabrics [26]. It is also possible to mix PB or other HCFs with magnetic nanoparticles and bind these with a polymeric binder to provide a structure and to enhance the separation process [27-30]. Another option is the creation of hybrid materials that can tackle several problems simultaneously by using anion exchangers, clays or surfactants [31, 32]. (Bio)sorption and combination of adsorbents with HCF are also options that have been widely investigated [23, 33-38]. Biomass materials are sometimes upgraded with other materials (magnetic nanoparticles) before their conjunction with HCF takes place [39].

3.1.5 Cesium measurement

In the following two manuscripts (paragraphs 3.4 and 3.5), two measurement methods for Cs are applied. The first measurement method is based on **gamma-ray spectroscopy** and the principles are described here according to [40]. For this purpose, a NaI(Tl) well-type detector is used, a high-efficiency scintillator for gamma-rays with sufficient resolution for energy separation. A NaI(Tl) scintillator has a good light yield, linearity and the I constituent has a high atomic number Z which is beneficial for photoelectric absorption ($\sim Z^{4.5}$).

A gamma-ray proton loses energy though ionization and excitation of the atoms of the NaI(Tl) crystal and through Bremsstrahling, creating fast electrons with a maximum energy equal to the energy of the incident gamma-photon. The detector must be sufficiently large to avoid the escape of these electrons. Photoelectric absorption liberates a photoelectron, carrying most of the gamma-ray energy, together with one or more low-energy electrons corresponding to the original binding energy of the photoelectron. Photoelectric absorption is the preferred process in gamma-ray spectroscopy, since a single peak appears at a total electron energy corresponding to the energy of the incident gamma-rays. Interfering with this photoelectric absorption is Compton scattering, when a recoil electron and a gamma-ray photon are scattered. A continuum of energy will be transferred to the electron, since the scattering angle can differ. The third interaction of gamma rays is pair production. If the gamma-ray energy exceeds 1.02 MeV (the energy required), an electron-positron pair is created and the excess energy appears as kinetic energy shared by the pair. This is typically found

in gamma-ray spectra as a peak at 1.02 MeV lower than the incident gamma-ray energy peak.

The detector used in the experiments is a 20x20 cm well-type detector with a well depth of 25.44 mm and well-diameter of 134.0 mm. This is considered as a very large detector, which is able to let all secondary particles interact with the detector. The efficiency of the detector set-up was determined using Monte Carlo simulations with the GSnrc-code and was near to 100% for the experiments, with less than 1% variation between the efficiency.

In **Inductively Coupled Plasma – Mass Spectrometry** (ICP-MS), a Cs containing solution is introduced as an aerosol in an argon plasma (only the smallest droplets, 3-6 µm, reach the plasma as an aerosol). The plasma is powered by an electromagnetic coil. This process results in ionization after desolvatation, vaporization and atomization. The positively charged ions can be separated using a mass spectrometer. A Perkin Elmer NeXION 350S is used for the experiments, which uses a quadrupole mass spectrometer that only separates ions of a certain mass-to-charge ratio for a given ratio of voltages between the rods. A quadrupole MS typically has a lower resolution, requiring a Collision/Reaction Cell (CRC) to remove isobaric and polyatomic interferences. CRCs can be operated in two modes: reaction mode, in which specific reaction gasses remove known isobaric and polyatomic interferences or collision mode, based on the kinetic energy discrimination (KED). During the KED process (used for Cs measurements), He atoms collide with the analyte and polyatomic interferences. A voltage bias at the cell exit exclude these polyatomic ions from the ion beam because of their lower residual energy.

The most important parameters in the determination of Cs by the two used measurement methods are displayed in Table 3-2.

Table 3-2 Operational parameters for Cs measurement using ICP-MS and gamma-ray spectroscopy

Parameter	ICP-MS	Gamma-ray spectroscopy (with NaI(Tl) well-type detector)
Environmental influence	A cleanroom is required especially for the determination of Al, Ca, Mg, Na, Si and Zn in ultratrace concentration (ppt range) is required	Lead shielding and background correction are needed.
Matrix/Sample properties	Liquid with up to 0.2% diluted salts in standard mode and up to 2% of acid. Up to 30% salt content is possible using a FAST FIAS micro-injection system. Concentrations up to 300 ppm can be measured.	Must fit in the open space in the well No specific sample preparation necessary.
Measurement time	20 samples/hour	Dependent on activity and desired level of (un)certainty. (In this project: ca. 6 minutes to reach 10 000 counts, 10 samples/hour)
Calibration	External calibration based on standard solutions. An internal standard is also added to each of the samples.	External calibration using solutions that were measured in the ionization chamber.

Table 3-2 continued

Parameter	ICP-MS	Gamma-ray spectroscopy (with NaI(Tl) well detector)
Detection limit	The limit of detection (LOD) quantifies the lowest quantity that can be distinguished from a blank value. $$LOD = \frac{3 * \sigma_B * C_S}{S_S - S_B}$$ σ_B: standard deviation of the blank C_S: concentration of the standard solution S_S: signal of the standard solution S_B: signal of the blank solution The limit of quantification (LOQ) is the lowest concentration at which the analyte can be measured at reasonable precision. $$LOQ = \frac{S_B * C_S}{S_S - S_B}$$ Practical detection limit: 0.001 µg/L for Cs in MQ for the Perkin Elmer NeXION 350S	The number of sample counts must exceed a value that depends on the background rate and uncertainty in the estimate of the background rate. [41] $$N_S^2 \geq k^2 * (N_S + N_B + \sigma_B^2)$$ N:number of counts N_S: number of counts of the sample N_B: number of counts of the background σ_B : uncertainty in the background estimate; k: chosen factor linked to the desired confidence The minimum detectable activity (MDA in Bq/ unit wt) [42]: $$MDA\left(\frac{Bq}{unit\ wt}\right) = \frac{2.71 + 4.66(\sigma_B)}{T * EFF * Y * wt}$$ T is the collect time (sec) EFF is the efficiency at the energy of interest Y is the branching ratio wt is the sample weight

Table 3-2 continued

Parameter	ICP-MS	Gamma-ray spectroscopy (with NaI(Tl) well detector)
Relative error	Result of several individual measurements in the optimal concentration range lead to a relative error of approximately 1%. QC standards are used for slope correction or recalibration. Recovery tests are performed using a spike solution added to a similar matrix.	$$\frac{\sigma_N}{N} = \frac{\sqrt{N}}{N}$$ [42] As the number of counts increases, the relative error decreases. In this research, approximately 10 000 counts per sample are counted, resulting in a relative error of approximately 1%.
Efficiency	A triple cone interface in combination with a quadrupole ion deflector (QID) is used for an efficient extraction of the plasma ion population and to avoid neutral particles to contribute to background. Efficiency of ionization is controlled by internal standard.	Calculated based on Monte Carlo analysis. In this project: 99-100%. Detector efficiency takes into account: - Geometric efficiency - Absorption efficiency - Sample efficiency - Relative efficiency
Dynamic linear range	Up to 9 magnitudes (10^9) using a dual mode detector, combining impulse and analog detection.	Dead time is a results of system electronics at high counting rates, but can be (partly) corrected.

Both ICP-MS and gamma-ray spectroscopy have inherent (dis)advantages. The high dynamic linear range, multi-element detection and low detection limits make the ICP-MS competitive to the gamma-ray spectroscopy for Cs. Detection limits for Cs-134 measurements can be decreased by using solutions that are more concentrated in Cs-134 compared to stable Cs. The greatest advantage of the ICP-MS is the easy sample handling and the auto-sampler introduction system, in combination with quick measurement times and robustness towards several solutions (e.g. salt content in sea water.) The greatest advantage of gamma-ray spectroscopy is the absence of sample preparation, which can result in an easy determination of the mass balance of the adsorption system. The properties of the sample (salt content, solid/liquid,..) can be accounted for using efficiency calculations.

3.2 Research questions

Since ACBSG had already proven to be a valuable adsorbent for removal of organic pollutants and chromium, the main question to be answered here is: can it also be used for Cs adsorption? And could it possibly be combined with Prussian Blue for enhanced removal?

The first focus of this research is to find a suitable adsorption and measurement system to determine Cs adsorption efficiency. In the first manuscript, "Adsorption of cesium on different types of activated carbon", Cs-134 is used as a tracer to measure total Cs concentration via gamma-ray spectrometry. This research was conducted at the JRC-IRMM facilities and provided valuable insights on the removal and measurement of radionuclides. A combination of PB with AC is produced by a simple adsorption process to investigate a possible synergy between the selective agent and the adsorptive properties of the AC. An overview of the research questions that are answered in the first part:

- Research of a feasible adsorption and measurement system for Cs-134 adsorption on AC

- Removal efficiency of Cs by 5 ACs, two commercial and 3 ACBSGs

- Influence of pre-adsorption of PB on AC on the adsorption efficiency

- pH dependency of the Cs adsorption on all the adsorbents

As the results of the first manuscript point out that the effects of PB pre-adsorption were not totally satisfactory, the second part focuses on the use of another hexacyanoferride (HCF) in combination with 2 selected ACs. This second manuscript is called "Enhanced cesium removal from real matrices by modified activated carbons". Since the selected incorporation methods are typically used for biomass, some of these methods were simplified, using the ACs adsorptive capacities as driving force for the modification. Stable Cs (Cs-133) measurements are performed by ICP-MS. Focus points in this part are:

- Production of hybrid adsorbents with a different modification grade

- Describing the leaching behavior of the created adsorbents in order to protect the environment

- Testing for Cs adsorption efficiency at 2 AC dosages

- Comparing Cs adsorption from 3 different media: Milli-Q water, reconstituted water and marine medium

3.3 References

[1] World Nuclear, Fukushima Accident, **2017**.

[2] I. Korsakissok, A. Mathieu, D. Didier, Atmospheric dispersion and ground deposition induced by the Fukushima Nuclear Power Plant accident: A local-scale simulation and sensitivity study, Atmospheric Environment, **2013**, 70, 267-279.

[3] Y.-H. Koo, Y.-S. Yang, K.-W. Song, Radioactivity release from the Fukushima accident and its consequences: A review, Progress in Nuclear Energy, **2014**, 74, 61-70.

[4] Y. Pontillon, G. Ducros, P.P. Malgouyres, Behaviour of fission products under severe PWR accident conditions VERCORS experimental programme—Part 1: General description of the programme, Nuclear Engineering and Design, **2010**, 240, 1843-1852.

[5] B. Sportisse, A review of parameterizations for modelling dry deposition and scavenging of radionuclides, Atmospheric Environment, **2007**, 41, 2683-2698.

[6] O. Masson, A. Baeza, J. Bieringer, K. Brudecki, S. Bucci, M. Cappai, F.P. Carvalho, O. Connan, C. Cosma, A. Dalheimer, D. Didier, G. Depuydt, L.E. De Geer, A. De Vismes, L. Gini, F. Groppi, K. Gudnason, R. Gurriaran, D. Hainz, Ó. Halldórsson, D. Hammond, O. Hanley, K. Holeý, Z. Homoki, A. Ioannidou, K. Isajenko, M. Jankovic, C. Katzlberger, M. Kettunen, R. Kierepko, R. Kontro, P.J.M. Kwakman, M. Lecomte, L. Leon Vintro, A.P. Leppänen, B. Lind, G. Lujaniene, P. Mc Ginnity, C.M. Mahon, H. Malá, S. Manenti, M. Manolopoulou, A. Mattila, A. Mauring, J.W. Mietelski, B. Møller, S.P. Nielsen, J. Nikolic, R.M.W. Overwater, S.E. Pálsson, C. Papastefanou, I. Penev, M.K. Pham, P.P. Povinec, H. Ramebäck, M.C. Reis, W. Ringer, A. Rodriguez, P. Rulík, P.R.J. Saey, V. Samsonov, C. Schlosser, G. Sgorbati, B.V. Silobritiene, C. Söderström, R. Sogni, L. Solier, M. Sonck, G. Steinhauser, T. Steinkopff, P. Steinmann, S. Stoulos, I. Sýkora, D. Todorovic, N. Tooloutalaie, L. Tositti, J. Tschiersch, A. Ugron, E. Vagena, A. Vargas, H. Wershofen, O. Zhukova, Tracking of Airborne Radionuclides from the Damaged Fukushima Dai-Ichi Nuclear Reactors by European Networks, Environmental Science & Technology, **2011**, 45, 7670-7677.

[7] The National Diet of Japan, The Fukushima Nuclear Accident Indepenten Investigation Commision, **2012**.

[8] H. Kato, Y. Onda, M. Teramage, Depth distribution of 137Cs, 134Cs, and 131I in soil profile after Fukushima Dai-ichi Nuclear Power Plant Accident, Journal of Environmental Radioactivity, **2012**, 111, 59-64.

[9] T. Fujiwara, T. Saito, Y. Muroya, H. Sawahata, Y. Yamashita, S. Nagasaki, K. Okamoto, H. Takahashi, M. Uesaka, Y. Katsumura, S. Tanaka, Isotopic ratio and vertical distribution of radionuclides in soil affected by the accident of Fukushima

Dai-ichi nuclear power plants, Journal of Environmental Radioactivity, **2012**, 113, 37-44.

[10] P. Bailly du Bois, P. Laguionie, D. Boust, I. Korsakissok, D. Didier, B. Fievet, Estimation of marine source-term following Fukushima Dai-ichi accident, J Environ Radioact, **2012**, 114, 2-9.

[11] S.C. Gad, T. Pham, Cesium A2 - Wexler, Philip, in: Encyclopedia of Toxicology (Third Edition), Academic Press, Oxford, **2014**, 776-778.

[12] U.S. Department of Health and Human Services, Toxicological profile for cesium, **2004**.

[13] G.T. Johnson, T.R. Lewis, W.D. Wagner, Acute toxicity of cesium and rubidium compounds, Toxicology and Applied Pharmacology, **1975**, 32, 239-245.

[14] P. Lestaevel, R. Racine, H. Bensoussan, C. Rouas, Y. Gueguen, I. Dublineau, J.-M. Bertho, P. Gourmelon, J.-R. Jourdain, M. Souidi, Césium 137 : propriétés et effets biologiques après contamination interne, Médecine Nucléaire, **2010**, 34, 108-118.

[15] R.G. Thomas, R.L. THomas, Lethality of Cs-137 and Sr-90 administered in combination to rats, Radiation Research, **1970**, 42, 282-291.

[16] National Aeronotic and Space Administration, Properties of selected radioisotopes - Part I: Unclassified Literature, Washington, D.C., **1968**.

[17] M.-M. Bé, Table de Radionucléides - Cs 134, LNHB, **2012**.

[18] A.N. Ratnikov, A.V. Vasiliev, R.M. Alexakhin, E.G. Krasnova, A.D. Pasternak, B.J. Howard, K. Hove, P. Strand, The use of hexacyanoferrates in different forms to reduce radiocaesium contamination of animal products in Russia, Science of The Total Environment, **1998**, 223, 167-176.

[19] N.A. Beresford, S. Fesenko, A. Konoplev, L. Skuterud, J.T. Smith, G. Voigt, Thirty years after the Chernobyl accident: What lessons have we learnt?, Journal of Environmental Radioactivity, **2016**, 157, 77-89.

[20] B.J. Howard, N.A. Beresford, G. Voigt, Countermeasures for animal products: a review of effectiveness and potential usefulness after an accident, Journal of Environmental Radioactivity, 2**001**, 56, 115-137.

[21] A. Mohammad, Y. Yang, M.A. Khan, P.J. Faustino, Long-term stability study of Prussian blue-A quality assessment of water content and cyanide release, Clinical toxicology (Philadelphia, Pa.), **2015**, 53, 102-107.

[22] F. Ricci, G. Palleschi, Sensor and biosensor preparation, optimisation and applications of Prussian Blue modified electrodes, Biosensors and Bioelectronics, **2005**, 21, 389-407.

[23] Lalhmunsiama, C. Lalhriatpuia, D. Tiwari, S.-M. Lee, Immobilized nickel hexacyanoferrate on activated carbons for efficient attenuation of radio toxic Cs(I) from aqueous solutions, Applied Surface Science, **2014**, 321, 275-282.

[24] C. Vincent, A. Hertz, T. Vincent, Y. Barré, E. Guibal, Immobilization of inorganic ion-exchanger into biopolymer foams – Application to cesium sorption, Chemical Engineering Journal, **2014**, 236, 202-211.

[25] D. Parajuli, A. Takahashi, H. Noguchi, A. Kitajima, H. Tanaka, M. Takasaki, K. Yoshino, T. Kawamoto, Comparative study of the factors associated with the application of metal hexacyanoferrates for environmental Cs decontamination, Chemical Engineering Journal, **2016**, 283, 1322-1328.

[26] G.-R. Chen, Y.-R. Chang, X. Liu, T. Kawamoto, H. Tanaka, D. Parajuli, M.-L. Chen, Y.-K. Lo, Z. Lei, D.-J. Lee, Prussian blue non-woven filter for cesium removal from drinking water, Separation and Purification Technology, **2015**, 153, 37-42.

[27] H.-M. Yang, K.S. Hwang, C.W. Park, K.-W. Lee, Sodium-copper hexacyanoferrate-functionalized magnetic nanoclusters for the highly efficient magnetic removal of radioactive caesium from seawater, Water Research, **2017**, 125, 81-90.

[28] H.-M. Yang, S.-C. Jang, S.B. Hong, K.-W. Lee, C. Roh, Y.S. Huh, B.-K. Seo, Prussian blue-functionalized magnetic nanoclusters for the removal of radioactive cesium from water, Journal of Alloys and Compounds, **2016**, 657, 387-393.

[29] K.S. Hwang, C.W. Park, K.-W. Lee, S.-J. Park, H.-M. Yang, Highly efficient removal of radioactive cesium by sodium-copper hexacyanoferrate-modified magnetic nanoparticles, Colloids and Surfaces A: Physicochemical and Engineering Aspects, **2017**, 516, 375-382.

[30] H.G. Mobtaker, T. Yousefi, S.M. Pakzad, Cesium removal from nuclear waste using a magnetical CuHCNPAN nano composite, Journal of Nuclear Materials, **2016**, 482, 306-312.

[31] G.-R. Chen, Y.-R. Chang, X. Liu, T. Kawamoto, H. Tanaka, D. Parajuli, T. Kawasaki, Y. Kawatsu, T. Kobayashi, M.-L. Chen, Y.-K. Lo, Z. Lei, D.-J. Lee, Cesium removal from drinking water using Prussian blue adsorption followed by anion exchange process, Separation and Purification Technology, **2017**, 172, 147-151.

[32] C.W. Park, B.H. Kim, H.-M. Yang, B.-K. Seo, J.-K. Moon, K.-W. Lee, Removal of cesium ions from clays by cationic surfactant intercalation, Chemosphere, **2017**, 168, 1068-1074.

[33] A.K. Vipin, B. Hu, B. Fugetsu, Prussian blue caged in alginate/calcium beads as adsorbents for removal of cesium ions from contaminated water, Journal of Hazardous Materials, **2013**, 258, 93-101.

[34] T. Nishikiori, S. Suzuki, Radiocesium decontamination of a riverside in Fukushima, Japan, Journal of Environmental Radioactivity, **2017**, 177, 58-64.

[35] K. Inoue, M. Gurung, B.B. Adhikari, S. Alam, H. Kawakita, K. Ohto, M. Kurata, K. Atsumi, Adsorptive removal of cesium using bio fuel extraction microalgal waste, Journal of Hazardous Materials, **2014**, 271, 196-201.

[36] D. Ding, Y. Zhao, S. Yang, W. Shi, Z. Zhang, Z. Lei, Y. Yang, Adsorption of cesium from aqueous solution using agricultural residue - Walnut shell: Equilibrium, kinetic and thermodynamic modeling studies, Water Research, **2013**, 47, 2563-2571.

[37] T. Lan, Y. Feng, J. Liao, X. Li, C. Ding, D. Zhang, J. Yang, J. Zeng, Y. Yang, J. Tang, N. Liu, Biosorption behavior and mechanism of cesium-137 on Rhodosporidium fluviale strain UA2 isolated from cesium solution, Journal of Environmental Radioactivity, **2014**, 134, 6-13.

[38] X. Liu, G.-R. Chen, D.-J. Lee, T. Kawamoto, H. Tanaka, M.-L. Chen, Y.-K. Luo, Adsorption removal of cesium from drinking waters: A mini review on use of biosorbents and other adsorbents, Bioresource Technology, **2014**, 160, 142-149.

[39] Z. Majidnia, A. Idris, Evaluation of cesium removal from radioactive waste water using maghemite PVA–alginate beads, Chemical Engineering Journal, **2015**, 262, 372-382.

[40] G.F. Knoll, Radiation Detection and Measurement, John Wiley & Sons, **2000**.

[41] Amptek Inc., How sensitive is the gamma-rad, **2017**

[42] Canberra, Spectrum analysis, **2010**

3.4 Adsorption of cesium on different types of activated carbon[7]

S. R. H. Vanderheyden[1], R. Van Ammel[2], K. Sobiech-Matura[2], K. Vanreppelen[1,3], S. Schreurs[3], W. Schroeyers[3], J. Yperman[1], R. Carleer[1]

[1]Research Group of Analytical and Applied Chemistry, CMK, Hasselt University, Diepenbeek, Belgium

[2]European Commission, Joint Research Centre, Institute for Reference Materials and Measurements, Geel, Belgium

[3]Research Group of Nuclear Technology, CMK, Hasselt University, Diepenbeek, Belgium

Abstract

The optimal conditions to remove radiocesium from water by adsorption on activated carbon (AC) were investigated. Two commercial ACs were compared to ACs prepared by steam activation of brewers' spent grain. The influence of pH and loading AC with Prussian Blue were studied. [134]Cs, measured by gamma-ray spectroscopy, served as a tracer for the Cs concentration. Column experiments showed that a neutral to acidic pH enhanced adsorption compared to high pH. Norit GAC 1240 had the highest adsorption capacity, 8.5 µg Cs g^{-1} AC for a column filtration. Sequential columns of Norit GAC 1240 removed 28.1± 2.8% of Cs per column.

3.4.1 Introduction

Produced only by anthropogenic sources, radioactive Cs isotopes are released into the biosphere by weapons testing, nuclear reactor accidents and controlled release

---

[7] References for this article can be found on page 146 in section 3.4.6

into waste water streams. These releases combined with its relatively long half-life ($T_{1/2} \approx 30$ years), makes ^{137}Cs the major contributor to the long term environmental radiation dose received by humans and other organisms [1]. During the nuclear accident at the Fukushima nuclear power plant, the estimated release of ^{137}Cs into the environment amounted to more than 12×10^{15} Bq. Additionally, the short-lived [134]Cs ($> 12 \times 10^{15}$ Bq, $T_{1/2} \approx 2$ years) and [136]Cs ($> 2 \times 10^{15}$ Bq, $T_{1/2} \approx 13$ days) were also released, raising the level of activity in the drinking water above the legally permitted levels in the nearby areas [2,3]. One estimates that these atmospheric releases are only a fraction of the releases from the Chernobyl nuclear power plant during the accident in 1986 [2]. The activity of Cs radioisotopes poses a radiotoxicity risk caused by external radiation exposure and internal radiation damage after inhalation of contaminated air or intake of contaminated food or water [4,5]. However, stable Cs in these concentrations is not known to be harmful. Cs is very mobile in aqueous environments because of its high solubility, but it strongly binds to soils and minerals. This promotes accumulation of Cs radioisotopes and contamination of the food chain [5,4,6]. Treatment of radioactive waste water contaminated with Cs isotopes is a challenging research area in environmental radiation protection [7].

Recently, a wide range of low-cost adsorbents were investigated for the removal of Cs from wastewater because other methods such as chelation and precipitation are rather ineffective for the removal of trace amounts of Cs [8-10]. Studies have been carried out using different organic and inorganic ion exchangers, such as Prussian blue (PB) and other hexacyanoferrates (HCF) [11-13]. HCFs have a major disadvantage: they exist mainly as micro-particles (particle diameter <100 nm). These micro-particles are hard to filtrate from aqueous solutions and can clog a fixed bed reactor causing a significant pressure loss. Recent research has shown that adsorption of cesium is a promising remediation method for contaminated liquid wastes, if the operating costs can be kept sufficiently low [7,14,15]. Combining HCF (nano)particles with a carrier material having beneficial characteristics could provide a practical and efficient material for Cs removal [9,12,16,17]. Incorporation of HCF on biosorbents provides a solution for the filtration problems associated with unbound HCF [9,17]. The incorporation of

these HCF in a porous material would lead to an increased amount of HCF for a specific volume, thereby increasing adsorption efficiency.

Activated carbon (AC), having high surface area and developed porosity is a low-cost and effective adsorbent for a wide range of pollutants [18,19]. AC has been used in research to remove radionuclides from waste water solutions in a relatively straightforward way compared to other methods [20]. AC has multiple surface functionalities, a high mechanical strength and a good resistance towards chemicals, heat and radiation [19,21]. Most of the AC produced presently is made by steam activation of mined coal. However, it might be economically interesting to produce AC from biomass by pyrolysis, followed by chemical or physical activation. During physical activation, a carbonised biomass is treated with a mildly oxidising gas at 750 – 900 °C to increase its porosity and surface area [18,22-25]. Carbonisation and activation of biomass has previously proven to produce economically valuable AC, if the source material has a consistent and lignin-rich composition [19,26-28]. Brewers spent grain (BSG) is an interesting source material for the preparation of AC because of its availability and high nitrogen content. This creates an in-situ nitrogenised AC, characterised by an increased amount of pyrrolic and pyridinic surface groups [29,30,27,31]. Because of changed acidic/basic surface characteristics and a more pronounced chemisorption mechanism, nitrogenised ACs have shown an improved adsorption towards multiple pollutants compared to normal AC [32-37]. Adsorption of Cs on ACs has been researched in the past, but with relatively high concentrations of Cs, generally 10 mg/L and higher [7,38,39].

In order to find an AC suitable for Cs removal from waste water, adsorption capacities for lower Cs concentrations are measured and presented in this paper. Furthermore, a simple HCF incorporation on the surface of the AC is tested, in order to find a synergistic effect between adsorption and the HCF ion exchangers. Focussing on low concentrations of Cs and different adsorption techniques, adsorption capacities are compared for different types of AC. A series of experiments was set up for the study in order to investigate the key adsorption parameters. This could provide good tools for future low-level adsorption experiments.

3.4.2 Experimental

The goal of this experiment was to study and optimise the removal of Cs from water using different ACs. To study the behaviour of the Cs, [134]Cs was used as a tracer. A standard Cs solution was irradiated to activate a fraction of the stable Cs to [134]Cs. The [134]Cs solution was brought in contact with AC under different experimental conditions. In this experiment the optimal settings for adsorption were tested by varying the AC, the pH and the adsorption technique.

Three adsorption techniques were evaluated: batch adsorption tests and two types of column tests. Batch adsorption tests were based on the equilibrium between the AC adsorbents (5 different types plus their modified form) and the Cs solution after 48 hours of shaking. Column adsorption tests resembled industrial adsorption filter systems and can be performed in two ways. Firstly, a single column containing the AC can be used multiple times to extract Cs from the same solution, until saturation of the AC surface is reached. This is referred to later on as a 'single column' experiment and is conducted with the 5 ACs. Secondly, a solution can be filtered through different sequential columns to remove Cs. This is referred to as 'sequential column' experiment and was performed only for Norit GAC 1240.

To prepare the solutions needed in the experiments, Milli-Q water and analytical grade reagents were used. All labware was cleaned with detergent and water prior to use. Glassware, centrifuge tubes and filtration columns were filled with a solution containing 20 mg L^{-1} of stable Cs having the same pH as the solution used in the experiments and left overnight in order to saturate their surfaces with stable Cs.

3.4.2.1 Activated carbon

Five different types of AC were used in the experiments. Three of them were prepared from BSG using a custom made pyrolysis/activation reactor as described previously in [27]. BSG was dried at 105±5 °C for 24 h and sieved to obtain a particle size smaller than 2 mm. These three ACs were prepared at different temperatures, using different steam activation durations and quantities of Milli-Q water: ACBSG05 (800 °C/30 min/10 mL), ACBSG06 (850 °C/45 min/15 mL) and ACBSG07 (800 °C/45 min/15 mL). For comparison, the two most widely used

commercially available ACs were used: Norit GAC 1240 (Cabot Corporation, Massachusetts, USA) and Filtrasorb400 (Chemviron Carbon, Seneffe, Belgium). Both of these ACs are made from steam-activated bituminous coal and have a more mesoporous structure. Their properties make them ideal for removal of a range of pollutants from waste water [40,41].

An important characteristic of AC is the point of zero charge (pH_{PZC}) as it determines at which pH the total surface charge of the AC is zero. A pH above the pH_{PZC} will cause the surface of the AC to be negatively charged, attracting the Cs cations to its surface. Solutions having $pH > pH_{PZC}$ will be tested to evaluate the influence of this attraction on adsorption.

The characteristics of the porosity of the AC were determined by analysis of the BET (Brunauer-Emmet-Teller) surface areas (total surface area S_{BET}, microporous surface area S_{micro} and exterior surface area S_{ext}), total porosity volume (V_T), micropore volume (V_{Micro}) and mesopore volume (V_{Meso}) by nitrogen (77 K) adsorption using an Autosorb AS-1 (Quantachrome, USA) [42,43]. The micropores are characterised by the Dubinin – Radushkevich method (volume micropores V_{Micro}) and the t-plot method using the De Boer method (micropore surface S_{micro} and extremal surface S_{ext}). Before analysis the samples were outgassed for 16 h at 200 °C in high vacuum. Experiments were performed by 'Department of Chemistry', Laboratory for Adsorption and Catalysis, University Antwerp, Belgium.

Table 3-3 displays these results. For the ACs from BSG, the BET surface increases with increasing activation (from ACBSG05 to ACBSG07 and to ACBSG06). The obtained BET surface for the ACs from BSG is around half (686 – 836 m²/g) of the BET surface from the commercial ACs (1468 -1483 m²/g). Higher and longer activation times increase the BET surface, micropore (V_{Micro}), mesopore (V_{Meso}) and the overall pore volumes (V_T) of all the samples. The V_{Micro}/V_T ratio decreased from 0.81 to 0.78, indicating that the mesopores gain a larger contribution to the total pore volume by increasing activation. This is also observed in the broadening of the average micropore diameter (L_0). In contrast to the commercial ACs, the ACBSGs have average pore diameter that is 2 times smaller than the commercial ACs.

Table 3-3 BET surfaces and pore volumes of the used ACs determined by nitrogen adsorption at 77 K

	S_{BET} (m²/g)	S_{micro} (m²/g)	S_{ext} (m²/g)	V_T (cm³/g)	V_{Micro} (cm³/g)	V_{Meso} (cm³/g)	L_0 (nm)	E_0 (kJ/mol)
ACBSG05	686	422	100	0.335	0.274	0.060	0.9	23.5
ACBSG06	836	506	151	0.439	0.342	0.097	1.3	19.9
ACBSG07	758	461	121	0.382	0.304	0.078	1.0	22.2
Norit GAC 1240	1468	532	725	0.827	0.599	0.228	2.6[*]	15.5
Filtrasorb F400	1483	833	432	0.859	0.604	0.256	2.6[*]	15.5

[*] The empirical correlation (Stoeckli formula) is only valid for L_0 values between 0.5 and 2.0 nm

A rough estimation of the pore size distribution of the micropores (Figure 3-5) is determined by means of the Density Functional Theory (DFT). The pore size distribution reveals that the ACBSGs consist of primarily pores with a diameter between 1 and 1.1 nm, followed by two secondary micropores 0.82 – 0.97 nm and 1.12 – 1.32 nm. In addition, wider micropores are found of about 2 nm. The pore size distribution in the mesopore range shows four peaks: at 3.7 nm, 4.9 nm, 5.3 nm and 5.8 nm respectively. An increase in temperature and activation increases the amount of micropores and mesopores, without increasing their size. When comparing with the pore size distribution of the commercial ACs, a very discrete distribution is obtained by the activation and pyrolysis of BSG.

Prussian Blue (PB) was fixed on the surface of each of these five ACs to create an AC-PB combination to enhance the adsorption capacity. Therefore, 1 g of AC was mixed with 150 mL of saturated PB solution and shaken for 48 hours. The pH of the solution was set at 7, to prevent dissociation of the PB in an acidic or basic environment [44,45]. The AC was then filtered off using ashless Whatman filters, washed with water and dried at 105±5 °C for 24 h. The PB concentration of the solution before and after adsorption was obtained indirectly by measuring the iron concentration in the solutions using ICP-AES (Optima 3300 DV, Perkin Elmer, Massachusetts, USA). The mass difference of PB was supposed to be bound to the AC. The mass of PB adsorbed on the surface of the AC is an important parameter to determine the extra amount of Cs that can be adsorbed. Both 5 ACs and 5 AC-PBs were used in the batch adsorption experiments.
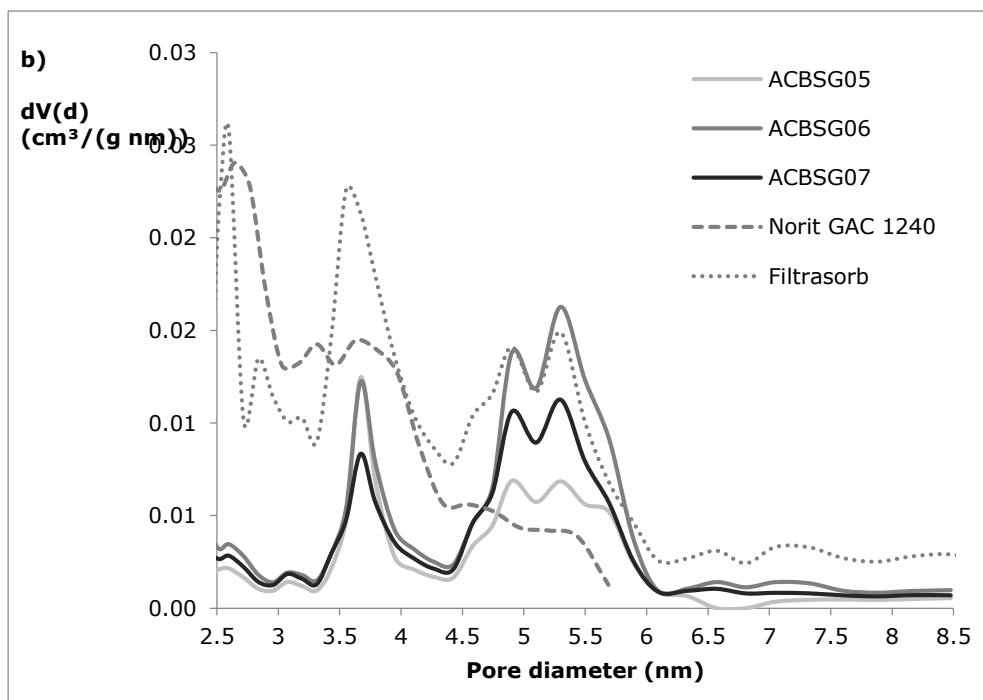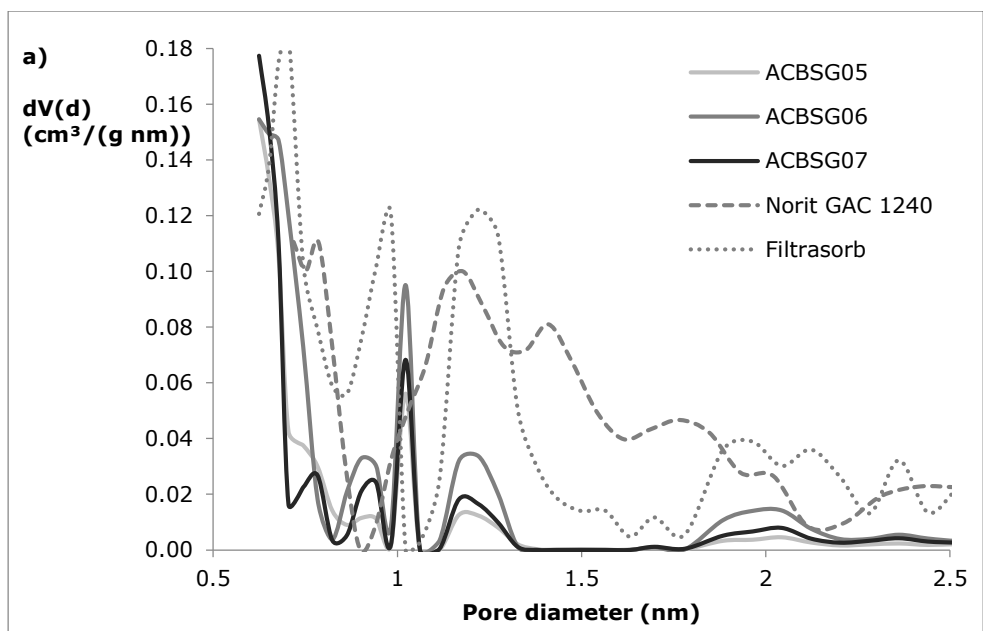
Figure 3-5 Pore size distribution of the ACs determined by DFT method for a) micropores; b) mesopores (2.5 – 8.5 nm)

Table 3-4 displays the mass of PB adsorbed on the AC expressed in mg g^{-1}. The observed differences in adsorbed amount might be related to the pore size distribution, allowing PB to move more freely in Norit GAC 1240, Filtrasorb 400 and ACBSG06. The latter was activated in the most severe conditions (850 °C/45 min/15 mL), which led to an increase in overall pore sizes, as described above, increasing the mobility of the colloidal PB molecules [46].

Table 3-4 Mass of PB adsorbed on the five different activated carbons used in this study

Type of AC	mg PB g^{-1} AC
Norit GAC 1240-PB	13.9 ± 0.1
Filtrasorb 400-PB	10.1 ± 0.1
ACBSG05-PB	1.6 ± 0.1
ACBSG06-PB	15.3 ± 0.1
ACBSG07-PB	3.3 ± 0.1

3.4.2.2 Solutions

In order to be able to monitor the behaviour of Cs in these experiments, a 1000 mg L^{-1} CsNO$_3$ standard solution was irradiated for 21 hours in the neutron flux of BR-1 at SCK·CEN (φ=3x10^{11} n cm^{-2} s^{-1}; σ=30x10^{-24} cm^{-2}) to activate part of the Cs to ^{134}Cs. The ^{134}Cs in the irradiated solution served as a tracer for the total Cs. The undiluted solution had an activity concentration of 50.93±0.74x10^3 Bq g^{-1}. The radiopurity of it was checked by measuring it on a HPGe detector. No impurities could be identified.

The solution was diluted to approximately 1:1000 in three steps. Dilution factors were determined gravimetrically and checked by measuring the activity of ^{134}Cs in the solution using an ionisation chamber and a well-type NaI(Tl) detector.

Previous work showed that the pH$_{PZC}$ of AC from BSG ranges from 10.6 to 10.8, and those of the used commercially available ACs from 11.5–11.7 [27]. Therefore, the pH of the working solutions was adjusted to 7, 10 and 12 using ammonia.

These working solutions had a [134]Cs activity concentration of 59.24±0.70, 59.67±0.70, 60.44±0.71 Bq g^{-1} corresponding to a Cs concentration of 1.16, 1.17 and 1.19 mg L^{-1} at pH 7, 10 and 12, respectively.

3.4.2.3 Gamma-ray spectrometry

The activity of the samples was determined by 4π gamma counting using a 20 x 20 cm NaI(Tl) well-type detector with a well-diameter of 25.4 mm and well-depth of 134.0 mm. In the NaI(Tl) well detector all the signals above the lower energy threshold of 50 keV were counted. All measurement results were corrected for background and decay. The total efficiency of the well-type NaI(Tl) detector was calculated using Monte Carlo simulations with the EGSnrc-code. The calculations were done using the same lower threshold of 50 keV. Furthermore, the different filling heights of solution in the used centrifuge tubes were individually modelled. The calculated efficiencies were close to 100% and showed a variation smaller than 1% between empty and completely filled tubes.

A gamma-ray spectrum of the [134]Cs solution obtained with the well-type NaI(Tl) detector is displayed in Figure 3-6. The lower energy threshold of 50 keV is clearly visible. The spectrum shows the transitions at 605 keV (p=98.21, $\gamma_{1,0}$) and 796 keV (p=85.73, $\gamma_{3,1}$) [47]. The peak at 1401 keV is the sum peak of these transitions, caused by the simultaneous detection of both gamma rays. At 1970 keV the gamma rays of 569, 605 and 796 are collected simultaneously.
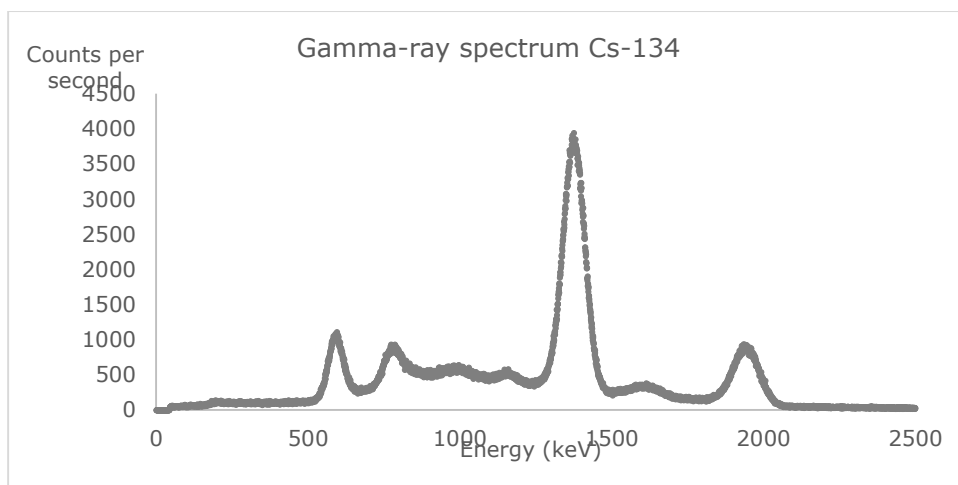
Figure 3-6 Gamma-ray spectrum of a [134]Cs solution measured in the well-type Na(Tl) detector

3.4.2.4 Batch adsorption experiment

The batch adsorption experiments were conducted using all 10 types ACs, i.e. 5 ACs both with and without fixed PB. Each of these ten ACs was tested for adsorption using three [134]Cs solutions of different initial pH (7-10-12) and similar activity.

Between 20 and 30 mg of AC and approximately 9 mL of Cs solution (approximately 60 Bq g^{-1} [134]Cs, corresponding to 1.2 mg L^{-1} Cs) at the desired initial pH (7, 10 or 12) were gravimetrically added into different centrifuge tubes (VWR High Performance 15 ml, VWR International, Leuven, Belgium). After shaking the tubes for 48 h in a Maxi-Mix III Vortex Mixer (Thermo Scientific, USA), each solution was filtered through a 75 mm funnel (VITLAB, Großostheim, Germany) with an ashless Whatman filter and the filtrated solution was stored in a second centrifuge tube. The filter containing the AC was dried and stored in a third centrifuge tube. All three centrifuge tubes (the empty centrifuge tube, the filtered solution and filter paper with AC) were measured in the well-type NaI(Tl) detector. This test was conducted in triplo for each type of AC. Adsorption capacities at equilibrium (q_e, in mg/g) were calculated as follows:

159

$$q_e = A_{filter} * k_{ac} / m_{AC} \qquad \text{Equation 3-1}$$

Were A_{filter} is the measured activity in the filter (in Bq), k_{ac} is the recalculation constant for activity to mass (in mg/Bq) and m_{AC} is the mass of the AC used (in g).

To prove there were no losses of ^{134}Cs during the experiment, a recovery experiment was set up. This experiment was conducted in exactly the same way prior to the batch adsorption experiment. Recovery rates were calculated for three ACs as the ratio between the activity of the solution in the centrifuge tube prior to shaking and the sum of the activities measured in the three centrifuge tubes after the adsorption experiment. A maximum of 0.7% deviation from 100% was found, indicating that the losses of activity throughout the adsorption procedure were minor.

3.4.2.5 Single column experiment

Adsorption of Cs on AC can be applied to both surface water (neutral to slightly acidic environment) and liquid waste treatment in decontamination units, where pH conditions can be more extreme. In order to test samples resembling the conditions described above and to find an optimal pH to promote column adsorption, solutions of different pH were tested: one acidic, one neutral and two basic. As a reference AC, Norit GAC 1240 was chosen for this experiment. Bio-rad Poly-Prep Chromatography Columns (0.8 x 4 cm) (Bio-Rad, California, USA) were filled with approximately 0.7 g of Norit GAC 1240 and pre-wetted with water. 11 mL of approximately 37 Bq g^{-1} ^{134}Cs solution at pH 4, 7, 10 and 12 was poured over these columns and collected, by gravity, in a centrifuge tube. The activity of the collected solution, as well as the activity remaining in the empty centrifuge tube, were both measured in the well-type detector. The collected solution was then poured over the column again. This cycle was repeated five times. Each test was conducted in duplo. After five cycles the column was measured in the well-type detector after air drying for 48 hours. Adsorption capacities (q) were calculated as mg Cs (calculated from the column activity) per gram of AC.

On the basis of the first tests the most effective pH was determined, 5 different ACs (Norit GAC 1240, Filtrasorb 400, ACBSG05, ACBSG06, ACBSG07) were used

in order to compare their performance. The column adsorption procedure was identical to the one described above. It was performed using 11 mL of approximately 37 Bq g^{-1} ^{134}Cs solution at pH 7.

For the column adsorption experiment a recovery experiment was also conducted. For this purpose, two columns filled with approximately 0.7 g of AC (Norit GAC 1240 and ACBSG07) were used. 11 mL of containing approximately 37 Bq g^{-1} of ^{134}Cs was then poured over each column and collected in a centrifuge tube. This process was repeated 5 times. The centrifuge tubes and column were measured as described above. The average recovery rate showed no loss during the column test.

3.4.2.6 Sequential column experiment

In this part of the experiment five columns were filled with approximately 0.7 g of Norit GAC 1240. 12 mL of approximately 37 Bq g^{-1} Cs solution at pH 7 was poured over the column and collected. After measuring the collected solution, it was poured successively over the four remaining identical columns and the activity of the solution was measured after each filtration. This test was conducted in duplo.

3.4.3 Results and discussion

3.4.3.1 Batch adsorption experiment

Batch adsorption tests using different ACs could reveal the difference between the commercial ACs and the AC from BSG. The influence of PB adsorption prior to Cs adsorption and the influence of pH on the amount of adsorbed Cs were also determined.
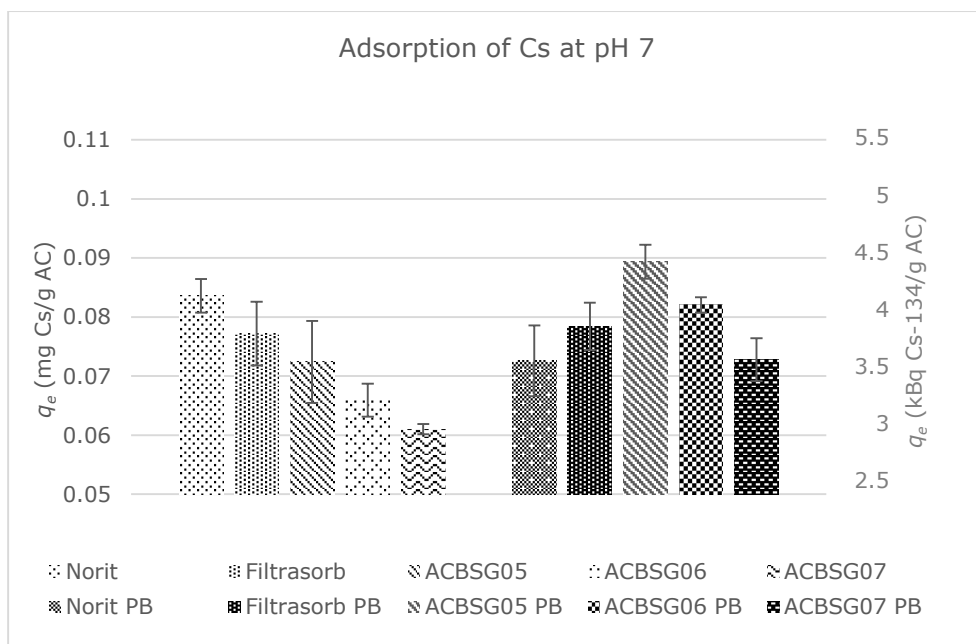
Figure 3-7 Adsorption capacities (q_e) of Cs on different ACs during batch adsorption at pH 7
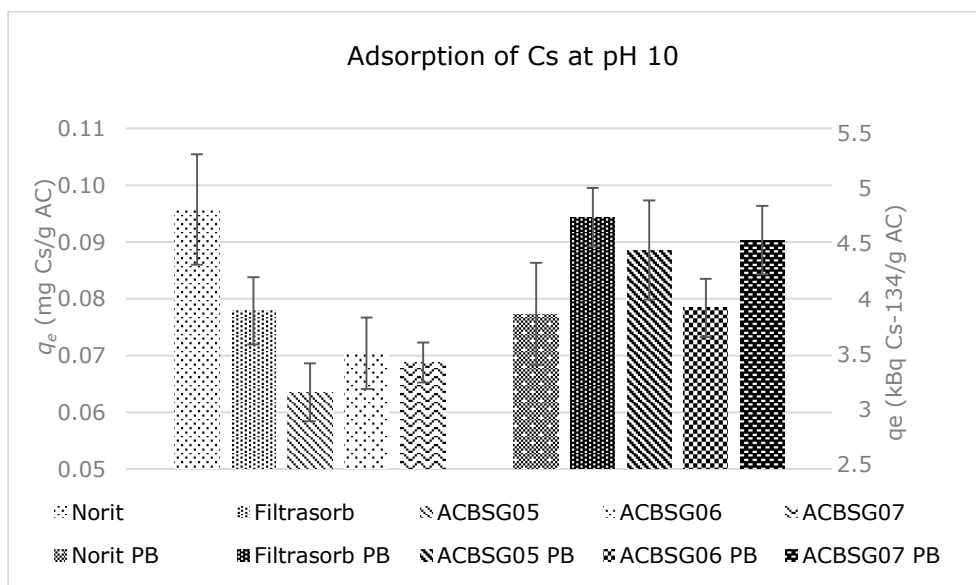
Figure 3-8 Adsorption capacities (q_e) of Cs on different ACs during batch adsorption at pH 10
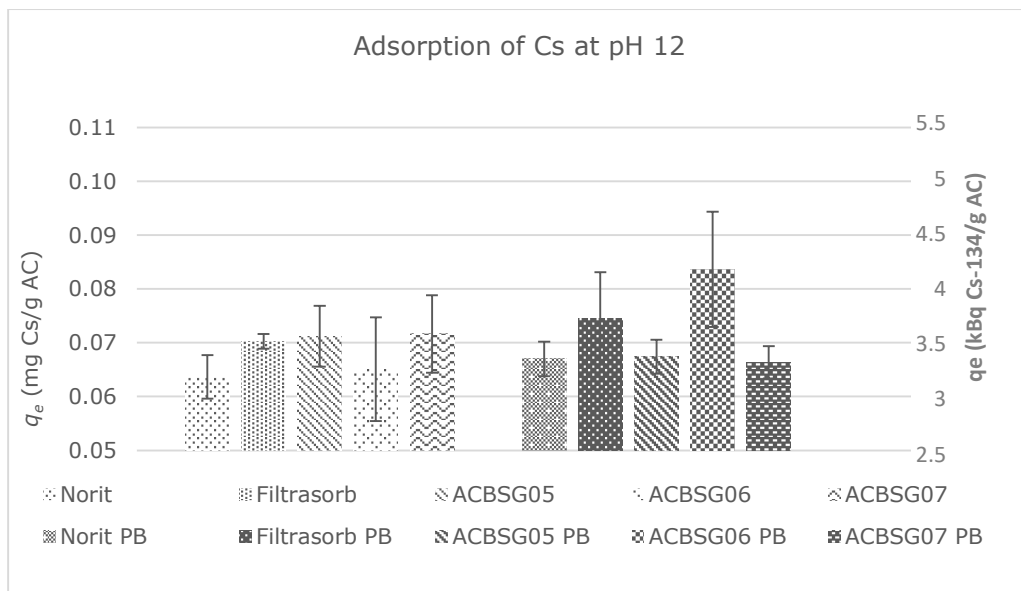
Figure 3-9 Adsorption capacities (q_e) of Cs on different ACs during batch adsorption at pH 12

The results of the batch adsorption experiments are displayed in Figure 3-7, Figure 3-8 and Figure 3-9. The untreated ACs are plotted on the left and the ACs with PB adsorbed on the right side. Error bars show the combined standard uncertainty. Statistical measurement uncertainties were calculated and proven to be insignificant compared to the standard deviations between the 3 different repeats of the experiments. For each pH the average activity concentrations and Cs concentrations before and after adsorption are displayed in Table 3-5. The average removal percentage is displayed at the different pH settings. Adsorption capacity at equilibrium is expressed as q_e (mg Cs adsorbed per gram AC).

The best adsorption capacity (q_e) was obtained at pH 10, although the differences between adsorption of solutions of different pH were not significant. At pH 12, all ACs were negatively charged, but this did not increase the adsorption of Cs on the AC. This may have been caused by the competition of adsorption between Cs and the high amount of ammonia present in the solution. The binding of PB on AC prior to Cs adsorption did not significantly promote the adsorption at any of the tested pH values. Furthermore, the dissociation of unbound PB happens above pH 8. This can explain the fact that AC with PB shows the same q_e values at pH 10

and 12 as for the unloaded AC. This experiment shows that the ACs have similar adsorption capacities in different circumstances. A removal of about 20% is limited compared to the results obtained by ion exchangers, where removal rate of above 70% are easily reached [48,16]. Some manuscripts report extremely low [39,49] removal percentages for Cs using AC. Kimura et al. [15] reported removal percentages up to almost 100%, but used AC dosages were approximately 30 times higher than in this manuscript. The ACs investigated seem to have an interesting affinity for Cs, even at lower dosage.

Table 3-5 Average measured (activity) concentrations before and after batch adsorption with calculated average removal for each tested pH

pH	Activity concentration before adsorption (Bq g^{-1})	Cs concentration before adsorption (mg L^{-1})	Activity concentration after adsorption (Bq g^{-1})	Cs concentration after adsorption (mg L^{-1})	Removal percentage
7	59.24 ± 0.70	1.16 ± 0.01	48.63 ± 1.86	0.95 ± 0.04	18.3 ± 3.0
10	59.67 ±0.70	1.17 ± 0.01	47.11 ± 1.25	0.93 ± 0.02	21.0 ± 1.7
12	60.44 ± 0.71	1.19 ± 0.01	49.24 ± 1.18	0.96 ± 0.02	18.5 ± 1.2

3.4.3.2 Single column adsorption

3.4.3.2.1 pH selection

Results of the column filtration of solution at different pH (4-7-10-12) are shown in Figure 3-10.

For pH 4 and pH 7, the adsorption capacity (q) increased with each cycle with a maximum q_e of about 0.0083 mg g^{-1} Cs on Norit GAC 1240. A higher pH drastically lowered the maximum adsorbed amount of Cs on the AC, to a q_e of 0.0033 mg g^{-1} at pH 10 and 0.0020 mg g^{-1} at pH 12 after 5 cycles. Additionally, *q* seems to decrease with each additional cycle. This effect was probably due to the competition of adsorption by the ammonia ion in the solutions, which explains why the lowest adsorbed amount is found at the highest pH. The competition between Cs and the ammonia ion may wash out the Cs already adsorbed on the AC, decreasing q after three cycles. A neutral to slightly acidic environment enhances Cs adsorption in comparison to a strongly basic environment.
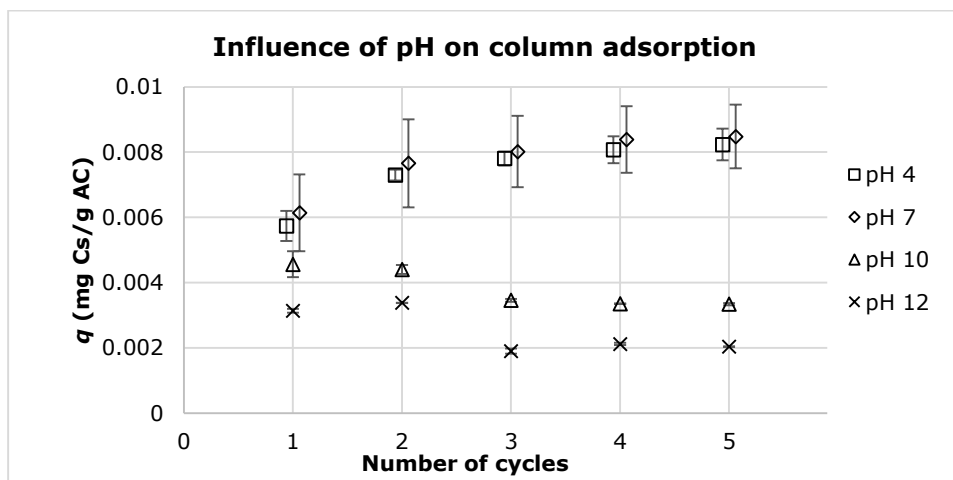
Figure 3-10 Adsorption capacities after 5 cycles of adsorption on a column filled with Norit GAC 1240 using solutions with different pH.

Data points have been artificially separated to enhance visibility.

3.4.3.2.2 AC selection

The commercial ACs show a significantly higher adsorption capacity q of Cs compared to the ACBSGs. Norit GAC 1240 reached its equilibrium adsorption capacity (q_e of 0.0085 mg g^{-1}) after 4 cycles, while q on Filtrasorb 400 still rose to 0.0075 mg g^{-1} after 5 cycles. Both commercial ACs are in granular form, making a better interaction between the surface of the AC and the Cs solution possible compared to the three ACBSGs, having a smaller particle size. The ACBSGs tended to stick together in the column with air still present in open spaces, causing possible channel formation. This resulted in a less efficient interaction between AC surface and solution. Additionally, this caused a limited contact time and smaller contact area for the ACBSGs. All 3 ACBSGs reached their equilibrium adsorption capacities after 2-3 cycles. ACBSG06 performed better compared to ACBSG05 and ACBSG07 (a q of 0.0050 mg g^{-1}, compared to 0.0024 mg g^{-1} and 0.0034 mg g^{-1} respectively), possibly due to the higher activation temperature used, creating a slightly wider pore distribution thus increasing the mobility of the Cs ions in aqueous solutions.
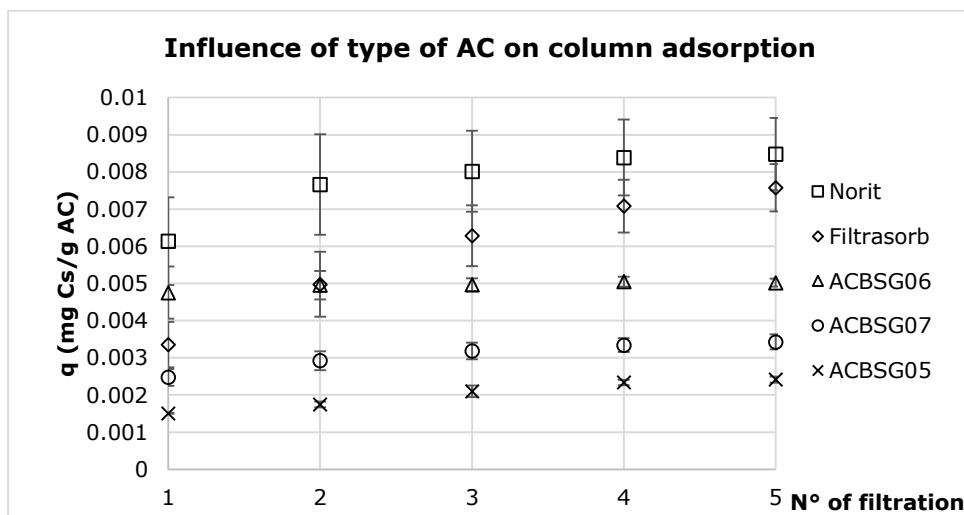
Figure 3-11 Adsorption capacities after 5 cycles of adsorption on 5 ACs using a solution of pH 7

3.4.3.3 Sequential column adsorption

Passing the solution through five columns filled with Norit GAC 1240 decreased the concentration from 36.3 ± 0.3 Bq g^{-1} (0.713 mg L^{-1} Cs) to 6.8 ± 0.9 Bq g^{-1} (0.135 mg L^{-1} Cs). For this test, the decrease showed a removal rate of $28.1\pm2.8\%$ of the initial Cs concentration per filtration. This result indicated that further removal of low levels of Cs is possible using sequential filtration steps. No equilibrium was reached during this experiment, as displayed in Figure 3-12.
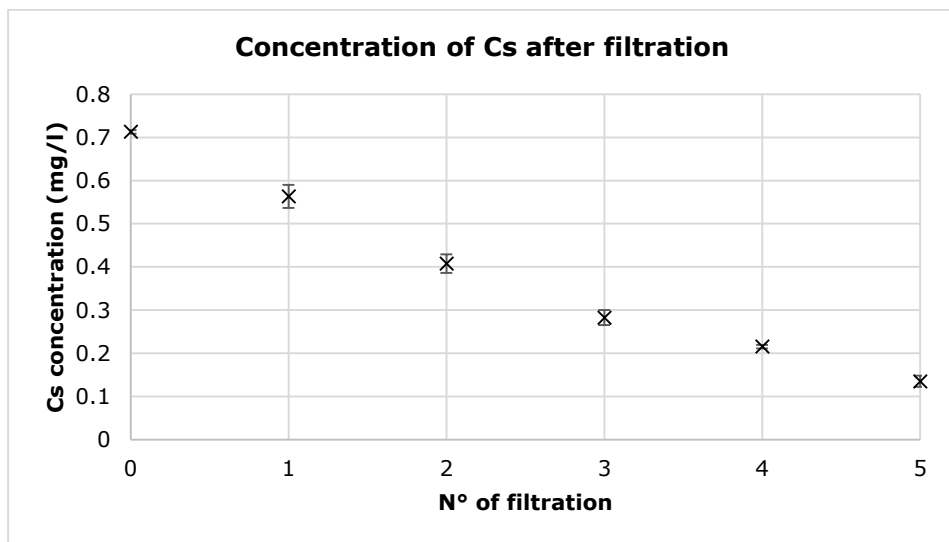
Figure 3-12 Decrease in Cs concentration after sequential column adsorption with Norit GAC 1240 GAC1240

3.4.4 Conclusions

This work studied the removal of low concentrations of Cs from aqueous solutions by AC. For measurement , ^{134}Cs served as a tracer for the total Cs concentration. A standard solution of Cs was irradiated in a neutron flux to provide a radiopure ^{134}Cs solution of which both the exact concentration of Cs and activity of the ^{134}Cs tracer were known. Batch experiments using a variety of ACs adsorbing Cs from solutions with different pH showed no significant difference between the adsorption capacities at equilibrium for Cs (expressed as q_e values in mg Cs per gram AC) on either commercial AC or AC from BSG. Also the difference in adsorption between the Cs solutions of different pH was not significant. Binding PB on the ACs prior to the adsorption of Cs showed no significant effect on the q_e for any of ACs. Because batch experiments revealed no difference between the ACs, column experiments were conducted. A column experiment with Norit GAC 1240 using 4 solutions with a different pH showed that a neutral to slightly acidic pH increased the adsorption of Cs. At a higher pH the effect of the competition with ammonia ions caused a decrease of q_e. For the lab-scale ACs the ACBSG06 (the AC activated at the highest temperature) reached the highest q_e. Both commercially available ACs (Filtrasorb 400 and Norit GAC 1240) had even higher q_e values. This was caused by the difference in physical properties of the AC. Using sequential column adsorption to remove low concentrations of Cs from aqueous solutions led to promising results, as a steady removal rate per cycle step was observed. An equilibrium state is expected to be reached after several stages, where further removal is ineffective. A study will be performed to confirm this. The experiment showed that AC has potential as a low-cost and effective adsorbent for removal of low Cs concentrations. Removal percentages and adsorption capacities were comparable or higher than in relevant literature. Feasibility studies on the application of the method described in this paper in the nuclear industry are planned to be conducted.

3.4.5 Acknowledgements

3.4.6 References

[1] F.W. Whicker, D.I. Jr. Kaplan, D.M. Hamby, K.A. Higley, T.G. Hinton D.J. Rowan, R.G. Schreckhise, Cesium-137 in the Environment: Radioecology and Approaches to Assessment and Management. NCRP Book No. 154 National Council on Radiation Protection and Measurements, **2007**.

[2] G. Steinhauser, A. Brandl, T.E. Johnson, Comparison of the Chernobyl and Fukushima nuclear accidents: A review of the environmental impacts, Science of The Total Environment, **2014**, 470–471, 800-817.

[3] TEPCO, Detailed analysis results in the port, discharge channel and bank protection at Fukushima Daiichi NPS (As of August 28), **2013**.

[4] P. Lestaevel, R. Racine, H. Bensoussan, C. Rouas, Y. Gueguen, I. Dublineau, J.-M. Bertho , P. Gourmelon, J.-R. Jourdain, M. Souidi, Césium 137 : propriétés et effets biologiques après contamination interne, Médecine Nucléaire, **2010**, 34, 108-118.

[5] Public Health Service, Toxicological profile for cesium. Agency for Toxic Substances and Disease Registry, **2004**.

[6] N. Kinoshita, K. Sueki, K. Sasa, J.-I.Kitigawa, S. Ikarashi, T. Nishimura T, Y.-S. Wong, Y. Satou, K. Handa, T. Takahashi, M. Sato, T. Yamagata, Assessment of individual radionuclide distributions from the Fukushima nuclear accident covering central-east Japan, Proceedings of the national academy of sciences, **2011**, 108, 19526-21952.

[7] X. Liu, G.-R. Chen, D.-J. Lee, T. Kawamoto, H. Tanaka, M.-L. Chen,Y.-K. Luo, Adsorption removal of cesium from drinking waters: A mini review on use of biosorbents and other adsorbents, Bioresource Technology, **2014**, 160, 142-149.

[8] D. Li, D.I. Kaplan, A.S. Knox, K.P. Crapse, D.P. Diprete, Aqueous 99Tc, 129I and 137Cs removal from contaminated groundwater and sediments using highly effective low-cost sorbents, Journal of Environmental Radioactivity, **2014**, 136, 56-63.

[9] D. Ding , Y. Zhao, S. Yang, W. Shi, Z. Zhang, Z. Lei, Y. Yang, Adsorption of cesium from aqueous solution using agricultural residue - Walnut shell: Equilibrium, kinetic and thermodynamic modeling studies, Water Research, **2013**, 47, 2563-2571.

[10] T. Lan, Y. Feng, J. Liao, X. Li, C. Ding, D. Zhang, J. Yang, J. Zeng, Y. Yang, J. Tang, N. Liu, Biosorption behavior and mechanism of cesium-137 on Rhodosporidium fluviale strain UA2 isolated from cesium solution. Journal of Environmental Radioactivity, **2014**, 134, 6-13.

[11] D. Parajuli, H. Tanaka, Y. Hakuta, K. Minami, S. Fukuda, K. Umeoka, R. Kamimura, Y. Hayashi, M. Ouchi, T. Kawamoto, Dealing with the aftermath of Fukushima Daiichi nuclear accident: decontamination of radioactive cesium enriched ash, Environmental Science & Technology, **2013**, 47, 3800-3806.

[12] D. Ding, Z. Lei, Y. Yang, C. Feng , Z. Zhang, Selective removal of cesium from aqueous solutions with nickel (II) hexacyanoferrate (III) functionalized agricultural residue–walnut shell, Journal of Hazardous Materials, **2014**, 270, 187-195.

[13] P.A. Haas, A review of information on ferrocyanide solids for removal of cesium from solutions, Separation science and technology **1993**, 28, 2479-2506.

[14]D. Ding, Z. Zhang, Z. Lei, Y. Yang, T.Cai, Remediation of radiocesium-contaminated liquid waste, soil, and ash: a mini review since the Fukushima Daiichi Nuclear Power Plant accident, Environmental Science and Pollution Research, **2015**, 23, 2249-2263.

[15] K. Kimura, M. Hachinohe, K.T. Klasson, S. Hamamatsu, S. Hagiwara, S. Todoriki, S. Kawamoto, Removal of Radioactive Cesium from Low-Level Contaminated Water by Charcoal and Broiler Litter Biochar, Food Science and Technology Research, **2014**, 20, 1183-1189.

[16] H. Parab, M. Sudersanan M, Engineering a lignocellulosic biosorbent – Coir pith for removal of cesium from aqueous solutions: Equilibrium and kinetic studies, Water Research, **2010**, 44, 854-860.

[17] A.E. Ofomaja, A. Pholosi, E.B. Naidoo, Application of raw and modified pine biomass material for cesium removal from aqueous solution, Ecological Engineering, **2015**, 82, 258-266.

[18] D.P. Mohan, C.U. Pittman Jr., Activated carbons and low cost adsorbents for remediation of tri- and hexavalent chromium from water, Journal of Hazardous Materials, **2006**, 762-811.

[19]H. Marsh, F. Rodríguez-Reinoso, Activated carbon, Elsevier Science & Technology books, **2006**.

[20] M.C. Montana, I. Serrano, R. Devesa, L. Matia, I. Vallés, Removal of radionuclides in drinking water by membrane treatment using ultrafiltration, reverse osmosis and electrodialysis reversal, Journal of Environmental Radioactivity, **2013**, 125, 86-92.

[21] S. Biniak, G. Szymanski, J. Siedlewski, A. Swiatkowski, The characterization of activated carbons with oxygen and nitrogen surface groups, Carbon, **1997**, 35, 1799-1810.

[22] P. McKendry, Energy production from biomass (part 2): conversion technologies, Bioresource Technology, **2002**, 83, 47-54.

[23] H.B. Goyal, D. Seal, R.C. Saxena, Bio-fuels from thermochemical conversion of renewable resources: A review, Renewable and Sustainable Energy Reviews, **2008**, 12, 504-517.

[24] R.C. Bansal, M. Goyal, Activated Carbon Adsorption. Taylor & Francis, Boca Raton, **2005**.

[25] J.A. Menéndez-Díaz, I. Martin-Gullón, Types of carbon adsorbents and their production. In: Activated Carbon Surfaces in Environmental Protection. Elsevier Ltd., **2005**.

[26] B.H. Hameed, A.A. Rahman, Removal of phenol from aqueous solutions by adsorption onto activated carbon prepared from biomass material, Journal of Hazardous Materials, **2005**, 160, 576-581.

[27] K. Vanreppelen, S. Vanderheyden, T. Kuppens, S. Schreurs, J. Yperman, R. Carleer, Activated carbon from pyrolysis of brewer's spent grain: Production and adsorption properties, Waste Management & Research, **2014**, 32(7), 634-45

[28] W. Tanthapanichakoon, P. Ariyadejwanich, P. Japthong, K. Nakagawa, S.R. Mukai, H. Tamon, Adsorption-desorption characteristics of phenol and reactive dyes from aqueous solution on mesoporous activated carbon prepared from waste tires, Water Research, **2005**,3 9, 1347-1353.

[29] S.I. Mussatto, G. Dragone, I.C. Roberto, Brewer's spent grain: generation, characteristics and potential applications, Journal of Cereal Science, **2006**, 43; 1-14.

[30] A.S.N. Mahmood, J.G. Brammer, A. Hornung, A. Steele, S. Poulston; The intermediate pyrolysis and catalytic steam reforming of Brewers spent grain, Journal of Analytical and Applied Pyrolysis, **2013**, 103, 328-342.

[31] G. Yang, H. Chen, H. Qin, Y. Feng, Amination of activated carbon for enhancing phenol adsorption: Effect of nitrogen-containing functional groups, Applied Surface Science, **2014**, 293, 299-305.

[32] A. Bagreev, S. Bashkova, T.J. Bandosz, Adsorption of SO_2 on activated carbons: The effect of nitrogen functionality and pore size, Langmuir, **2002**, 18, 1257-1264.

[33] A. Bagreev, J.A. Menendez, I. Dukhno, Y. Tarasenko, T.J. Bandosz, Bituminous coal-based activated carbons modified with nitrogen as adsorbents of hydrogen sulfide, Carbon, **2004**, 42, 469-476.

[34] R.A. Hayden, Method for reactivating nitrogen-treated carbon catalysts. Google Patents, **1995**.

[35] E.G. Lorenc-Grabowska, G.; Diez, M.A., Kinetics and equilibrium study of phenol adsorption on nitrogen-enriched activated carbons, Fuel, **2012**.

[36] S. Matzner, H.P. Boehm, Influence of nitrogen doping on the adsorption and reduction of nitric oxide by activated carbon, Carbon, **1998**, 36, 1697-1709.

[37] T.J. Bandosz, C.O. Ania, Surface chemistry of activated carbons and its characterization. In Activated carbon surfaces in environmental remediation, Bandosz, Elsevier: **2006**; 159-229.

[38] K.-C. Song, H.K. Lee, H. Moon, K.J. Lee, Simultaneous removal of the radiotoxic nuclides Cs137 and I129 from aqueous solution, Separation and Purification Technology, **1997**, 12, 215-227.

[39] M. Caccin, F. Giacobbo, M. Da Ros, L Besozzi, M. Mariani, Adsorption of uranium, cesium and strontium onto coconut shell activated carbon, Journal of Radioanalytical and Nuclear Chemistry, **2012**, 297, 9-18.

[40] Cabot Corporation, Safety data sheet - Norit GAC 1240, **2015**.

[41] Calgon Carbon, Filtrasorb 400 - Granular Activated Carbon, **2015**.

[42] R.S. Mikhail, S. Brunauer, E.E. Bodor, Investigations of a complete pore structure analysis, Journal of Colloid and Interface Science, **1968**, 26, 45-53.

[43] P. Klobes, K. Meyer, R.G. Munro, Porosity and Specific Surface Area Measurements for Solid Materials, National Institute of Standards and Technology, Washington, **2006**.

[44] A. Mohammad, Y. Yang, M.A. Khan, P.J. Faustino, Long-term stability study of Prussian blue-A quality assessment of water content and cyanide release, Clinical toxicology, **2015**, 53, 102-107.

[45] F. Ricci , G. Palleschi, Sensor and biosensor preparation, optimisation and applications of Prussian Blue modified electrodes, Biosensors and Bioelectronics, **2005**, 21, 389-407.

[46] K. Vanreppelen, Towards a circular economy – Development, characterisation, techno-economic analysis and applications of activated carbons from industrial rest streams. UHasselt, **2016**.

[47] M.-M. Bé, Table de Radionucléides - Cs 134, LNHB, **2012**.

[48] Lalhmunsiama, C. Lalhriatpuia , D. Tiwari, S.-M. Lee, Immobilized nickel hexacyanoferrate on activated carbons for efficient attenuation of radio toxic Cs(I) from aqueous solutions, Applied Surface Science, **2014**, 321, 275-282.

[49] J. Brown, D. Hammond, B.T. Wilkins, Handbook for Assessing the Impact of a Radiological Incident on Levels of Radioactivity in Drinking Water and Risks to Operatives at Water Treatment Works: Supporting Scientific Report Oxfordshire, **2008**.

3.5 Enhanced cesium removal from realistic matrices by nickel-hexacyanoferrate modified activated carbons[8]

S. R. H. Vanderheyden[a], J. Yperman[a], R. Carleer[a], S. Schreurs[b]

[a] Hasselt University, Centre for Environmental Sciences, Research Group of Analytical and Applied Chemistry, Agoralaan – Building D, 3590 Diepenbeek, Belgium; e-mail: jan.yperman@uhasselt.be; robert.carleer@uhasselt.be

[b] Hasselt University, Centre for Environmental Sciences, Research Group of Nuclear Technology, Agoralaan – Building H, 3590 Diepenbeek, Belgium; e-mail: sonja.schreurs@uhasselt.be

* Corresponding author: Sara R.H. Vanderheyden, sara.vanderheyden@uhasselt.be +3211 268211

Abstract

After nuclear disasters, radioactive cesium partitions to soils and surface water, where it decays slowly. Hexacyanoferrates (HCF) have excellent cesium removal properties but their structure is typically powdery. Many carrier materials, such as biomass or magnetic particles, have been used to provide a strong form of these HCF that can be used in filters. This research uses the adsorptive properties of activated carbon (AC) to easily incorporate an HCF and provide good structural properties to the end material. These HCF-modified ACs show drastically improved adsorption properties towards Cs after one, two and three modification cycles. The activated carbon from brewer's spent grain with one modification cycle removes more than 80% of 1 mg/L Cs in a sea water solution and more than 98% of 1 mg/L Cs from surface water at a low AC dosage (0.5g AC/L). Iron and nickel

---

[8] References for this article can be found on page 163 in section 3.5.5

leaching is studied and found to be dependent on the type of AC used and the leaching solution. Iron leaching can be problematic in surface and seawater, whereas nickel leaching is especially pronounced in seawater.

3.5.1 Introduction

Even more than 6 years after the accident at the Fukushima Daichii Nuclear Power Plant on March 11th 2011, the environmental contamination with Cs-137 ($T_{1/2} \cong$ 30 years) poses one of the greatest challenges. The most contaminated area contains more than 1000 kBq/m² of Cs-137 and Cs-134 ($T_{1/2} \cong 2$ years) and spans a vast 645 km² of which 66% are broadleaf and evergreen needle leaf forest [1]. Deposition of tree litter causes the cesium to deposit on the ground, where it could possibly be removed. If the litter is not removed timely, the decomposition of biomass will cause the Cs to leach into the soil, where it can easily be retained by clays and organic matter [1-4] Leaching of Cs and erosion of contaminated soils is a problem that could contaminate ground- and surface water on the long term [5-8]. Many factors, such as soil type, salt content and amount of precipitation influence the distribution of Cs in waterways, causing it to be concentrated or diluted at specific locations [6, 9, 10].

Removal of cesium from aqueous solutions is typically performed by using Prussian Blue (PB, Iron(III) hexacyanoferrate(II)) as an adsorbent [11, 12]. There are some disadvantages of the use of PB, such as its very fine particle size distribution, making it difficult to use in filters. Its dissociation in basic solutions and cyanide formation in acidic solutions make pH control a crucial factor for Cs removal [13, 14]. Research has mostly focused on stabilization and granulation of PB [12, 14-18], or the use of different hexacyanoferrates (HCF) [19-22]. HCFs are very selective for Cs ion exchange since their crystal structure has lattices comparable to the hydrated ion size of Cs^+, but not big enough to be permeated by other alkali ions such as Na^+ [20, 23, 24]. Nickel-HCF (C_6FeN_6Ni) has recently gained more attention because of its stability and practical procedures to integrate

it on different types of carrier materials. This integration can be performed with a straightforward two-step adsorption process and requires no special equipment. This grants the ion exchanger chemical and physical strength and tackles some of the typical problems with HCF [25-28].

Activated carbon (AC) is a good adsorbent for both organic and inorganic pollutants from aqueous solutions owing to its porous structure and large surface area. Previous research has shown a wide variation in adsorption capacities measured for Cs on AC. Some manuscripts report extremely low [29, 30] removal percentages for Cs using AC. Some authors report higher removal percentage, but used very high AC dosages or Cs concentrations, enhancing the removal percentage [31, 32]. In order to improve physical properties of an HCF and the adsorption properties of Cs on AC, a combination of these two materials is proposed in this research.

3.5.2 Methods and materials

The goal of these experiments is to enhance removal of Cs by combining the adsorptive capacities of AC and HCF. Therefore, Ni-HCF is incorporated in different ratios on two ACS. After characterization, these new adsorbents are then used to remove low concentrations (1 mg/L) of Cs from Milli-Q, fresh and salt water by using reconstituted water solutions.

All used reagents were of analytical grade (unless otherwise specified) and Milli-Q water was used for the preparation of all solutions.

3.5.2.1 AC production and properties

After drying for 24 h at 105±5 °C, BSG is sieved through a 2 mm sieve. In the horizontal semi-continuous reactor designed by the research group, 40 g of BSG is pyrolysed and activated, yielding approximately 8 g of AC. The reactor is stirred by an internal screw and nitrogen or water are added through an inlet. The exact reactor set-up is described in [33]. The BSG is heated up in a nitrogen flow (70 ml/min) at a rate of 10 °C/min up to a temperature of 850 °C. An isothermal period of 45 minutes follows, during which 15 mL of H_2O is added. After cooling down, the produced ACBSG06 is sieved to particle sizes between 63 μm and 1

mm. Norit GAC1240 (Cabot Corporation, USA) was obtained to compare all results to a commercial AC and also sieved to particle sizes between 63 µm and 1 mm.

These ACs are both suited for removal of several pollutants from waste water, but have some distinct differences. ACBSG06 has higher nitrogen (x4) and ash (x2) content compared to Norit GAC1240. The pH_{PZC} (point of zero charge) is defined as the pH at which the total surface charge of the AC is zero and depends mostly on surface functionalities. ACBSG06 has a pH_{PZC} of 10.8, whereas Norit GAC1240 has a pH_{PZC} of 11.5. The surface area (Brunauer-Emmett-Teller, BET) is 1468 m²/g for Norit GAC1240 and 836 m²/g for ACBSG06 [Table 3-3 on page 154] The pore size distribution can be found in Figure 3-5 at page 156.

3.5.2.2 Modification of AC

Incorporation of Ni-HCF on Norit GAC1240 and ACBSG06 is performed using alternate adsorption of Ni^{2+} and potassium ferricyanide ($K_3[Fe(CN)_6]$), according to [25]. This method was initially used for the modification of biomass, but the acid washing step is skipped, since AC has good adsorptive properties.

Two solutions are used: solution A is a 0.5 M solution of $NiCl_2$ (p.a.) in Milli-Q water. Solution B contains 0.5 M $K_3[Fe(CN)_6]$).$3H_2O$ in Milli-Q water. 20 mL of solution A is added to 5 g of AC and shaken at 25°C for 16 hours. The AC is filtered using ashless filters (Rotilabo A14, Roth) and washed with Milli-Q water three times. 10 mL of solution B is added and this mixture is shaken for 24 hours at 30°C. The sample is filtered and washed with Milli-Q three times. Then it is dried at 60 °C for 48 hours. This process is used 1 to 3 times on both of the ACs, providing ACs with different modification rate. Both NoritGAC1240_1 and ACBSG06_1 have gone through this process once, NoritGAC1240_2 and ACBSG06_2 twice, and NoritGAC1240_3 and ACBSG06_3 three times. The unnumbered samples are unmodified Norit GAC1240 and ACBSG06.

3.5.2.3 Characterisation

Ash content determination is performed using a TGA 2950 (TA instruments), with a heating rate of 20 °C/min in a nitrogen atmosphere up to 550 °C. Afterward, oxygen addition ensures burning of all organic components.

For Elemental Analysis (CHNS-O) a Thermo Finnigan Element Analysis Flash EA 1112 is used after standardisation with BBOT (2,5-bis (5-tert-butyl-benzoxazol-2-yl) thiophene)). O content is calculated by difference. Samples are measured in quadruplicate.

Leaching of iron and nickel from the ACs and modified ACs is tested in three media: Milli-Q water, reconstituted standard water and reconstituted sea water prepared as in "3.5.2.4 Cesum adsorption tests". 200 mg of AC is added to 50 mL of solutions and shaken for 24 h at room temperature. After filtration through ashless filters, the iron and nickel concentrations of the liquid samples are measured by ICP-OES. This test is performed in duplo and the results are discussed in section 3.5.3.1.2 on page 183.

3.5.2.4 Cesium adsorption tests

Cs solutions are prepared using a 1000 mg L^{-1} $CsNO_3$ standard solution (CertiPur, VWR). All used Cs solutions have an initial concentration of approximately 1 mg Cs/L.

In a first phase, Cs is adsorbed from pure Milli-Q water at two AC dosages (0.5 g/L and 4 g/L). This will be referred to as low and high dosage experiments in the following sections. 15 or 120 mg of AC is added to 30 mL of 1 mg/L Cs solution and shaken for 24 hours at room temperature. The solutions are then filtered using ashless filters. Cs concentration is determined by ICP-MS. This experiment is conducted in triplo for both AC dosages.

This adsorption experiment is then repeated using two standard solutions with 1 mg/L Cs. The first solution is a reconstituted standard (sweet) water, based on ISO 6341 and "OECD series on testing and assessment number 29: Guidance document on transformation/dissolution of metals and metal compounds in aqueous media". The reconstituted standard water contains following salts: $NaHCO_3$ (65.7 mg/L), KCl (5.75 mg/L), $CaCl_2.2H_2O$ (294 mg/L), $MgSO_4.7H_2O$

(123 mg/L). A natural buffering capacity with CO_2 in air keeps the solution at pH 8 [34]. To simulate removal of Cs from sea water, a standard marine medium is used according to ASTM E729-96. The total salt content is 34±0.5 g/kg and its pH is buffered at 8. Following salts are added to 890 ml of Milli-Q in this order to create the marine medium: NaF (3 mg), $SrCl_2.6H_2O$ (20 mg), H_3BO_3 (30 mg), KBr (100 mg), KCl (700 mg), $CaCl_2.2H_2O$ (1.47 g), Na_2SO_4 (4.00 g), $MgCl_2.6H_2O$ (10.72 g), NaCl (23.5 g), $Na_2SiO_3.9H_2O$ (20 mg), $NaHCO_3$ (200 mg). The solution is then diluted to 1 L.

A low AC dosage experiment yields a high value of the adsorption capacity q_e of an AC. In this paper, this is considered to be an estimate for the maximal value. It is defined as:

$$q_e = \frac{\text{mg of cesium}}{\text{g of AC}}$$

Equation 3-2

High dosage experiments lead to an estimate of the maximal percentage removal that can be achieved in an industrial setting and is defined as:

$$\text{Removal efficiency} = \frac{\text{Cs concentration removed } (\frac{mg}{L})}{\text{Initial metal concentration } (\frac{mg}{L})} * 100\%$$

Equation 3-3

Distribution coefficients are calculated to compare the efficiency of the different adsorbents according to:

$$K = \frac{q_e \, (\frac{mg}{g})}{\text{Remaining Cs equilibrium concentration } (\frac{mg}{L})}$$

Equation 3-4

3.5.3 Results and discussion

3.5.3.1 Characterisation of AC

3.5.3.1.1 Ash content and elemental composition

Ash content and the elemental composition (CHNS-O) are displayed in percent by mass in Table 3-6. A significantly higher nitrogen content was found for ACBSG06 compared to Norit GAC1240 in [33]. The nitrogen surface functionalities enhance the adsorption of metals from solutions, improving the efficiency of the modification because nickel is adsorbed more easily [35]. As the number of modification cycles increases, the ash and nitrogen content of the samples increase, while the carbon content decreases. This is expected since more Ni-HCF is building up on the surface. The only exception is the difference between ACBSG06_2 and ACBSG06_3, where the total ash content is approximately the same, suggesting no more uptake of modification chemicals is happening. The surface of ACBSG06_3 seems to be more oxidized compared to the ACBSG06_2.

From this data, calculations can be made to estimate the ratio of the HCF that is adsorbed onto the surface of the AC. The ratio is calculated using the elemental composition of Ni-HCF and the results of the ash determination and elemental analysis for C and N. For the modified AC, the amount of incorporated HCF increases with the number of modification cycles. For ACBSG this ranges from 8.8±1.7% for ACBSG06_1 to 20.3±0.6% for ACBSG06_2 and 27.0±2.8% for ACBSG06_3. As noted before, the modification is less efficient for Norit GAC1240, with lower ratios of HCF incorporated in the modified samples. These range from 5.5±1.0% for Norit GAC1240_1 to 14.0±2.0% for Norit GAC1240_2 and 18.2±1.6% for Norit GAC1240_3. Only two modification cycles are needed for ACBSG06 to achieve a higher ratio of HCF in the sample than cannot even be achieved with three modifications for Norit GAC1240.

Table 3-6 Ash content and elemental analysis of ACBSG06 and Norit GAC1240 and their modifications in mass percent (wt%)

Sample	Ash (%)	C (%)	H (%)	N (%)	S (%) *	O (%) (from difference) **
ACBSG06[33]	17.73 ± 1.03	70.46 ± 0.85	1.19 ± 0.10	2.13 ± 0.04	< DL	8.48 ± 1.34
ACBSG06_1	19.47 ± 0.60	65.85 ± 1.92	1.12 ± 0.10	3.04 ± 0.01	< DL	10.52 ± 2.02
ACBSG06_2	22.56 ± 0.10	61.28 ± 0.88	1.24 ± 0.35	3.70 ± 0.15	< DL	11.22 ± 0.96
ACBSG06_3	22.32 ± 0.10	54.96 ± 0.21	1.09 ± 0.38	4.04 ± 0.06	< DL	17.59 ± 0.45
Norit GAC1240[36]	7.9 ± 0.1	85.30 ± 2.10	0.6 ± 0.1	0.80 ± 0.10	< DL	5.40 ± 2.11
Norit GAC1240_1	9.45 ± 0.80	81.46 ± 0.51	1.42 ± 0.64	1.21 ± 0.03	< DL	6.46 ± 1.15
Norit GAC1240_2	12.04 ± 0.90	75.88 ± 1.10	1.27 ± 0.29	2.01 ± 0.04	< DL	8.80 ± 1.45
Norit GAC1240_3	14.69 ± 0.90	75.57 ± 0.94	0.94 ± 0.57	3.11 ± 0.25	< DL	6.06 ± 1.33

(*) <DL : below detection limit limit (for S, approximately 0.2%)   (**) O calculated as 100% - Ash – C – H – N – S

3.5.3.1.2 Leaching in used media

Leaching experiments show the amount of iron and nickel that can be leached into a solution from the adsorbents based on their dry weight. The duration of the experiment (24 h) is considered long enough to provide a conclusion on the total amount that can be leached. Figure 3-13 shows the results for the amount of iron leached in all media. Care should be taken when using ACs for purification of water. The effluent water (in which Cs is removed) should not pollute surface water and has to stay below the EPA criterion of 1 mg of iron per liter for protection of aquatic life [37]. Normal ACs only leach a minimal amount of iron: 1 µg/g for Norit GAC1240 and 2µg/g for ACBSG06. Unreacted iron on the surface of the adsorbent is the cause of leaching of both iron and nickel for the modified ACs. As the modification rate increased, the amount leached increases in both Milli-Q and OECD standard water, except for ACBSG06_3, which leached less iron. As stated before, the ACBSG06_03 does not differ significantly to ACBSG06_2 in their elemental compositions, so the iron might have been effectively adsorbed by the third adsorption of the nickel solution. The oxidation of the surface might have led to more stable iron compounds on the surface. The use of marine medium decreases the leached amount of iron as the amount of modification cycles increases. The ionic strength of this medium is too high to permit iron to leach.

Figure 3-14 shows the leaching results for nickel. The leaching of nickel is limited in Milli-Q water compared to OECD standard water and marine medium. Norit GAC1240 and its modifications show considerable less leaching of nickel compared to the modifications of ACBSG06. ACBSG06_3 leaches more nickel compared to the other modifications, suggesting some unreacted nickel is still present on the surface after modification and additional washing is necessary. Even in marine medium, nickel is leached out easily. The saltwater aquatic life is only protected when nickel concentrations stay below 8.2 µg L-1 for continuous exposure and below 74 µg L-1 in regard to acute toxicity [37]. To reach these limit values, additional washing or the use of less concentrated reagents is proposed for future research.
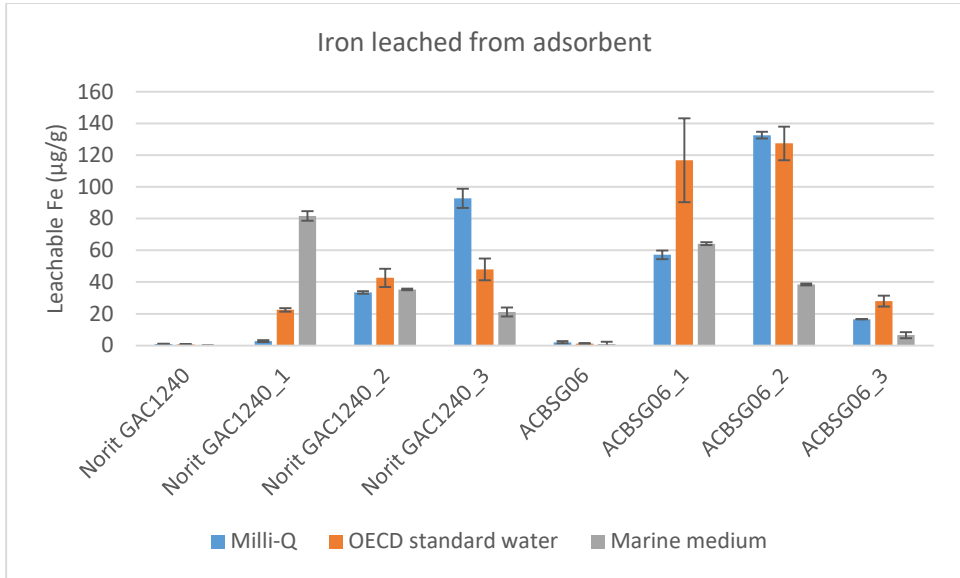
Figure 3-13 Leaching of iron from the adsorbents in different media
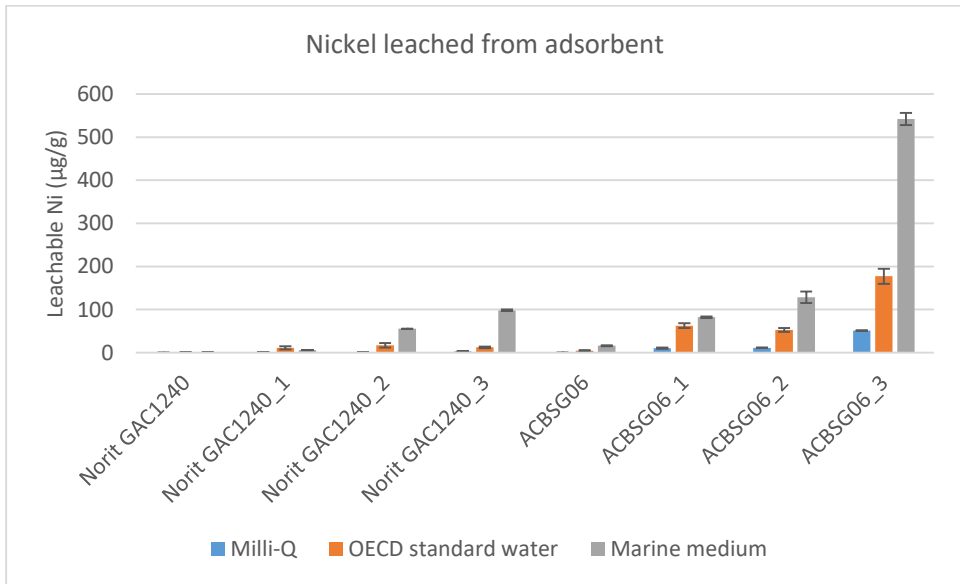
Figure 3-14 Leaching of nickel from the adsorbents in different media

3.5.3.2 Adsorption of Cs from different aqueous media

Figure 3-15 displays the removal percentages for each (modified) AC in the three solutions for high dosage. At high AC dosage (4 g AC/L) the unmodified ACs are able to remove Cs better from the solutions in this order: Milli-Q > OEXD Standard Water > Maritime medium. The presence of competing ions is preventing the effective adsorption of Cs ions. These ions, such as K^+ and Na^+, which are predominant in the standard water and marine medium, can adsorb on free negatively charged spaces on the AC surface. This way, adsorption sites can only partly become occupied by adsorbed Cs. In the marine medium, almost no Cs is removed by either unmodified Norit GAC1240 or ACBSG06. The best results for unmodified AC are reached for Norit GAC1240, that is able to remove up to approximately 25% of the Cs from the Milli-Q solution. Modified ACs all adsorb approximately 99.9 – 100% of the Cs present in the solution at this high AC dosage, whatever the medium or ionic strength. The number of modification cycles has no influence if the AC is used at this high AC dosage.
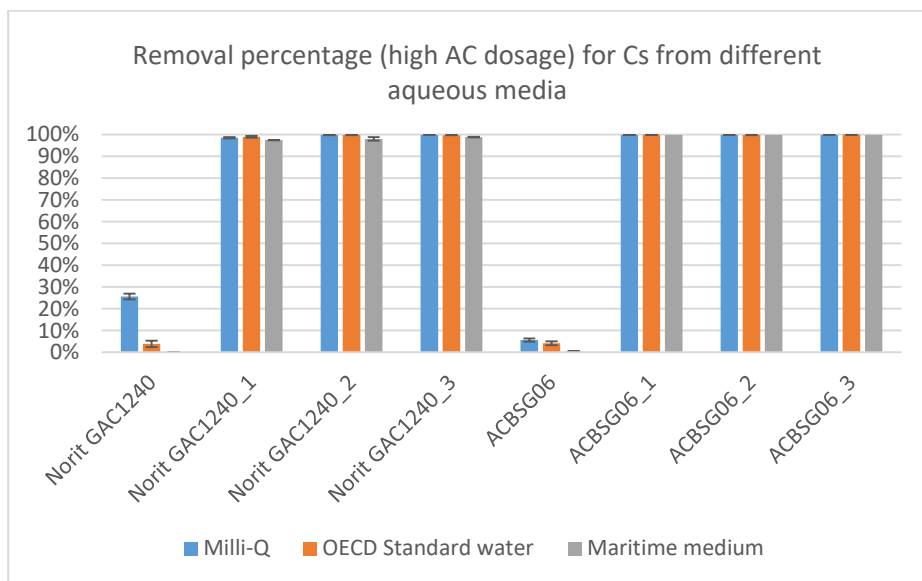
Figure 3-15 Removal percentage of cesium for different (modified) ACs at a dosage of 4g AC/L
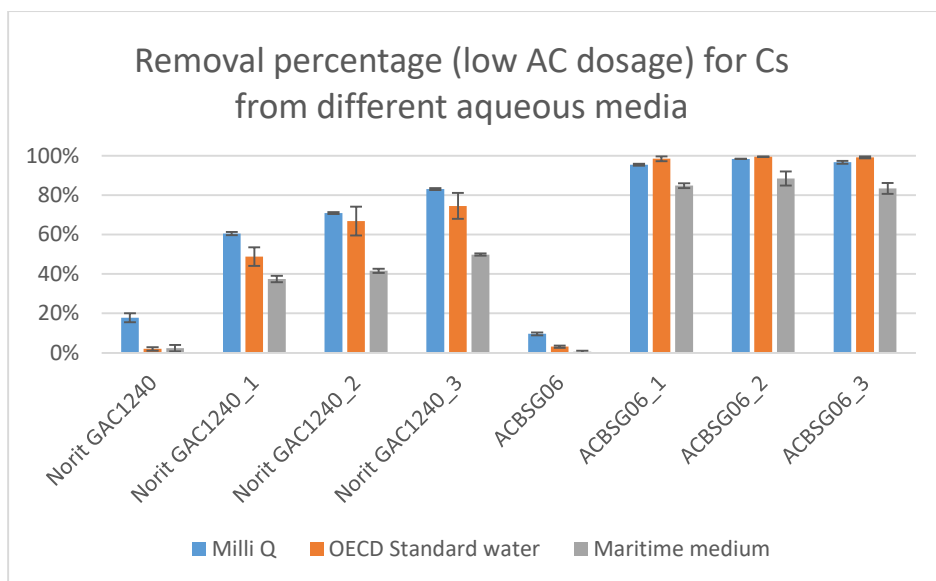
Figure 3-16 Removal percentage of cesium for different (modified) ACs at a dosage of 0.5g AC/L

The removal percentage for each medium and each (modified) AC at a low dosage (0.5 g AC/L) is displayed in Figure 3-16. The unmodified ACs are less efficient at Cs removal compared to each modified AC. The highest removal percentage for Cs from Milli-Q water is 17.8% for Norit GAC1240. The HCF in the modified ACs is able to adsorb the small hydrated Cs ions in its crystal lattice, while blocking the bigger hydrated ions as Na+ and K+ out The modified ACs all show extremely improved adsorption properties for each of the media. However, removal from marine medium is always less efficient than from OECD standard water and Milli-Q. This effect is more pronounced for the modifications of Norit GAC1240. These modifications also exhibit an improved adsorption depending on the number of modification cycles. Removal percentage for OECD standard water goes up from 48% for one modification to 67 and 75% for two or three modifications. This means even more cycles might be needed to reach a maximal removal of Cs. The modified ACBSG06 ACs all perform equally, suggesting just one modification cycle is needed to provide maximal results, with Cs removal higher than 98% in OECD standard water and approximately 85% from maritime medium. This effect is caused by the higher nitrogen content, making the ACBSG06 more suited for the modification.

The same conclusions can be reached using Figure 3-17, that shows the adsorption capacities for Cs for low AC dosage. When almost all Cs is removed, q_e reached a value of approximately 1800 µg Cs/ g AC, but this might still be an underestimate of the amount that could be adsorbed onto the surface when the maximum adsorption capacity is reached. As the available Cs in the solution is depleted, all Cs is adsorbed to the surface, but not all the available adsorption sites might be occupied. The q_e values for the ACBSG06 modification are therefore a minimal estimate of the q_e. For this exact reason, q_e values are all limited to a minimum of approximately 245 µg/g for all the modified ACs at high dosage.
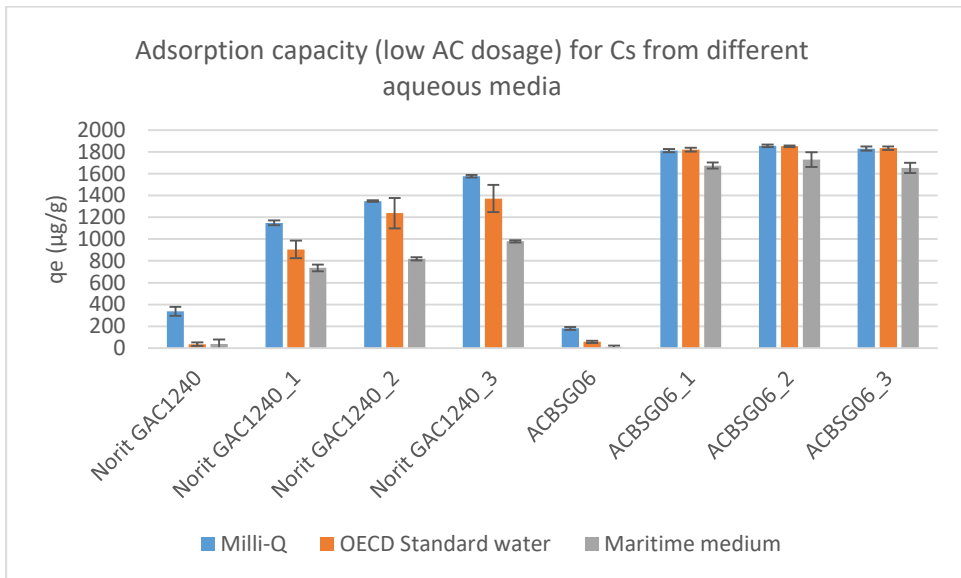
Figure 3-17 Adsorption capacity for different (modified) ACs at a dosage of 0.5 g/L

Distribution coefficients are calculated to compare results for adsorption at low AC dosage and are displayed in Table 3-7. These K values express a ratio of the amount of Cs on the surface compared to the equilibrium Cs concentration in the solution after adsorption. Since the removal of Cs at high AC dosage leads to very low equilibrium Cs concentrations of less than 1% of the initial concentration, these distribution coefficients are very high and are heavily influenced by experimental variation.

187

Table 3-7 Distribution coefficients (K) for the adsorbents at low AC dosage in Milli-Q (MQ), standard OECD water (SW) and marine medium (MM)

Sample	K_{MQ}	K_{SW}	K_{MM}
ACBSG06	0.21	0.06	0.01
ACBSG06_1	42	130	11
ACBSG06_2	120	450	15
ACBSG06_3	72	260	10
Norit GAC1240	0.43	0.04	0.04
Norit GAC1240_1	3.1	1.9	1.2
Norit GAC1240_2	4.9	4.1	1.4
Norit GAC1240_3	9.9	5.8	2.0

For modified ACBSG06 samples, the equilibrium concentrations of Cs are also very low, especially for OECD standard water, so these results might be an underestimate of K_{SW}. Comparison of K values between unmodified and modified AC also show what was visible in the removal percentages: modification leads to a higher distribution coefficient and removal percentage. The increase in number of modification cycles increases the distribution coefficient significantly for Norit GAC1240, but has no importance for ACBSG06, that performs best after even one modification. When K values are compared for the different media, a decrease of K is seen with increase of ionic strength. An exception is the comparison between Milli-Q and standard OECD water for modified ACBSG06, since these ACs reach slightly higher removal percentages in standard water.

3.5.4 Conclusion

Modification of an AC using Ni-HCF is a straightforward method, using alternating impregnation of nickel and potassium ferricyanide. This method performs more efficiently on a slightly nitrogenized AC, because the nickel is more efficiently adsorbed on these surfaces. This means AC from BSG is more suited for this application compared to Norit GAC1240 due to its in-situ generated nitrogen functionalities. The ash content of the adsorbents increases as more impregnation cycles are performed, but there is a maximal amount of Ni-HCF that can be incorporated. However, it is not necessary to reach this maximal amount for efficient adsorption properties. Even at low dosages of 0.5 g AC/L the ACBSG06 sample, only once impregnated, removes more than 98% of the Cs present in a standard water solution, mimicking surface water. Using this ACBSG06_1, approximately 84% of Cs is removed from a 1 mg/L Cs in seawater solution. Leaching of the Ni-HCF is tested by comparing leaching of nickel and iron in the three used media. In standard water (surface water) and marine medium (seawater) leaching of iron can be problematic. In contrary, nickel leaching is more prominent in sea water compared to surface water, but has a more pronounced toxicity. For use in industrial settings, ABSG06_01 is the most interesting modified AC produced: it reaches high removal percentages in each medium and only needs minimal modification cycles. An additional washing step can be introduced in the modification step to minimize leaching of nickel and iron.

3.5.5 References

[1] S. Hashimoto, S. Ugawa, K. Nanko, K. Shichi, The total amounts of radioactively contaminated materials in forests in Fukushima, Japan, **2012**, 2, 416.

[2] H. Mukai, S. Motai, T. Yaita, T. Kogure, Identification of the actual cesium-adsorbing materials in the contaminated Fukushima soil, Applied Clay Science, **2016**, 121, 188-193.

[3] S. Harada, M. Yanagisawa, Evaluation of a method for removing cesium and reducing the volume of leaf litter from broad-leaved trees contaminated by the Fukushima Daiichi nuclear accident during the Great East Japan Earthquake, Chemosphere, **2017**, 172, 516-524.

[4] Y. Huang, N. Kaneko, T. Nakamori, T. Miura, Y. Tanaka, M. Nonaka, C. Takenaka, Radiocesium immobilization to leaf litter by fungi during first-year decomposition in a deciduous forest in Fukushima, Journal of Environmental Radioactivity, **2016**, 152, 28-34.

[5] K. Murota, T. Saito, S. Tanaka, Desorption kinetics of cesium from Fukushima soils, Journal of Environmental Radioactivity, **2016**, 153, 134-140.

[6] K. Sakuma, A. Kitamura, A. Malins, H. Kurikami, M. Machida, K. Mori, K. Tada, T. Kobayashi, Y. Tawara, H. Tosaka, Characteristics of radio-cesium transport and discharge between different basins near to the Fukushima Dai-ichi Nuclear Power Plant after heavy rainfall events, Journal of Environmental Radioactivity, **2017**, 169, 137-150.

[7] S. Iwagami, Y. Onda, M. Tsujimura, M. Hada, I. Pun, Vertical distribution and temporal dynamics of dissolved 137Cs concentrations in soil water after the Fukushima Dai-ichi Nuclear Power Plant accident, Environmental Pollution, **2017**, 230, 1090-1098.

[8] J. Pumpanen, M. Ohashi, I. Endo, P. Hari, J. Bäck, M. Kulmala, N. Ohte, 137Cs distributions in soil and trees in forest ecosystems after the radioactive fallout – Comparison study between southern Finland and Fukushima, Japan, Journal of Environmental Radioactivity, **2016**, 161, 73-81.

[9] M. Onodera, A. Kirishima, S. Nagao, K. Takamiya, T. Ohtsuki, D. Akiyama, N. Sato, Desorption of radioactive cesium by seawater from the suspended particles in river water, Chemosphere, **2017**, 185, 806-815.

[10] M. Naulier, F. Eyrolle-Boyer, P. Boyer, J.-M. Métivier, Y. Onda, Particulate organic matter in rivers of Fukushima: An unexpected carrier phase for radiocesiums, Science of The Total Environment, **2017**, 579, 1560-1571.

[11] P. Lestaevel, R. Racine, H. Bensoussan, C. Rouas, Y. Gueguen, I. Dublineau, J.-M. Bertho, P. Gourmelon, J.-R. Jourdain, M. Souidi, Césium 137 : propriétés et effets biologiques après contamination interne, Médecine Nucléaire, **2010**, 34, 108-118.

[12] K. Minami, K. Sakurai, R. Kanai, Y. Asanuma, T. Kawasaki, Y. Kojima, T. Kobayashi, R. Kamimura, T. Kawamoto, Radiocesium removal system for environmental water and drainage, Water Research, **2016**, 107, 29-36.

[13] A. Mohammad, Y. Yang, M.A. Khan, P.J. Faustino, Long-term stability study of Prussian blue-A quality assessment of water content and cyanide release, Clinical toxicology (Philadelphia, Pa.), **2015**, 53, 102-107.

[14] F. Ricci, G. Palleschi, Sensor and biosensor preparation, optimisation and applications of Prussian Blue modified electrodes, Biosensors and Bioelectronics, **2005**, 21, 389-407.

[15] G.-R. Chen, Y.-R. Chang, X. Liu, T. Kawamoto, H. Tanaka, A. Kitajima, D. Parajuli, M. Takasaki, K. Yoshino, M.-L. Chen, Y.-K. Lo, Z. Lei, D.-J. Lee, Prussian blue (PB) granules for cesium (Cs) removal from drinking water, Separation and Purification Technology, **2015**, 143,146-151.

[16] D. Parajuli, H. Tanaka, Y. Hakuta, K. Minami, S. Fukuda, K. Umeoka, R. Kamimura, Y. Hayashi, M. Ouchi, T. Kawamoto, Dealing with the aftermath of Fukushima Daiichi nuclear accident: decontamination of radioactive cesium enriched ash, Environmental Science & Technology, **2013**, 47, 3800-3806.

[17] C. Jeon, Removal of cesium ions from aqueous solutions using immobilized nickel hexacyanoferrate-sericite beads in the batch and continuous processes, Journal of Industrial and Engineering Chemistry, **2016**, 40, 93-98.

[18] R. Chen, H. Tanaka, T. Kawamoto, M. Asai, C. Fukushima, H. Na, M. Kurihara, M. Watanabe, M. Arisaka, T. Nankawa, Selective removal of cesium ions from wastewater using copper hexacyanoferrate nanofilms in an electrochemical system, Electrochimica Acta, **2013**, 87, 119-125.

[19] H.G. Mobtaker, T. Yousefi, S.M. Pakzad, Cesium removal from nuclear waste using a magnetical CuHCNPAN nano composite, Journal of Nuclear Materials, **2016**, 482, 306-312.

[20] D. Parajuli, A. Takahashi, H. Noguchi, A. Kitajima, H. Tanaka, M. Takasaki, K. Yoshino, T. Kawamoto, Comparative study of the factors associated with the application of metal hexacyanoferrates for environmental Cs decontamination, Chemical Engineering Journal, **2016**, 283, 1322-1328.

[21] Y. Okamura, K. Fujiwara, R. Ishihara, T. Sugo, T. Kojima, D. Umeno, K. Saito, Cesium removal in freshwater using potassium cobalt hexacyanoferrate-impregnated fibers, Radiation Physics and Chemistry, **2014**, 94, 119-122.

[22] H. Zhang, X. Zhao, J. Wei, F. Li, Removal of cesium from low-level radioactive wastewaters using magnetic potassium titanium hexacyanoferrate, Chemical Engineering Journal, **2015**, 275, 262-270.

[23] T. Vincent, C. Vincent, Y. Barré, Y. Guari, G. Le Saout, E. Guibal, Immobilization of metal hexacyanoferrates in chitin beads for cesium sorption: synthesis and characterization, Journal of Materials Chemistry A, **2014**, 2, 10007-10021.

[24] Lalhmunsiama, C. Lalhriatpuia, D. Tiwari, S.-M. Lee, Immobilized nickel hexacyanoferrate on activated carbons for efficient attenuation of radio toxic Cs(I) from aqueous solutions, Applied Surface Science, **2014**, 321, 275-282.

[25] D. Ding, Y. Zhao, S. Yang, W. Shi, Z. Zhang, Z. Lei, Y. Yang, Adsorption of cesium from aqueous solution using agricultural residue - Walnut shell: Equilibrium, kinetic and thermodynamic modeling studies, Water Research, **2013**, 47, 2563-2571.

[26] D. Ding, Z. Lei, Y. Yang, C. Feng, Z. Zhang, Selective removal of cesium from aqueous solutions with nickel (II) hexacyanoferrate (III) functionalized agricultural residue–walnut shell, Journal of Hazardous Materials, **2014**, 270, 187-195.

[27] H. Parab, M. Sudersanan, Engineering a lignocellulosic biosorbent – Coir pith for removal of cesium from aqueous solutions: Equilibrium and kinetic studies, Water Research, **2010**, 44, 854-860.

[28] A.E. Ofomaja, A. Pholosi, E.B. Naidoo, Application of raw and modified pine biomass material for cesium removal from aqueous solution, Ecological Engineering, **2015**, 82, 258-266.

[29] M. Caccin, F. Giacobbo, M. Da Ros, L. Besozzi, M. Mariani, Adsorption of uranium, cesium and strontium onto coconut shell activated carbon, Journal of Radioanalytical and Nuclear Chemistry, **2012**, 297, 9-18.

[30] J. Brown, D. Hammond, B.T. Wilkins, Handbook for Assessing the Impact of a Radiological Incident on Levels of Radioactivity in Drinking Water and Risks to Operatives at Water Treatment Works: Supporting Scientific Report Oxfordshire, **2008**.

[31] K. Kimura, M. Hachinohe, K.T. Klasson, S. Hamamatsu, S. Hagiwara, S. Todoriki, S. Kawamoto, Removal of Radioactive Cesium (134Cs plus 137Cs) from Low-Level Contaminated Water by Charcoal and Broiler Litter Biochar, Food Science and Technology Research, **2014**, 20, 1183-1189.

[32] S. Khandaker, T. Kuba, S. Kamida, Y. Uchikawa, Adsorption of cesium from aqueous solution by raw and concentrated nitric acid–modified bamboo charcoal, Journal of Environmental Chemical Engineering, **2017**, 5, 1456-1464.

[33] K. Vanreppelen, S. Vanderheyden, T. Kuppens, S. Schreurs, J. Yperman, R. Carleer, Activated carbon from pyrolysis of brewer's spent grain: Production and adsorption properties, Waste Management & Research, **2014**, 32(7), 634-45

[34] Guidance Document on Transformation/Dissolution of Metals and Metal Compounds in Aqueous Media, in: OECD Environment, **2001**.

[35] L. Largitte, T. Brudey, T. Tant, P.C. Dumesnil, P. Lodewyckx, Comparison of the adsorption of lead by activated carbons from three lignocellulosic precursors, Microporous and Mesoporous Materials, **2016**, 219, 265-275.

[36] S.R.H. Vanderheyden, R. Van Ammel, K. Sobiech-Matura, K. Vanreppelen, S. Schreurs, W. Schroeyers, J. Yperman, R. Carleer, Adsorption of cesium on different types of activated carbon, Journal of Radioanalytical and Nuclear Chemistry, **2016**, 310, 301-310.

[37] Environmental Protection Agency, National recommended water quality criteria, **2004.**

3.6 Chapter conclusions

In both papers ACs and hybrid HCF-AC adsorbents are tested for Cs removal. The first paper proves that a system with a Cs-134 tracer is a promising system to study Cs adsorption. The used batch adsorption system was unable to demonstrate differences between ACs, probably owing to a lower mixing efficiency compared to previous tests. The binding of PB on AC also has no influence on adsorption. Column adsorption tests prove a slight promotion of adsorption in acidic media. Adsorption decreases with increasing pH. The lower surface area of the ACBSG results in lower adsorption capacities for Cs compared to two commercially available ACs. More testing on cyclical column adsorption should be done, especially with the new promising Ni-HCF/AC materials prepared in the second manuscript included in this chapter.

In section 3.5, Ni-HCF is incorporated into AC using an adsorption method. The higher nitrogen content of the ACBSG results in a stronger affinity of nickel to bind to its surface and a higher grade of modification per step. A maximal amount of Ni-HCF to be bound to the surface is found, but it is not necessary to have this amount on the surface for maximal Cs removal. The hybrid adsorbents are very efficient at Cs removal from three different media: Milli-Q water, reconstituted surface water and reconstituted marine medium. The influence of salt content is minimal, making the hybrid materials suitable for use in various conditions. Leaching of the materials should be monitored but not problematic as the Cs adsorption capacity is sufficiently high to use a low AC-HCF dosage.

The major results from this chapter are:

- The set-up of a workable system using Cs-134 as a tracer for Cs adsorption
- Column tests are more promising than batch adsorption experiments shaken at low velocity
- The incorporation of PB on AC by adsorption does not promote adsorption and is not pH-stable

- The incorporation of Ni-HCF by a two phase adsorption system provides excellent results for Cs removal from various media at low and intermediate dosage

4 The use of activated carbons as adsorbent for problematic metals in Flemish surface water

4.1 The use of activated carbons as adsorbent for problematic metals in Flemish surface water[9]

S. R. H. Vanderheyden[a], J. Yperman[a], R. Carleer[a], S. Schreurs[b]

[a] Hasselt University, Centre for Environmental Sciences, Research Group of Applied and Analytical Chemistry, Agoralaan – Building D, 3590 Diepenbeek, Belgium; e-mail: jan.yperman@uhasselt.be; robert.carleer@uhasselt.be

[b] Hasselt University, Centre for Environmental Sciences, Research Group of Nuclear Technology, Agoralaan – Building H, 3590 Diepenbeek, Belgium; e-mail: sonja.schreurs@uhasselt.be

Abstract

Two commercially available activated carbons (ACs) are compared to a biomass-based AC from brewer's spent grain (ACBSG) for their ability to adsorb inorganic species from aqueous solutions. A selection is made of several metals and metalloids that are at risk of being problematic in surface water in Flanders (As, Cd, Co, Cu, Pb, U, V, Zn). After screening the adsorption efficiency using 10 mg/L metal ion concentrations in Milli-Q water, the influence of reconstituted standard water is also determined. The final goal is the study of the adsorption capacity and removal percentages of 5 selected metals (Cd, Co, U, V, Zn) as a single element and in mixtures at trace and ultratrace concentrations (0.44 µg/L – 61 µg/L, depending on the species) using realistic AC dosages (0.5 and 4 g/L). For the single element solutions, a significant statistical difference between the ACs is found for Co, V and Zn. For Co and Zn, ACBSG06 performs significantly better at both low and high AC dosage. Mixed solutions cause a decrease in adsorption capacity and removal percentage for each AC for each species. Furthermore, Co and U affect Cd adsorption. For Zn adsorption, ACBSG06 performs significantly

---

better than the commercial ACs. Leaching tests suggest that relatively high amounts of Al and As are released from commercial ACs.

Keywords

4.1.1 Introduction

Flanders, in the North of Belgium, has a historical issue with pollution of surface water because of heavy metal industries. The Flemish Environmental Agency (Vlaamse Milieumaatschappij, VMM) monitors arsenic, barium, cadmium, chromium, cobalt, copper, mercury, molybdenum, lead, nickel, uranium, vanadium and zinc concentrations in surface water at more than 300 measuring points. The total number of measurement points exceeding the environmental quality limit values, exhibits a declining tendency, however, certain metals and metalloids remain problematic. The number of measurement points exceeding the limit values is most prominent for Co (47.5%), U (34.3%), As (19.5%), V (7.5%), Zn (14.0%), and Cd (2.7%) (2015) [1]. Flemish environmental quality limit values for selected metals and metalloids in surface water are displayed in Table 4-1.

Table 4-1 Flemish environmental quality limit values (averaged over a year) for selected metals in surface water. Taken from [2]

Metal	As	Cd	Co	Cu	Pb	U	V	Zn
Limit value (µg/L)	3	0.08-0.25*	0.5	7	7.2	1	4	20

*Dependent on water hardness, varying from 0.08 µg/L when<40 mg $CaCO_3$/L dissolved and 0.25 µg/L when ≥200 mg $CaCO_3$/L dissolved

Whilst mostly known for its capacity to adsorb organic molecules, activated carbon (AC) has also been proven as an efficient adsorbent for several individual metal ions [3-8]. Real-life applications for adsorption often have multiple contaminants present. The influence of multiple elements can create a competitive adsorption system, leading to synergic or antagonistic adsorption of a specific element [8-11]. Modeling has shown the possibility of a multi-anchored system where one metal ion is physisorbed onto several surface functionalities simultaneously [12]. The most important parameters for efficient metal adsorption are solution pH, the

types of surface functionalities able to form complexes with the metals and the point of zero charge (pH_{PZC}) of the AC [13]. At high pH, insoluble hydroxides are formed for some metal ions and will precipitate. At pH lower than the ACs pH_{PZC}, the surface is positively charged, creating repulsion between the surface and any metal cation.

In this study, AC from brewer's spent grain (BSG) will be compared to two commercial types of AC: Norit GAC1240 and Filtrasorb F400. ACBSG proved already to be an interesting adsorbent for removal of organic and inorganic compounds, due to its enhanced amount of surface groups and chemical properties [14-16]. ACBSG typically has a nitrogen content that is approximately three times higher than in commercial ACs, but their BET surface is only half of the BET surface of commercial ACs. Furthermore, comparing the amount of surface groups to commercial samples, a similar amount of acidic surface groups is found, but the amount of basic surface groups is doubled. This in-situ nitrogenized AC is examined for removal of several metal ions and their combinations in surface water. The focus of this research is its applicability in engineering and real-life situations: after a preselection, mixtures of metal ions will be adsorbed from reconstituted standard water on AC. The discussion is based on a statistical analysis of the large experimental adsorption dataset. Both ion concentrations and AC dosage will be kept low to simulate realistic adsorption scenarios.

4.1.2 Methods and materials

The goal of these experiments is to compare the removal of several metal ions from waste water by different ACs. One AC is prepared from BSG using pyrolysis and steam activation, two other ACs are commercially available: Norit GAC1240 and Filtrasorb F400. To compare metal adsorption, a series of tests is set up. A first screening experiment categorizes metal ions according to adsorption affinity from Milli-Q water. A second experiment to determine the influence of a more realistic set-up (surface water) with reconstituted standard water is performed using the same concentrations as the first experiment. Finally, the use of AC for removal of ultratrace concentrations of metal ions from surface water is evaluated for single metal solutions and combinations.

All used reagents were of analytical grade (unless otherwise specified) and Milli-Q water was used for the preparation of all solutions.

4.1.2.1 AC production and properties

According to [14] and [15]

BSG was dried for 24 h at 105 ± 5 °C and sieved to particle sizes smaller than 2 mm. 40 g of BSG was pyrolysed and activated in a rotating horizontal reactor. The heating rate was set at 10 °C/min up to 850 °C, after which 15 mL of H_2O was injected during a 45 min isothermal period. The N_2 flow was set at 70 mL/min. This resulted in the production of ACBSG06. Norit GAC 1240 (Cabot Corporation, USA) and Filtrasorb F400 (Chemviron Carbon, Belgium) were used for comparison of the adsorption performance.

The main differences between ACBSG06 and the commercial ACs are the higher nitrogen (4x) and the higher ash (2x) content. The pH_{PZC} can be found in Table 2-1 on page 73. The surface area (Brunauer-Emmett-Teller, BET) is 1468 m²/g for Norit GAC1240 and 836 m²/g for ACBSG06 [Table 3-3 on page 154] The pore size distribution can be found in Figure 3-5 at page 156.

4.1.2.2 Screening AC for metal adsorption

In order to estimate the adsorption affinity of several metal ions, adsorption on AC from Milli-Q water with pH 2 and 7 is tested for 6 species (As, Cd, Co, U, V, Zn) individually. For Cu and Pb, adsorption is only tested at pH 2 as hydroxide precipitation already occurs at pH ≥ 7. Solutions with an arbitrary concentration of 10 mg/L of each metal ion and metalloid ion are prepared using Milli-Q water and the pH is adjusted to 2 and 7 using nitric acid (0.1 M) and sodium hydroxide (0.1 M). Used salts and standard solutions (VWR CertiPUR) are displayed in Table 4-2.

Table 4-2 Metal and metalloid species used in the experiments with their predominant ions at pH 2 and 7 according to speciation diagrams

Metal species	Dissolved salt	Predominant ions at pH 2	Predominant ions at pH 7
As	H_3AsO_4 in 0.5 mol/L HNO_3*	$H_2AsO_4^-$, H_3AsO_4 [17, 18]	$H_2AsO_4^-$ $HAsO_4^{2-}$ [17, 18]
Cd	$Cd(NO_3)_2 \cdot 4H_2O$ (Merck, p.a.)	Cd^{2+} [19]	Cd^{2+} [19]
Co	$Co(NO_3)_2 \cdot 6H_2O$ (Merck, p.a.)	Co^{2+} [20]	Co^{2+} [20]
Cu	$Cu(NO_3)_2 \cdot 3H_2O$ (Merck, p.a.)	Cu^{2+} [19]	N.A.
Pb	$Pb(NO_3)_2$ in 0.5 mol/L HNO_3 (Merck, p.a.)	Pb^{2+} [19]	N.A.
U	U(VI) in 2-5% HNO_3 (Chemlab, Plasma HiQu)**	UO_2^{2+} [21]	$(UO_2)_2CO_3(OH)_3^-$ $UO_2(OH)_2$*** [21]
V	VO_2SO_4 in 0.5 mol/L H_2SO_4 (Merck, p.a.)	VO_2^{2+} $V_{10}O_{26}(OH)_2^{4-}$ [22, 23]	$V_3O_9^{3-}$ $V_4O_{12}^{4-}$ [22, 23]
Zn	$Zn(NO_3)_2 \cdot 6H_2O$ (Fluka, p.a.)	Zn^{2+} [19]	Zn^{2+} [19]

N.A.: Not applicable, * Arsenic acid CertiPUR standard solution, 1000 mg/L As ** Uranium (VI+) standard solution, 1000 mg/L U *** Water in equilibrium with CO_2

30 mL of the 10 mg/L metal solution at the appropriate pH is added to 15 and 120 mg of each AC. This mixture is shaken for 24 hours at 25°C, filtrated through ashless paper filters and metal concentration is determined using ICP-OES (Perkin Elmer Optima 8300) after acidification of the samples. The concentration of the added solution (initial metal concentration) is also determined and the difference in concentration is used for the calculations. This experiment is conducted in twofold. AC dosages correspond to 0.5 g/L and 4g/L, in this paper labelled 'low AC dosage' and 'high AC dosage' respectively. A low AC dosage is preferred to

estimate the maximal adsorption capacity q_e of an AC, an important theoretical quality parameter. It is defined as:

$$q_e = \frac{(c_{initial} - c_{equilibrium}) * V}{m_{AC}}$$

Where $c_{initial}$ (mg/L) is the concentration of the chosen ion in the solution added to the vial, $c_{equilibrium}$ (mg/L) the concentration of the species after filtration (at equilibrium, i.e. 24 h), V the added volume (L) and m_{AC} (g) is the amount of AC added to the vial.

High AC dosage experiments lead to an estimate of the maximal percentage removal that can be achieved in an industrial setting and is defined as:

$$Removal\ percentage = \frac{c_{initial} - c_{equilibrium}}{c_{initial}} * 100\%$$

An additional benefit of the adsorption method using two different AC dosages is shown when the value for q_e or the removal percentage of an experiment is approximately equal at both AC dosages. Figure 4-1 shows a conceptual adsorption isotherm using a 10 mg/L starting solution of a target ion. The x-axis corresponds to the equilibrium concentration, which is inversely proportional to the removal percentage, which increases when the AC dosage is increased. Two specific zones are pointed out in the figure: one zone with an almost constant q_e value and one zone with an almost constant removal percentage.

When the results for q_e are similar for an experiment at both low and high AC dosage, this implies that q_e is a measure for the maximal adsorption capacity that can be obtained using this adsorbent. The values of the removal percentage may vary significantly while the q_e stays constant. To improve the removal efficiency, more AC can be added to the system to increase the removal percentage.

A similar removal percentage between the experiments with low and high AC dosage proves that the AC has already adsorbed a maximal amount at low AC dosage and increasing the dosage will not increase the removed amount drastically. When the removal percentage is adequately high, this is a promising result for the use in industrial settings. The q_e value is an understatement of the maximal value that could be theoretically reached.
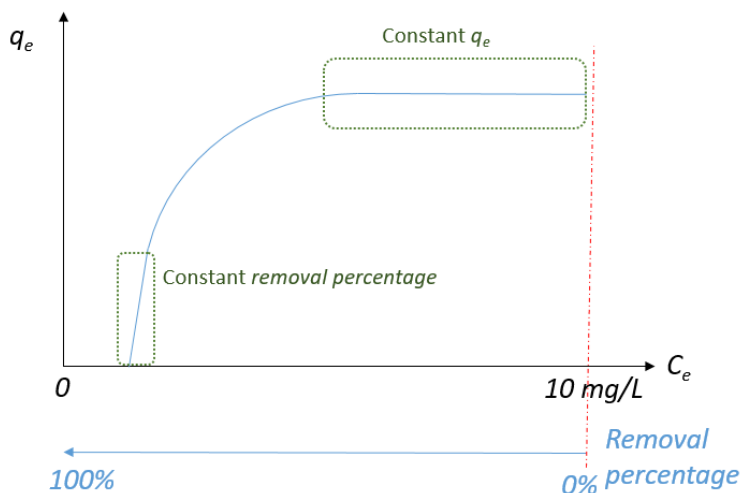
Figure 4-1 Conceptual adsorption isotherm

4.1.2.3 Metal removal from reconstituted standard water

In order to estimate the effects on adsorption of an environmental matrix, a metal adsorption study was performed in reconstituted standard water. This standard water is based on ISO 6341 and "OECD (Organisation for Economic Co-operation and Development) series: testing and assessment number 29: Guidance document on transformation/dissolution of metals and metal compounds in aqueous media". The following components make up the standard water: $NaHCO_3$ (65.7 mg/L), KCl (5.75 mg/L), $CaCl_2.2H_2O$ (294 mg/L), $MgSO_4.7H_2O$ (123 mg/L). The CO_2 present in the air provides a natural buffering capacity, keeping the solution buffered at pH 8 [24].

To study the influence of the ionic strength, adsorption was first tested with 10 mg/L of pure metal solutions in reconstituted standard water. For a more realistic situation, the experiment was also performed with trace metal concentration. For this, solutions were prepared with standard water, spiked with a metal concentration that was slightly higher than the legal limit values for surface water (Table 4-1). Based on the adsorption results at pH 7, following trace concentration solutions were prepared: 0.4 µg/L Cd, 2.5 µg/L Co, 0.5 µg/L U, 20 µg/L V and 60 µg/L Zn. Measurements of trace concentration are performed using ICP-MS (Perkin Elmer NeXION 350S). Adsorption tests were also performed at low and

205

high AC dosage for solutions with combinations of these metals. Binary, tertiary, quaternary and quinary systems were all set up using the metal concentrations stated above. For each metal, this will lead to 16 combinations for adsorption experiments performed in twofold for each AC, requesting a statistical analysis.

4.1.2.4 Statistical analysis

The amount of data involved in the adsorption experiments and the interdependence between the results make the interpretation a challenge. In order to determine which results for adsorption capacity or percent removal are significantly different from each other, statistical analyses were performed.

Statistical analyses are first performed for the experiments with trace ion concentrations. Analyses are based on the presence of metal or metalloid ions (present= 1/not present= 0) and not on the specific concentrations of that ion in each set of experiments. To investigate whether AC type and/or dosage influence adsorption capacity and/or removal percentage, statistical analyses are first performed on the adsorption capacity and removal percentage data for the experiments with only one metal ion per solution. Next, statistical analyses are extended on the data of all metal ion mixtures, using a model including all two-way interactions. All statistical analyses are performed using R version 3.4.2.

Linear regression is used to determine which factors have a significant influence on adsorption capacity and removal percentage. Backward model selection is performed, removing the least significant term in each step (based on a significance level of $p \leq 5\%$). Significance is determined based on an overall F-test for each factor. The final model contains only significant terms.

When significant factors have more than 2 levels (i.e. AC type, interactions), pairwise comparisons are performed to determine differences between the levels. If there was no difference after this multiple testing correction, the factor could be removed from the model. Tukey's test is used for this purpose, calculating all pairwise comparisons at the same time.

4.1.2.5 Determination of leachable ions

In order to estimate the amount of heavy metals released from the AC into Milli-Q and reconstituted standard water, leaching tests are set up. 200 mg of AC is

added to 50 mL of either Milli-Q or reconstituted standard water. Each mixture is shaken for 24 h at room temperature and filtered through ashless filters. ICP-OES is used to measure Ca, Mg and Na. Concentrations of Al, As, Cd, Co, Cu, Fe, Pb, U, V and Zn are determined via ICP-MS.

4.1.3 Results and discussion

4.1.3.1 Adsorption screening: removal of single ions in Milli-Q water

The results of the two-point adsorption screening for several metals can be found in Table 4-3. For each metal on AC adsorption, q_e values and removal percentages are given at low and high AC dosage, at pH 2 and pH 7.

For solutions with pH 2 and for both commercial ACs: As, Cd, Co, Cu, Pb, V and Zn show no adsorption affinity at **low** AC dosages, only for U up to 2-3% adsorption percentages could be measured. For Filtrasorb F400 and ACBSG06, the similar q_e values prove that this low value is already the maximal value, but the addition of more AC might increase the removal percentage. ACBSG06 is the only AC at **low** dosage that adsorbs a small amount of Cu and V and up to 11% of U.

In the case of **high** AC dosages at pH 2, improved results are obtained for most metal ions and all ACs, except for Zn, where still no adsorption can be noticed on any AC. For Cd and Co, only for ACBSG06 limited adsorption performance can be measured at high AC dosage. For As, low adsorption removal percentages are found for all ACs. For V, moderate values are obtained for Filtrasorb F400 and Norit GAC1240 with 10 and 12% respectively, but for ACBSG06 higher removal percentages are realized up to 37%. For Cu and Pb, rather low removal percentages are recorded for a high AC dosage of Filtrasorb F400 and Norit GAC1240, however for ACBSG06 much higher removal percentages are realized: 11% for Cu and even 47% for Pb. A critical amount of AC is needed to initiate adsorption of Pb on ACBSG06, as there was no adsorption at low AC dosage. Also removal of U at high AC dosage is most efficient for ACBSG06. ACBSG06 is able to remove 85% of U, whereas Norit GAC1240 and Filtrasorb F400 remove only 44% and 22% of U, respectively.

Adsorption at pH 7 is improved for most metals, but for the neutral/anionic As species still no affinity for adsorption on any of the ACs is noticed. The pH of the solution is still below PZC, but more of the surface groups will be negatively charged compared to the pH 2 solution, allowing electrostatic forces to attract more of the other metal cations to the surface. The q_e values at low AC dosage give an estimation of the theoretical maximal adsorbed amount q_{max}. For Cd, ACBSG06 reaches 6.24 mg/g, compared to 4.82 and 4.27 mg/g for Filtrasorb F400 and Norit GAC1240 respectively. All the ACs reach similar q_e values for Co (3.04-3.51 mg/) and V (3.99 – 4.25 mg/g), suggesting that the difference between the ACs does not influence this adsorption behaviour. Filtrasorb F400 reaches the highest value for U adsorption of 10mg/g, followed by Norit GAC1240 with 9.1 mg/g and "only" 7.9 mg/g for ACBSG06, completely different from the behavior at pH 2. The biggest difference between the ACs can be found for Zn, which is barely adsorbed onto Filtrasorb F400 (2.2 mg/g) and Norit GAC1240 (1.4 mg/g), but adsorbs quite well on ACBSG06 (10 mg/g). In addition, the q_e values are also similar for the commercial samples, suggesting that the adsorption sites on the AC surface are optimally occupied.

When studying the removal percentages at **high** AC dosage at pH 7, the biggest difference between the ACs is now found for Cd. At high AC dosage, the commercial ACs are able to remove 40-50% of Cd from the solution, compared to 95% of ACBSG06. Co removal % are the lowest for Norit GAC1240 (52%) and the highest for Filtrasorb F400 (71%); with ACBSG06 performing averagely (62%). ACBSG06 also performs averagely for U removal (71%) compared to Filtrasorb F400 (81%) or Norit GAC1240 (60%). The removal percentage of V varies between 42% for ACBSG06, 46% for Filtrasorb F400 and 55% for Norit GAC1240. Zn removal is very efficient for Filtrasorb F400 and ACBSG06 (94% and 97% respectively) but somewhat lower for Norit GAC1240 (86%). At **high** AC dosage, ACBSG06 is the most efficient in removing Cd and Zn, Filtrasorb F400 in removing Co and U, and Norit GAC1240 in removing V.

Table 4-3 Adsorption capacities (qe, in mg/g) and percentage removal of Filtrasorb F400, Norit GAC1240 and ACBSG06 for several metals (10 mg/L) in a Milli Q water matrix at pH 2 and 7 (except Cu and Pb, only at pH 2)

Metal 10 mg/L	Milli-Q / pH 2				Milli-Q / pH 7			
	Low AC dosage		High AC dosage		Low AC dosage		High AC dosage	
	q_e (mg/g)	% removal	q_e (mg/g)	% removal	q_e (mg/g)	% removal	q_e (mg/g)	% removal
Filtrasorb F400								
As	≈ 0*	≈ 0%	0.06	2%	≈ 0	≈ 0%	≈ 0	≈ 0%
Cd	≈ 0	≈ 0%	≈ 0	≈ 0%	4.8	23%	1.3	48%
Co	≈ 0	≈ 0%	≈ 0	≈ 0%	3.4	16%	1.9	71%
Cu	≈ 0	≈ 0%	0.13	5%				
Pb	≈ 0	≈ 0%	0.05	2%				
U	0.55	3.0%	0.53	22%	10	57%	1.8	81%
V	≈ 0	≈ 0%	0.21	10%	4.3	22%	1.1	46%
Zn	≈ 0	≈ 0%	≈ 0	≈ 0%	2.2	13%	1.9	94%
Norit GAC1240								
As	≈ 0	≈ 0%	0.04	2%	≈ 0	≈ 0%	≈ 0	≈ 0%
Cd	≈ 0	≈ 0%	≈ 0	≈ 0%	4.3	20%	1.0	40%
Co	0.10	≈ 0%	≈ 0	≈ 0%	3.0	14%	1.4	52%
Cu	≈ 0	≈ 0%	0.11	4%				
Pb	≈ 0	≈ 0%	0.12	5%				
U	0.30	2.0%	1.1	44%	9.1	51%	1.3	60%
V	≈ 0	≈ 0%	0.31	12%	4.7	25%	1.3	55%
Zn	≈ 0	≈ 0%	≈ 0	≈ 0%	1.4	9%	1.7	86%
ACBSG06								
As	≈ 0	≈ 0%	0.10	4%	≈ 0	N.A.	≈ 0	≈ 0%
Cd	≈ 0	≈ 0%	0.05	2%	6.2	30%	2.5	95%
Co	≈ 0	≈ 0%	0.08	3%	3.5	16%	1.7	62%
Cu	0.30	1.0%	0.29	11%				
Pb	≈ 0	≈ 0%	1.2	47%				
U	2.0	11%	2.1	85%	7.9	45%	1.6	71%
V	0.52	3.0%	0.92	37%	4.0	21%	1.0	42%
Zn	≈ 0	≈ 0%	≈ 0	≈ 0%	10	63%	2.0	97%

*≈ 0 / ≈ 0%.: no significant difference found between starting and equilibrium concentration

4.1.3.2 Removal of high metal concentrations from reconstituted standard water (pH ≥ 7)

The adsorption experiments with reconstituted standard water are only performed for Cd, Co, U, V and Zn since As adsorption is ineffective and Cu and Pb precipitate at this pH. As can be seen from Table 4-4. The use of reconstituted standard water decreases adsorption capacities and removal percentages compared to Milli-Q water. The presence of competing ions in the solution due to the matrix of reconstituted standard water has less impact on the general adsorption performance of ACBSG06 than on the performance of both commercial ACs. There is an electrical diffused double layer between the AC and adsorbate species in solution, of which the thickness is expanded when more electrolytes are present in the solution [25]. This expansion prevents the approach of the ions to the surface and leads to lower adsorption because of a weakened electrostatic attraction. Furthermore, the presence of the ions that make up the reconstituted water can lead to a competition for adsorption. These two effects lead to a less effective adsorption of the target ions in the solution. However, ACBSG06 has a significantly higher amount of surface groups per area, (higher number of surface groups and a lower BET surface area) which will assumedly compensate for the increase of the thickness of the boundary layer.

Use of the reconstituted standard water has a different effect for each metal ion and AC. The q_e values at **low** AC dosage show a decline for each AC for each species except for Zn. The influence of the matrix on Cd adsorption capacity is limited for ACBSG06, which only decreases from 6.2 mg/g to 6.0 mg/g, in contrast to the commercial samples, which decrease from 4.8 to 1.9 mg/g (Filtrasorb F400) and from 4.3 to 1.8 mg/g (Norit GAC1240). For Co, the decrease in adsorption capacity is approximately equal for each AC. Adsorption capacities for U decreased drastically (more than 10 times) for the commercial samples, whereas the q_e value for ACBSG06 is only half of the value as in Milli-Q water. V adsorption capacities decreased only slightly for each AC. Adsorption capacities for Zn increased significantly for the commercial samples, compared to the Milli-Q adsorption experiments. This suggests that for Zn adsorption, chemisorption is more pronounced than the electrostatical attraction in the commercial ACs. The increase in ionic strength can assist the transport of the Zn ions to the surface, which is

repulsive towards the Zn ions and enables them to chemisorb (formation of covalent bonds) onto the surface functionalities [26], for ACBSG06 the q_e value is lowered to 7.2 mg/g, suggesting that Zn also adsorbs electrostatically on this surface. It is still more efficient than Filtrasorb F400 (4.8 mg/g) and Norit GAC1240 (5.6 mg/g), but the difference between these adsorbents is less pronounced.

At **high** AC dosages, Cd adsorption shows a strong decrease, compared to the Milli-Q water experiments, (- 38%) in the removed amount for Filtrasorb F400, in contrast to a slight decrease (-9%) for Norit GAC1240 and almost no influence (-3%) for ACBSG06. Furthermore, the removal percentage is not increased with increasing AC dosage for Filtrasorb, suggesting this is the highest removal percentage that can be reached in this experiment. The increase in ionic strength strongly decreases the % removal of Co for both Filtrasorb F400 (-22%) and ACBSG06 (-37%), but only 7% for Norit GAC1240. The adsorption of U is lowered for the commercial ACs (-49% and – 40% for Filtrasorb F400 and Norit GAC1240 respectively) but remains higher at circa 73% for ACBSG06. The presence of the matrix ions decreases V uptake for all ACs, resulting in equivalent % removal values for each AC of 31-37%. Lastly, the removal of Zn at high AC dosages seems almost unaffected by the addition of salts, confirming that chemisorption is the most prominent adsorption mechanism.

Table 4-4 Adsorption capacities (qe, in mg/g) and percentage removal of Filtrasorb F400, Norit GAC1240 and ACBSG06 for several metals (10 mg/L) in a reconstituted standard water matrix

Metal 10 mg/L	Reconstituted standard water			
	Low AC dosage		High AC dosage	
	q_e (mg/g)	% removal	q_e (mg/g)	% removal
Filtrasorb F400				
Cd	1.9	10%	0.24	10%
Co	1.8	10%	1.3	55%
U	0.99	5.1%	0.80	32%
V	3.4	18%	0.86	37%
Zn	4.8	24%	2.2	89%
Norit GAC1240				
Cd	1,8	9.3%	0.75	31%
Co	1.2	6.3%	1.1	48%
U	0.67	3.4%	0.48	20%
V	3.5	18%	0.72	31%
Zn	5.6	28%	2.3	90%
ACBSG06				
Cd	6.0	32%	2.2	92%
Co	1.4	7.4%	0.95	39%
U	3.2	16%	1.8	73%
V	3.1	16%	0.82	35%
Zn	7.2	37%	2.4	97%

4.1.3.3 Statistical analysis of the removal of trace ion concentrations from reconstituted standard water

4.1.3.3.1 Single ion removal

The adsorption experiment in reconstituted standard water is repeated using trace concentrations of the selected metal species (Cd: 0.24 µg/L, Co: 1.4 µg/L, U: 4.5 µg/L, V: 22 µg/L, Zn: 50 µg/L). Since the concentrations in this experiment are different from both the previous experiments and from each other, it will be impossible to compare the ACs in a quantitative way. The lower starting concentration will result in higher removal percentages, but lower q_e values. The averaged experimental results for each AC and analyte ions are displayed in Table 4-5. The statistical analysis of the raw data is performed as discussed in section 4.1.2.4. The report with relevant data, p-values and conclusions can be found in paragraph 4.2 on page 229. Relevant data and p-values are selected for this discussion.

Statistical analysis of the raw data of this realistic adsorption set-up for single ion removal concluded that – even if there might be differences between the values displayed in Table 4.5- there are <u>no significant statistical differences</u> between each of the ACs for **Cd** and **U** adsorption since the spread of the raw experimental data is big. Each of the ACs performs similarly. The analysis also proves that the only factor determining adsorption capacity and removal percentage is the increasing AC dosage, which increases the removal percentage (Cd: +16.4%; U: +13.6%) and decreases the adsorption capacity (Cd: -0.24 µg/g; U: -0.49 µg/g).

The pairwise comparison for the removal percentage of **V** shows a significant difference between Filtrasorb F400 and the other two ACs with respectively p-values of 0.0019 (Filtrasorb F400/Norit GAC1240) and 0.0032 (Filtrasorb F400/ACBSG06) at both high and low AC dosages. Filtrasorb F400 has a calculated removal percentage that is approximately 14% lower than the other two ACs at both AC dosages. There is no significant difference in the performance of Norit GAC1240 and ACBSG06 for the V removal percentage (p=0.9032).

Table 4-5 Adsorption capacities (qe, in mg/g) and percentage removal of Filtrasorb F400, Norit GAC1240 and ACBSG06 for several metals (trace concentrations) in a reconstituted standard water matrix at pH 8

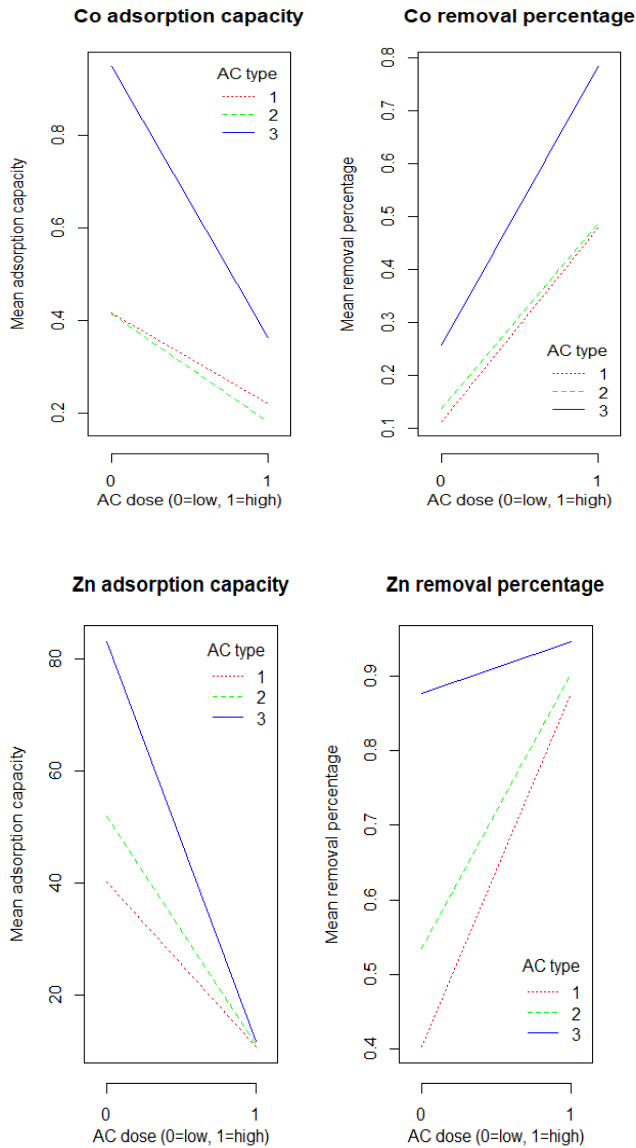| Metal Trace concentration	Reconstituted standard water			
	Low AC dosage		High AC dosage	
	q_e (µg/g)	% removal	q_e (µg/g)	% removal
Filtrasorb F400				
Cd	0.28	59%	0.05	81%
Co	0.41	14%	0.18	47%
U	0.59	66%	0.09	80%
V	22	49%	3.97	71%
Zn	52	53%	11.23	90%
Norit GAC1240				
Cd	0.28	58%	0.05	77%
Co	0.42	16%	0.22	47%
U	0.56	62%	0.08	74%
V	27	60%	4.9	88%
Zn	40	40%	11	88%
ACBSG06				
Cd	0.29	61%	0.04	70%
Co	0.95	26%	0.36	78%
U	0.58	65%	0.09	79%
V	26	58%	4.9	88%
Zn	83	88%	12	95%

Figure 4-2 Statistical pairwise comparison of adsorption capacity and removal percentage for each AC for Co (top) and Zn (bottom) removal using single ion solutions.

AC type: 1= Norit GAC1240; 2= Filtrasorb F400; 3=ACBSG06.

Low AC dosage = 0.5 g/L, high AC dosage = 4g/L

Mean adsorption capacity in µg/g. Lines display statistical connection, not adsorption behaviour.

215

For Co and Zn removal, significant statistical differences between the ACs are found for both adsorption capacities and removal percentages for the single ion solutions. The statistical outcomes are visually summarized in Figure 4-2, where lines indicate a statistical trend and not actual adsorption isotherm behaviour.

From Figure 4-2 it can be concluded that ACBSG06 always has a higher adsorption capacity and removal percentage for **Co** at low and high AC dosage, while the commercial samples perform similarly. From Table 4-5 it can also be observed that the removal percentage for ACBSG06 for Co is approximately double compared to the commercial ACs at **low** AC dosage. Norit GAC1240 and Filtrasorb do not differ significantly at low AC dosage (p=1 for q_e and p=0.8587 for % removal) or high AC dosage (p= 0.9967 for q_e and 0.9968 for % removal). ACBSG06 differs statistically from both Norit GAC1240 and Filtrasorb F400 for % removal of Co at **high** AC dosage (both p= <0.001), but this is not the case for q_e (p=0.6104 and p=0.4039 respectively). However, at **low** AC dosage, the statistical difference between the commercial ACs and ACBSG06 is significant for both q_e and % removal (p= 0.0024 for q_e and p=0.0035 for removal % for Norit GAC1240/ACBSG06; p= 0.0122 for q_e and 0.0181 for removal % for Filtrasorb F400/ACBSG06). The statistical difference between ACBSG06 and the commercial ACs was not observed at higher **Co** concentrations of 10 mg/L, suggesting that the higher amount of surface groups per area benefits the ACBSG06 at low ion concentrations, as the possible complexation sites are more available.

For **Zn** at **low** AC dosage, there is no significant statistical difference between Filtrasorb F400 and Norit GAC1240 (p=0.4272 for q and p=0.4756 for % removal), but differences compared to ACBSG06 are significant (all p < 0.02). At **high** AC dosage, the difference for q_e and % removal is within experimental error (as can also easily been seen from Figure 4-2) for all the ACs for Zn removal, and no statistical differences can be observed. Since the removal percentage for ACBSG06 is almost similar at both dosages it reaches its maximum removal percentage at a lower dosage than the commercial samples and is more interesting for economical use in industrial installations.

4.1.3.3.2 Mixed ions removal

In order to estimate the influence of other metal and metalloid ions on the adsorption of the five selected elements, adsorption experiments are also performed using several mixtures. In general, the analyses showed lower adsorption capacities and lower removal percentages for each AC when mixtures are used compared to the single ion solutions. This can be attributed to competition effects, lowering the amount of possible complexation sites that are available to the ions. The metal ions will be individually discussed when statistically significant differences are found.

As mentioned above, **Cd removal** is not influenced by the type of AC. When other metal ions are added to the solution, the adsorption capacity at a low AC dosage is 0.05 µg/g lower and the removal percentage at high AC dosage is 38% lower compared to the single element solutions. It can be concluded that the presence of metal ions generally causes a small decrease in adsorption efficiency of **Cd**. A significant effect of **V** was found, decreasing the removal percentage with approximately 9% (p=0.059). An interaction between **Co** and **U** was also found to be significant on the adsorption capacity of **Cd** when they are both present in the solution. The interaction is still significant after correcting for multiple testing. These data are presented in Figure 4-3 and Figure 4-4, showing that the adsorption capacity or removal percentage is highest when both **Co** and **U** are not present (Co=0 and U=0). However, the presence of both of these ions (Co=1 and U=1) at the same time increases adsorption efficiency of **Cd** (both q_e and removal percentage) compared to the presence of either of these ions on their own.

For **Co, U and V removal**, no significant statistical effects are found, nor for individual ACs or influence of other elements. The average data for adsorption of these ions from mixed solutions are displayed in Table 4-6, with p values <0001 except for the removal percentage for U. This result shows that the maximal amount of U is removed by each AC. Results are averaged for each of the AC data, since there is no significant difference between the ACs. The adsorption capacity and removal percentage are considerably lower than for the pure solutions (Table 4-5), except for the q_e for **Co**. In comparison to Figure 4-2, q_e values and removal percentages are lower for ACBSG06.
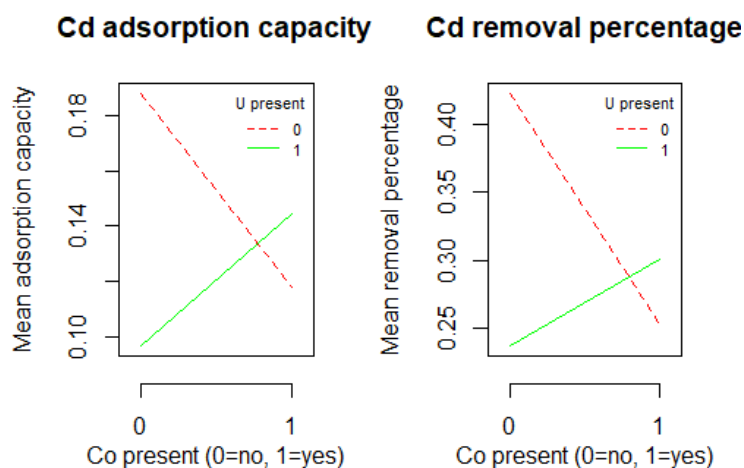
Figure 4-3 Influence of Co and U on the Cd removal
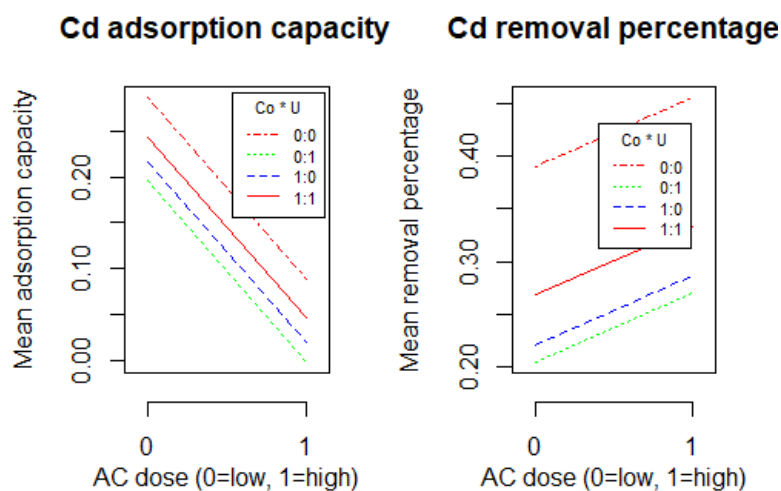
Figure 4-4 The influence of Co*U interactions on Cd removal

Table 4-6 Average adsorption capacities and removal percentages at low and high AC dosage of Co, U and V in mixtures

Metal	Low AC dosage		High AC dosage	
	q_e (µg/g)	% removal	q_e (µg/g)	% removal
Co	0.64	12%	0.22	35%
U	0.26	30%*	0.04	30% *
V	11.48	29%	2.28	44%

*: no significant statistical difference between high and low AC dosage

For the **removal of Zn**, no significant statistical effects are found for the other ions present in the solution. There are however still effects of the individual ACs on the adsorption capacity, but not on the removal percentage. For the adsorption capacity, there is no significant statistical difference between the two commercial samples, but they are both significantly (both $p < 0.001$) different from ACBSG06. The maximum adsorption capacity of ACBSG06 will probably be higher than for the commercial samples, yet this has to be investigated. The effect can also be observed in Figure 4-5. The adsorption capacities and removal percentages are also found to be lower than for the single ion solutions, due to general competition effects.
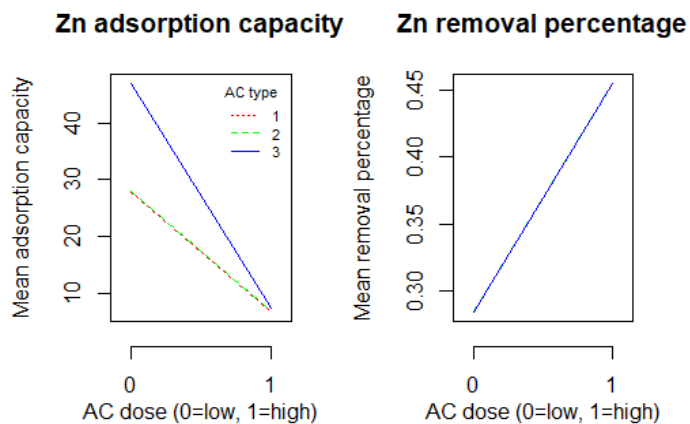
Figure 4-5 Adsorption capacity and removal percentage for Zn in mixtures

4.1.3.4 Leaching of metals from AC

The results of the leaching experiments for the three ACs are displayed in Table 4-7. Results were calculated accounting for the metal ion concentrations in Milli-Q and standard water measured by ICP-MS and ICP-OES. Measurements below detection limit are reported when the target element is not present in detectable concentration.

Table 4-7 Leaching of metals from the AC in Milli-Q and reconstituted standard water

Leachable metal (µg/g AC)	Norit GAC1240		Filtrasorb F400		ACBSG06	
	Milli-Q	Standard water	Milli-Q	Standard water	Milli-Q	Standard water
Al	0.26	9.15	0.26	25.7	0.25	0.06
As	<0.02	0.99	0.03	3.48	0.09	0.07
Cd	<0.01	<0.01	<0.01	<0.01	<0.01	<0.01
Co	0.04	0.03	0.04	0.02	0.03	0.03
Cu	0.18	0.31	0.18	0.32	0.25	0.33
Fe	<0.50	<0.50	<0.50	0.62	0.78	1.17
Pb	<0.01	<0.01	0.03	<0.01	0.11	0.13
U	<0.01	<0.01	<0.01	<0.01	<0.01	<0.01
V	0.01	0.05	0.01	0.35	<0.01	0.03
Zn	1.04	0.31	0.61	0.30	0.55	0.31
Other ions (mg/g AC)						
Ca	0.11	<0.01	0.12	<0.01	0.45	<0.01
Mg	<0.01	<0.01	<0.01	<0.01	1.322	<0.01
Na	0.05	<0.01	<0.01	<0.01	0.18	<0.01

For Ca, Mg and Na the ACs are very prone to leaching into Milli-Q, but the effect is not measurable when the samples are introduced to the reconstituted standard water, presumably because equilibrium with the ions in the solutions is set. The leaching of Ca, Mg and Na is more pronounced for the ACBSG06, since it has nearly double the ash content compared to the commercial AC. Cd and U are the only metal species that are not leached for any of the studied ACs. The most prominent results are the high amounts of Al and As that leach from commercial ACs in reconstituted standard water. The leaching of As is especially significant for Filtrasorb F400 in reconstituted standard water and might have to be monitored due to its toxicity, since the WHO health guideline states that As concentrations in water should not exceed 10 µg/L [27]. The concentration of As would already exceed the environmental limit of 3 µg/L when a very low AC dosage of 3 g/L for Norit GAC1240 and less than 1 g/L for Filtrasorb F400 is used [2]. Only a fraction of the amount of As compared to the commercial samples is leached by ACBSG06, for which the As leaching seems unaffected by the matrix.

ACBSG06 leaches an amount of Pb that might be problematic in surface waters at AC dosages higher than 10 g/L, as the environmental limit is at 1.2 µg/L [2]. Fe is leached by Filtrasorb F400 in reconstituted standard water and for ACBSG06 in both media. Zn leaching in Milli-Q is more pronounced for the commercial samples (Norit GAC 1240 > Filtrasorb F400 > ACBSG06), but using reconstituted standard water provides similar results for each of the ACs.

4.1.4 Conclusion

The most problematic inorganic ionic species in Flemish surface water are Co, U, As, V, Zn and Cd. For these elements, an adsorption screening is performed using solutions of pH 2 and pH 7. The two commercial ACs, Filtrasorb F400 and Norit GAC1240, have lower removal percentages at high (4g/L) AC dosage for Cd, Co and Zn compared to the ACBSG06. An adsorption experiment with Cu and Pb was also performed with solutions of pH 2. The commercial ACs do not remove these elements effectively, but ACBSG06 at high AC dosage is able to remove up to 47% of Pb.

The use of reconstituted standard water increases the ionic strength and generally decreases adsorption capacities and removal percentages. The strongest decrease in removal percentage was perceived for Cd removal by Filtrasorb F400 at high AC dosage, which is 38% lower than in the single ion solution. The influence of ionic strength is different for each metal and each AC. The increase of ionic strength shows no to little influence for Zn adsorption on any of the ACs, suggesting that for Zn, chemisorption is the most important adsorption mechanism. At high AC dosage, ACBSG06 is the most efficient in removing Cd and Zn, Filtrasorb F400 is the most efficient in removing Co and U, and Norit is the most efficient GAC1240 in removing V.

Removal of trace concentrations of ions and mixtures was analysed by statistical methods to account for two-way interactions. When single element solutions were adsorbed, no significant statistical differences for the ACs were found for Cd and U removal (76% and 78% removal at high AC dosage respectively). For V, Filtrasorb F400 performed significantly worse than the other samples. For Co and Zn, ACBSG06 significantly performed better than both commercial samples.

Analysis of mixed metal removal adsorption experiments showed that all adsorption capacities and removal percentages decrease in comparison with the single element adsorption experiments. For Co, U and V no significant statistical effects of other metals or AC type were found. Cd removal was not influenced by AC type, but presence of V or both Co and U decrease adsorption capacity and removal percentage. For Zn adsorption at low AC dosage, the use of ACBSG06 leads to significantly higher adsorption capacity.

Leaching experiments revealed that leaching of As can be problematic for commercial ACs and leaching of Pb for ACBSG06. Filtrasorb F400 also leaches Al, Fe and Zn. ACBSG06 has a very limited leaching behavior, except for Fe.

Acknowledgement

4.1.5 References

[1] Vlaamse Milieumaatschappij, Zware metalen in het grondwater in Vlaanderen, in: Afdeling Operationeel waterbeheer VMM, Dienst Grondwaterbeheer, Aalst, **2015**.

[2] Vlaamse regering, VLAREM II: Bijlage 2.3.1. Basismilieukwaliteitsnormen voor oppervlaktewater in, **2003**.

[3] C.M. Park, J. Han, K.H. Chu, Y.A.J. Al-Hamadani, N. Her, J. Heo, Y. Yoon, Influence of solution pH, ionic strength, and humic acid on cadmium adsorption onto activated biochar: Experiment and modeling, Journal of Industrial and Engineering Chemistry, **2017**, 48, 186-193.

[4] F. Di Natale, A. Lancia, A. Molino, D. Musmarra, Removal of chromium ions form aqueous solutions by adsorption on activated carbon and char, Journal of Hazardous Materials, **2007**, 381-390.

[5] P.G.J.-M.P. Ciffroy, M. K., Kinetics of the adsorption and desorption of radionuclides of Co, Mn, Cs, Fe, Ag and Cd in freshwater systems: experimental and modelling approaches, Journal of Environmental Radioactivity, **2001**, 55, 71-91.

[6] S.X. Liu, X. Chen, X.Y. Chen, Z.F. Liu, H.L. Wang, Activated carbon with excellent chromium(VI) adsorption performance prepared by acid-base surface modification, Journal of Hazardous Materials, **2007**, 315-319.

[7] E. Asuquo, A. Martin, P. Nzerem, F. Siperstein, X. Fan, Adsorption of Cd(II) and Pb(II) ions from aqueous solutions using mesoporous activated carbon adsorbent: Equilibrium, kinetics and characterisation studies, Journal of Environmental Chemical Engineering, **2017**, 5, 679-698.

[8] A. Nieto-Márquez, A. Pinedo-Flores, G. Picasso, E. Atanes, R. Sun Kou, Selective adsorption of Pb^{2+}, Cr^{3+} and Cd^{2+} mixtures on activated carbons prepared from waste tires, Journal of Environmental Chemical Engineering, **2017**, 5, 1060-1067.

[9] R. Tovar-Gómez, M.d.R. Moreno-Virgen, J. Moreno-Pérez, A. Bonilla-Petriciolet, V. Hernández-Montoya, C.J. Durán-Valle, Analysis of synergistic and antagonistic adsorption of heavy metals and acid blue 25 on activated carbon from ternary systems, Chemical Engineering Research and Design, **2015**, 93, 755-772.

[10] T. Bohli, A. Ouederni, N. Fiol, I. Villaescusa, Evaluation of an activated carbon from olive stones used as an adsorbent for heavy metal removal from aqueous phases, Comptes Rendus Chimie, **2015**, 18, 88-99.

[11] I.A. Aguayo-Villarreal, A. Bonilla-Petriciolet, R. Muñiz-Valencia, Preparation of activated carbons from pecan nutshell and their application in the antagonistic adsorption of heavy metal ions, Journal of Molecular Liquids, **2017**, 230, 686-695.

[12] L. Sellaoui, T. Depci, A.R. Kul, S. Knani, A. Ben Lamine, A new statistical physics model to interpret the binary adsorption isotherms of lead and zinc on activated carbon, Journal of Molecular Liquids, **2016**, 214, 220-230.

[13] V.C. Srivastava, I.D. Mall, I.M. Mishra, Adsorption of toxic metal ions onto activated carbon: Study of sorption behaviour through characterization and kinetics, Chemical Engineering and Processing: Process Intensification, **2008**, 47, 1269-1280.

[14] K. Vanreppelen, S. Vanderheyden, T. Kuppens, S. Schreurs, J. Yperman, R. Carleer, Activated carbon from pyrolysis of brewer's spent grain: Production and adsorption properties, Waste Management & Research, 32 (**2014**) 634-645.

[15] S.R.H. Vanderheyden, R. Van Ammel, K. Sobiech-Matura, K. Vanreppelen, S. Schreurs, W. Schroeyers, J. Yperman, R. Carleer, Adsorption of cesium on different types of activated carbon, Journal of Radioanalytical and Nuclear Chemistry, **2016**, 310, 301-310.

[16] S.R.H. Vanderheyden, K. Vanreppelen, J. Yperman, R. Carleer, S. Schreurs, Chromium(VI) removal using in-situ nitrogenized activated carbon prepared from Brewers' spent grain, Adsorption, **2017**, 24, 147-156.

[17] Arsenic: Medical and Biologic Effects of Environmental Pollutants, National Acadamies Press, **1977**.

[18] A.M. Ure, C.M. Davidson, Chemical Speciation in the Environment, Blackie Academix & Professional, **2002**.

[19] M.G.A. Vieira, A.F. De Almeida Neto, M.G. Carlos da Silva, C.C. Nóbrega, A.A. Melo Filho, Characterization and use of in natura and calcined rice husks for biosorption of heavy metal ions from aqueous effluents, Brazilian Journal of Chemical Engineering, **2012**, 29, 619-633.

[20] R.N. Collins, A.S. Kinsela, The aqueous phase speciation and chemistry of cobalt in terrestrial environments, Chemosphere, **2010**, 79, 763-771.

[21] A. Krestou, D. Panias, Uranium (VI) speciation diagrams in the UO2 2+ / CO3 2- / H2O system at 25°C, The European Journal of Mineral Processing and Environmental Protection, **2004**, 4, 113-129.

[22] L. Zeng, C.Y. Cheng, A literature review of the recovery of molybdenum and vanadium from spent hydrodesulphurisation catalysts, Part II: Separation and purification, Hydromettalurgy, **2009**, 98.

[23] J. Livage, Hydrothermal Synthesis of Nanostructured Vanadium Oxides, Materials, **2010**, 3, 4175-4195.

[24] Guidance Document on Transformation/Dissolution of Metals and Metal Compounds in Aqueous Media, in: OECD Environment: Health and Safety Publications, **2001**.

[25] (L. Chávez-Guerrero, R. Rangel-Méndez, E. Muñoz-Sandoval, D. A. Cullen, D. J. Smith, H. Terrones and M. Terrones, Production and detailed characterization of bean-husk based carbon: Efficient cadmium (II) removal from aqueous solutions, Water Research, **2008**, 42, 3473–3479.

[26] G. Newcombe, M. Drikas, Adsorption of NOM onto activated carbon: Electrostatic and non-electrostatic effects, Carbon, **1997**, 35, 1239-1250.

[27] World Health Organization, Guidelines for drinking-water quality: Fourth edition, **2011**.

4.2 Supplementary materials

Summary of the report of the statistical analysis by Cécile Kremer

In this report the ACs are named as follows:

AC1 = Norit GAC1240

AC2 = Filtrasorb F400

AC3 = ACBSG06

4.2.1 Cd models

4.2.1.1 Analysis of single ion removal

→ only significance of AC dosage

Adsorption capacity (q)

	Estimate	**Standard error**	***p*-value**
(Intercept)	0.2847	0.0107	<.0001
AC dose (high)	-0.2393	0.0151	<.0001

Removal percentage (%)

	Estimate	**Standard error**	***p*-value**
(Intercept)	0.5966	0307	<.0001
AC dose (high)	0.1638	0.0434	.0037

There is a significant effect of AC dosage. There is no significant effect of AC type. The adsorption capacity at high AC dosage is 0.2393 lower than at low AC dosage. The removal percentage is 0.1638 higher compared to low AC dosage.

Cd adsorption capacity   **Cd removal percentage**
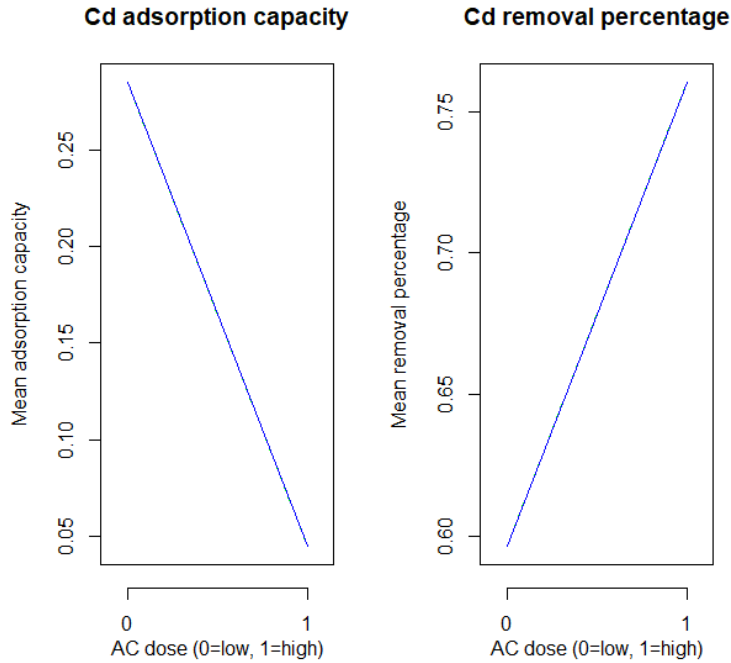
4.2.1.2 Analysis with 2-way interactions:

Adsorption capacity (q)

	Estimate	Standard error	*p*-value
(Intercept)	0.2356	0.0135	<.0001
AC dose (high)	-0.1975	0.019	<.0001
Co	0.0055	0.0095	.5625
U	0.0161	0.0095	.0923
Co*U	0.0294	0.0095	.0022

Removal percentage (%)

	Estimate	Standard error	p-value
(Intercept)	0.3174	0.0284	<.0001
AC dose (high)	0.065	0.0323	.0449
Co	0.0281	0.0162	.0832
U	0.0359	0.0162	.0271
V	-0.0896	0.0324	.0059
Co*U	0.0599	0.0162	.0003

There is a significant effect of AC dosage: high AC dosage results in a significantly lower adsorption capacity (0.1975 lower) and higher removal percentage (0.065 higher). There is a significant effect for the presence of V: a lower removal percentage (0.0896 lower than without V).

There is also a significant interaction between Co and U: the effect of Co is dependent on the presence of U in the mixture and the effect of U is dependent on the presence of Co. Pairwise comparisons are performed to confirm this difference

Pairwise comparisons for Co*U

	p-value for q	p-value for %
0:1 − 0:0	.0195	<.0001
1:0 − 0:0	.1140	.002
1:1 − 0:0	.5076	.0499
1:0 − 0:1	.8962	.9861
1:1 − 0:1	.3873	.5046
1:1 − 1:0	.8128	.7201

The interaction is still significant after correction for multiple testing.

For example: there is a significant difference between 'No Co, U present' and 'No Co and No U'

                                                                    0:1   -   0:0

The figure below shows that the adsorption capacity is lower for 'No Co, U present' than for 'no co and no U'.

Cd adsorption capacity   **Cd removal percentage**
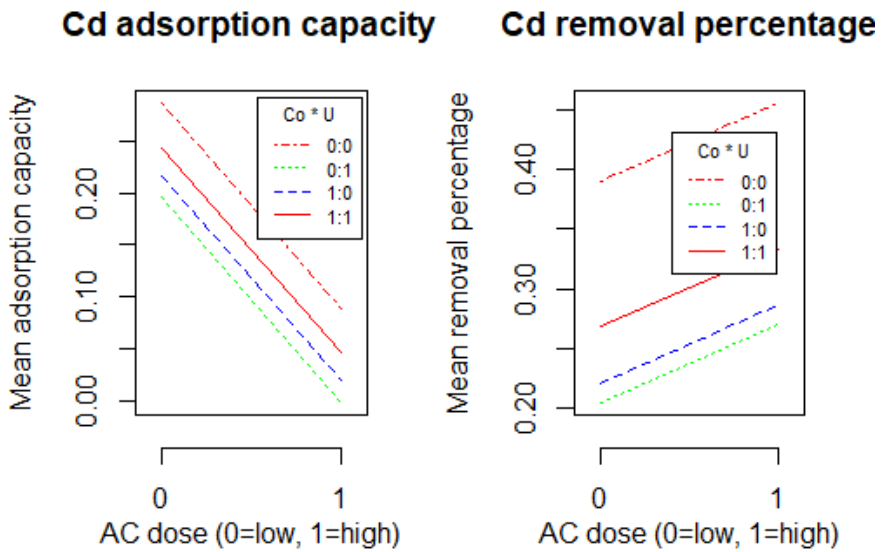
The effect of AC dosage (figure below) is the same for the adsorption capacity as with the single ion solution. The removal percentage is lower than for the single ion removal. This is also visible when the estimates from both tables are compared (single ion removal vs. model with interactions.)

Cd adsorption capacity
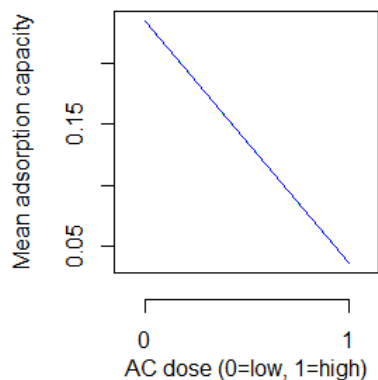
Cd removal percentage
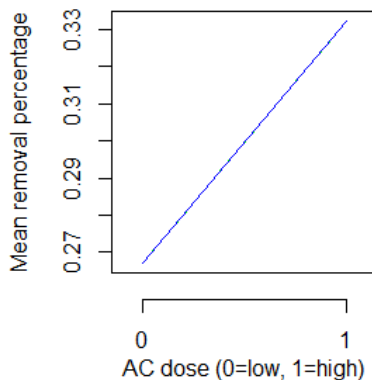
The effect of Co*U interaction is displayed in the figure below. The adsorption capacity is highest when Co and U are both not present.

Cd adsorption capacity
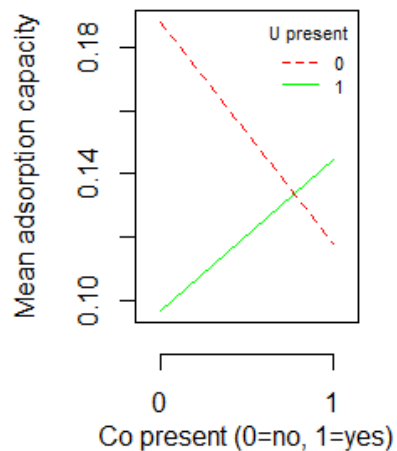
Cd removal percentage
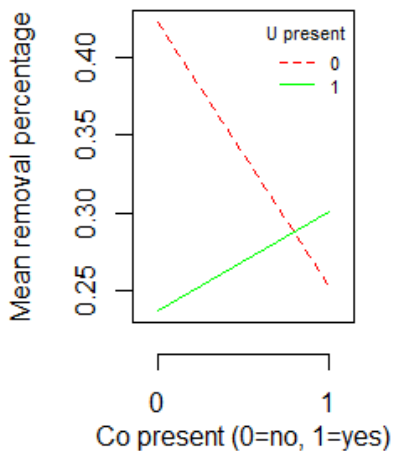
4.2.2 Co models

4.2.2.1 Analysis of single ion removal

→ **significant interaction of AC type * AC dosage**

Adsorption capacity (q)

	Estimate	**Standard error**	***p*-value**
(Intercept)	0.4163	0.0614	<.0001
AC type 2	-0.0016	0.0868	.9861
AC type 3	0.5311	0.0868	.0009
AC dose (high)	-0.1956	0.0868	.065
AC type 2 * AC dose (high)	-0.0367	0.1227	.7747
AC type 3 * AC dose (high)	-0.3896	0.1227	.0192

Removal percentage (%)

	Estimate	**Standard error**	***p*-value**
(Intercept)	0.113	0.0157	.0004
AC type 2	0.0248	0.0222	.3067
AC type 3	0.1445	0.0222	.0006
AC dose (high)	0.3654	0.0222	<.0001
AC type 2 * AC dose (high)	-0.015	0.0313	.6489
AC type 3 * AC dose (high)	0.1613	0.0313	.0021

There is an interaction between AC type and AC dosage: the effect of AC type is different for low vs high AC dosage.

Pairwise comparisons for ACtype*ACdosis

	p-value voor q	*p*-value voor %
1:1 − 1:0	.3339	<.0001
2:0 − 1:0	1	.8587
2:1 − 1:0	.2058	<.0001
3:0 − 1:0	.0066	.0048
3:1 − 1:0	.9847	<.0001
2:0 − 1:1	.3405	<.0001
2:1 − 1:1	.9967	.9968
3:0 − 1:1	.0013	.0004
3:1 − 1:1	.6104	<.0001
2:1 − 2:0	.2103	<.0001
3:0 − 2:0	.0065	.0124
3:1 − 2:0	.9865	<.0001
3:0 − 2:1	<.001	.0004
3:1 − 2:1	.4039	<.0001
3:1 − 3:0	.0039	<.0001

Example: the difference between AC3 and AC1 at low dosages are significant. (3:0) −(1:0)

Co adsorption capacity
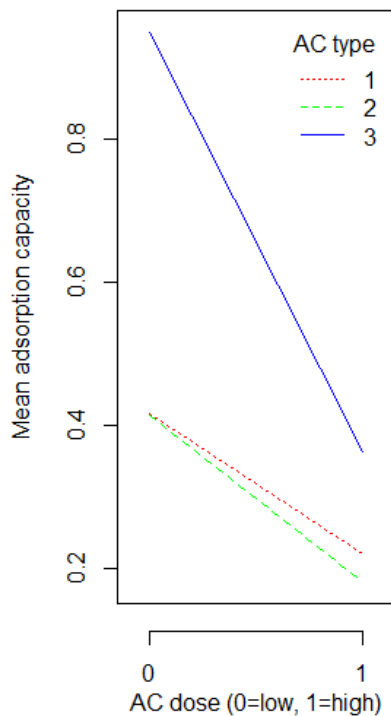
Co removal percentage
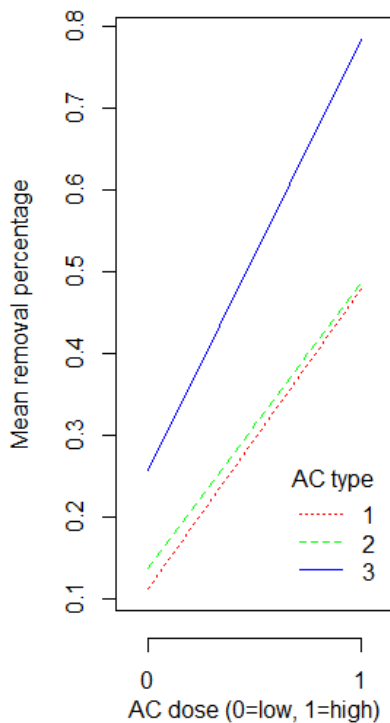
4.2.2.2 Analysis with 2-way interactions:

Adsorption capacity (q)

	Estimate	**Standard error**	*p*-value
(Intercept)	0.6439	0.0383	<.0001
AC dose (high)	-0.4196	0.0541	<.0001

Removal percentage (%)

	Estimate	Standard error	*p*-value
(Intercept)	0.1251	0.0196	<.0001
AC dose (high)	0.2252	0.0277	<.0001

There is a significant effect of AC dosage. The adsorption capacity at high AC dosage is 0.4196 lower than at low dosage and the removal percentage at high dosage is 0.2252 higher than at low dosage. This effect can also be seen in the following figure.
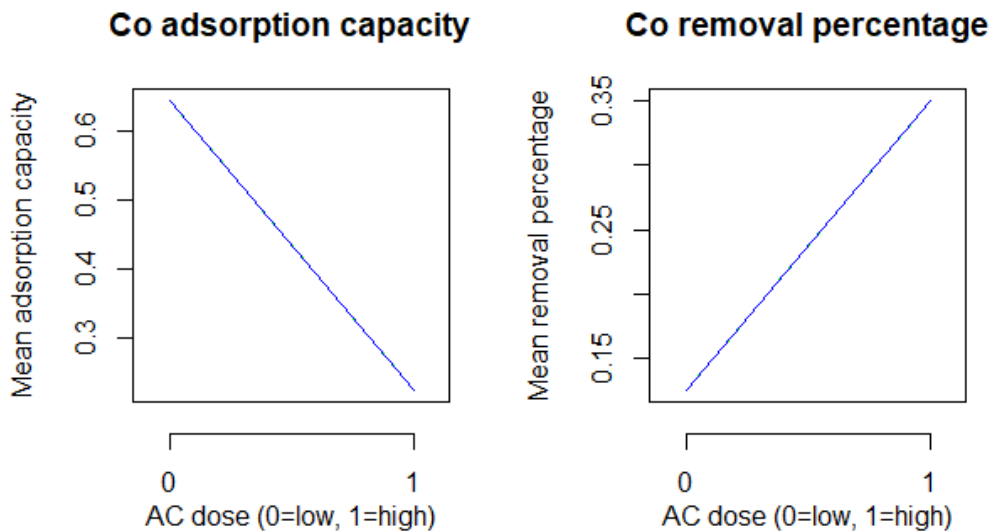
→ **Adsorption capacity and removal percentage are lower than for the single ion removal**

The effect of AC dosage seems to be less strong than compared to the single ion removal. There was however an interaction of AC type that is absent here, so these figures cannot be compared.

4.2.3 U models

4.2.3.1 Analysis of single ion removal

→ only AC dosage is significant

Adsorption capacity (q)

	Estimate	**Standard error**	***p*-value**
(Intercept)	0.5774	0.0097	<.0001
AC dose (high)	-0.4903	0.0138	<.0001

Removal percentage (%)

	Estimate	**Standard error**	***p*-value**
(Intercept)	0.6428	0.0157	<.0001
AC dose (high)	0.1355	0.0222	.0001

Only the effect of AC dosage is significant. At high AC dosage the adsorption capacity is 0.4903 lower, and the removal percentage is 0.1355 higher. This effect can be seen on the figures below.

U adsorption capacity
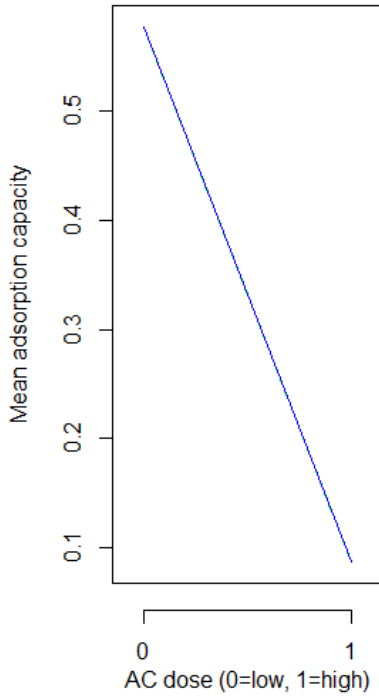
U removal percentage
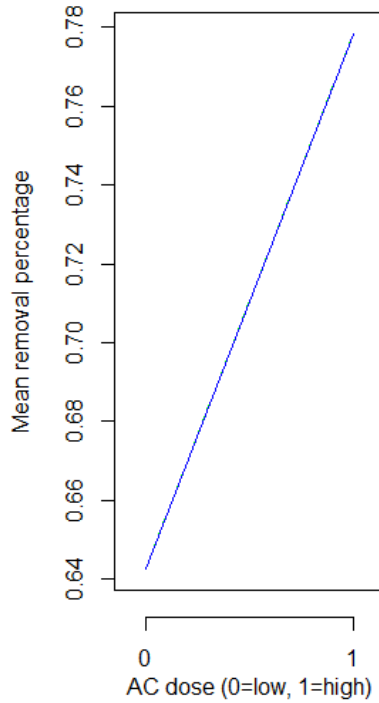
4.2.3.2 Analysis with 2-way interactions:

Adsorption capacity (q)

	Estimate	Standard error	*p*-value
(Intercept)	0.2563	0.0134	<.0001
AC dose (high)	-0.2193	0.019	<.0001

Removal percentage (%)

	Estimate	Standard error	*p*-value
(Intercept)	0.3044	0.0159	<.0001

There is a significant effect of AC dosage for the adsorption capacity (0.2193 lower at high AC dosage). There is no significant difference in the removal percentage between high and low AC dosage.
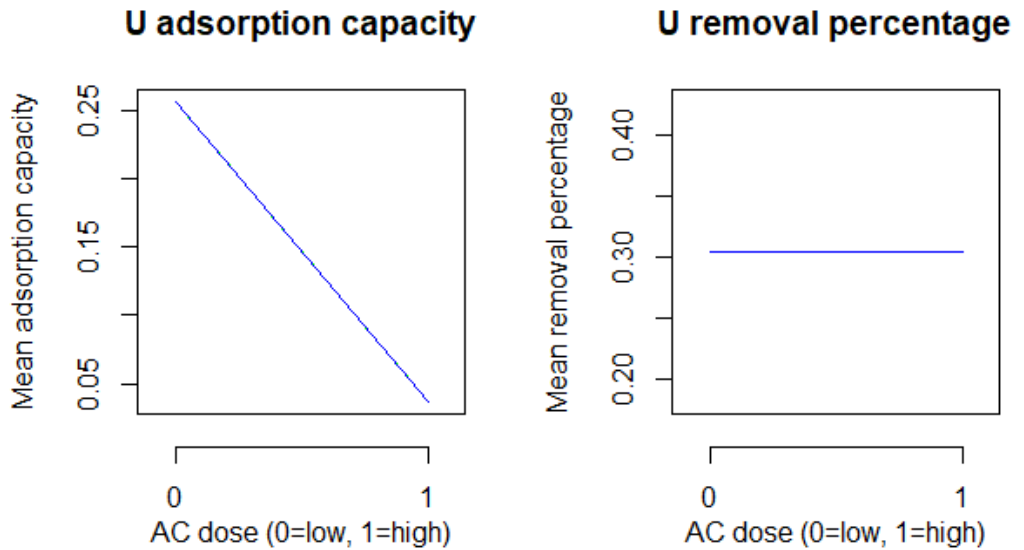
→ **Adsorption capacity and percent removal lower than for single ion removal**

4.2.4 V models

4.2.4.1 Analysis of single ion removal

→ AC type and dosage significant

Adsorption capacity (q)

	Estimate	**Standard error**	***p*-value**
(Intercept)	24.8411	0.8237	<.0001
AC dose (high)	-20.2443	1.1649	<.0001

Removal percentage (%)

	Estimate	**Standard error**	***p*-value**
(Intercept)	0.6061	0.022	<.0001
AC type 2	-0.1412	0.0269	.0008
AC type 3	-0.0117	0.0269	.6766
AC dose (high)	0.267	0.022	<.0001

There is a significant effect of AC dosage: the adsorption capacity is 20.24 lower at high AC dosage compared to low AC dosage and the removal percentage is 0.267 higher.

AC type 2 (Filtrasorb F400) has a significantly lower (0.1412) removal percentage than AC1 (Norit GAC1240). Pairwise comparisons are performed to determine which ACs differ significantly. From this comparison it can be concluded that type 2 and 1, as well as type 2 and 3 are significantly different.

	p-value voor %
2 − 1	.0019
3 − 1	.9032
3 − 2	.0032

V adsorption capacity
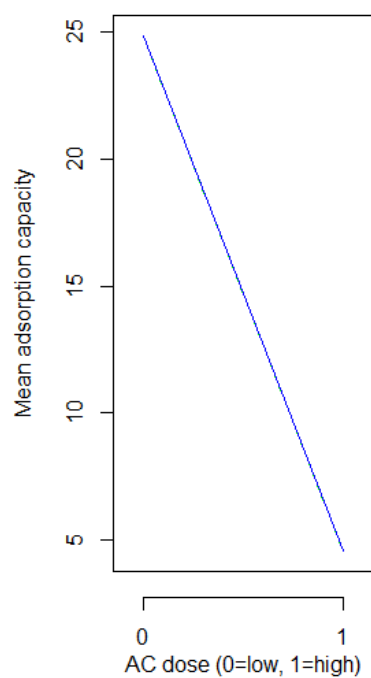
V removal percentage
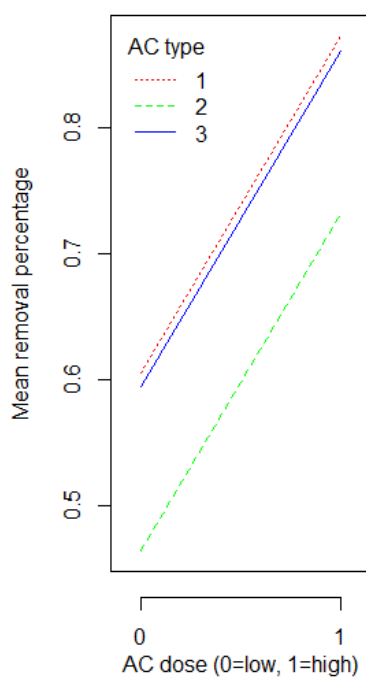
4.2.4.2 Analysis with 2-way interactions:

Adsorption capacity (q)

	Estimate	Standard error	*p*-value
(Intercept)	11.4813	0.6043	<.0001
AC dose (high)	-9.2839	0.8547	<.0001

Removal percentage (%)

	Estimate	Standard error	*p*-value
(Intercept)	0.2895	0.0269	<.0001
AC dose (high)	0.1531	0.0381	<.0001

There is a significant effect of AC dosage. At high AC dosage the adsorption capacity is 9.2839 lower than at low AC dosage and the removal perentage is 0.1531 higher.
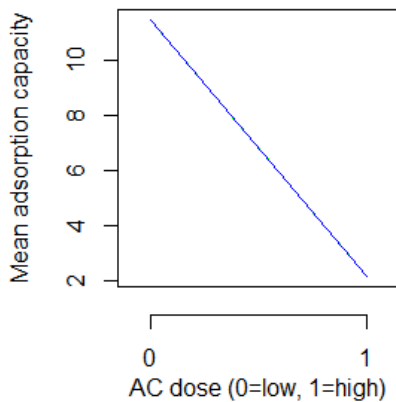
➜ q and percent removal are both lower than for the single ion removal

The effect of AC dosage is less pronounced that for the single ion removal. This can only be said with surety for the adsorption capacity, as the AC type also has an influence on the removal percentage for the single ion removal.

4.2.5 Zn models

4.2.5.1 Analysis of single ion removal

→ significant interaction of AC type * AC dosage for both q and removal percentage

Adsorption capacity (q)

	Estimate	**Standard error**	***p*-value**
(Intercept)	40.276	4.069	<.0001
AC type 2	11.606	5.755	.0903
AC type 3	42.671	5.755	.0003
AC dose (high)	-29.353	5.755	.0022
AC type 2 * AC dose (high)	-11.299	8.138	.2144
AC type 3 * AC dose (high)	-41.857	8.138	.0021

Removal percentage (%)

	Estimate	**Standard error**	***p*-value**
(Intercept)	0.4038	0.0485	.0002
AC type 2	0.1308	0.0686	.1052
AC type 3	0.4737	0.0686	.0005
AC dose (high)	0.4737	0.0686	.0005
AC type 2 * AC dose (high)	-0.106	0.097	.3165
AC type 3 * AC dose (high)	-0.4053	0.097	.0058

There is an interaction between AC type and AC dosage: the effect of type of AC is different for low vs high dosage. The effect of type and dosage cannot be interpreted separately. A pairwise comparison is performed to determine which AC*ACdosage differ significantly from each other.

Pairwise comparisons voor ACtype*ACdosis

	p-value voor q	*p*-value voor %
1:1 − 1:0	.0164	.0035
2:0 − 1:0	.4272	.4756
2:1 − 1:0	.0171	.0027
3:0 − 1:0	.0024	.0035
3:1 − 1:0	.0186	.0017
2:0 − 1:1	.0029	.018
2:1 − 1:1	1	.999
3:0 − 1:1	<.001	1
3:1 − 1:1	.9999	.903
2:1 − 2:0	.0031	.0129
3:0 − 2:0	.0122	.0181
3:1 − 2:0	.0034	.0074
3:0 − 2:1	<.001	.999
3:1 − 2:1	1	.9835
3:1 − 3:0	<.001	.9034

Zn adsorption capacity
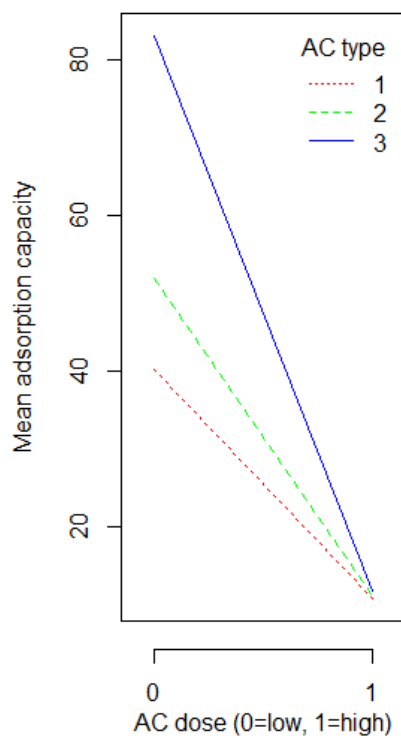
Zn removal percentage

247
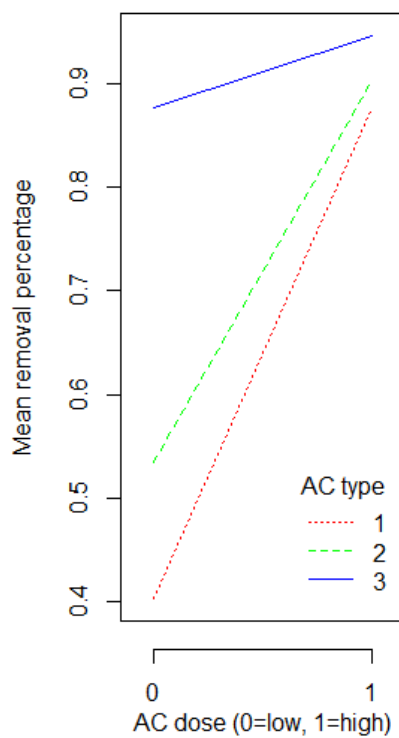
4.2.5.2 Analysis with 2-way interactions:

Adsorption capacity (q)

	Estimate	**Standard error**	*p*-value
(Intercept)	27.7393	3.2875	<.0001
AC type 2	0.2866	4.6492	.9509
AC type 3	19.1792	4.6492	<.0001
AC dose (high)	-21.0218	4.6492	<.0001
AC type 2 * AC dose (high)	-0.1274	6.5749	.9846
AC type 3 * AC dose (high)	-18.6392	6.5749	.0048

There is an interaction between AC type and AC dosage. The effects cannot be interpreted individually.

Pairwise comparisons voor ACtype*ACdosis

	p-value voor q
1:1 − 1:0	.0001
2:0 − 1:0	1
2:1 − 1:0	.0001
3:0 − 1:0	.0006
3:1 − 1:0	.0002
2:0 − 1:1	<.0001
2:1 − 1:1	1
3:0 − 1:1	<.0001
3:1 − 1:1	.9999
2:1 − 2:0	.0001
3:0 − 2:0	.0008
3:1 − 2:0	.0002
3:0 − 2:1	<.0001
3:1 − 2:1	.9999
3:1 − 3:0	<.0001

Example: there is a significant difference for adsorption capacity between AC1 with a low or high AC dosage. (1:1) − (1:0)

Removal percentage (%)

	Estimate	Standard error	*p*-value
(Intercept)	0.2895	0.0269	<.0001
AC dose (high)	0.1531	0.0381	<.0001

A higher AC dosage significantly increases the removal percentage with 0.1531.
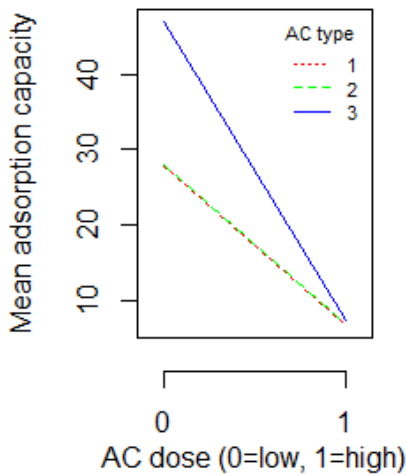
→ **Adsorption capacity and removal percentage lower than for single ion removal.**

The effect of AC dosage is less pronounced that for the single ion removal. This can only be said with surety for the adsorption capacity, as the AC type also has an influence on the removal percentage for the single ion removal.

5 Summary, conclusions and perspectives

Climate change and the increasing need for resources have turned the interest of industry and legislation towards the use of biomass. A comprehensive summary of the properties of biomass and conversion methods is given in **chapter 1**. Its potential as energy carrier has been known for a long time, but the possibilities to produce new materials by using conversion methods have created a new-found research interest. Since certain chemical elements are enriched or depleted in specific biomass materials, new materials can be created keeping this characteristic in mind. Production of new materials with certain properties or in-situ created functionalities is one of the options that can be explored for biomass. The use of biomass has an impact on the environment and technical installations, but also on economy and social structures in rural regions.

The biomass used throughout this project is brewer's spent grain (BSG). BSG is produced after the malting process during beer brewing. It consists of the leftover materials from the barley after its sugars and starches have been extracted. Roughly 270 500 tons of BSG are produced globally in one year and most of this is fed to ruminants. However, BSG contains a high amount of indigestible fibers and causes an increased methane production. A high water content up to 85% induces rapid degradation, demanding a quick drying and processing technology. With roughly 70% of cellulose, hemicellulose and lignin on a dry basis, BSG is an ideal material for biotechnological applications. Its high content of nitrogen creates a promising precursor for new materials with in-situ generated nitrogen functionalities, using pyrolysis as conversion method.

During the pyrolysis, biomass is thermally cracked in an oxygen-poor environment. The organic constituents break down into smaller parts and create an energy-dense gas (bio-gas) of which a part condenses at room temperature

(bio-oil) and a solid third fraction: (bio-) char. The latter contains unconverted solid, carbonaceous residues and a small mineral fraction. Its structural and chemical properties highly depend on the input material and pyrolysis conditions. The use of heated steam burns off carbon groups in a process called activation, converting the char into activated carbon (AC). With a high surface area and a multitude of surface functionalities this AC has good adsorptive properties. For BSG, the result of pyrolysis and steam activation is an in-situ nitrogenized ACBSG.

In **chapter 2**, ACBSG and two commercial ACs (Norit GAC1240 and Filtrasorb F400) are studied for the removal of chromium(VI) from aqueous solutions. Results show that the measurement methods to determine Cr concentration should not be limited to one oxidation state, but both total Cr and Cr(VI) concentrations should be considered. The difference between total Cr and Cr(VI) concentration is the amount of in-situ formed Cr(III). Single measurements of Cr(VI) result in an overestimation of the amount of Cr removed and lead to a higher apparent adsorption capacity (q_{app}). This q_{app} is an estimate of the Cr(VI) adsorbed plus the amount of Cr(VI) reduced to Cr(III). Whereas the 'true' adsorption capacity (q_e) should only account for the adsorbed amount of Cr as Cr(VI). This typical reduction behaviour also leads to a new adsorption isotherm shape, with a maximal removal percentage for total chromium at an AC dosage of approximately 0.75 g/L. Above this dosage, more Cr(VI) is reduced into Cr(III), which is less efficiently adsorbed, leading to a lower removal percentage for total Cr. In comparison with the two industrial ACs, ACBSGs have slightly better removal percentages for Cr(VI) at low dosages of 0.4 g/L (up to 97% for ACBSG06 compared to 91% for Filtrasorb F400). Similar removal percentages (>99%) for Cr(VI) at AC dosages above 1.2 g/L are found for all studied ACs. When the removal of the total Cr is considered, ACBSGs reached a higher removal percentage at the optimal AC dosage of 0.75 g/L, up to 87% for ACBSG05, compared to 73% for both commercial samples. The reduction reaction is more pronounced for the commercial samples because of their lower oxygen and nitrogen content. Experimental data for the kinetic behaviour of the adsorption of both Cr(VI) and total Cr show that the ACBSGs also have a faster removal rate than the two commercial ACs because of the slower reduction reaction.

The second part of **chapter 2** describes the performance for chromium adsorption on modified AC. Two modification methods are performed on four AC samples: two selected ACBSGs and both commercial ACs. The first modification method is an acid/basic washing of the samples with diluted nitric acid and sodium hydroxide. This results in a more oxidized surface. The O/C ratio increases by a factor 8 and 4 for Norit GAC1240 and Filtrasorb F400 respectively, but only by a factor 2 for the ACBSGs, as they have a higher initial oxygen content. These oxygen functionalities should enhance the Cr adsorption by preventing the reduction to Cr(III) and making more sites available for complexation; it is found however that the total amount of surface functionalities decreases drastically for each AC. This results in lower adsorption capacities and removal percentages for Cr(VI) and total chromium compared to unmodified ACs. The second modification method is based on grafting of a copolymer with a quaternary ammonium end group, able to form complexes with Cr. The copolymer structure partly blocks the porous structure of the AC, so no synergy between the two materials is noticed. The adsorption capacities and removal percentages do not show the typical optimum. At AC dosages below 0.8 g/L, it removes Cr(VI) more efficiently than unmodified ACs, but it performs worse for total Cr removal. Above 0.8 g/L, the removal percentages for all studied ACs are again similar. Removal rate of Cr(VI) is the highest for the unmodified ACs, whereas the copolymerized ACs have a faster removal rate for total Cr.

The knowledge collected in **chapter 2** can be the basis for interesting new lines of research. The adsorption behaviour with a typical AC dosage optimum is now described for the Cr(VI) oxyanion, but other oxyanions are also susceptible to oxidation reactions. It would be interesting to determine the adsorption behaviour of other problematic oxyanions such as As(V)/As(III) (AsO_4^{3-}/ AsO_3^{3-}) (also considering the disappointing results from **chapter 4**); Fe(VI)/Fe(III) (FeO_4^{2-}/Fe^{3+}); Mn(VII)/Mn(II) (MnO_4^-/Mn^{2+}). Since a lot of adsorption experiments in literature are performed using sulphate salts, the effect of its reduction from sulfate (SO_4^{2-}) to sulfite (SO_3^{2-}) might also influence the surface chemistry and adsorption equilibria. Since the oxidation/reduction effect, resulting in an optimal dosage, is more pronounced for the ACBSG, it would be interesting to look into the mechanism of this effect: "is it particularly caused by a smaller BET surface,

the higher amount of surface functionalities or the nitrogen content?" The comparison of different ACs with different (known) properties can be a helpful tool here.

As the result of the copolymerization reaction is an AC with blocked porous structure, it would be interesting to explore alternatives that can overcome the current drawbacks. The conditions of finding a new (organic) modification would be: a) a molecule/compound that can be synthesized in very thin layers or clusters, b) with a selectivity towards Cr(VI) and c) showing a limited reduction to Cr(III). If a suitable agent can be found, it would be challenging to prove synergy with the activated carbon, that provides surface area and bulk density. Furthermore, the regeneration of the polymer/AC should be looked at, e.g. by washing the hybrid adsorbent with eluting solvents. The incorporation of current state-of-the-art nanoparticles or inorganic adsorbents into the AC is also a valuable research topic.

The adsorption of cesium on several ACs is the topic of **chapter 3**. Cs is a contaminant that is rarely found, except in the vicinity of nuclear (disaster) sites, where it is present as Cs-134 and Cs-137. Different measurement methods for Cs are described in this chapter and are published in two articles. In the first paper, Cs concentration is measured by gamma-ray spectrometry. To obtain a tracer material, a stable Cs-133 solution is irradiated to create Cs-134. In the second article, Cs concentrations are measured by ICP-MS.

In the first part of **chapter 3,** Cs adsorption from aqueous solutions at different pH (7/10/12) is tested on 5 ACs: 3 ACBSGs and the two commercial ACs. For experiments in batch, the removal percentage is approximately 21% at a pH 10, with no significant differences between the ACs. Raising the pH even higher to pH 12 is unsuccessful due to competition effects causing a decrease in adsorption efficiency. Incorporation of Prussian Blue on the AC does not create a hybrid material able to remove more Cs. Furthermore, Prussian Blue has a low stability when pH differs from 7. When a single column filled with AC is used several times for a Cs solution with different pH (4/7/10/12), the adsorption capacity increases if the pH is neutral to slightly acidic. For the basic solutions, the adsorption capacity decreases with cycle number because the Cs ions are washed off of the

AC by ammonia. When the adsorption capacity of the 5 ACs is compared during several cycles, the commercial ACs show a higher adsorption capacity (approximately 8.5 µg/g for Norit) compared to ACBSGs (5.0 µg/g for ACBSG06). This effect is caused by the particle size distribution, resulting in channel formation in the columns filled with the ACBSGs. The ACBSGs tend to stick together, creating preferential pathways. This effect is not observed for the commercial ACs. When a Norit GAC1240 column is used 5 sequential times, the removal percentage of each cycle was 28.1% on average.

In the second part of **chapter 3**, a hybrid material is created by incorporation of nickel hexacyanoferrate (Ni-HCF) on two ACs: ACSBSG06 and Norit GAC1240. Ni-HCF is a selective adsorbent for Cs, but has a very fine granular structure. Incorporation of Ni-HCF on AC has some major advantages: the structural properties of the Ni-HCF are supported by the carrier material, adsorbing part of the Cs. The incorporation of Ni-HCF is carried out by a two-step adsorption procedure, performing very efficiently as the AC surface is a good adsorbent itself. This adsorption procedure is repeated one, two and three times for each AC. The hybrid materials are first tested for their leaching behaviour of nickel and iron, both present in the Ni-HCF. The amount of iron leached in Milli-Q or standard (fresh) water increases when the number of modification cycles increases. For salt water (marine medium), the amount of iron leached is limited and decreases with increasing number of modifications. Nickel leaching is most problematic in sea water for ACBSG06, with a maximum release of 540 µg/g for the threefold modified ACBSG06.

Adsorption of Cs on the hybrid materials is compared to unmodified ACs at two dosages. At a high AC dosage (4 g/L), each modified AC removed nearly 100% of Cs in all aqueous media (Milli-Q - sweet water - salt water). At low dosage (0.5 g/L), differences between the hybrid adsorbents are emphasized. The Norit GAC1240 modifications show an increase in removal percentage as the number of modification cycles increases and a decrease in removal percentage as the ionic strength of the aqueous media increases. Threefold modified Norit GAC1240 at low dosage reaches a removal percentage of 83% in Milli-Q, 75% in sweet and 50% in salt water. ACBSG06 reaches higher but equivalent removal percentages for each of the modification cycles, implying that a single modification cycle

already provides the most efficient hybrid adsorbent. The removal percentages are higher than those for the commercial AC: 95, 98 and 84% for Milli-Q, sweet and salt water respectively.

This chapter describes new ideas and methodologies and could initiate future research into decontamination using biomass-based AC. A combination of techniques used in the two manuscripts can lead to effective adsorption systems with a highly precise measurement method. If the leaching problems associated with the Ni-HCF are solved (by washing, diluting the reagent concentrations up to the most efficient concentration or re-using reagent solutions during the modification steps), the modified ACs are able to be used in water-phase systems very effectively. A further improvement of the hybrid adsorbent would be pelletization, after which it can be used in column filters without the current problems (channel formation, sticking,) caused by the particle size distribution. Pelletization of the adsorbent could also add a significant benefit for dedicated applications: if the adsorbent is sufficiently mechanically robust, it can be mixed with Cs-contaminated soils. Using washing methods or natural percolation (rain), the Cs will leach out of the soil and into the adsorbent pellets, that can be sieved off of the de-contaminated soil afterwards. To test this decontamination method, gamma-ray spectrometry is a valuable measurement method as it can measure the Cs concentrations at (very) low levels in each of the fractions without chemical processing. A mass balance can be easily calculated based on the Cs activity in the soil, the adsorbent and the water before and after decontamination. Of course, it would be ideal to develop more specific adsorbents for radionuclides or other pollutants and to be able to make adsorbent mixtures that are specific to the decontamination site.

The last chapter, **chapter 4**, focuses on the removal of metals and metalloids from surface water by AC. A selection of ionic species is made based on data from the Flemish Environmental Agency (VMM) (As, Cd, Co, Cu, Pb, U, V, Zn). Experiments are based on a simplified two-point adsorption test at low (0.5 g AC/L) and high (4 g AC/L) AC dosage. An adsorption screening, removing 10 mg/L of each selected species from Milli-Q water at pH 2 or 7, shows that adsorption using acidic solutions is limited except for U. At pH 7, ACBSG06 has higher removal percentages than two commercial ACs for Cd, U and Zn. Increasing the ionic

strength by using a reconstituted surface water solution instead of Milli-Q has different effects for each AC and metal species. Zn adsorption is least influenced by the ionic strength, whereas the removal percentages of the other metals decrease slightly to drastically (up to an 80% decrease for Cd adsorption on Filtrasorb F400). Statistical analyses are used to determine the influence of AC type and adsorbate mixtures when the concentrations of the metals and metalloids were lowered in reconstituted water. Single ion experiments show that there are no differences between the ACs for Cd and U. Norit GAC1240 and ACBSG06 perform similarly for V (Filtrasorb F400 reaches approximately 14% lower removal percentages). For Co and Zn, ACBSG06 has significantly higher removal properties.

The influence of mixtures is surveyed by adsorption of binary, tertiary, quaternary and quinary mixtures of the 5 selected species (Cd, Co, U, V and Zn). For Cd removal the type of AC does not make a difference, but the competitive presence of U and Co decreases the removal. The influence of other selected ions on Co, U and V removal was insignificant and no significant differences were found between the ACs. Zn adsorption is still most effective on ACBSG06, but no influences of other metals were found. Finally, leaching experiments in reconstituted water show that Al and As leach more from commercial ACs, with a very high leachability of As for Filtrasorb F400, that also leaches Fe and Zn in high concentrations. ACBSG06 has a high leachability for Fe compared to commercial AC.

The biggest challenge that is faced in chapter 4 is the limited availability of data. There is no data available in literature that can be comparable to the current set-up as described in this chapter since the research focus here lies on (very) low concentrations and realistic AC dosages have to be considered. But also the amount of achieved data is limited, especially when looking into statistical analyses. A multiplication of the amount of adsorption data would definitely lead to more statistical significance, but is also paired with copious amounts of technical lab-work. More data per experiment would also enlarge the differences between the ACs and the influences of individual metals.

6 Besluit, samenvatting en perspectieven

De klimaatverandering en voortdurende nood aan materialen verplichten industrie en wetgeving zich meer te richten op het gebruik van biomassa. Het potentieel van biomassa als energiedrager was al langer bekend, maar de mogelijkheden om nieuwe materialen te kunnen produceren met behulp van verschillende conversiemethodes hebben een hernieuwde onderzoeksinteresse opgewekt. Omdat bepaalde chemische elementen in meer of mindere mate aanwezig zijn in specifieke biomassa's kunnen nieuwe materialen gemaakt worden met specifieke karakteristieken. De productie van nieuwe materialen met specifieke eigenschappen of in-situ geproduceerde functionaliteiten is een optie die onderzocht wordt. De voordelen van het gebruik van biomassa hebben niet alleen een directe impact op het milieu en technische installaties, maar ook op de economie en de sociale structuren in landbouwgebieden.

De biomassa die in dit project geselecteerd wordt is draf (Brewer's spent grain, BSG). Draf wordt geproduceerd tijdens het mouten in het bierbrouwproces. Het bestaat uit de restanten van gerst, nadat alle suikers en zetmeelverbindingen geëxtraheerd zijn. Er wordt wereldwijd ruwweg 270 500 ton draf geproduceerd per jaar, waarvan het merendeel gevoederd wordt aan herkauwers. Draf bevat echter ook een grote hoeveelheid onverteerbare vezels en veroorzaakt een grotere methaanproductie. Het hoge watergehalte tot 85% zorgt voor een snelle microbiële degradatie, waardoor een snelle droog- en verwerktechnologie vereist is. Gezien draf op droge basis bestaat uit ongeveer 70% cellulose, hemicellulose en lignine is het een ideaal materiaal voor biotechnologische toepassingen. Het hoge stikstofgehalte maakt draf een veelbelovende precursor voor het produceren van nieuwe materialen met in-situ gegenereerde stikstoffunctionaliteiten geïntroduceerd via pyrolyse.

Tijdens het pyrolyseproces wordt biomassa thermisch gekraakt in een zuurstofarme omgeving waardoor organische componenten in kleinere stukjes worden afgebroken. Er ontstaan verschillende fracties in dit proces: een energierijk gas (biogas), dat gedeeltelijk condenseert bij kamertemperatuur (bio-olie) en een derde vaste fractie: (bio-)char. Dit laatste bevat onvolledig geconverteerde vaste koolachtige residu's en een kleine minerale fractie. De structurele en chemische eigenschappen zijn sterk afhankelijk van het startmateriaal en de pyrolyse-omstandigheden. Bovendien kan met behulp van verhitte stoom koolstof afgbrand worden tijdens een activatieproces. Op deze manier wordt er actieve kool (AC, activated carbon) geproduceerd. Door zijn hoog specifieke oppervlakte met diverse oppervlaktefunctionaliteiten bezit AC goede adsorptie-eigenschappen. Voor draf zorgt pyrolyse gecombineerd met activatie voor een in-situ genitrogeneerde AC (ACBSG).

In hoofdstuk 2 worden ACBSG en twee commercieel beschikbare ACs (Norit GAC1240 en Filtrasorb F400) bestudeerd voor het verwijderen van chroom(VI) uit waterige oplossingen. De resultaten tonen aan dat de gebruikte meetmethodes voor Cr zich niet mogen beperken tot één oxidatietoestand maar dat concentraties van zowel totaal Cr als Cr(VI) gemeten moeten worden. Het verschil tussen totaal Cr en Cr(VI) concentraties is de hoeveelheid Cr(III) die gevormd is tijdens het verwijderingsproces. Metingen van enkel Cr(VI) resulteren in een overschatting van de verwijderde hoeveelheid Cr en leiden tot een hogere schijnbare adsorptiecapaciteit (q_{app}). Deze q_{app} is een maat voor de som van verwijderde Cr(VI) en de fractie van Cr(VI) die gereduceerd is naar Cr(III). De reële adsorptiecapaciteit (q_e) zou enkel rekening moeten houden met de hoeveelheid Cr die als Cr(VI) is geadsorbeerd. Dit typische reductiegedrag zorgt ook voor een nieuwe adsorptie-isotherm, met een maximum verwijderingspercentage voor totaal chroom bij een AC dosage van ongeveer 0,75 g/L. Boven deze AC dosage wordt Cr(VI) sterker gereduceerd naar Cr(III), dat op zijn beurt slechter geadsorbeerd wordt. Dit leidt tot een lager verwijderingspercentage voor Cr totaal. In vergelijking met de twee industriële ACs hebben de ACBSGs een beperkt beter verwijderingspercentage voor Cr(VI) bij dosages van 0,4 g/L (tot 97% voor ACBSG06, vergeleken met 91% voor F400). Vergelijkbare verwijderingspercentages (>99%) voor Cr(VI) werden voor alle bestudeerde ACs

gevonden bij dosages hoger dan 1,2 g/L. Wanneer gekeken wordt naar de verwijdering van totaal Cr, hebben de ACBSGs een hoger verwijderingspercentage bij een optimale AC dosage, tot 87% voor ACBSG05, vergeleken met 73% voor beide commerciële ACs. De reductiereactie is meer uitgesproken in de commerciële ACs wegens hun lagere zuurstof- en stikstofgehalte. De experimentele data voor de adsorptiekinetiek van zowel Cr(VI) als totaal Cr tonen aan dat de ACBSGs een sneller verwijderingstempo hebben dan de commerciële ACs door de tragere reductiereactie.

Het tweede deel van hoofdstuk 2 beschrijft de prestaties van gemodificeerde AC voor de adsorptie van chroom. Twee modificatiemethodes zijn toegepast op 4 AC stalen: 2 geselecteerde ACBSGs en beide commercieel beschikbare stalen. De eerste modificatiemethode is een zuur/base wasproces van de stalen en maakt gebruik van verdunde salpeterzuur- en natriumhydroxideoplossingen. Dit resulteert in een geoxideerd oppervlak. De ratio O/C stijgt met een factor 8 en 4 voor respectievelijk Norit GAC1240 en Filtrasorb F400, maar slechts met een factor 2 voor beide ACBSGs, die initieel al een hoger zuurstofgehalte bevatten. Deze zuurstoffunctionaliteiten zouden de Cr-adsorptie kunnen verbeteren door het verhinderen van de reductie naar Cr(III) en het incorporeren van complexatiesites. De resultaten tonen echter dat het totaal aantal oppervlaktefunctionaliteiten drastisch daalt voor elke AC. Dit resulteert in lagere adsorptiecapaciteiten en verwijderingspercentages voor zowel Cr(VI) als totaal chroom, dit in vergelijking met ongemodificeerde ACs. De tweede modificatiemethode is gebaseerd op het enten van een copolymeer met een quaternaire ammoniumeindgroep die complexen kan vormen met Cr. De structuur van het copolymeer blokkeert echter gedeeltelijk de poreuze structuur van de AC, dus wordt er geen synergetisch effect door de combinatie van de twee materialen vastgesteld. Bij AC dosages onder de 0,8 g/L verwijdert deze gemodificeerde AC Cr(VI) efficiënter dan ongemodificeerde AC, maar presteert hij minder goed voor de verwijdering van totaal Cr. Boven 0,8 g/L zijn de verwijderingspercentages voor alle bestudeerde ACs vergelijkbaar. Het verwijderingstempo voor Cr(VI) is het snelst voor ongemodificeerde ACs, maar de gecopolymeriseerde ACs bieden een snellere verwijdering van totaal Cr.

De kennis die opgebouwd is in hoofdstuk 2 kan de basis bieden voor uitdagende nieuwe onderzoekslijnen. Het adsorptiegedrag met een typisch optimum voor de AC dosis is nu beschreven voor het Cr(VI) oxyanion, maar andere oxyanionen zijn ook onderhevig aan oxidatie/reductie reacties. Het zou daarom nuttig zijn om het adsorptiegedrag van andere oxyanionen te onderzoeken, zoals As(V)/As(III) (AsO_4^{3-}/ AsO_3^{3-}) (ook in het licht van de teleurstellende adsorptieresultaten van hoofdstuk 4; Fe(VI)/Fe(III) (FeO_4^{2-}/Fe^{3+}) en Mn(VII)/Mn(II) (MnO_4^-/Mn^{2+}). Omdat veel adsorptie-experimenten in de literatuur worden uitgevoerd met sulfaatzouten is mogelijk dat het effect van de reductie van sulfaat (SO_4^{2-}) naar sulfiet (SO_3^{2-}) ook de oppervlakte-chemie en het adsorptiegedrag beïnvloedt. Omdat het oxidatie/reductie effect, resulterend in een optimale AC dosis, meer uitgesproken is voor ACBSG is het ook aangewezen het mechanisme van dit effect te onderzoeken: "wat is de rol van een kleiner specifiek oppervlak, een hogere hoeveelheid oppervlaktefunctionaliteiten en het stikstofgehalte?" Het vergelijken van verschillende ACs met verschillende (gekende) eigenschappen kan hier nieuwe perspectieven bieden.

Gezien het resultaat van de copolymerisatiereactie een AC is met een geblokkeerde poreuze structuur is het aangewezen om alternatieven te exploreren. De voorwaarden voor het vinden van een nieuwe (organische) modificatie zijn: a) een molecule die gesynthetiseerd kan worden in erg dunne lagen of in clusters, b) met een selectiviteit voor Cr(VI) en c) die weinig reductie naar Cr (III) veroorzaakt. Als een geschikt agens gevonden wordt kan dit aanleiding geven tot een synergie met AC, die specifiek oppervlak en bulkdichtheid voorziet. Verder zouden ook de regeneratiemogelijkheden van de polymeer/AC-verbinding kunnen onderzocht worden door het hybride adsorbens te wassen met geschikte solventen. Het incorporeren van hedendaagse state-of-the-art nanopartikels of inorganische adsorbentia is ook een waardevolle uitbreiding van dit onderzoek.

De adsorptie van cesium op verschillende ACs is het onderwerp van hoofdstuk 3. Cs is wereldwijd een zeldzame vervuiling, behalve in de buurt van nucleaire (ramp)gebieden, waar het voorkomt als Cs-134 en Cs-137. Verschillende meetmethodes voor de bepaling van Cs-concentraties worden beschreven in dit hoofdstuk, opgebouwd uit twee artikels. De eerste paper is gebaseerd op het

meten van de Cs concentratie via gammaspectrometrie. Een stabiele Cs-133 oplossing wordt bestraald om Cs-134 te produceren. In het tweede artikel worden Cs concentraties bepaald via ICP-MS.

In het eerste deel van hoofdstuk 3 wordt de adsorptie van Cs uit waterige oplossingen bij een verschillende pH (7/10/12) getest op 5 ACs: 3 ACBSGs en de twee commerciële ACs. Voor de batch-experimenten wordt er een verwijderingspercentage van ongeveer 21% gevonden bij pH 10, zonder significante verschillen tussen de ACs onderling. Het verhogen van de pH tot 12 is geen succes: er treedt competitie op en de adsorptie-efficiëntie daalt. Het incorporeren van Pruisisch Blauw op de AC creëert geen nieuw hybride materiaal dat meer Cs kan verwijderen. Bovendien is Pruisisch Blauw erg onstabiel als de pH te veel afwijkt van 7. Wanneer een enkele kolom gevuld met AC meermaals wordt gebruikt om Cs oplossingen met verschillende pH (4/7/10/12) te filteren stijgt de adsorptiecapaciteit als de pH neutraal tot lichtjes zuur is. Voor de basische oplossingen daalt de adsorptiecapaciteit wanneer het aantal gebruikscycli stijgt door het uitwassen van de Cs-ionen door de aanwezige ammoniak. Wanneer de adsorptiecapaciteit van de 5 ACs vergeleken worden tijdens de verschillende cycli, geven de commerciële ACs een hogere adsorptiecapaciteit (ongeveer 8,5 µg/g voor Norit) vergeleken met de ACBSGs (5,0 µg/g voor ACBSG06). Dit effect wordt veroorzaakt door de deeltjesgrootteverdeling en resulteert in kanaalvorming in de kolommen met ACBSG en wordt niet waargenomen voor de commerciële ACs. De ACBSGs kleven samen, waardoor voorkeurspaden gecreëerd worden. Wanneer 5 Norit GAC1240 kolommen achtereenvolgens gebruikt worden is het verwijderingspercentage per kolom gemiddeld 28.1%.

In het tweede deel van hoofdstuk 3 wordt een hybride materiaal geproduceerd door het incorporeren van nikkelhexacyanoferraat (Ni-HCF) op 2 ACs: ACBSG06 en Norit GAC1240. Ni-HCF is een selectief adsorbens voor Cs, maar heeft een zeer fijne granulaire structuur. Het incorporeren van Ni-HCF in AC heeft een aantal grote voordelen: de structurele eigenschappen van Ni-HCF worden gesteund door het dragermateriaal (de AC) dat zelf ook een deel van het Cs adsorbeert. Deze incorporatie gebeurt met een tweestaps adsorptieprocedure die erg efficiënt verloopt omdat de AC zelf een goed adsorbent is. Deze incorporatie wordt een-,

twee- en driemaal uitgevoerd voor elke AC. De geproduceerde hybride materialen worden eerst getest voor het uitlooggedrag van ijzer en nikkel, beiden aanwezig in de Ni-HCF. De hoeveelheid uitgeloogd ijzer in Milli-Q of standaard (zoet) water stijgt wanneer het aantal uitgevoerde modificatiecycli toeneemt. In zout water (marine medium) is er weinig uitloging van ijzer en de uitgeloogde hoeveelheid daalt met stijgend aantal modificatiecycli. Nikkeluitloging is erg problematisch in zout water voor ACBSG06, met een maximale uitloging voor het driemaal gemodificeerd staal tot 540 µg/g.

Adsorptie van Cs op de hybride materialen wordt vergeleken met adsorptie op ongemodificeerde AC bij twee AC dosages. Bij een hoge AC dosage (4g/L) verwijderde elke gemodificeerde AC bijna 100% van het aanwezige Cs in alle oplossingen (Milli-Q, zoet water, zeewater). Bij een laag AC dosage (0,5 g/L) worden de verschillen tussen de hybride adsorbentia beklemtoond. De gemodificeerde versies van Norit GAC1240 tonen een verhoging van het verwijderingspercentage wanneer het aantal modificatiecycli stijgt en een verlaging van het verwijderingspercentage wanneer de ionische sterkte van de oplossing stijgt. Driemaal gemodificeerde Norit GAC1240 behaalt bij lage AC dosage tot 83% verwijdering in Milli-Q, 75% in zoet water en 50% in zout water. ACBSG06 bereikt hogere maar gelijkaardige verwijderingspercentages voor elke modificatie: één enkele modificatiecyclus is al voldoende voor het produceren van het efficiëntste hybride adsorbens. Het verwijderingspercentage is hoger dan voor de commerciële AC: 95, 98 en 84% voor respectievelijk Milli-Q, zoet en zout water.

De nieuwe ideeën en methodologieën beschreven in dit hoofdstuk kunnen nieuw onderzoek over decontaminatie met behulp van biomassa-gebaseerde AC initiëren. Een combinatie van de beschreven technieken kan leiden tot zeer efficiënte adsorptiemedia met erg precieze meetmethodes. De uitlogingsproblemen geassocieerd met de Ni-HCF verhinderen momenteel dat de gemodificeerde ACs zeer gemakklijk kunnen worden ingezet in waterzuivering. Een verdere verbetering van het hybride adsorbens zou pelletiseren zijn, waarna het kan gebruikt worden in kolommen zonder de huidige problemen (kanaalvorming, aan elkaar plakken,...) die te maken hebben met de deeltjesgrootteverdeling. Het pelletiseren van het adsorbent zou ook een extra

voordeel toevoegen voor een mogelijke applicatie: als het hybride adsorbent voldoende robuust is kan het gemengd worden met Cs-gecontamineerde aarde. Door nabehandeling (wassen met water) natuurlijke uitloging (beregening) kan Cs uit de bodem uitgeloofd worden en geadsorbeerd worden op de adsorbent pellets, die achteraf van de gecontamineerde aarde afgezeefd kunnen worden. Om deze decontaminatiemethode te testen is gamma-spectrometrie een waardevolle meetmethode omdat de (zeer lage) Cs concentraties in elke fractie kunnen gemeten worden zonder chemische behandeling. Een massabalans kan eenvoudig bepaald worden gebaseerd op de Cs activiteit in de aarde, het water en de pellets vóór en na decontaminatie. Natuurlijk zou het ideaal zijn meer specifieke adsorbentia te ontwikkelen voor radionuclides. Hiervan zouden dan adsorbent mengsels kunnen gemaakt worden die specifiek voor de decontaminatie site worden samengesteld.

Het laatste hoofdstuk, hoofdstuk 4, focust op de verwijdering van metalen en metalloïden uit oppervlaktewater door AC. Een selectie van ionen werd gemaakt op basis van de expertise van de Vlaamse Milieumaatschappij (As, Cd, Co, Cu, Pb, U, V, Zn). De experimenten zijn uitgevoerd als een vereenvoudigde tweepuntstest bij lage (0,5 g AC/L) en hoge (4 g AC/L) AC dosage. Een adsorptiescreening waarbij 10 mg/L van elk gekozen ion verwijderd wordt uit een oplossing van Milli-Q met pH 2 of 7 toont aan dat het gebruik van zure oplossingen leidt tot gelimiteerde adsorptie, behalve voor uranium. Het verhogen van de ionische sterkte door het gebruik van een gereconstitueerd oppervlaktewater in de plaats van Milli-Q heeft verschillende effecten voor elke AC en ion. Bij pH 7 heeft ACBSG06 een hoger verwijderingspercentage dan de twee commerciële ACs voor Cd, U en Zn. Zn adsorptie wordt het minst beïnvloed door de ionische sterkte, in tegenstelling tot de verwijdering van andere metalen die lichtjes tot erg drastisch vermindert (een vermindering tot 80% voor Cd adsorptie op Filtrasorb F400). Statistische analyses worden gebruikt om de invloed van het AC type en de adsorbaat mengsels te bepalen wanneer de concentratie van metalen en metalloïden heel laag is in gereconstitueerd oppervlaktewater. Experimenten waarbij slechts 1 probleemion aanwezig is tonen aan dat er geen verschillen zijn tussen de ACs voor adsorptie van Cd en U. Norit GAC1240 en ACBSG06 presteren gelijkaardig voor V (waarbij Filtrasorb F400 ongeveer 14% minder V verwijdert).

Voor Co en Zn heeft ACBSG06 beduidend betere verwijderingseigenschappen dan de commerciële ACs.

De invloed van mengsels wordt onderzocht door adsorptie van twee-, drie-, vier- en vijfvoudige mengsels van de 5 geselecteerde ionen (Cd, Co, U, V en Zn). Voor het verwijderen van Cd maakt het type AC geen verschil, maar de competitieve aanwezigheid van U en Co verlagen wel de verwijderingsefficiëntie. De invloed van de geselecteerde ionen op verwijdering van Co, U en V was onbeduidend en er worden ook geen significante verschillen tussen de verschillende ACs gevonden. De adsorptie van Zn is nog steeds het meest effectief op ACBSG06, maar er wordt ook geen invloed van andere metalen gevonden. Tenslotte tonen uitloogproeven in gereconstitueerd water aan dat zowel Al als As meer uitlogen uit commerciële ACs, met een erg hoge uitloging van As voor Filtrasorb F400, dat bovendien ook hogere concentraties Fe en Zn uitloogt. ACBSG06 heeft een hoge uitloogbaarheid voor Fe in vergelijking met commerciële AC.

Het grootste probleem voor de beschreven experimenten in hoofdstuk 4 is de beperkte beschikbaarheid van data. In de literatuur zijn er geen data beschikbaar die vergelijkbaar zijn met de gegevens verkregen met de opstelling zoals beschreven in hoofdstuk 4, mede door het feit dat zeer lage concentraties moeten verwijderd worden met realistische AC dosissen. Ook het aantal verkregen experimentele gegevens zijn te beperkt, zeker met het oog op statistische analyses. Een veelvoud van de hoeveelheid adsorptiedata zou zeker leiden tot meer statistische significantie, maar gaat ook gepaard met significante experimentele belasting. Meer data per experiment zou ook de verschillen tussen de ACs en de individuele metaalionen uitvergroten.

7 List of publications

2018

Journal Contribution

Vanderheyden, Sara; Vanreppelen; Kenny; Yperman, Jan; Carleer, Robert & Schreurs, Sonja (2018). *Chromium(VI) removal using in-situ nitrogenized activated carbon prepared from brewers' spent grain.*
In: Adsorption, 24, p. 147-156 [Article - cat: A1]

Vanderheyden, Sara; Yperman, Jan; Carleer, Robert & Schreurs, Sonja (2017). *Enhanced cesium removal from realistic matrices by modified activated carbons*.
In: Chemosphere, 202, 569-575**.** [Article – cat: A1]

Vanderheyden, Sara; Yperman, Jan; Carleer, Robert & Schreurs, Sonja (2017). *The use of activated carbons as adsorbent for problematic metals in Flemish surface water*
In: Adsorption, **submitted**

2017

Journal Contribution

Vanderheyden, Sara; Yperman, Jan; Carleer, Robert & Schreurs, Sonja (2017). *Activated carbon modification resulting in an enhanced Cr(VI) removal.*
In: Desalination and Water Treatment, **in press.** [Article – cat: A1].

Conference Material

Vanderheyden, Sara; Yperman, Jan; Schreurs, Sonja & Carleer, Robert (2017). *Activated carbon modification resulting in an enhanced Cr(VI) removal.*
In: PhD Scientific Workshop Week: "Bringing knowledge into practice", Santiago de Cuba, Cuba, 06-11/11/2017. [Presentation - cat: C2]

Vanderheyden, Sara; Van Ammel, Raf; Sobiech-Matura, Katarzyna; Schreurs, Sonja; Yperman, Jan & Carleer, Robert (2017). *Adsorption of caesium on different types of activated carbon.*
In: EUFRAT User Meeting "Progress of Nuclear Data Measurements using JRC's unique facilities", Geel, Belgium, 04-07/12/2017. [Paper - cat: C2]

Vanderheyden, Sara; Van Ammel, Raf; Sobiech-Matura, Katarzyna; Vanreppelen, Kenny; Schreurs, Sonja; Schroeyers, Wouter; Yperman, Jan & Carleer, Robert (2017). *Adsorption of caesium on different types of*

activated carbon.
In: EUFRAT User Meeting "Progress of Nuclear Data Measurements using JRC's unique facilities", Geel, Belgium, 04-07/12/2017. [Presentation - cat: C2]

Vanderheyden, Sara; Schreurs, Sonja; Yperman, Jan & Carleer, Robert (2017). *Modication of activated carbons from brewers' spent for chromium(VI) adsorption.*
In: ATHENS 2017 5th International Conference on Sustainable Solid Waste Management, Athens, 21-24/6/2017. [Presentation - cat: C2]

2016

Journal Contribution

Vanderheyden, Sara; Van Ammel, R.; Sobiech-Matura, K.; Vanreppelen, Kenny; Schreurs, Sonja; Schroeyers, Wouter; Yperman, Jan & Carleer, Robert (2016). *Adsorption of cesium on different types of activated carbon.*
In: JOURNAL OF RADIOANALYTICAL AND NUCLEAR CHEMISTRY, 310(1), p. 301-310. [Article - cat: A1 - Validation: ecoom 2017]

2015

Conference Material

VANDERHEYDEN, Sara; VAN AMMEL, Raf; SOBIECH-MATURA, Katarzyna; Vanreppelen, Kenny; SCHREURS, Sonja; Schroeyers, Wouter; Yperman, Jan & Carleer, Robert (2015). *Comparison of adsorption properties of Cs on different types of activated carbon.*
In: ENVIRA2015 International Conference on Environmental Radioactivity: New Challenges with New Technologies, Thessaloniki, 21-25/09/2015. [Presentation - cat: C2]

Schreurs, Sonja; Carleer, Robert; Yperman, Jan; Pontikes, Yiannis; Hult, Mikael; Vanreppelen, Kenny; Maggen, Jens; Vanderheyden, Sara; Croymans-Plaghki, Tom; Vandevenne, Niels & Schroeyers, Wouter (2015). *Targeted treatment of selected waste streams to produce added value materials.*
In: Topical Day: Dealing with environmental contamination: from response to risk assessment, SCK-CEN, Mol - Belgium, 26/11/2015. [Presentation - cat: C2]

2014

Journal Contribution

VANREPPELEN, Kenny; VANDERHEYDEN, Sara; KUPPENS, Tom; SCHREURS, Sonja; YPERMAN, Jan & CARLEER, Robert (2014). *Activated carbon from pyrolysis of brewer's spent grain: Production and adsorption properties.*

In: Waste Management & Research, 32 (7), p. 634-645. [Article - cat: A1 - Validation: ecoom 2015]

2013

Proceedings Paper

VANREPPELEN, Kenny; VANDERHEYDEN, Sara; KUPPENS, Tom; SCHREURS, Sonja; CARLEER, Robert & YPERMAN, Jan (2013). *Activated Carbon from Pyrolysis of Brewer's Spent Grain: Production and Adsorption Properties.*
 Klemeš, J.J.; Varbanov, P.; Ababneh, A.; Østergaard, P.A.; Connolly, D.; Kafarov, V.; Krajačić, G.; Lund, H.; Mathiesen, B.V.; Mohsen, M.; Möller, B.; Perković, L.; Sikdar, S.K.; Vujanović, M. (Ed.). Proceedings of the 8th Conference on Sustainable Development of Energy, Water and Environment Systems (SDEWES 2013). [Full Paper - cat: C1]

Conference Material

VANREPPELEN, Kenny; VANDERHEYDEN, Sara; KUPPENS, Tom; SCHREURS, Sonja; CARLEER, Robert & YPERMAN, Jan (2013). *Activated Carbon from Pyrolysis of Brewer's Spent Grain: production and Adsorption Properties.*
In: 8th Conference on Sustainable Development of Energy, Water and Environment Systems, Dubrovnik, 22-27/09/2013. [Presentation - cat: C2]